INVESTIGATING THE ROLE OF MUTANT HUNTINGTIN IN ALTERED TRANSCRIPTION IN HUNTINGTON'S DISEASE

by

Haibei Hu

Submitted in partial fulfillment of the requirements
for the degree of Doctor of Philosophy

at

Dalhousie University
Halifax, Nova Scotia
July 2007

Your file Votre référence
ISBN: 978-0-494-31498-2
Our file Notre référence
ISBN: 978-0-494-31498-2

DALHOUSIE UNIVERSITY

To comply with the Canadian Privacy Act the National Library of Canada has requested that the following pages be removed from this copy of the thesis:

Preliminary Pages
- Examiners Signature Page (pii)
- Dalhousie Library Copyright Agreement (piii)

Appendices
- Copyright Releases (if applicable)

This work is dedicated to my parents

TABLE OF CONTENTS

LIST OF FIGURES

LIST OF TABLES

ABSTRACT

Inheritance of one copy of the *huntingtin* gene with an extended CAG repeat causes Huntington's Disease (HD). People with HD gradually develop a triad of clinical symptoms that involve motor dysfunction, cognition deficits and psychiatric disturbances. Currently, there is no effective treatment for HD. The most distinct neuropathology in HD is a gradual loss of GABAergic medium spiny projection neurons in the caudate and putamen. Studies from animal models of HD have demonstrated that the amino terminus of mutant huntingtin (N-mHtt) accumulates in the nucleus and that levels of a specific subset of mRNAs decrease in some neurons. How N-mHtt reduces synthesis of mRNA in a cell- and gene-specific manner is currently unknown. In this study, we employed a systematic approach to explore the mechanism whereby N-mHtt exerts transcriptional repression in transgenic HD mice, and in cell culture and *in vitro* models of HD. We chose to study phosphodiesterase 10A (PDE10A) as a model of mutant huntingtin-affected genes. We performed detailed analyses of gene structure and tissue-specific expression of PDE10A and studied the affects of N-mHtt on the expression of this gene. N-mHtt decreased transcription from the striatal-specific PDE10A2 promoter but not from a testis-specific PDE10A1 promoter. Reduced transcription was caused by decreased transcription initiation specifically from two of three transcription start sites in young R6/1 transgenic HD mice. N-mHtt present in the brains of R6/1 mice did not alter the DNA binding activities of 125 of 345 transcription factors prior to the time that transcription of PDE10A2 began to decrease. Using a cell-free system, we determined that soluble monomer form of wild-type and mutant huntingtin were associated with the transcription preinitiation complexes. Together, the data do not support the current hypotheses that N-mHtt sequesters transcription factors from promoters. Rather, it appears that N-mHtt directly associates with and may change the composition of the complexes of proteins that make up the basal transcription machinery. This direct association with the transcription machinery may block communication between the transactivation domains of promoter-specific factors and the cell-specific components in the core transcription machinery.

LIST OF ABBREVIATIONS USED

2-D	Two-Dimensional
TAP	Tobacco Acid Pyrophosphatase
3-NP	3-Nitropropionic Acid
5' RLM-RACE	5' RNA-Ligase Mediated Rapid Amplification of cDNA Ends
AHRARNT	Aryl Hydrocarbon Receptor /Ah Receptor Nuclear Translocator Heterodimers
ANOVA	Two-Way Analysis of Variance
AP1	Activating Protein 1
ARE	AU-Rich Response Element
C	Carboxy
CB1	Cannabinoid Receptor Type 1
CBP	cAMP Response Element Binding Protein Binding Protein
CNS	Central Nervous System
Co-IP	Co-Immunoprecipitation
CtBP/p300	C-Terminal Binding Protein
DARPP32	Dopamine Responsive Phosphoprotein 32 Kda
ddH_2O	Double-Distilled H_2O
DRPLA	Dentate-Rubral And Pallido-Luysian Atrophy
DTT	Dithiothreitol
ECL	Enhanced Chemiluminescence
EDTA	Ethylenediaminetetraacetic Acid
Egr1	Early Growth Response 1

EMSA	Electromobility Shift Assay
EST	Expressed Sequence Tag
FBS	Fetal Bovine Serum
fmol	Fento Moles
GABA	Gamma-Aminobutyric Acid
GAD65	Glutamic Acid Decarboxylase 65
GC-1	GC-Box Elements
GST	Glutathione *S*-Transferase
HBSS	Hank's Balanced Salt Solution
HD	Huntington's Disease
HDAC	Histone Deaceylation
Hdh	Mouse *Huntingtin* Gene
HPRT	Hypoxanthine Guanine Phosphoribosyltransferase
Hrs	Hours
KCl	Potassium Chloride
KH_2PO_4	Mono Potassium Phosphate
mGluR	Glutamte Receptors
Min	Minutes
MMLV-RT	Moloney Murine Leukemia Virus Reverse Transcriptase
MyoD	Myogenic Regulatory Factor D
MZF-1	Myeloid Zinc Finger 1
N	Amino
Na_2HPO_4	Disodium Hydrogen Phosphate

NaCl	Sodium Chloride
NcoR	Nuclear Receptor Co-Repressor
NES	Nuclear Export Signal
NF1	Nuclear Factor –1
NFkappaB	Nuclear Factor Kappa B
NGF-IA	Nerve Growth Factor Inducible Factor A
NGFI-C	Early Growth Response Protein-1C
NGFR	Nerve Growth Factor Receptor
NIIs	Neuronal Intranuclear Inclusions
NLS	Nuclear Localization Signal
NMDA	N-Methyl-D-Aspartic Acid
nmol	Nano Moles
NOS	Nitric Oxide Synthase
NRSF	Neuron Restrictive Silencing Factor
nt	Nucleotides
P/CAF	P300/CBP Associated Factor
PBS	Phosphate-Buffered Saline
PCR	Polymerase Chain Reaction
PDE	Phosphodiesterase
PGC-1α	Peroxisome Proliferation Activator Receptor (PPAR) Gamma-Coactivator 1α
pmol	Pico Moles
PMSF	Phenoylmethylsulfonyl Fluoride

polyQ	Polyglutamine
PVDF	Polyvinylidene Fluoride
QA	Quinolinic Acid
qRT-PCR	Quantitative Reverse Transcriptase-PCR
RNA pol II	RNA Polymerase II
RPA	Ribonuclease Protection Assay
RXR	Retinoid X Receptor
SAHA	Suberoylanilide Hydroxamic Acid
SBMA	Spinal And Bulbar Muscular Atrophy
SCA	Spinocerebellar Ataxia
SDS	Sodium Dodecyl Sulfate
SDS-PAGE	Sodium Dodecyl Sulfate-Polyacrylamide Gel Electrophoresis
Sec	Seconds
SFM	Serum Free Media
Sp1	Specific Protein 1
SSC	Chloride-Sodium Citrate
SSRI	Selective Serotonin Reuptake Inhibitors
TAF	TBP-Associated Factors
TBP	TATA Box Binding Protein
TdT	Terminal Deoxynucleotidyl Transferase
Tet	Tetracycline
TR	Thyroid Hormone Receptor
TUNEL	Terminal Transferase dUTP Nick End Labeling

U	Units
UV	Ultraviolet
VDR	Vitamin D Receptor
YAC	Yeast Artificial Chromosome

ACKNOWLEDGEMENTS

Doing a Ph.D. in Eileen's lab is one of the best things that ever happened to me. I would like to give my deepest and warmest gratitude to my supervisor Dr. Eileen Denovan-Wright. I thank her for giving me enough faith and strength like no one else to face all the challenges of this research career. I thank her for giving me enormous guidance to become a thinker and not simply a "doer". I am mostly grateful for her persistence and patience in helping me improve my professional English writing. I would also like to thank her for her true friendship with regards to life, people, cooking, yoga and most recently fashion from Italy; as well as many other ingredients in life. This has been such a wonderful journey. Thank you for everything !

I would like to thank present and past members in Eileen's lab including Geraldine, Marissa, Elizabeth and Matt, in particular. I want to thank them for making the lab such a joyful place to work and for teaching me enough "googleable" English terms to survive. I especially want to thank Geraldine for teaching me several techniques in the lab, for her stimulating discussions, and her genuine friendship in many aspects. Thanks GG! I would also like to acknowledge Min Huang, Kathleen Murphy and Janette Nason for their excellent technical support throughout this study. My special thanks go to Dr. Anna-Maria Szczesniak, Dr. Robert Gilbert and Marissa Attis for helping me in many academic and non-academic circumstances. I truly appreciate your constant support! I would like to thank the many fellow graduate students and postdoctoral fellows in the Vision 2000 lab for their help and companionship that made this lab a wonderful place to work. I also want to give my thanks to the Department of

Pharmacology for its continuous support for graduate students and for providing me with a great training environment to become a better researcher.

I am extremely grateful for all the support and love from my family. I want to thank my parents for encouraging me to get an advanced education overseas and for constantly giving me the courage, faith and confidence to face the challenges in my life. I am mostly indebted to my mother, who came from China to help me while I was writing my thesis. Thank you for everything, Mom.

I wish to thank Dr. Elena Cattaneo, Dr. Beverly Davidson and Dr. Xiao-Jiang Li for providing various reagents as gifts for this research. I would also like to acknowledge the Huntington Society of Canada (HSC) and the Nova Scotia Health Research Foundation (NSHRF) for PhD studentships throughout this degree. This research work was funded by the Canadian Institute of Health Research (CIHR) and HSC.

CHAPTER 1

Introduction

1.1 Huntington's Disease (HD)

Huntington's Disease was first described as an unique form of chorea by a physician named George Huntington in 1872. Three distinct features including its heritability, a tendency for patients to experience insanity and commit suicide, and a manifestation of the disease in adulthood, are associated with the chorea. This chorea bears the physician's name and is now called Huntington's Disease (HD) (Huntington, 1872). HD is an inherited neurological disorder that equally affects men and women with an incidence of 4 to 7 per 100,000 worldwide (Harper, 1992). Inheritance of the disease gives rise to a progressive, selective neuronal cell death associated with a triad of symptoms that include motor dysfunctions, cognitive deficits, and psychiatric disturbances (Bates *et al.*, 2002). The disease onset is usually in mid-life but can vary from early childhood until old age and the duration of the disease ranges from 10 to 25 years after onset of motor symptoms (Harper, 1992; Vonsattel & DiFiglia, 1998).

Clinical Features of HD

There is variability in the symptoms at different stages of HD progression and among patients (Brandt *et al.*, 1984; Harper, 1992). Motor dysfunction consists of involuntary movements and impaired voluntary movements. Involuntary movements include chorea, dystonia, irregular jerking and rigidity. Impaired voluntary movements involve the limbs and trunk and musculature of the respiratory, laryngeal, pharyngeal, oral and nasal systems. As such, HD patients suffer from gait disturbances, impaired pursuit with saccadic intrusions, lack of fine motor coordination, difficulty in swallowing and impairments of speech. The combination of involuntary movements and impairment

of fine motor skills ultimately causes great functional impairment and a poor quality of life (Ross *et al.,* 1997). Cognitive difficulties usually begin about the same time as abnormal movements. Patients develop aphasia (loss of ability to use language), agnosia (loss of cognition and ability to learn), global dementia (loss of memory) and delirium (Brandt *et al.,* 1984). Other significant components of HD are the psychiatric symptoms that occur before the onset of the movement disorders in up to 50% of HD patients (Nance, 1998). Depression, aggression, irritability, apathy, and mood swings are the most common symptoms of HD patients, which can be accompanied by delusions, hallucinations and/or schizophrenia-like syndrome. These psychiatric symptoms may be behaviorally expressed as aggressive outbursts, impulsiveness, social withdrawal, and suicide (Jensen *et al.,* 1993).

Neuropathology of HD brains

The most prominent neuropathology in HD brains is selective neurodegeneration in the basal ganglia, mainly in the caudate and putamen. Other brain regions that are affected in HD, but to a lesser extent, include certain neuronal populations in the thalamus, subthalamus, and substantia nigra, as well as pyramidal neurons in layers III, V and VI of the cortex and CA1 of the hippocampus (Vonsattel, 1983). Loss of neurons in the caudate and putamen show a gradient, with the earliest and most extensive loss in the dorsal and medial regions of the structure, and progressive loss in ventral and lateral regions as the disease progresses. Despite selective vulnerability to cell death of the medium spiny projection neurons, which are the most abundant type of neurons in the caudate and putamen, the large and medium aspiny interneurons survive throughout the

progression of HD (Vonsattel & DiFiglia, 1998). Neuronal loss in HD is followed by reactive astrocytosis and gliosis, and the number and size of reactive glia are proportional to the degree of neuronal loss (Stevens *et al.*, 1988). A 0 to 4 relative grading scale of gross and microscopic neurodegeneration, based primarily on changes in the caudate and putamen, has been used to semi-quantitatively categorize the severity of HD in post-mortem brains (Vonsattel *et al.*, 1985). Cell death in the caudate and putamen reflects vulnerability of these cells and this may have inadvertently focused research on understanding changes that occur in this region without considering that HD may have negative effects caused by common mechanisms throughout the brain. Patients, which at the time of death had brains classified as grade 0, manifest HD symptoms but do not have detectable neurodegeneration in the caudate putamen (Caramins *et al.*, 2003). These facts demonstrate that symptoms precede detectable neurodegeneration. Clinical symptoms of HD can not be attributed directly to the degree of atrophy and degeneration in the caudate and putamen. Functional changes in structures outside of the caudate and putamen, such as the cortex, hippocampus, cerebellum and white matter, may play significant roles in non-motor symptoms and the clinical heterogeneity observed among HD patients (Rosas *et al.*, 2003; Lafosse *et al.*, 2007).

Inheritance and discovery of the HD *gene*

Analysis of many HD pedigrees in Venezuela from 1983 to 1993 clearly delineated the inheritance of HD (Gusella *et al.*, 1993). HD is characterized by equal incidence in both sexes, equal transmission by both sexes, and a clear autosomal dominant pattern of inheritance. In 1993, the genetic cause of HD was identified using

material derived from the well-defined HD pedigree in Venezuela. HD is caused by an abnormal expansion of the polymorphic CAG trinucleotide repeat in exon 1 of the *Interesting Transcript (IT15)* gene, later named the *HD* gene (Huntington's Disease Collaborative Research Group, 1993). The *HD* gene is located on the short arm of chromosome 4 (4p16.3) and contains 67 exons that code for a 3144 amino acid, 350 kDa huntingtin protein. The chromosomal position accounts for the autosomal pattern of inheritance of HD. The CAG repeat is translated into a polyglutamine (polyQ) tract within the N-terminus of the huntingtin protein. Members of the general population who do not have HD have 35 or fewer CAG repeats at this position of the *HD* gene, although the locus is clearly polymorphic like many other microsatellite repeats in the human genome. HD patients have more than 35 contiguous CAG repeats. There is an inverse correlation between the number of CAG repeats and the age of onset in HD (Duyao *et al.*, 1993), but the strength of this correlation varies considerably. The strongest correlation between repeat length and age of onset applies to the largest CAG repeats (55 to 250 repeats), which are frequently associated with juvenile onset of disease (Nance *et al.*, 1999; Geevasinga *et al.*, 2006). The majority of HD patients have 40 to 50 CAG repeats and the age of onset/repeat length correlation is much weaker for this group of HD patients (Brinkman *et al.*, 1997). Patients having an allele with 35-38 CAG repeats are considered to be at risk for developing the disease but may not develop HD phenotypes during their lifespan (Rubinsztein *et al.*, 1996). The mutant *HD* allele that is inherited from affected fathers tends to increase in the size of CAG repeat found in the gene of the offspring (Trottier *et al.*, 1994). Most of the patients who suffer from juvenile-onset HD inherit the *HD* allele from their fathers. The juvenile form of the disease is characterized

by bradykinesia, rigidity, dystonia and epilepsy rather than chorea seen in the adult-onset of HD (Geevasinga *et al.,* 2006). Genotype-phenotype correlation studies show that the size of CAG repeats is inversely correlated with severity of brain pathology, but not with the development of psychiatric features or rate of dece in HD patients, suggesting CAG expansion may be directly related to cell vulnerability but sequences surrounding the CAG expansion may be attributed to the psychiatric symptoms. These studies indicate that the expansion of CAG located within the *HD* gene may contribute to neuronal dysfunction, which occurs decades prior to neurodegeneration (Lovestone *et al.,* 1996). Analysis of the Venezuelan HD kindred demonstrated that variability in age of onset has both genetic (in addition to the inheritance of an abnormal CAG repeat) and environmental components (Wexler *et al.,* 2004). HD patients acquire the mutant alleles from the preceding generation in majority of HD cases (95%) and <5% show sporadic mutation that is independent of non-paternal transmission (Huntington's Disease Research Collaborative Research Group, 1993). Heterozygous HD patients with one mutant allele show indistinguishable features compared to patients with two mutant alleles indicating an autosomal dominant feature of HD (Durr *et al.,* 1999; Wexler *et al.,* 1987)

Current treatments

There is currently no effective treatment for preventing or delaying the progression of HD. The treatments that are available for HD patients target chorea and psychotic symptoms (Bonelli & Hofmann, 2004; 2007) (Table 1-1). Antichorea

Table 1-1. Possible therapeutic approaches for HD[1].

Pharmacology approaches	Drugs used	Mechanism of action	Target	Side-effects
Sedatives, Psychiatric agents, Mood stabilizer, Cognitive enhancers[2]	Carbamazepine, risperidone, clozapine quetiapine	Anti-psychotics Anti-depressants SSRI	Depression, psychiatric symptoms	Insomnia, tremor, anxiety, seizures, sleepiness
	Olanzapine Tetrabenazine Haloperidol Pimozide	Dopamine-depleting agents	Chorea, hyperkinetic movements	Sedation, Parkinsonian symptoms, depression, insomnia
	Isoniazid Muscimol THIP Baclofen	GABAergic agonists	Dystonia, seizures	Sedation, or no effect
	Diazepam	Anti-cholinergic drugs	Dystonia	All anti-cholinergic side-effects, dry mouth, nausea
	Amantadine Remecemide Riluzole Ketamine	NMDA antagonists	Reduce excitotoxicity through NMDA receptors	No improvement in chorea symptoms, decline in memory
Strategies targeted at specific HD processes[4]	Minocycline Miraxion	Caspase inhibitors	Inhibit caspase activation, anti-apoptosis	N/D[3]
	Co-enzyme Q10, remacemide Creatine	Mitochondrial enhancers	Generate energy and maintain cell viability	N/D
	Memantine	Glutamate receptor blocker	Inhibit excitotoxicity	N/D
	Congo red Intrabodies	Aggregate inhibitor	Inhibit the formation of aggregates	N/D
	Sodium butyrate	HDAC inhibition	Increase transcription	N/D
	Antisense, RNAi	Gene and protein silencing	Decrease mutant protein	N/D

Pharmacology approaches	Drugs used	Mechanism of action	Target	Side-effects
Reparative strategies	Primary cells, stem cells, human fetal striatal tissues	Transplantation repair	Replacing dying striatal neurons	No changes or modest benefits

[1]Rego & Almeida, 2005; Handley *et al.,* 2006; Bonelli & Hofmann, 2004.
[2]Drugs that were used in human clinical trials.
[3]Not determined in human clinical trials.

treatments include typical neuroleptics and atypical neuroleptics. Typical neuroleptic drugs that are occasionally used in HD patients include the dopamine-depleting agent tetrabenazine and the antipsychotics fluphenzine, haloperidol and pimozide. Patients on these medications have less chorea but have motor dysfunction including impairment of gait, speech and swallowing may be exacerbated and dystonia may be worsened. These negative aspects of drug treatment, in addition to the common side effects of these drugs such as sedation, insomnia, parkinsonism, depression and akathisia, limit their clinical use (Bonelli & Hofmann, 2004). Psychiatric symptoms are often treated with selective serotonin reuptake inhibitors (SSRI), for depression, anxiety disorders and obsessive/compulsive symptoms in HD. In other cases, patients receive typical antidepressants such as haloperidol. Drugs that enhance mitochondrial metabolism (coenzyme Q_{10}, remacemide, creatine), anti-inflammatory agents that may have antiapoptotic properties (minocycline) and aggregate inhibitors (Congo red) all have been proposed to be promising therapies for HD (Handley *et al.,* 2006). However, conflicting findings of these reagents in animal models of HD and incomplete understanding of their pharmacological mechanisms prevent their use in human clinical trials (Table 1-1). Therapies currently available for different stages of HD patients can only temporarily ease symptoms of chorea at the expense of worsening functional tasks; these treatments do not slow the progression of the disease (Handley *et al.,* 2006). Reducing symptoms, decreasing disability and improving quality of life are the goals of managing HD. Achieving these goals requires an understanding and appreciation of how this genetic disorder developed at cellular and molecular levels (Rego & Almeida, 2005).

1.2 Function of Wild-Type Huntingtin

Expression of the HD gene

Despite the very specific pattern of neurodegeneration observed in HD, wild-type huntingtin and mutant huntingtin are both ubiquitously expressed, with the highest levels of huntingtin protein being found in CNS neurons and the testes of humans and rodents (Trottier *et al.,* 1995; Sharp *et al.,* 1995; Fusco *et al.,* 1999). The function(s) of normal huntingtin protein are not completely understood due to its large size and lack of sequence similarity to other proteins of known function (Bhide *et al.,* 1996; Hackam *et al.,* 1998; Martindale *et al.,* 1998). An *HD* homolog is present in all vertebrates and recent data indicate that members of the basal chordates also express a *HD* homolog suggesting an ancient history and conservation of this protein after the divergence of the chordates from other species (Gissi *et al.,* 2006). Huntingtin is present in the nucleus, cell body, dendrites and nerve terminals of neurons. Subcellular fractionation and immuno-localization studies suggest that huntingtin is associated with the Golgi apparatus, endoplasmic reticulum and mitochondria and plays a role in vesicle trafficking, clathrin-mediated endocytosis, neuronal transport, postsynaptic signaling and regulation of apoptosis (Trottier *et al.,* 1995).

Huntingtin knock-out mouse models

The idea that huntingtin has a specific function during development has been supported by studies on inactivation of the mouse *huntingtin (Hdh)* gene using a knock-out strategy where the *Hdh* gene is disrupted by null mutation (Duyao *et al.,* 1995; Nasir *et al.,* 1995; Zeitlin *et al.,* 1995). In all cases, nullizygous mouse embryos die at

approximately embryonic day 7.5, indicating an important role of huntingtin protein in embryogenesis. Two different heterozygous knock-out models display no neurologic phenotype (Duyao *et al.,* 1995; Zeitlin *et al.,* 1995), suggesting that one copy of normal huntingtin is sufficient to support early development. This observation is consistent with a human study in which a woman carrying a balanced translocation with a breakpoint between exon 40 and 41 of the *HD* gene expressed one copy of a normal *HD* gene but showed normal phenotype (Ambrose *et al.,* 1994). These studies suggest that the dominant feature of HD is not due to the inactivation of the normal *HD* allele. Conditional knockout of the *HD* gene using the Cre/*loxP* site-specific recombination strategy has shown that loss of expression of huntingtin protein in the brain and testis at embryonic day 15 and postnatal day 5 results in a progressive degenerative neuronal phenotype and sterility, indicating that huntingtin is required for the development of young embryos and the maturation and maintenance of the postnatal brain (Dragatsis *et al.,* 2000). Information from knock-out models argue against the possibility that the loss of the wild-type *HD* allele is the primary cause of HD and that low levels of wild-type huntingtin may influence disease progression.

Proteolytic cleavage of huntingtin protein

Huntingtin contains three consensus sites for cellular proteases. These cleavage sites are located at amino acid 548, 552 and 586 catalyzed by caspase 3 (Wellington *et al.,* 1998), caspase 2 (Hermel *et al.,* 2004) and caspase 6 (Graham *et al.,* 2006), respectively. Cleavage generates different fragments of huntingtin and the N-terminal accumulates and is ubiquinated in the striatum compared to those in the cortex (Mende-

Mueller *et al.*, 2001). The rodent striatum is the structure that has equivalent functions to the caudate and putamen in the human brain. Various sizes of N-terminal fragments and full-length wild-type huntingtin are present in the nucleus although the cleaved N-terminus and wild-type huntingtin protein lack a typical nuclear localization signal (NLS) (Hoogeveen *et al.*, 1993). The presence of nuclear export signal (NES) at the carboxy-terminus of huntingtin may explain a higher level of amino-terminal fragments than full-length protein in the nucleus (Hilditch-Maguire *et al.*, 2000; Tao & Tartakoff, 2001). The mechanisms whereby wild-type huntingtin is translocated into the nucleus are not clearly understood and it is suggested that it is associated with nuclear transport complexes that contain proteins having NLS (Takano & Gusella, 2002).

1.3 Animal Models of HD

Early HD models

Before the *HD* gene was discovered, it was thought that excitotoxicity and impaired mitochondrial function in the caudate and putamen were the cause of the disease. This hypothesis was based on observations that injection into the rodent striatum with excitatory amino acids preferentially caused cell death of the same type of neurons that are selectively lost in HD patients. Intrastriatal injection of the N-methyl-D-aspartic acid (NMDA) receptor agonist quinolinic acid (QA) in rats and non-human primates results in selective loss of gamma-aminobutyric acid producing (GABAergic) projection medium spiny neurons (MSN) and preservation of large aspiny interneurons such as those containing acetylcholinesterase or nitric oxide synthase (NOS), neuropeptide Y and somatostatin (Ferrante *et al.*, 1985; Beal *et al.*, 1986; Hantraye *et al.*, 1990). Systemic

injection of mitochondrial toxins such as malonic acid or 3-nitropropionic acid (3-NP) also causes chronic selective degeneration of striatal MSNs, which can be attenuated by treatment with NMDA receptor antagonists (Beal *et al.,* 1993; Greene *et al.,* 1993), suggesting that mitochondrial dysfunction in HD is a part of NMDA receptor-mediated excitotoxicity signaling in striatal neurons. These animal models of HD recapitulate selective striatal cell death and some behavioral features seen in HD patients, but they can not explain the fact that grade 0 HD patients develop HD symptoms without striatal neurodegeneration. In addition, the distribution of the NMDA receptors in the brain does not correspond to the areas of the brain most affected with HD (Luthi-Carter *et al.,* 2003). Therefore, these models only represent a late event that occurs in HD and excitotoxicity and mitochondrial dysfunction are likely secondary effects that follow early neuronal dysfunction in HD.

Genetic models of HD

Many genetic models of HD have been established. The models include genetic manipulation of cells from various sources and transgenic organisms including *Drosophila* (Agrawal *et al.,* 2005; Marsh & Thompson, 2006), *Caenorhabditis elegans* (Parker *et al.,* 2004), mice (Mangianni *et al.,* 1996; Hodgson *et al.,* 1999; Schilling *et al.,* 1999; Reddy *et al.,* 1998; Wheeler *et al.,* 2000; Shelbourne *et al.,* 1999; Lin *et al.,* 2001), and rats (Nguyen *et al.,* 2006). These models have greatly contributed to the study of different stages of the disease and have been most useful in the study of early stages of the disease that precede, and may be independent from, cell death.

HD is an autosomal dominant disease and the major aspects of the disease are caused by a gain of function of the mutant protein although a loss of 50% of the amount of wild-type huntingtin protein in some neurons, and undefined genetic and environment factors contribute to a lesser extent to HD onset and progression (Rosenblatt *et al.*, 2001). The gain of function(s) in HD can be specifically examined in transgenic mouse models of the disease where the mice have a copy of either a part or the entire human mutant *HD* gene with an expanded CAG repeat in exon 1 and two normal copies of the endogenous mouse *HD* gene. Many transgenic models have been established and they differ in the location of the site of insertion, the promoter used for driving the transgene expression and the size of the huntingtin gene being inserted (Table 1-2). The full-length transgenic models include the full-length human *huntingtin* gene in yeast artificial chromosome (YAC) driven by its own promoter with 128Q, 72Q, 46Q or 18Q (YAC72) (Hodgson *et al.*, 1999; Zeron *et al.*, 2002; 2004; Graham *et al.*, 2006; Shehadeh *et al.*, 2006; Weydt *et al.*, 2006; Metzler *et al.*, 2007) and the full-length human huntingtin transgene driven by the CMV promoter with 89Q and 48Q (Reddy *et al.*, 1998). Although the full-length transgenic model YAC72 displays the striatal specific neurodegeneration at 12 months (Hodgson *et al.*, 1999), they do not have behavioral abnormalities and appearance of neuronal intranuclear inclusions (NII) until 7 months and 11 months of age, respectively, prior to cell death, reinforcing the idea that neuronal dysfunction is a direct correlation to behavioral abnormalities. Since different N-terminal fragments of mutant huntingtin are found in the human brain (Davies *et al.*, 1997), different truncated transgenic models

Table 1-2. Transgenic and knock-in mouse models of HD[1].

Models	Promoter used/length of polyQ	Onset of Rotarod impairment	Clasping	Other Symptoms	Appearance of NII	Cell loss and brain atrophy	Life span
Transgenic models[2]	Human promoter, YAC full-length gene with either 72Q or 46Q	N/D[4]	YAC72Q, onset by 3 months	Hyperactive, circling, gait ataxia by 9 months	N-terminal antibody specific NII in striatum by 12 months	Cell loss in the striatum by 12 months	> 1 year
	CMV promoter, full-length gene with 89Q	N/D	4 months	Hyperactive circling, end-stage hypoactive	Few inclusion throughout brain by	20% cell loss in some animals	2-3 years
	Mouse prion promoter, N-terminal 171 aa with 82Q	8-12 weeks	5 months	Tremor, abnormal gait, hypokinesis	Striatum, cortex, hippocampus, amygdale, diffused NII by 6 months	Degeneration in the striatum	5-6 months
	Human promoter, exon 1, R6/2 line, 140-150Q	5 weeks	8 weeks	Tremor, abnormal gait, weight loss, learning deficits, hypokinesis, diabetes	First detected by 3.5 weeks NII throughout brain, fewer in dendritic spines	No neurodegeneration, frontal cortex, dorsal striatum and cerebellar cell loss at late stage, brain atrophy	12-15 weeks
	Human promoter, exon 1, R6/1 line, 110-115Q	15-16 weeks	20-30 weeks	Tremor, gait disturbances, weight loss, learning deficits	First appear by 8 weeks, NII throughout brain	No neurodegeneration, brain atrophy	30 weeks up to 1 year
	Tet-on/off promoter, exon 1, 94Q	4 weeks	28 weeks	Mild tremor, jerky motion by 20 weeks, hypoactive by 36 weeks	First appear at 18 weeks, aggregate staining in gene-on mice in the striatum and cortex	No report on neurodegeneration, brain atrophy and progressive striatal atrophy	32 to 40 weeks

Models	Promoter used/length of polyQ	Onset of rotarod impairment	Clasping	Other Symptoms	Appearance of NII	Cell loss and brain atrophy	Life span
Knock-in models[3]	Endogenous mouse HD gene promoter (Hdh) knock-in model, 111Q, 92Q	None	None	None	First appear at 9-11 months, CALB-positive striatal neurons, cortex, olfactory tubercle	None	2-3 years
	Hdh promoter, 150Q	40 weeks	Appear at 40-50 weeks	Clasping, gait deficits at 25 weeks	First appear at 12-13 months, Striatum, nuclear accumbens, cortical layers III and IV	None	2-3 years

[1]Adapted from Rubinsztain, 2002; Meade *et al.*, 2002.
[2]Hodgson *et al.*, 1999; Schilling *et al.*, 1999; Reddy *et al.*, 1998, 1999; Mangianni *et al.*, 1996.
[3]Wheeler *et al.*, 2000; Shelbourne *et al.*, 1999; Lin *et al.*, 2001.
[4]Not determined.

containing different N-terminal fragments have been established. The R6 lines contain exon 1 of the human *HD* gene under the control of the human HD promoter (Mangiarini *et al.,* 1996). The human transgene is expressed ubiquitously but at levels that are lower than the levels of endogenous mouse huntingtin and the two lines carry the CAG repeat expansion of encoding the first 89 amino acids of human huntingtin with either ~115 polyglutamines (N89-115Q in R6/1) or ~150 polyglutamines (N89-150Q in R6/2 mice). Both R6 lines develop the same neurological phenotypes with onset of overt motor dysfunction at approximately 8 weeks in R6/2 hemizygotes, 16 to 20 weeks in R6/1 hemizygotes (Mangiarini *et al.,* 1996). The mouse line developed by Schilling *et al.* (1999) expresses the N-terminal 171 amino acid mouse huntingtin transgene with 82Q, 44Q or 18Q driven by the mouse *prion* gene promoter (N171-82Q). The N171-82Q mice develop a phenotype starting at 2-3 months of age, depending on the expression level of the transgene. Due to unstable transgene expression, only 1% of neurons develop intranuclear inclusions. Another truncated model of HD contains exon 1 of human huntingtin with 94Q driven by Tet-on/off promoter, which shows a reversible HD phenotype (Yamamoto *et al.,* 2000). All of these transgenic mice show one or more abnormal motor behaviors including hindlimb clasping following tail suspension, abnormal gait, hyper- or hypoactivity and poor rotarod performance. The details of the different promoter and constructs used, phenotypes, brain pathology and life span are presented in Table 1-2. The mouse models that express a full-length copy of *HD* gene, unlike truncated transgenic models, are highly useful for examining the post-translational modifications and proteolytic cleavage during the pathogenesis of HD. However, these mice take up to 1.5 years to develop HD-like symptoms (Hodgson *et al.,* 1999) and,

therefore, have limited practical use for experimentation and testing potential therapeutics. The truncated models, on the other hand, can not be used for studying proteolytic cleavage, but the relatively fast onset of HD-like symptoms makes them practical and inexpensive to use. There seems to be a stronger correlation between age of onset and the development of HD phenotypes in truncated models than in full-length models, suggesting that the truncated model may model important aspects of the human condition.

The R6/1 and R6/2 models were used in this study (Mangiarini *et al.,* 1996). These mice express the exon 1 of human huntingtin transgene under the control of the human huntingtin promoter with 115Q (R6/1) and 150Q (R6/2). The levels of transgene expression are ~31% and 75% of the levels of endogenous huntingtin in R6/1 and R6/2 mice, respectively. The onset and the rate of progression of HD-like symptoms like tremor, abnormal gait, weight loss, learning deficits, hypokinesia are inversely correlated with the length of CAG repeat within the transgene in each line (Table 1-2), as is observed in humans (Duyao *et al.,* 1993). Intranuclear inclusions widely occur in the brains of R6 mice but show high density in the cortex and the striatum and they appear to be ubiquinated (Davies *et al.,* 1997), similar to inclusions seen in the postmortem HD brains (DiFiglia *et al.,* 1997). Due to their close resemblance to the human condition and relative faster onset compared to full-length transgenic models, they are the most widely used models for understanding the earliest gain of function of the N-terminus of mutant huntingtin prior to cell death as well as for *in vivo* testing of therapeutic agents (Li *et al.,* 2005).

Knock-in HD mouse models have an extended CAG repeat inserted into the mouse huntingtin gene (*Hdh*). Mice that are homozygous or heterozygous for the mutation can be raised and studied. Because knock-in HD mice carry the mutation in an appropriate genomic and protein context, they are the most faithful genetic models for the human condition (Levine *et al.*, 1999; Shelbourne *et al.*, 1999; Wheeler *et al.*, 1999; Lin *et al.*, 2001). However, knock-in mice develop behavioral abnormalities very slowly and subtly compared to transgenic models with the same length of polyQ (Shelbourne *et al.*, 1999). Several knock-in models have been generated with polyQ lengths ranging from 50 to 150Q. The only clear indication of the development of a progressive neurological phenotype has been reported in the 150Q line, which showed hind-limb clasping, impaired rotarod ability and gait disturbances at 40-50 weeks (Lin *et al.*, 2001). Knock-in mice have a mixed effect from gain of function of the mutant allele and loss of function of the normal allele, studying transgenic mice gives an advantage of only examining the gain of function of the mutant allele.

One distinct aspect of all the genetic models above is that there is very little cell loss and no clear neurodegeneration even at the late stage of HD (Mangiarini *et al.*, 1996; Schilling *et al.*, 1999; Bjorkqvist *et al.*, 2005; Smith *et al.*, 2006), providing further evidence that neurodegeneration is a late event during the progression of HD and not directly causal to the development of symptoms.

1.4 Aggregates in the Neuropathogensis of HD

NIIs are a hallmark of HD and are present in brain tissue of HD patients (DiFiglia *et al.*, 1997; Gutekunst *et al.*, 1999), in transgenic mouse models (Davies *et al.*, 1997;

Hodgeson *et al.*, 1999; Schilling *et al.*, 1999), and in cell culture models of HD (Wang *et al.*, 1999; Jana *et al.*, 2000; Zemskov & Nukina, 2003). The aggregates are immunoreactive to antisera raised against the N-terminus of huntingtin, but not to internal or C-terminal epitopes, as well as the anti-ubiquitin antibody suggesting that aggregates contain ubiquinated N-terminal huntingtin. The immunoreactive NIIs are not present in wild-type animals and normal human brains (DiFiglia *et al.*, 1997). The cleaved N-terminus of mutant huntingtin specifically promotes aggregate formation. This is consistent with studies showing that the proteolytic cleavage of huntingtin liberates the amino terminus of both the wild-type and mutant form of the protein but the mutant form collects in the nucleus, whereas the N-terminus of wild-type huntingtin is detectable as a diffuse protein in the cytoplasm (Hoogeveen *et al.*, 1993).

Mutant huntingtin protein is capable of forming abnormal protein-protein interactions (Harjes & Wanker, 2003). It appears that the polyQ region can form a "polar zipper" structure where antiparallel β-strands of polyQ are linked together by hydrogen bonds between the main chain amides (Perutz *et al.*, 1995). The polar zipper hypothesis has been supported by *in vitro* studies using purified glutathione *S*-transferase (GST)-HD exon 1 fusion proteins (Hollenbach *et al.*, 1999; Scherzinger *et al.*, 1999). The formation of SDS-insoluble huntingtin aggregates, similarly to β-amyloid plaques found in Alzheimer's Disease (Harper & Lansbury, 1997) and α-synuclein Lewy bodies in Parkinson's Disease (Wood *et al.*, 1999), occur by a nucleation-dependent polymerization mechanism (Scherzinger *et al.*, 1999). This means that the formation of the aggregate in the nucleus is a rate-limiting step and is dependent on protein concentration, and in the HD case, on the length of polyQ (Hollenbach *et al.*, 1999;

Scherzinger *et al.,* 1999; Gutekunst *et al.,* 1999). According to Perutz's model, at specific concentrations and polyQ length, soluble proteins or protein fragments change from a random coil structure into a hydrogen-bonded hairpin, which form dimers, trimers and longer oligomers. The hairpin structure slowly forms a nucleus of structured oligomers in an intermediate structure, which subsequently increases in molecular weight via the recruitment of more fragments or interacting proteins and becomes an ordered fibrillar structure, or aggregate (Perutz *et al.,* 1995). Ultimately, aggregates reach a size that, with appropriate staining, can be viewed by histological means.

It is still controversial whether NIIs are pathologic, coincidental or neuroprotective in HD (Sisodia, 1998; Yu *et al.,* 2002; Bates, 2003; Shastry, 2003; Arrasate *et al.,* 2004). One controversy arises from the fact that neurons with inclusions do not correspond to the neurons that show the most prominent neuronal dysfunction. In R6/2 mice, NIIs increase in size and prevalence more rapidly in the cortex than in the striatum (Meade *et al.,* 2002). However, reduced mRNA level of cannabinoid receptor type 1 (CB1) was found in the striatum and very few isolated cortical neurons despite the fact that the CB1 mRNA are expressed in neurons throughout the cortex and the striatum (Denovan-Wright & Robertson, 2000; McCaw *et al.,* 2004). In the striatum, NIIs are larger and more frequent in large interneurons, which are spared in HD, compared to medium spiny projection neurons, which are selectively affected in HD (Meade *et al.,* 2002). In post-mortem HD brains, the cerebral cortex has the highest number of aggregates whereas the aggregates in the caudate nucleus are comparatively rare (DiFiglia *et al.,* 1997; Gutekunst *et al.,* 1999). A second controversy stems from whether NIIs are functionally correlated to neurodegeneration. Several studies have argued

against a direct association between NIIs and neurodegeneration (Saudou *et al.,* 1998; Arrasate *et al.,* 2004; Schaffar *et al.,* 2004; Slow *et al.,* 2005). The formation of NIIs found in a cell culture model of HD does not contribute to cell toxicity (Saudou *et al.,* 1998). The full-length transgenic mice YAC72 do not show any detectable aggregates despite behavior abnormality and striatal degeneration at 12 months of age (Hodgson *et al.,* 1999). The shortstop mice containing exon 1 and 2 of human huntingtin transgene do not develop behavioral abnormalities and neurodegeneration despite widespread neuronal inclusions in the brain (Slow *et al.,* 2005). Striatal neurons die without the formation of NIIs but the presence of NIIs predicts the improved survival of neurons in a cell culture model of HD (Arrasate *et al.,* 2004). These studies suggest that the formation of NII does not contribute to neurodegeneration and vice versa. A third controversy comes from studies that both blocking and promoting the formation of inclusions appear to be beneficial to ameliorate HD symptoms. Azo-dye Congo red binds preferentially to β-sheets containing amyloid fibrils, inhibits polyQ oligomerization and promotes the clearance of expanded polyQ repeats *in vitro* (Heiser *et al.,* 2000; Smith *et al.,* 2001; Poirier *et al.,* 2002). Chronic treatment of R6/2 mice with Congo red appears to clear aggregates from the brain and improve weight loss and motor function after the onset of symptoms at 8 weeks and extend the lifespan (Sanchez *et al.,* 2003). However, a similar study suggests that systematic infusion of Congo red does not improve motor, behavioral deficits, weight loss and cognitive function in R6/2 mice (Wood *et al.,* 2007). The opposing observations using Congo red in the same mouse model indicate that whether the clearance of aggregate by Congo red contributes to improved neuronal function remains uncertain. Importantly, since Congo red can not pass the blood brain barrier and

it is difficult to see how intranuclear aggregates in the brain are disrupted by Congo red unless the drug gets into the brain. On the other hand, promoting inclusion formation in cellular models of HD prevents huntingtin-mediated proteasome dysfunction and lessens cell pathology (Bodner *et al.*, 2006), suggesting that inclusions may be a means for cells to remove the toxic form of mutant huntingtin and survive longer.

The controversies regarding the role of aggregates during HD pathogenesis is associated with a key question: What form of mutant huntingtin is most toxic? All data from cells and animal models of HD rely on the expression of soluble monomeric forms of huntingtin with extended polyQ as the precursor of aggregate formation. Following the expression of the transgene proteins in transgenic mice or following transfection of huntingtin constructs in cells, toxicity could come from the monomer, misfolded monomer, intermediate aggregates or some form of mature aggregates. All these states are present and they could directly cause neuronal dysfunction prior to the manifestation of behavioral abnormalities and the detectable NIIs. *In vivo* studies tend to rely on the immunoreactivity of the N-terminal huntingtin antibody EM48 or anti-ubiquitin antibody for the detection of NIIs without necessarily linking different forms of mutant huntingtin during the aggregation process with the neuronal dysfunction or neuronal death. Moreover, there is evidence that human huntingtin-specific antibodies are highly specific to different forms of the protein (Miller *et al.*, 2005; Wolfgang *et al.*, 2005), such that measurement of the presence or absence of human huntingtin in different studies presented in the published literature may not represent an accurate picture of the states of the disease in relation to the presence of the protein, the form of the protein or the subcellular distribution of the protein. On the other hand, terminal transferase dUTP nick

end labeling (TUNEL) is usually employed as a means to quantify cell death in most of papers on HD but this technique cannot be used to quantify cells that are in the process of dying from those that are not functioning properly but will survive. Using siRNA molecules for lowering the synthesis of mutant huntingtin *in vivo* appears to improve the HD-like symptoms and reverse the decreased DARPP32 and preproenkephalin mRNAs in HD transgenic mice (Harper *et al.,* 2005; Rodriguez-Lebron *et al.,* 2005). Using a Tet-on/off system, Yamamoto *et al* (2000) provided *in vivo* evidence that stopping synthesis of mutant huntingtin in HD94 mice controlled by a Tet-on/off promoter for a period of time results in a reversal of hind limb clasping phenotype and recovery of dopamine D1 receptor levels. These data suggest that soluble huntingtin causes neuronal dysfunction and ultimately leads to behavioral abnormalities in HD. It has been proposed that aggregate formation in neurons represents a coping mechanism in cells. Aggregrate formation would reduce the concentration of toxic, soluble mutant huntingtin when mutant huntingtin reached a specific concentration in neurons (Arrasate *et al.,* 2004). Transient expression of various lengths of mutant huntingtin construct does not show NIIs but altered cell function, such as aberrant protein-protein interactions (Li *et al.,* 1995; Wanker *et al.,* 1997; Kahlem *et al.,* 1998; Sittler *et al.,* 1998; Boutell *et al.,* 1999; Borrell-Pages *et al.,* 2006), altered gene expression (Boutell *et al.,* 1999; McCampbell *et al.,* 2000; Shimohata *et al.,* 2000; Steffan *et al.,* 2000; Nucifora *et al.,* 2001; Dunah *et al.,* 2002; Li *et al.,* 2002; van Roon-Mom *et al.,* 2002; Zhai *et al.,* 2005; Cui *et al.,* 2006; Kazantsev & Hersch, 2007), changes in vesicular trafficking (Hilditch-Maguire *et al.,* 2000; Trettel *et al.,* 2000; Trushina *et al.,* 2006; Tagawa *et al.,* 2007), suggesting these processes precede the formation of NIIs. Taken together, it appears that soluble N-

terminal huntingtin with an extended polyQ tract within the nucleus may initiate a cascade of events that lead to neuronal dysfunction. Following changes in cell physiology in response to the initial changes induced by mutant huntingtin throughout the brain, cognitive, psychiatric and motor impairment develop followed by selective neurodegeration. The intracellular changes that have been studied are summarized in figure 1-1.

1.5 Early Changes in Specific Gene Expression in HD

The N-terminal fragment of mutant huntingtin readily enters the nucleus. This observation leads to studies of gene expression in the striatum using microarrays and gene-specific surveys (Cha *et al.,* 1998; Cha *et al.,* 1999; Denovan-Wright & Robertson, 2000; Luthi-Carter *et al.,* 2000; 2002; Chan *et al.,* 2002; Hebb *et al.,* 2004; McCaw *et al.,* 2004; Gomez *et al.,* 2006; Desplats *et al.,* 2006). Among ~6000 mRNAs surveyed in the striatum of R6/2 mice, Luthi-Carter *et al.* (2000) determined that only 1 to 2% of genes had differences in relative expression, among which were genes involved in neurotransmitter signaling and second messenger systems. This early study examined changes in gene expression in 6 week-old R6/2 mice which already have detectable NIIs and rotarod disabilities (Mangiarini *et al.,* 1996; Luesse *et al.,* 2001; Meade *et al.,* 2002). Genes that are responsive to inflammatory mediators were also increased at this time point but those involved in mitochondrial functions, caspase activation and apoptosis related signaling did not change until a time point (12 weeks) when the R6/2 mice are

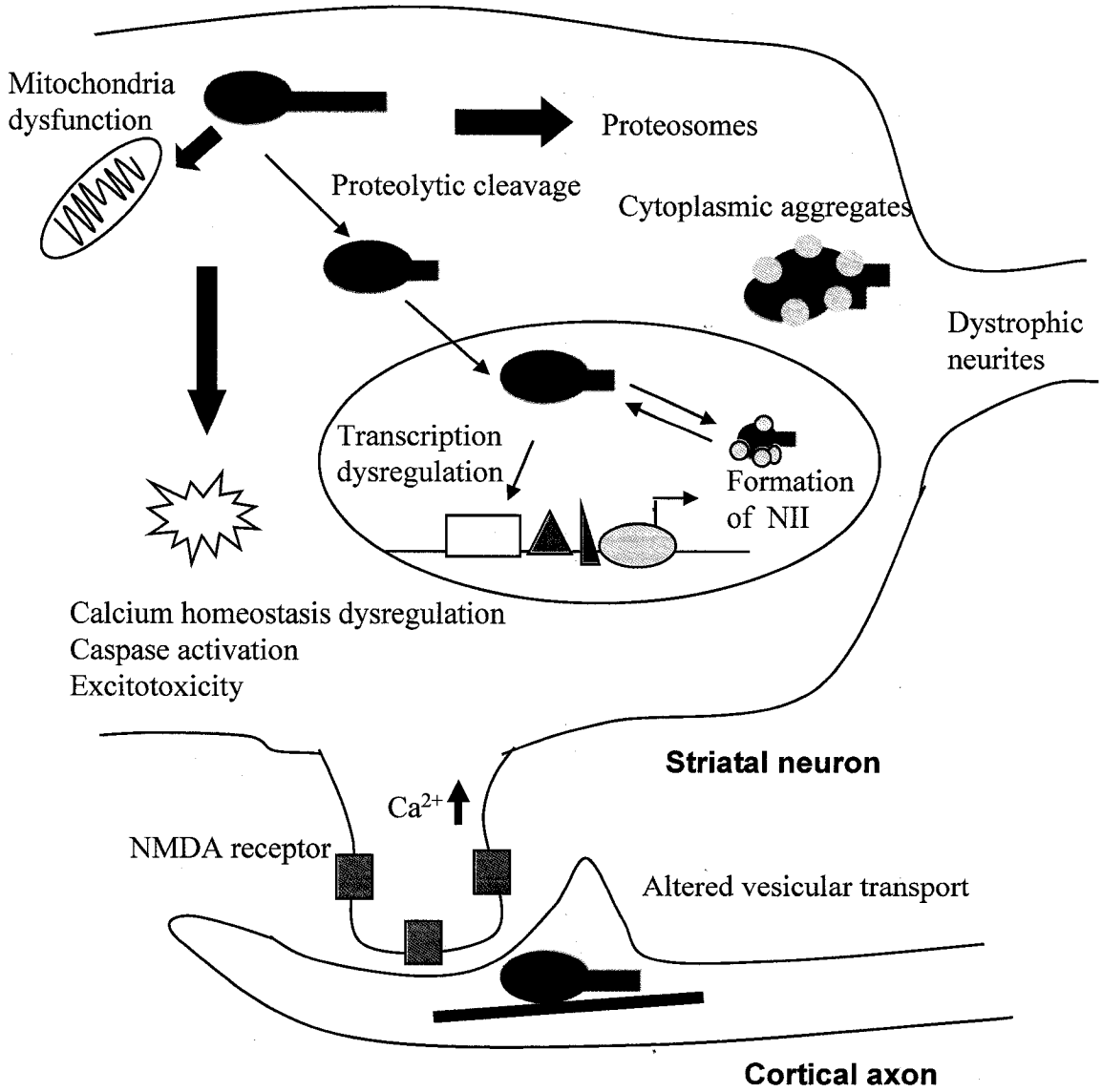

Figure 1-1. Intracellular changes that have been demonstrated to occur in transgenic mice and cells. Full-length mutant huntingtin is cleaved by proteases in the cytoplasm, leading to the formation of cytoplasmic and neuritic aggregates. Cleaved N-terminus of mutant huntingtin translocates to the nucleus where it affects transcription and forms NIIs through abnormal protein-protein interactions. Mutant huntingtin also affects mitochondria function, calcium homeostasis, caspase activity which all lead to excitotoxcity of striatal neuron. Excitotoxicity can be mediated by NMDA receptors, which leads to Ca^{2+} influx. Mutant huntingtin alters axonal transport thus that less trophic supports such as BDNF can be obtained from the cortical neurons. (NIIs, neuronal intranuclear inclusions) (Borrel-Pages *et al.,* 2006 and Li & Li, 2006 and references therein)

severely disabled and close to death. This supports the notion that excitotoxic pathways altered by HD are a late event and maybe secondary to the initial alteration of mRNAs involved in second messenger systems and that cell death and apoptosis pathways are not altered due to absence of striatal neurodegeneration in these mice. Genes whose expression is affected in 6 week-old R6/2 are also affected in 4 month-old N171-82Q transgenic mice; at this time point, the N171-82Q mice also show behavioral abnormalities. The mRNA changes in the cerebellum in 12 month-old N171-82Q mice have been compared to transgenic mice containing the larger N-terminus of huntingtin protein HD46 (964 amino acids of the N-terminal human huntingtin protein with 46Q) and full-length transgenic model YAC72 mice (Chan *et al.,* 2002). It appeared mRNAs involved in signaling and neurotransmitter receptors do not change in mice expressing larger N-terminus or full-length fragment of mutant huntingtin protein (Chan *et al.,* 2002), supporting that altered gene expression governing second messenger and neurotransmitter receptor signaling is specific to the short N-terminal model of HD transgenic mice. This again reinforces the rationale that the N-terminal model is a better model to study the most early and prominent mRNA alterations.

HD, in fact, belongs to a family of neurodegenerative diseases caused by expansion of polyQ in different proteins. This family includes dentate-rubral and pallido-luysian atrophy (DRPLA), spinal and bulbar muscular atrophy (SBMA) and the spinocerebellar ataxia (SCAs) 1, 3, 6, 7, 17 (Helmlinger *et al.,* 2006; Riley & Orr, 2006). These polyQ diseases all show adult onset and progressive neurodegeneration and each possesses a unique pattern of neurodegeneration in different regions of the brain, suggesting that the common disturbances of these diseases are related to polyQ but the

unique disturbances may be related to polyQ in the context of specific proteins. Luthi-Carter *et al.* (2002b) found overlapping gene expression changes at fully symptomatic ages of mouse models of DRPLA, SCA7, SBMA and HD (N171-82Q and R6/2 transgenic mice), indicating that these changes are associated with long-term expression of polyQ-containing proteins that is unlikely to reflect a protein-context dependent effect. In other words, protein-context dependent changes in gene expression are directly associated with neuronal dysfunction and ultimately neurodegeneration in a specific population of neurons in each of these polyQ diseases.

Microarray data from grade 0 HD human brains, which do not have neurodegeneration, show that the altered mRNAs in HD display a regional pattern that parallels the known pattern of neurodegeneration: caudate > motor cortex > cerebellum (Hodge *et al.,* 2006), indicating that regional-specific neuronal dysfunction precedes neurodegeneration. These authors also observed that there is a similar group of genes affected in the cortex and the striatum, indicating the striatal neurons and cortical neurons share similar molecular mechanism of HD-induced neuronal dysfunction. Although many studies have focused on the striatum, changes in the cortex might not be excluded from the pathogenesis in HD.

All microarray studies have suggested that a specific set of striatal mRNA are decreased prior to NII formation and they are not associated with neuronal death. It remains to be determined whether changes of this group of genes reflect an immediate neuropathogenesis caused by mutant huntingtin and how these early changes lead to behavioral phenotypes before the abnormal aggregation is initiated.

1.6 Transcriptional Dysregulation in HD

Overwhelming evidence indicates that the behavioral phenotypes seen in mouse models of HD are caused by neuronal dysfunction. Decreased mRNAs of selective neurotransmitter receptors, including CB1, glutamate receptors (mGluR1 and mGluR3), dopamine D1 and dopamine D2 receptors, were found in R6 transgenic models prior to the onset of the behavior abnormalities (Cha *et al.,* 1998; Cha *et al.,* 1999; Denovan-Wright & Robertson, 2000). Decreased mRNA and proteins of signaling molecules such as dopamine responsive phosphoprotein 32 kDa (DARPP32), phosphodiesterase (PDE) 10A and PDE1B, preproenkephalin were found in R6 models, knock-in models and early grade autopsy tissues of HD (Augood *et al.,* 1996; Bibb *et al.,* 2000; Menalled *et al.,* 2000; Hebb *et al.,* 2004; Gomez *et al.,* 2006). These studies strongly suggest that the N-terminus of mutant huntingtin in the nucleus in R6 models affects transcription of these genes, which might be one of earliest molecular alterations directly caused by the mutant protein (Fig. 1-2). However, it remains largely unknown how the N-terminus of mutant huntingtin causes the levels of specific mRNAs to decrease while not affecting levels of other genes that are co-expressed in the same cells such as glutamic acid decarboxylase 65 and 67 (GAD65, GAD67) (Menalled *et al.,* 2000) and NMDA receptor type 1 (NMDA-R1) (Chen-Plotkin *et al.,* 2006).

In the nucleus, many huntingtin binding partners have been identified by yeast two hybrid, co-immunoprecipitation (Co-IP), and GST-pull down assays. These include

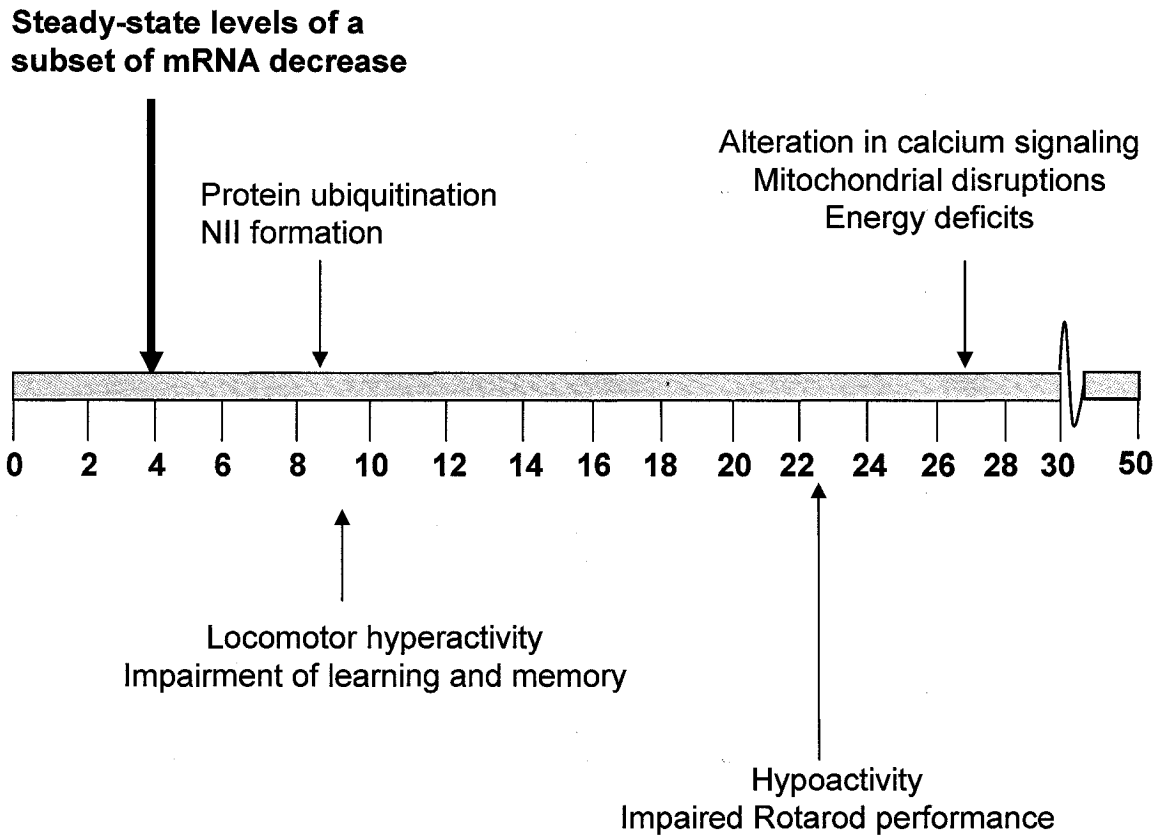

Figure 1-2. Illustration of the progression of HD in R6/1 transgenic mice. The light blue bar represents the life span R6/1 mice. Several key pathologic events that occur in R6/1 mice are illustrated above or under the bar. Their time of occurrence are indicated by arrows toward the bar. (Mangiarini *et al.*, 1996; Li *et al.*, 2005 and references therein)

cAMP response element binding protein (CREB) binding protein (CBP) (McCampbell *et al.*, 2000; Nucifora *et al.*, 2001; Shimohata *et al.*, 2000), specific protein 1 (Sp1) (Li *et al.*, 2002; Dunah *et al.*, 2002), TATA box binding protein (TBP) (van Roon-Mom *et al.*, 2002), p53 (Steffan *et al.*, 2000; Bae *et al.*, 2005), C-terminal binding protein (CtBP/p300), p300/CBP associated factor (P/CAF) (Chai *et al.*, 2001; Kegel *et al.*, 2002), nuclear co-repressor protein (NCoR) (Boutell *et al.*, 1999) and transcription association factor II130 (TAFII130) (Dunah *et al.*, 2002). However, it is not known how these ubiquitously expressed factors functionally cause decreased transcription of a specific set of mRNA in HD. Some mRNAs for transcription factor themselves are altered in the caudate nucleus of grade 0 HD human brain (Hodges *et al.*, 2006), implying that mutant huntingtin might have a cascade effect on transcription by decreasing expression levels of certain transcription factors that then further perturb regulation of gene expression.

Involvements of Sp1, CBP and basal transcription machinery in HD

Sp1 is a ubiquitously expressed transcriptional activator whose major function is to recruit the general transcription complex TFIID to DNA (Courey & Tjian, 1988). TFIID is a large multiprotein complex which contains TBP and multiple TBP-associated factors (TAFs) (Albright & Tjian, 2000). It has been shown that the N-terminal mutant huntingtin protein interacts with Sp1 in a polyQ-length dependent manner in the brains of R6/2 mice and human HD patients by *in vitro* binding and immunoprecipitation studies (Dunah *et al.*, 2002; Li *et al.*, 2002). Transiently expressed full-length mutant huntingtin decreases the promoter activity of the dopamine D2 receptor gene in primary striatal cells. Over-expression of Sp1 and TAFII130, one of components in TFIID, rescues the

repressed promoter activity and cell toxicity induced by mutant huntingtin (Dunah *et al.*, 2002). The soluble form of mutant huntingtin inhibits Sp1 binding to the promoter of nerve growth factor receptor (NGFR) thus suppressing NGFR transcriptional activity (Li *et al.*, 2002). Based on these observations, therefore, it is hypothesized that mutant huntingtin sequesters Sp1 from binding to its target promoter sites and decreases transcription. However, one important question that has not been addressed in these studies is how ubiquitously expressed Sp1 interacting with soluble mutant huntingtin causes transcriptional dysregulation of a subset of genes. Moreover, the role of Sp1 in mutant huntingtin-induced transcription dysregulation has been challenged by the finding that there is increased Sp1 expression and DNA binding activity in the brains of R6/2 mice and PC12 cell model of HD (Qiu *et al.*, 2006). Suppression of Sp1 expression by Sp1 siRNA in PC12 cells expressing mutant huntingtin ameliorates the cell toxicity. Treatment of mithramycin A, an antibiotic that selectively blocks Sp1 binding to GC rich region, abolishes the 3-NP induced cell toxicity in PC12 cells (Qiu *et al.*, 2006). The authors concluded that inhibition of Sp1 is neuroprotective. However, the 3-NP lesion model of HD is a model that only represents a pattern of striatal neurodegeneration, which is a late stage event during the progression of HD in animal models and HD patients thus not the underlying mechanism of HD (Beal *et al.*, 1993; Borlongan *et al.*, 1997; Brouillet *et al.*, 1999). Increased expression of Sp1 might be a compensatory event accompanying excitoxicity. Amelioration of cell toxicity by mithramycin treatment may not be directly associated with correction of Sp1 mediated transcriptional dysregulation but likely through a Sp1 independent mechanism. Therefore, the role of Sp1 in mutant huntingtin mediated transcriptional repression remains unclear.

Several polyQ disease proteins have compromised CRE-mediated transcription. CBP have been detected in aggregates of several polyQ-containing disease proteins including androgen receptor (SBMA disease protein) (McCampbell *et al.,* 2000), ataxin-3 (SCA3 causing protein) (Chai *et al.,* 2001) and atrophin 1 (DRPLA disease protein) (Nucifora *et al.,* 2001), implying a common transcriptional defect mediated by CBP in all three diseases. CBP has been found in mutant huntingtin-containing aggregate, both *in vivo* and *in vitro.* It appeared that the interaction between CBP and mutant huntingtin protein is mediated either through the polyQ-rich activation domain (Nucifora *et al.,* 2001) or the acetytransferase domain (Steffan *et al.,* 2000). Inactivation of CBP histone acetyltransferase activity by mutant huntingtin can lead to decreased histone acetylation. Since decreases in histone acetylation are associated with transcriptional silencing and this could conveniently explain transcriptional repression in HD, increasing histone acetylation by histone deaceylation (HDAC) inhibitor may provide a strategy for compensating for decreased transcription in HD. HDAC inhibitors suberoylanilide hydroxamic acid (SAHA) and sodium butyrate dramatically improve body weight and motor performance and extend the lifespan in R6/2 mice (Ferrante *et al.,* 2003; Hockly *et al.,* 2003). These drugs show neuroprotective effects in the PC12 inducible model, fruitfly model and *C. elegans* model of HD (Steffan *et al.,* 2001; Igarashi *et al.,* 2003; Bates *et al.,* 2006). However, it is intriguing how treatment with HDAC inhibitors, which, in theory, broadly increases histone acetyltransferase activity, would specifically increase transcription of some reduced mRNAs in HD.

Recently, using an *in vitro* transcription system with individually purified transcription factors TFIIA, TFIIB, TFIIE, TFIIF and affinity purified TFIID, TFIIH,

RNA polymerase II (RNA pol II), Zhai *et al.* (2006) showed that increasing amounts of TFIID, TFIIF and Sp1 can rescue mutant huntingtin mediated transcriptional repression of the dopamine D2 receptor gene. They also showed that increasing amounts of TFIIB and RNA pol II further decrease the mutant huntingtin-mediated transcriptional repression on the D2 promoter, suggesting that saturation of these two factors has negative effects on transcription. The authors did not comment on this observation. Human TFIIF is composed of two subunits RAP30 and RAP74 and association of these two subunits is required for normal function of TFIIF (Robert *et al.*, 1998). Anti-RAP30 antibody is able to co-immunoprecipitate mutant huntingtin in striatal extracts isolated from heterozygous knock-in HD mice and such interaction is present in COS7 cells co-transfected with RAP30 and mutant huntingtin. Over-expression of RAP30 in primary striatal neurons can rescue mutant huntingtin mediated repression of the D2 receptor promoter and prevent cell death. However, this study fails to address whether such interaction is specific between ubiquitously required RAP30 and mutant huntingtin and whether such interaction is present in non-affected genes in the striatum of HD transgenic models and HD patients.

Unresolved puzzles of transcription dysregulation in HD

Based on the information available regarding the expression of mutant huntingtin and the natural history of the disease, our working hypothesis is that the mutant huntingtin protein causes transcriptional dysregulation of a specific subset of genes early in HD progression and that this abnormal function of mutant huntingtin initiates a cascade of events that leads to progressive loss of function and ends in cell death of some

cells. While previous studies have demonstrated that mutant huntingtin interacts with transcription factors, these studies may represent experimental systems that allow interactions to occur even though such interactions may not occur *in vivo* because of low affinity or inter- or intracellular segregation of the proteins. None of the interactions between mutant huntingtin and individual ubiquitous proteins explain how mutant huntingtin causes reduction of transcription in a cell-, gene- and temporal-specific manner.

1.7 Objectives

Whatever the actual consequence of alteration of the regulation of any one gene or even all affected genes, HD is caused by mutant huntingtin. As such, our goal was to contribute to the understanding of the abnormal function of mutant huntingtin with respect to transcription. Specifically, we hoped to clarify the unresolved features of altered transcription in HD. Understanding the mode of transcription in these systems would help identify key mediators in mutant huntingtin-induced early molecular events that lead to neuronal dysfunction. In this study, we employed a systematic approach using one gene as a model to explore how the N-terminus of mutant huntingtin exerts transcriptional repression. The criteria for choosing the model gene were 1) this gene is highly expressed in the striatum, yet not confined in expression solely to the striatum, 2) expression of this gene is not normally regulated in response to neuronal activity, natural aging, or other pathogenic states, 3) there is evidence that the mRNA levels of this gene decreased relatively early in one HD animal model, 4) the gene is expressed in other places in the brain and body such that we could compare gene expression in various

tissues and in the presence of mutant huntingtin, and 5) the gene is an important signaling molecule and there is a body of literature on its normal function thus allowing us to link the mechanism of transcriptional dysregulation to general neuronal dysfunction. Phosphodiesterase (PDE) 10A was chosen for this study because it met several of the criteria. PDE10A is an enzyme that hydrolyzes second messengers, cyclic AMP and cyclic GMP (cGMP), regulating many biologic processes (Hebb & Harold, 2007; Xie *et al.*, 2006). PDE10A belongs to a large and diverse PDE family including 11 family members that differ in biochemical properties, tissue and cellular expression pattern and substrate specificities (Beavo, 1995; Soderling & Beavo, 2000). Among the family, PDE10A, PDE1B and PDE4 and PDE7B are highly expressed in the brain (Polli & Kincaid, 1992; Hebb *et al.*, 2004; Reyes-Irisarri *et al.*, 2005). The PDE10A and PDE1B mRNAs are decreased in several HD transgenic models and human HD patients (Luthi-Carter *et al.*, 2000; Chan *et al.*, 2002; Luthi-Carter *et al.*, 2002a; Hebb *et al.*, 2004; Desplats *et al.*, 2006; Hodges *et al.*, 2006). Understanding the mechanism whereby mutant huntingtin alters PDE10A gene expression in mice, cells and *in vitro* models of HD may provide a new strategy to understand the specificity of transcriptional dysregulation via mutant huntingtin.

To determine the mechanism of mutant huntingtin-induced transcriptional dysregulation, the specific experiments completed during the course of this study were designed to answer the following questions:

1. What is the spatial distribution, onset and rate of decline, and final steady-state mRNA levels of PDE10A?

2. What is the structure of the gene, mRNA and the control region(s) of PDE10A in the brain and in other tissues?
3. Are all PDE10A isoforms equally susceptible to the effects of mutant huntingtin?
4. Does the expression of mutant huntingtin alter the rate of transcription or the stability of mRNAs encoded by mutant huntingtin-affected genes?
5. What are the functional promoters of each of the genes that have altered transcription initiation and are there "mutant huntingtin-response elements" within the PDE10A promoters?
6. Does mutant huntingtin act within a neuron to directly affect transcription or does mutant huntingtin alter intracellular signaling that in turn alters gene expression?
7. Does mutant huntingtin affect transcription factor activity or chromatin structure or both?
8. Are changes in transcription factor activity due to a direct interaction of mutant huntingtin protein?
9. Can we identify protein factors that directly interact with mutant huntingtin and affect promoter activity?
10. Can we test the contribution of mutant huntingtin-interacting proteins or block the effects of mutant huntingtin on transcription?

Our goal was to define the aberrant function of mutant huntingtin with respect to the abnormal expression of one gene that may illustrate common mechanisms of mutant

huntingtin-induced transcriptional dysregulation. In addition to contributing to the understanding of HD, this work may also contribute to our understanding of coordinated neuron-specific gene expression.

CHAPTER 2

Materials and Methods

2.1 Animals

Wild-type (C57B/β/6J), R6/1 [B6CBA-Tg(HDexon1)61Gpb/2J] and R6/2 [B6CBA-Tg(HDexon1)62Gpb/1J] mice (Mangiarini *et al.*, 1996) were originally purchased from Jackson Laboratory (Bar harbor, ME, USA). The R6/1 and R6/2 transgenic lines were established and maintained by crossing hemizygous carrier R6/1 and R6/2 males with wild-type females. All protocols were in accordance with the guidelines detailed by the Canadian Council on Animal Care and approved by University Committee on Animal Care at Dalhousie University. Mice were genotyped at the time of weaning (3 weeks of age) and at the time of death using a piece of ear-punch tissue. All chemical reagents were from Fisher Scientific Canada unless otherwise specified. The tissue was digested in 100 µl lysis buffer [10 mM Tris-HCl, pH 8.0, 5 mM ethylenediaminetetraacetic acid (EDTA), pH 8.0, 50 mM sodium chloride (NaCl), 0.5% Tween 20 (v/v) and 20 mg/ml proteinase K (Roche Applied Science, IN, USA)] at 55°C for 4 hours (hrs). Twenty microliters of lysate was then neutralized with 180 µl of neutralization buffer from REDExtract-N-Amp Ready Mix for Blood kit (Sigma-Aldrich Canada, Oakville, ON) and 5 µl of final mixture was used as a template for polymerase chain reaction (PCR) following instructions from the same kit. PCR was performed using primers HD1 and HD-trans (Table 2-1) to amplify a region of the human HD transgene. To isolate tissue, mice were deeply anaesthetized using sodium pentobarbital (65 mg/kg). For isolating RNA, following decapitation, dissected striata and testes were rapidly frozen in liquid nitrogen and stored at -80°C. For *in situ* hybridization, brains were immediately stored at –80°C. For isolating nuclear fractions, striatal tissues were

Table 2-1. PCR primers and oligonucleotides.

Name	Source	Direction	Sequence
		RT-PCR	
P1	Exon 1[1]	Sense	5'-TGGAAAAATTATATGGTTTGACG-3'
P2	Exon 25	Antisense	5'-CCACGGAGTAGCCGACGTCTGAAC-3'
P3	Exon 1a	Sense	5'-ACATGGAAGATGGACCCTCTA-3'
P4	Exon 25	Antisense	5'-AGGATGAGGTATCTTCTGGAATAATC-3'
		qRT-PCR	
RT1	Intron 1a	Antisense	5'-TGATGGGCGGTCCCGAACGTCCCT-3'
RT2	Exon 5	Antisense	5'-GCCCGTGTCCAGGCGCTGCTCTATGTA G-3'
HPRT S	NM013556[2]	Sense	5'-GCTGGTGAAAAGGACCTCT-3'
HPRT AS	NM013556	Antisense	5'-CACAGGACTAGAACACCTGC-3'
		***In situ* hybridization**	
HD40	Exon14	Antisense	5'-GACCAATGTCAAAGTGGAATAGCTCGA TGTCCCGGC-3'
HD1	Exon 25	Antisense	5'-GAACATGTAGCATATACTCCAGACAAC AGATCATATGG-3'
HD88	Exon 1a	Antisense	5'-GGACGCTCAAGGGAGCTGCCTCTTGT-3'
		5'RLM-RACE	
GSP1	Exon 1a	Antisense	5'-GCCGCCAAAGAGTTCGGCCACC –3'
GSP2	Exon 1a	Antisense	5'-TTGAATCGCAGGCGAGAGGAAGAG -3'
GSP3	Exon 1	Antisense	5'-GCAGCTCAGCTCTTGGGTTTGGCATCA C-3'
GSP4	Exon 1	Antisense	5'- GGTCTTCCAGCTCAGCTCCCTCTGGTC A-3'
		Genotyping	
HD1	XM003405	Sense	5'AGGGCGTGTCAATCATGCTGG3'
HDtrans	XM003405	Antisense	5'GGACTTGAGGGACTCGAA3'

Name	Source	Direction	Sequence
PCR of the PDE10A2 promoter			
*Bgl*II-HD93	AY360383	Sense	5'AGATCTTGGTTGAGGGGAGTCGGCAAG 3'
*Hind*III-HD94	AY360383	Antisense	5'AAGCTTGCCGCCAAAGAGTTCGGCCACC3'
HD80	AY360383	Sense	5'AGTACAGTGGGCCTGAGCCTGGCCC3'
HD91	AY360383	Antisense	5' GAAAATCCGAGGAGTCCGCG 3'
BglII-HD95	AY360383	Sense	5'AGATCTTCATCTTCCTGGTACTTCTGGCCG 3'
*Bgl*II-HD96	AY360383	Sense	5'AGATCTACAAGAGGCAGCTCCCTTGAGCG TCC3'
*Hind*III-HD97	AY360383	Antisense	5'AAGCTTGTCCTCCTCCTCCGCCGCCGC3'
PCR of the GAD65 promoter			
mGAD65-P1	AB032757	Sense	5'GGTACCTCAGCTCTCACCCACTCCAAGA3'
mGAD65-P3	AB032757	Antisense	5'CTCGAGGTTCTGCTAGACTGGCGCTG3'

[1]Exon numbers as defined in Genbank Accession Number:AY360383.
[2]Genbank accession number.

dissected and put in a ice-cold petri dish temporarily until nuclear extraction. All efforts were made to minimize the number of animals used.

2.2 Total RNA and Genomic DNA Isolations

Total RNA isolation

Total RNA was isolated from frozen striata and testes of various ages of wild-type and R6 mice using Trizol™ reagent (Invitrogen, Burlington, ON). All buffers, reagents, glasswares and plasticwares were treated to be RNase-free as described in Sambrook *et al.* (2000). Striata dissected from a mouse (15~20 mg) or testes from a mouse (30 mg) was homogenized in 200 µl of Trizol using a motored pestle. Trizol reagent (800 µl) was added to the homogenate and mixed well. The mixture was incubated at room temperature for 5 minutes (min). Chloroform (0.2 ml) (Fisher Scientific, Mississauga, ON) was added to the homogenate and the homogenate was subjected to centrifugation at 12,000 x *g* at 4°C for 15 min. The RNA in the aqueous phase was removed to a clean microfuge tube and 500 µl of isopropyl alcohol (Fisher Scientific) was added. The mixture was inverted several times and incubated on ice for 10 min to precipitate the RNA. The mixture was centrifuged at 12,000 x *g* at 4°C for 10 min to obtain the RNA pellet. The pellet was washed once with 75% (v/v) ethanol and centrifuged at 7,500 x *g* at 4°C for 5 min. The RNA pellet was air dried for 10 min at room temperature and dissolved in RNase-free H_2O at 55°C for 5 min. The RNA was stored at -80°C.

Genomic DNA isolation

Genomic DNA was isolated following a standard protocol (Sambrook *et al.*, 2001). Striatal tissue from one mouse (15-20 mg) was incubated in 4 ml lysis buffer [20

mM Tris-HCl, 5 mM EDTA pH 8.0, 400 mM NaCl, 1% (w/v) SDS, 25 μg/ml RNase A/T1] with gentle shaking for 20 min at room temperature. After incubation, 45 μl of 0.5 M EDTA and 20 μl of 20 mg/ml Proteinase K were added and the mixture was allowed to gently shake overnight at 55°C. An equal volume of phenol:chloroform:isoamylalchol (25:24:1) (pH 8.0) (Invitrogen) was added to the lysate and the mixture was subjected to centrifugation at 2,500 x *g* for 5 min. An equal volume of isopropyl alcohol was added to the recovered aqueous phase and the solution was subjected to centrifugation at 12,000g for 15 min at 4°C. The DNA pellet was dissolved in 0.6 ml of TE buffer [10 mM Tris-HCl, 1 mM EDTA, pH 8.0] at 4°C overnight with shaking. The DNA was stored at -20°C. RNA and DNA concentration was determined by spectrophotometry at 260 nm and 280 nm (Sambrook *et al.,* 2001).

2.3 PCR and Plasmid Construction

Polymerase chain reaction

Polymerase chain reaction (PCR) was employed to obtain PCR fragments for cloning and *in vitro* transcription. Primers used in PCR are listed in Table 2-1. A typical PCR reaction was performed in a 20 μl reaction containing a final concentration of 1 × QIAGEN hot start polymerase buffer, 20% Q-solution, 500 μM dNTP (Fermentas, Burlington, ON, Canada), 0.5 μM the sense primer, 0.5 μM the antisense primer and 2 unites (U) of QIAGEN hot start polymerase (QIAGEN, Mississauga, ON, Canada). For amplifying the promoter regions of PDE10A and GAD65, 5 ng of genomic DNA was used in both PCR reactions. The PCR parameter started with incubation at 95°C for 15 min to activate Hotstart polymerase, followed by 35 cycles of denaturation at 95°C for 1

min, annealing at 58°C (PDE10A) or at 62°C (GAD65) for 2 min and extension at 72°C for 1 min, followed by a 10 min extension at 72°C.

Plasmid construction

PCR products were resolved in agarose gels in 0.5 × TBE buffer [44.5 mM Tris, 44.5 mM Boric acid, 1 mM EDTA and 0.25 μg/ml of ethidium bromide and visualized under ultraviolet (UV) illumination. PCR products were excised from the gel and gel-purified using GenElute Gel Extraction Kit as per the manufacturer's instructions (Sigma-Aldrich). Purified PCR products were ligated into pGEM-T vector using the pGEM-T TA cloning system I (Promega, Madison, WI, USA). Ligation reaction was incubated at 4°C overnight with a 3:1 ratio of insert to vector. The ligated DNA was then recovered from the ligation buffer following ethanol precipitation to remove salt and then resuspended in 5 μl of double-distilled H_2O (ddH_2O). One to five microliters of ligated DNA (~ 20-50 ng) was electroporated into DH10B™-T1^R electrocompetent cells (Invitrogen) according to a standard electrotransformation protocol in Sambrook *et al* (2000). Colonies were inoculated in 3 ml 2 × YT broth [1.6% (w/v) tryptone, 1% yeast extract (w/v), 0.5% NaCl (w/v)] overnight at 37°C. Purification of plasmid DNA was performed using the GenElute Plasmid Miniprep Kit (Sigma-Aldrich).

For constructing PDE-pGL3 and GAD65-pGL3 constructs, pGEM-T plasmids containing inserts of appropriate size were digested using *Bgl*II/*Hind*III (for PDE-PGL3) and *Sac*I/*Xho*I (for GAD65-pGL3) to release cohesive-end insert DNA . Cohesive-end inserts were then ligated with compatible cohesive-end pGL3 basic vector (Promega). Ligation, electrotransformation, inoculation and minipreps were the same as described above. The constructs containing > 1 kb insert DNA were commercially sequenced

(York University, ON, Canada). The constructs that contained < 1 kb insert DNA were sequenced using T7 Sequencing™ Kit (GE Healthcare Lifescience) following the manufacturer's protocol.

2.4 RT-PCR

Reverse transcription-PCR (RT-PCR) was used to amplify PDE10A splice variants from the mouse striatum and testis. One microgram of total RNA (10 µl volume, in RNase-free H_2O) and 0.1 µg of oligodeoxythymidine [primer ($p(dT)_{12-18}$)] (Invitrogen) were mixed and denatured at 95°C for 5 min and cool rapidly on ice. A mixture of 200 mM dNTP, 40 U of RNasin® Ribonuclease Inhibitor (Promega) and 5 U of reverse transcriptase PowerScript™ (BD bioscience, Palo Alto, CA, USA) were added to the annealed primer and RNA and allowed to incubate at 42°C for 1 hour, followed by heating at 70°C for 5 min to denature the reverse transcriptase. For amplifying PDE10A cDNAs, 1 µl of RT reaction was used in RT-PCR. Primers used in RT-PCR are listed in Table 2-1.

2.5 Northern Blotting

A Northern blot was prepared by fractionating 10 µg of total RNA isolated from wild-type mice striata and testes on a 1% denaturing formaldehyde agarose gel following standard protocols (Sambrook *et al.*, 2001). Methods for radiolabelling the probe, hybridization and post -hybridization washes are described in (Denovan-Wright *et al.*, 1998). The hybridization probe was obtained by PCR amplification of the coding region of PDE10A cDNA. The PCR product (25 ng) was denatured at 95°C for 3 min and

radiolabelled in a 10 µl reaction containing 50 µCi [α-^{32}P]dCTP (3000 Ci/mmol) (Perkin Elmer, Wellesley, MA, USA) and the Ready-to-Go dCTP labelling reaction bead (GE Healthcare Lifescience) at 37°C for 30 min. Unincorporatated nucleotides were removed using a Sephadex G-25 column (GE Healthcare Lifescience). The activity of the purified probe was determined in a Beckman liquid scintillation counter (LS6000) as counts per min (c.p.m.). The blot was subjected to a 4 hrs pre-hybridization step in prehybridization buffer [50% formamide, 5 × sodium chloride-sodium citrate (SSC), 1 × Denhardt's reagent (Sigma), 20 mM sodium phosphate (pH 6.8), 0.2% sodium dodecyl sulfate (SDS), 5 mM EDTA, 10 mg/ml poly A, 50 mg/ml sheared salmon sperm DNA, 50 mg/ml yeast RNA] at 42°C. After prehybridization, the blot was incubated with radiolabelled probe (5×10^6 c.p.m./ml) allowing annealing between probe and target RNA in hybridization buffer [50% formamide, 5 × SSC, 10% dextran sulfate, 1 × Denhardt's reagent, 20 mM sodium phosphate, pH 6.8, 0.2% SDS, 5 mM EDTA, 10 mg/ml poly A, 50 mg/ml sheared salmon sperm DNA, 50 mg/ml yeast RNA] at 42°C overnight. Post-hybridization washes were performed in 2 × SSC, 0.1% SDS at 55°C for 15 min once, then in 1 × SSC, 0.1% SDS at 55°C for three times with 15 min each. The wet blot was wrapped in Saran wrap and then exposed to Biomax MS film (Kodak, Guelph, ON, Canada) with intensifying screen at -80°C for 24-48 hrs.

2.6 *In Situ* Hybridization Analysis

In situ *Hybridization*

Two oligonucleotide probes (HD40 and HD1) (Table 2-1) were used for *in situ* hybridization. For probe preparation, 10 pmol oligonucleotide was 3' end-labelled with 50 µCi of [α-^{33}P]dATP (3000 Ci/mmol) (Perkin Elmer) and 75 U of terminal

deoxynucleotidyl transferase (TdT) enzyme (Promega) in 1 × TdT buffer at 37°C for 90 min. Unincorporated radionucleotides were removed from the labelled probe using exclusion chromatography (MicroSpin G-25 columns, GE Healthcare Lifescience). Frozen brains were cut coronally on the cryostat with 14-15 μm thickness and placed on superfrost slides (Fisher Scientific) and stored in -80°C until use. Slides with frozen brain sections were thawed at room temperature, fixed in 4% (w/v) paraformaldehyde in 0.1 M phosphate-buffer for 5 min, rinsed twice in 1 × phosphate-buffered saline (PBS) [137 mM NaCl, 2.7 mM potassium chloride (KCl), 10 mM disodium hydrogen phosphate (Na_2HPO_4), 2 mM mono potassium phosphate (KH_2PO_4)], then rinse once in 2 × SSC for 20 min, and air dried for 30 min. Two hundred microliters hybridization buffer containing 50% deionized formamide, 5 × SSC, 1 × Denhardt's solution, 20 mM sodium phosphate, (pH 6.8), 0.2% SDS, 5 mM EDTA, 10% (w/v) dextran sulphate, 50 μg/ml sheared salmon sperm DNA, 50 μg/ml yeast RNA and 1 × 10^6 c.p.m./ml of labelled probes were added to the top of the slides. Slides were then coverslipped with Para film and allowed to incubate at 42°C overnight in a humidified chamber. Following hybridization, slides were washed in 1 × SSC four times at 58°C with 30 min each wash, 0.5 × SSC four times at 58°C with 30 min each wash, 0.25 × SSC four times at 58°C with 15 min each wash. Lastly, slides were dipped once in RNase-free H_2O and allowed to dry at room temperature overnight. Hybridization signal was then captured by exposing dried slides to Biomax MR film (Kodak) for 10 to 30 days at room temperature.

Quantitative analysis of PDE10A mRNA

The hybridization signal of PDE10A mRNA from *in situ* hybridization was analyzed by Kodak 1D Image Analysis software. Optical density (OD) was measured in

the striatum and the background hybridization of the medial septum of each section was subtracted from the OD value of the striatum. Data was subjected to a two-way analysis of variance (ANOVA) assessing the influence of genotype (wild-type, R6/1 and R6/2) and age (3-29 weeks of ages) of independent group of mice (N=4 for each age and each genotype). Tukey's honestly significant multiple comparisons were employed to identify differences in PDE mRNA expression among wild-type, R6/1 and R6/2 mice at specific ages. The rate of decline in PDE10A mRNA levels in R6/2 and R6/1 mice was fit with the equation $y = y^o + ae^{-bx}$ using SigmaPlot (Systat Software Inc, Point Richmond, CA, USA).

2.7 Quantitative RT-PCR

Quantitative RT-PCR (qRT-PCR) was used to determine the number of copies of mature and unspliced PDE10A2 primary transcript in cDNA samples derived from the striatum of wild-type and HD transgenic mice using the LightCycler thermal cycler system. A mixture of cDNAs was synthesized in RT reactions with gene-specific primers (RT1, RT2 and HPRT-AS) using Moloney Murine Leukemia Virus Reverse Transcriptase (MMLV-RT) (Promega) following the manufacturer's instructions. Negative control RT reactions, which included all components except MMLV-RT for each sample, were also analyzed by qRT-PCR to determine levels of genomic DNA that were present in total RNA samples prior to cDNA synthesis. The PCR reactions contained 1 μl of cDNA or no RT negative control, 0.2 μM sense and antisense primers, 2 mM or 4 mM magnesium chloride ($MgCl_2$) for primary and mature PDE10A2 cDNA, respectively, and 2 μl of LightCycler-DNA FastStart SYBR® Green I Mix containing

nucleotides, buffer, and hot start *Taq* DNA polymerase. Reactions were performed simultaneously to analyze cDNA samples derived from striata of 3, 5, 6 and 12 week-old mice. The PCR conditions involved 10 min at 95 ^{o}C to activate *Taq* DNA polymerase, 45 cycles of 95 ^{o}C for 15 seconds (sec), 68 ^{o}C for 5 sec and 72 ^{o}C for 15 sec. Fluorescent signal was measured at the end of each extension phase. Hypoxanthine guanine phosphoribosyltransferase (HPRT) cDNA was amplified with HPRT sense and antisense primers using similar conditions except for annealing at 65^{o}C (Table 2-1). The amount of products from no RT negative control that corresponded to trace amount of genomic DNA was subtracted from the copy number of the PDE10A2 primary and mature cDNAs. The copy number of PDE10A2 primary and mature cDNAs was normalized to the copy number of HPRT cDNA. Normalized cDNA levels were subjected to two-way analysis of variance and the 0.05 level of significance was adopted for all comparisons.

2.8 5'RLM-RACE

The First Choice™ RLM-RACE kit (Ambion, Austin, TX, USA) was used to prepare a cDNA library. Total wild-type RNA was treated with calf intestinal phosphatase (CIP) to remove the 5' phosphate from all RNAs that did not have a 7-methylguanosine cap, as well as from any trace genomic DNA. The RNA was then divided into two samples. One aliquot was exposed to Tobacco Acid Pyrophosphatase (+TAP) to remove 7-methylguanosine caps from the 5' end of the mature mRNAs leaving a free 5' phosphate. The other aliquot did not receive TAP treatment (-TAP) and served as a control for the effectiveness of the initial CIP treatment. Adapter RNA was ligated to the 5' phosphate groups on +TAP and control (-TAP) RNA using T4 RNA

ligase. M-MLV reverse transcriptase and random decamers were used to synthesize single-stranded cDNA. PCR amplification of the 5' ends of PDE10A cDNA included the 5' RACE outer adapter primer and one of two outer gene-specific primers (GSP1 and GSP 2) followed by nested PCR using the 5' RACE inner primer and corresponding inner gene-specific primers (GSP3 and GSP 4) (Table 2-1). PCR conditions for both the first and second rounds of amplification were: 94°C for 3 min, followed by 35 cycles of 94°C for 30 sec, 60°C for 30 sec, 72°C for 30 sec, followed by a final extension of 72°C for 10 min. The PCR products were fractionated in 2% agarose gels, gel-purified, cloned and sequenced as described in plasmid construction.

2.9 Ribonuclease Protection Assay

Synthesis of riboprobes

5'RLM-RACE clones were used as templates to synthesize riboprobes according to the instructions provided with Lign'Scribe and Maxiscript kits (Ambion). The plasmid DNA was linearized by restriction digestion. Maxiscript was performed at 37°C for 60 min in a 20 μl reaction containing 1 × transcription buffer, 0.5 mM ATP, 0.5 mM UTP, 0.5 mM GTP, 0.3 mM CTP, 0.2 mM Biotin-14-CTP (Invitrogen) and RNA polymerase mix. After incubation, DNase I (1 U) (Promega) was added to the mixture to remove template DNA. The RNA products were fractionated on a 5% polyacrylamide/8 M urea gel, visualized by UV shadowing, extracted from the gel and purified. The exon 1a-specific probe (RPA-P1) was 170 nucleotides in length, and contained 112 nts of PDE10A cRNA sequence, 38 nts of 5'RACE inner primer sequence and 20 nts of T7 promoter sequence. The exon 1-specific probe (RPA-P2) was 522 nts in length and

consisted of 460 nts PDE10A cRNA sequence, 38 nts 5'RACE inner primer sequence and 20 nt T7 promoter sequence. All riboprobes were stored at -80°C until use.

Ribonuclease Protection Assays

RPA were performed using the RPAIII™ kit (Ambion) and RNA isolated from various weeks of wild-type and R6/1 mice striata. Each probe (500 pg) was combined with 10 µg of total RNA and precipitated with 0.5 M ammonium acetate and 50% ethanol at -20°C for 30 min. The RNA mixture was recovered by centrifugation at 14,000 x *g* for 20 min at 4°C and resuspended in 10 µl hybridization buffer from RPAIII kit. The RNA was then denatured at 95°C for 5 min and allowed to hybridize at 42°C overnight. Control reactions included 2 pg probe only, and 500 pg probe with excess yeast RNA. After hybridization, all samples, except the sample containing 2 pg probe only, were subjected to a 30 minute RNase digestion using a 1:100 dilution of RNase A/T1 at 37°C. Digestion products and a biotinylated Century Plus RNA ladder (Ambion) were fractionated on a 5% polyacrylamide/8M gel, and transferred to Hybond N+ membrane (GE Healthcare Lifescience). Bands were visualized by chemiluminescent detection using Supersignal chemiluminescent detection kit following manufacturer's instruction (Pierce Biotechnology, Rockford, IL, USA).

2.10 Western Blotting

Striatal nuclear extract isolation

Isolation of nuclear extract from the forebrains of wild-type and R6/1 mice was performed according to Sambrook *et al* (2001). Forebrain tissue was dissected from

wild-type and R6/1 mice of different ages on ice. The tissue was homogenized in tight-fitting Dounce homogenizer in 2 ml ice-cold tissue homogenization buffer [10 mM HEPES-KOH (pH 7.6), 25 mM KCl, 0.15 mM spermine, 0.5 mM spermidine, 1 mM EDTA pH 8.0, 2 M sucrose, 10% glycerol, 0.5 mM phenoylmethylsulfonyl fluoride (PMSF), 1 μg/ml Leupeptin, 1 μg/ml Pepstatin]. To monitor lysis of cells, 10 μl of the cell suspension was mixed with an equal volume of 0.4% Trypan blue dye (Invitrogen) and examined under a microscope equipped with a 20 × objective until 80-90% of the cells were lysed and appeared blue. The cell homogenate was layered with 1 ml ice-cold tissue homogenization buffer in polyallomer ultracentrifuge tube (Beckman) and centrifuged at 103,900 x *g* in Beckman TLA100.1 rotor in Optima™ TLX Ultracentrifuge (Beckman Coulter, Mississauga, ON, Canada) for 40 min at 4°C. Supernatants (cytoplasmic extract) were removed into a new 1.5 ml eppendorf tube and stored at -80°C until use. Nucleic pellets were resuspended in 1 ml of ice-cold tissue resuspension buffer [5 mM HEPES-KOH (pH 7.9), 1.5 mM $MgCl_2$, 0.5 mM dithiothreitol (DTT), 0.5 mM PMSF, 26% glycerol]. Sodium chloride (5 M) was added into the resuspended nuclei in a drop-wise fashion to a final concentration of 300 mM. The nucleic mixture was allowed to incubate on ice for 30 min and recovered by centrifugation at 103,900 x *g* in Beckman TLA100.2 rotor for 20 min at 4°C. The supernatant (300 mM NaCl-soluble nuclear extract) was aliquoted. The nucleic pellet (300 mM NaCl-insoluble nuclear extract) was resuspended and homogenized in 0.32 M sucrose. Total proteins, cytoplasmic extract, 300 mM NaCl-soluble nuclear extract, 300 mM NaCl-insoluble nuclear extract were subjected to bicinchoninic acid (BCA) assay to determine the protein concentrations using BCA Protein Assay Reagent (Pierce).

Western Blotting Analysis

For Western blotting analysis, protein samples were subjected to 7.5% or 10% sodium dodecyl sulfate-polyacrylamide gel electrophoresis (SDS-PAGE) in 1 × running buffer [25 mM Tris, 250 mM glycine, pH 8.3, 0.1% SDS (w/v)], and transferred to polyvinylidene fluoride (PVDF) membrane (Fisher Scientific) in transfer buffer [48 mM Tris base, 39 mM glycine, 20% methanol] for 1 hr at 4°C with constant 100 V. Blots were incubated in blocking buffer [137 mM NaCl, 10 mM Tris, 0.1% Tween-20 and 5% skim milk] for 1 hr. After blocking, the blot was incubated with primary antibody in blocking buffer at 4°C overnight with gentle shaking. The next day, the blot wash washed in 20 ml wash buffer [137 mM sodium chloride, 10 mM Tris, 0.1% tween-20 (Sigma)] for 3 times with 20 min each, followed by incubation with peroxidase conjugated secondary antibody in blocking buffer. Blots were washed 3 times with 20 min each in 20 ml wash buffer following incubation with secondary antibody. Bound primary antibodies were detected using enhanced chemiluminescence (ECL) kit and Hyperfilm ECL high performance film (GE Healthcare Lifescience). Primary and secondary antibody dilutions used to detect NGF-IA, VDR, Sp1, CREB, NFkappaB and mutant huntingtin are listed in Table 2-2.

2.11 Electromobility Shift Assay

Double-stranded oligonucleotides (Table 2-3) containing consensus recognition sequences for different transcription factors were individually end-labelled using [γ-^{32}P]ATP (3000 Ci/mol) (Perkin-Elmer) and T4 Polynucleotide Kinase (Fermentas). The labelling reaction was performed in a 10 µl reaction mixture containing 1 × forward

Table 2-2. Antibodies used for Western blotting analyses.

Name[1]	Size (kDa)	SDS-PAGE (%)	Primary dilution	Secondary dilution	Commercial source[2]
NGF-IA	80	7.5%	1:1000	1:1000	Santa Cruz
VDR	55	7.5%	1:5000	1:1000	Chemicon
SP1	~105	10%	1:1000	1:1000	Santa Cruz
CREB	~45	7.5%	1:1000	1:1000	Chemicon
NFkappaB	105	7.5%	1:1000	1:1000	Chemicon
Hum I	~ 300	10%	1:500	1:2000	New England
Anti-Histidine	--	10%	1:50	1:1000	Chemicon

[1]NGF-IA, nerve growth factor inducible factor A or Egr1, early growth response 1; VDR, vitamin D receptor; Sp1, specific protein 1; CREB, cAMP responsive element binding protein; NFkappaB, nuclear factor kappa B.
[2]Santa Cruz, Santa Cruz Biotechnology; Chemicon, Chemicon Internationl; New England, New England Peptide.

reaction buffer (Fermentas), 3.5 pico moles (pmol) of double-stranded DNA, 10 μCi [γ-^{32}P]ATP (Perkin Elmer) and 10 U of T4 Polynucleotide Kinase (Fermentas) at 37°C for 10 min. After the incubation, the reaction was terminated with addition of 1 μl of 0.5 M EDTA to the mixture. Probes were purified and radioactivity of the probe was counted as described before. DNA-binding reactions were carried out for 20 min at room temperature in a mixture of 10 μl containing 1× gel shift binding buffer (Promega), 0.035 pmol of labelled oligonucleotide (~50,000 c.p.m.) and 5 μg of 300 mM NaCl-soluble nuclear extract from wild-type or HD mouse striata (see striatal nuclear extract isolation). For competition experiments, 100 × molar excess of unlabelled oligonucleotide was pre-incubated with the reaction mixture for 10 min at room temperature before the addition of radiolabelled probe. The reaction mixtures were fractionated on 4% native polyacrylamide gel in 0.5 × TBE buffer. The gels were dried and exposed to BioMax MS (Kodak) with an intensifying screen at -80°C for 12-24 hrs.

2.12 *In Vitro* DNase I Footprinting

In vitro DNase I footprinting assay was used to examine protein-DNA interactions on the PDE10A promoter *in vitro*. A 418 bp of PDE10A2 promoter fragment was generated by PCR amplification using sense primer HD80 and antisense primer HD88 (Table 2-1) which amplifies the -392 to +26 region of the PDE10A2 promoter. Sense primer HD80 was end-labelled using T4 Polynucleotide Kinase in a 10 μl reaction mixture containing 1 × forward reaction buffer (Fermentas), 5 pmol of primer, 70 μCi [γ-^{32}P]ATP (Perkin-Elmer) and 10 U of T4 Polynucleotide Kinase (Fermentas) at 37°C for 30 min. The radiolabelled probe was purified as described in Northern blotting.

Table 2-3. Sequence of double-strand DNA probes used in EMSA analysis.

Name[1]	Double-stranded DNA sequence	Cold Probes[2]
TR (DR-4)	5′AGCTTCAGGTCACAGGAGGTCAGAGAGCT 3′ 3′TCGAAGTCCAGTGTCCTCCAGTCTCTCGA 5′	RXR
RXR (DR-1)	5′AGCTTCAGGTCAGAGGTCAGAGAGCT 3′ 3′TCGAAGTCCAGTCTCCAGTCTCTCGA 5′	VDR(DR-3)
VDR (DR-3)	5′AGCTTCAGGTCAAGGAGGTCAGAGAGCT 3′ 3′TCGAAGTCCAGTTCCTCCAGTCTCTCGA 5′	RAR
AP1	5′CGCTTGATGAGTCAGCCGGAA 3′ 3′GCGAACTACTCAGTCGGCCTT 5′	Sp1
Sp1	5′ATTCGATCGGGGCGGGGCGAGC 3′ 3′TAAGCTAGCCCCGCCCCGCTCG 5′	AP1
CREB	5′AGAGATTGCCTGACGTCAGAGAGCTAG 3′ 3′TCTCGAACGGACTGCAGTCTCTCGATC 5′	NFkappaB
NFkppaB	5′AGTTGAGGGGACTTTCCCAGG 3′ 3′TCAACTCCCCTGAAAGGGTCC 5′	CREB

[1]TR (DR-4), thyroid hormone receptor (direct repeat 4); RXR (DR-1), retinoid X receptor (direct repeat 1); VDR, vitamin D receptor; AP1, activating protein 1; Sp1, specific protein 1; CREB, cAMP responsive element binding protein; NFkappaB, nuclear factor kappa B.
[2]Cold probes (100 X) used for competition.

Ten micrograms of 300 mM NaCl-soluble nuclear extract from 5 week-old wild-type or R6/1 transgenic HD mice was incubated for 20 min at room temperature with 50,000 c.p.m. of labelled 418 bp PDE10A2 promoter fragment in binding buffer [50 mM Tris-HCl (pH 8.0), 100 mM KCl, 12.5 mM $MgCl_2$, 1mM EDTA, 20% glycerol and 1 mM DTT]. After a 20 min incubation, 50 µl of 5 mM calcium chloride ($CaCl_2$) and 10 mM $MgCl_2$ was added to the reaction mixture and allowed to equilibrate for 1 min before adding 0.15 U DNase I (Promega) for 2.5 min. DNase I digestion was then terminated by adding 90 µl stop buffer [200 mM NaCl, 30 mM EDTA, 1% SDS (w/v) and 100 µg/ml yeast RNA] to the reaction mixture. Digested DNA was extracted with phenol:chloroform:isoamyl alcohol (25:24:1) (pH 8.0) (Invitrogen), precipitated with ethanol and finally resuspended in 10 µl of loading dye [10 mM EDTA (pH 7.5), 97.5% deionized formamide]. The samples were denatured at 95°C for 3 min and fractionated on 4% PAGE/8 M urea gels in buffer gradient established by 0.5 × TBE in the top buffer chamber and 1 × TBE in the bottom buffer chamber. The gel was dried and exposed to BioMax MS (Kodak) film with an intensifying screen at -80°C for 1-3 days.

2.13 Cell Culture and Transfection

Generation of unidirectional deletion constructs of PDE-PGL3

Ten micrograms of full-length PDE-PGL3 plasmid was sequentially digested with *Kpn*I and *Bgl*II at 37°C followed by ethanol precipitation at -20°C. The linearized plasmid DNA was recovered by centrifugation and resuspended in 44 µl of ddH_2O. Exonuclease treatment started with incubation of linear plasmid DNA with 1 × Exonuclease III buffer at 20°C for 10 min, followed by addition of 200 U of Exonuclease

III (Fermentas) to a total volume of 50 µl. Exonuclease III degrades double-stranded DNA from a *Kpn*I digested end (5' overhang) releasing 5'-mononucleotides from the 3'-ends of DNA strands and producing stretches of single-stranded DNA. Two microliters of ExoIII/DNA reaction mixture were removed at 10 sec intervals to another eppendorf tube containing 15 µl 5 × Mung Bean buffer (New England Biolab, Pickering, ON, Canada) until all ExoIII-treated DNA was removed. The DNA mixture was then incubated at 68°C for 15 min to inactivate ExoIII and further incubated with 10 U of Mung Bean Nuclease at 30°C for 30 min to remove stretches of single-stranded DNA producing ligatable ends of double-stranded DNA with various lengths. The DNA mixture was extracted using phenol:chloroform extraction and ethanol precipitation. DNA was recovered by centrifugation and finally resuspended in 20 µl ddH_2O. Five microliters of linear plasmid DNA mixture was allowed to undergo intramolecular ligation in a 10 µl reaction containing 1 × ligation buffer and 10 U of T4 DNA ligase (Promega). Ligated DNA products were transformed into electrocompetent *E.coli.* cells as described previously. The DNA sequences of eight independent clones containing different sizes of the PDE10A promoter were determined using the dideoxy sequencing method as described in section 2.3.

Cell culture and transfections

ST14A and derivatives that stably express the first 548 amino acids of huntingtin with 15 CAG repeats (N548wt-15Q) or 128 CAG repeats (N548hd-128Q) were kindly provided by Dr. Elena Cattaneo (Cattaneo & Conti, 1998; Rigamonti *et al.*, 2000). Cells were cultured at the permissive temperature of 33°C in Dulbecco's modified Eagle

medium (DMEM) (Invitrogen) supplemented with 10% fetal bovine serum (FBS) (HyClone, Logan, UT, USA) as described in Cattaneo & Conti (1998). Human embryonic kidney cells 293 (HEK293) were cultured in Dulbecco's modified Eagle medium supplemented with 10% horse serum (HyClone). Cells were grown in an incubator at 37°C with humidified 5% CO_2 and 95% air.

Plasmid constructs used in transfection experiments included pEGFP-N1 (BD bioscience), pDsRed1-N1 (BD bioscience), phRL-TK (Promega), pGL3-PDE10A, pCMV-Exon1-115Q and pCMV-Exon 1-22Q. pCMV-Exon1-115Q and pCMV-Exon1-22Q each contained part of the 5'-UTR, the coding region within exon 1 with 115 CAG repeats (Exon 1-115Q) or 22 CAG repeats (Exon 1-22Q), and part of intron 1 of human huntingtin as described in Rodriguez-Lebron *et al.* (2005).

All transfection experiments were performed following the instructions in Lipofectamine and Lipofectamine Plus Reagents kit (Invitrogen). For promoter deletion analyses, DNA mixture containing 0.2 μg of each deletion construct, 0.2 μg of pEGFP-N1, 0.05 μg of phRL-TK was incubated with 4 μl Lipofectamine Plus Reagent (Invitrogen) in 25 μl serum free media (SFM) at room temperature for 15 min. After incubation, 25 μl of SFM containing 1 μl Lipofectamine reagent was added to the mixture and allowed to further incubate at room temperature for 15 min. Fifty microliters of DNA/Lipofectamine mixture was added to either 50,000 N548wt-15Q cells or 50,000 N548mu-128Q cells in 200 μl SFM. On the next day, cells were washed with Hank's Balanced Salt Solution (HBSS) (HyClone) twice and replaced with ST14A growth media [DMEM supplemented with 10% fetal bovine serum (FBS)]. After 48 hrs post-transfection, cells were harvested for luciferase analysis. For transfections in ST14A

parental cells and HEK293 cells, 0.2 μg of PDE10A-P14-pGL3, 0.2 μg of pCMV-Exon 1-115Q or pCMV-Exon 1-22Q, 0.05 μg of pDsRed1-N1, and 0.05 μg of phRL-TK were transfected into 50,000 cells using the same procedure described above.

Luciferase activity

Cells were harvested 48 hours post-transfection and subjected to Dual Luciferase Assay (Promega). Cells were washed with 1 × PBS once and incubated with 100 μl 1 × Passive Lysis buffer at room temperature for 15 min. Cell lysates were subjected to two freeze-thaw cycles and collected by centrifugation at 12,000 x *g* for 1 min at 4°C. Ten microliters of cell lysate was used for dual luciferase assay following the manufacturer's protocol (Promega). Firefly luciferase activity was normalized to *Renilla* luciferase activity expressed from phRL-TK. Normalized data was subjected to two-way ANOVA and the 0.05 level of significance was adopted for all comparisons.

2.14 TranSignal Protein/DNA Array

TranSignal protein/DNA array was performed according to manufacturer's protocol (Panomics, Rewood, CA, USA). Five microgram of wild-type and R6/1 forebrain nuclear extract (300 mM NaCl-soluble) were mixed with 10 μl TranSignal Probe Mix (Panomics) in a 20 μl reaction and allowed to incubate at 15°C for 30 min. Following incubation, the mixture was fractioned in a 2% agarose gel in chilled 0.5 × TBE at 120 volts for 20 min. Protein-DNA complexes were excised from the gel and solublized with Extraction buffer A (Panomics). The bound probes were allowed to bind to Gel Extraction Beads (Panomics) and eluted from the beads in ddH_2O. For

hybridization, each array membrane was incubated with 4.5 ml of pre-warmed Hybridization buffer provided and then hybridized with the eluted probe (denatured at 95°C for 3 min) overnight at 42°C. After hybridization, each membrane was washed with 50 ml Hybridization Wash I [2 × SSC/0.5% SDS] at 42°C twice with 20 min each time, followed by 50 ml Hybridization Wash II [0.1 × SSC/0.5% SDS] at 42°C twice with 20 min each. After washes, blots were subjected to chemilumniscent detection. Blots were incubated with 1 × Blocking Buffer at room temperature for 15 min and then with a 1:1000 dilution of Streptavidin-HRP conjugate in the same buffer for 15 min. Each blot was washed with 20 ml 1 × Wash buffer for 3 times, followed by incubation with 1 × Detection Buffer at room temperature for 5 min. Hybridization signals on each blot were captured after 5 min incubation with 2 ml of substrate working solution and exposure to ECL hyperfilm (GE Healthcare Lifescience) for 10~60 min at room temperature.

2.15 TranSignal Transcription Reporter Array

TranSignal Transcription Reporter Assay was performed according to manufacturer's protocol (Panomics). TranSignal Reporter plamid mix (20 μl), 1 μg of pCMV-Exon 1-22Q or pCMV-Exon 1-115Q, 0.05 μg of pEGFP-N1 were co-transfected into 5×10^5 ST14A cells using Lipofectamine and Lipofectamine Plus Reagents (Invitrogen) using transfection procedure described above. Total RNA was isolated from transfected cells 48 hs post-transfection using the Trizol method as described above.

One microgram of total RNA and 6 μl of Transcription Reporter Array Primer were heated at 70°C for 2 min then 42°C for 2 min. The reverse transcriptase reaction

was performed at 42°C for 1 hr in a reaction mixture containing 12 µl Labelling Mix, 1 µl Biotin-dUTP, 1 µl MMLV-Reverse Transcriptase (Promega) and RNA/primer mixture. cDNA probes were denatured in 1 × Denaturing Solution at 68°C for 20 min and then neutralized in 1 × Neutralization Buffer at 72°C for 10 min. Labelled cDNA probes were then hybridized with the TranSignal Transcription Reporter Assay Membranes. Hybridization signal was detected with chemilumniscent detection. Hybridization and detection were the same as described for TranSignal Protein/DNA array.

2.16 Synthesis of Recombinant Huntingtin Protein *In Vitro*

Constructs pET-N171-23Q and pET-N171-87Q, which were kindly provided by Xiao-Jiang Li (Emory University, USA), contain cDNAs encoding the N-terminus of human huntingtin (amino acid 1 to 171 tagged with six histidines at the N-terminus of the recombinant protein fragment (Li *et al.*, 2002). These fusion proteins contained either 23Q (N171-23Q) or 87Q (N171-87Q). BL21 (DE3) bacterial cells (Invitrogen) were electro-transformed with 1 ng of either constructs and grown at 37°C overnight in 50 ml 2 × YT broth (Kenamycin, 50 µg/ml) until OD at 600 nm reached 0.6. After induction with 1 mM isopropyl-β-D-thiogalactopyranoside (IPTG) (Sigma) for 2 hrs, cells were recovered by centrifugation at 5000 rpm for 5 min and lysed in 8 ml of binding buffer [5 mM imidazole, 500 mM NaCl, 20 mM Tris-HCl, pH 8.0, 25 mM β-mercapthethanol, 0.1% nonidet P40 (NP40), 1 mM PMSF]. Lysates were allowed to bind to Ni-NTa columns (Invitrogen) at room temperature for 1 hr with gentle shaking. After binding, the column was washed three times with binding buffer containing 50 mM imidazole to remove unbound protein and cellular debris. Proteins that were bound to the column

were eluted with 5 ml elution buffer [400 mM imidazole, 500 mM NaCl, 20 mM Tris-HCl pH 8.0, 25 mM β-mercapthethanol, 0.1% NP40, 1 mM PMSF]. Eluted fractions were collected (1 ml/tube, from elution 1 to elution 5). Elution 1 was desalted using Zeba Desalt Spin Columns (Pierce) and stored at -80°C for *in vitro* transcription assay. Desalted N171-23Q and N171-87Q proteins and a series of known concentrations of BSA (4, 6, 8, 10, 12, 20, 25, 30 ng) were fractioned in one 7.5% SDS-PAGE gel, followed by silver staining. Densitometric analysis of silver-stained bands was performed using Kodak ID Image analysis software. The concentration of N171-23Q and N171-87Q were measured by comparing the OD of each band to a standard curve established by BSA.

2.17 *In Vitro* Transcription

The insert from the PDE10A2 promoter construct P6 (-433/+278) was amplified using primers HD80 and HD79 (Table 2-1). The GAD65 promoter (-503/+600) was amplified using primers mGAD-P1 and mGAD-P2 (Table 2-1). PCR products were resolved on a 0.8% agarose gel, followed by gel-purification as described before. The amount of DNA was calculated based on the relative intensity of the band and a comparable band in 1 kb GeneRuler DNA quantification ladder (Fermentas). The *in vitro* transcription reaction was performed using HeLaScribe Nuclear Extract *in vitro* Transcription System (Promega). The procedure started with pre-incubation of DNA and protein in a reaction mixture containing 126 fento moles (fmol) of PCR product, 1 × transcription buffer [20 mM HEPES (pH7.9), 100 mM KCl, 0.2 mM EDTA, 0.5 mM DTT, 20% (v/v) glycerol, 0.2 mM PMSF], 6 mM $MgCl_2$, 8 U of Hela Nuclear extract

with or without purified N171-23Q and N171-87Q at 30°C for 30 min. After pre-incubation, 1 μl dNTP mix containing 400 μM each of rCTP, rATP, rUTP and 16 μM rUTP and 10 μCi of [α-^{32}P]rGTP were added to the mixture and the mixture was allowed to incubate at 30°C for 30 min. The reaction was terminated by adding 175 μl Stop buffer (Promega) [0.3 M Tris-HCl (pH 7.4), 0.3 M sodium acetate, 0.5% (w/v) SDS, 2 mM EDTA and 3 μg/ml of yeast RNA]. *In vitro* synthesized RNAs were extracted with 200 μl of phenol:chloroform:isoamyl alcohol (25:24:1) (pH 8.0) (Invitrogen) and precipitated at -20°C from at least 1 hr to overnight. Following precipitation, RNA was recovered by centrifugation at 14,000 x *g* at 4°C for 20 min. RNA pellets were then resuspended in 10 μl loading dye [49% (v/v) formamide, 0.05% bromophenol blue (w/v), 0.05% xylene cyanol (w/v) and 5 mM EDTA], followed by denaturation at 95°C for 5 min. Denatured RNAs were resolved on a 4% polyacrylamide/8 M urea gel. The gel was dried and exposed to BioMax MS (Kodak) film with intensifying screen at -80°C for 1-3 days. The OD of the film background was subtracted from the OD of the 550 nt transcript from the PDE10A2 promoter and the 436 nt transcript from the GAD65 promoter in the presence of different amounts of N171-87Q and N171-23Q. The net OD of the each transcript was normalized to the OD of the transcript detected in HeLa alone.

For aggregation experiment *in vitro*, a peptide containing 20 polyglutamine and 2 lysine residue (polyQ) at two ends was obtained by custom synthesis from the Keck Center at Yale University (New Haven, CT, USA). Another peptide containing a 19 amino acids of polyproline-rich sequence (PQLPQPPPQAQPLLPQPQC) was obtained by custom synthesis from New England Peptide (Gardner, MA, USA). Lyophilized power for both peptides were dissolved in RNase-free H_2O. Aggregation was performed

by preincubating 1.5 pmol of N171-22Q or N171-87Q with various amounts of polyQ or polyP at 37°C for either 10 min or 2.5 hrs before the mixture was added to the *in vitro* transcription reactions. *In vitro* transcription reactions were performed the same as described above.

2.18 Silver Staining

Silver staining was used for staining proteins that have been fractioned on a SDS-PAGE gel. Following electrophoresis, the gel was incubated with 50% methanol for 3 times with 20 min each time, and then with RNase-free H_2O twice with 30 min each time. The gel was immersed in staining solution [0.4% $AgNO_3$ (w/v), 7.56% NaOH (w/v) and 1.4% ammonium sulfate (v/v)] for 90 min, followed by thorough rinse with RNase-free H_2O twice with 5 min each. The gel was developed in solution containing 0.005% citric acid (w/v) and 0.05% formaldehyde (v/v) for ~10 min and the development reaction was terminated by replacing developing solution with stop solution [45% methanol, 10% acetic acid]. Stained gels were scanned and subjected to densitometric analysis using Kodak ID Image analysis software.

2.19 Protein Binding With Dynabead-Coupled DNA

Labeling of promoter DNA with Dynabead M-280 Streptavidin

A PDE10A2 promoter fragment was PCR amplified using 5' biotin-labelled antisense primer HD79 and sense primer HD80 (Table 2-1). The PCR conditions were the same as described in PCR and plasmid construction for the PDE10A promoter except that the extension time in each cycle of DNA synthesis was 30 sec. A GAD65 promoter

was amplified using biotin-labelled sense primer mGAD-P1 and antisense primer mGAD-P3 using the same PCR conditions as described for the GAD65 promoter. PCR products were gel-purified and quantified on an agarose gel as described above. Before labelling, 1 mg of Dynabeads M-280 Streptavidin (Invitrogen) was washed 3 times in 100 µl of 2 × Binding & Wash Buffer [5 mM Tris-HCl, pH 7.5, 0.5 mM EDTA and 1 M NaCl] and finally resuspended in the same buffer to a final concentration of 5 µg/µl. Five picomoles of PCR products were mixed with the resuspended Dynabeads M-280 Streptavidin and allowed to incubate at room temperature with rotation for 30 min. To separate the beads from unbound DNA, the bead/DNA mixture was put on magnet for 2 min, followed by 3 washes with 2 × Binding & Wash buffer. The Dynabead-Streptavidin labelled DNA was resuspended in 1 × transcription buffer giving a final concentration of 126 fmol/µl and stored at 4°C.

Analysis of proteins that interact with the Dynabead-labelled promoters

A reaction mixture containing 126 fmol of Dynabead-labelled DNA, 1 × transcription buffer, 6 mM $MgCl_2$, 1.5 pmol of purified huntingtin fusion protein (His-23Q or His-87Q) and 8 U of Hela Nuclear extract was incubated at 30°C for 30 min. After incubation, proteins that interacted with the Dynabead-labelled DNA were separated from unbound proteins by placing the mixture on a Dynal magnetic particle concentrator (MPC) (Invitrogen) for 2 min. Unbound proteins were removed. The Dynabead-labelled promoters and the proteins that bound to Dynabead-labelled DNA were washed twice with 100 µl 1 × transcription buffer. The bound proteins were separated from the Dynabead-labelled promoter DNA by resuspending the Dynabead-

labelled DNA and proteins in 1 × SDS sample buffer [10% (v/v) glycerol, 5% (v/v) β-mercaptoethanol, 3% (w/v) SDS and 62.5 mM Tris-HCl (pH6.8)] and incubating the mixture at 95°C for 10 min. Proteins were fractionated on a 7.5% SDS-PAGE gel and the proteins were visualized after the gel was subjected to silver staining.

2.20 Two-Dimensional SDS-PAGE

Two-dimensional SDS-PAGE was used to separate proteins that interacted with the Dynabead-labelled promoter. The first dimension that separates proteins on their isoelectric points (pIs) was performed in Bio-Rad Biorad Protean® IEF Cell following manufacturer's instructions. After the pre-incubation and two washes, the bound proteins were separated from the Dynabead-labelled promoter DNA by heating the Dynabead-labelled DNA and proteins in 25 μl of 0.1% SDS at 95°C for 10 min. One hundred microliters of rehydration buffer was added to the resuspended proteins. The proteins were absorbed onto a precast immobilized pH gradient IPG gel strip (7 cm, pH gradient 5-8) (Bio-Rad) with constant 50 voltages (V) for 16 hrs at room temperature. After rehydration, proteins were allowed to focus to their pIs with a focusing program in Bio-Rad Biorad Protean® IEF Cell: S1, 250 V, 15 min; S2, linear, 4000 V, 2 hrs; S3, rapid, 10000 vhrs and S4, 500 V, hold. After the completion of focusing, the IPG gel strip was washed in 2.5 ml of equilibration buffer I for 10 min and then in 2.5 ml of equilibration buffer II for 10 min at room temperature with gentle shaking. The IPG gel strips containing the proteins that had migrated to their pIs were placed onto 7.5% SDS-PAGE gels for separation of proteins on the second dimension based on their molecular weight. The second dimension was subjected to electrophoresis with constant 250 V for 40-45

min in 1 × running buffer as described before. The separated proteins were visualized by silver staining as described above.

CHAPTER 3

Mutant Huntingtin Affects the Rate of Transcription of Striatum-Specific Isoforms of Phosphodiesterase 10A

The majority of work in this chapter has been published in:

Hu, H., McCaw, E.A., Hebb, A.L., Gomez, G.T. & Denovan-Wright, E.M. (2004) Mutant huntingtin affects the rate of transcription of striatum-specific isoforms of phosphodiesterase 10A. *Eur J Neurosci*, **20**, 3351-3363.

3.1 Introduction

Inheritance of a *HD* gene with an expansion of a CAG repeat causes HD. (Huntington's Disease Collaborative Research Group, 1993). Despite expression of mutant huntingtin throughout the brain and body (Sharp *et al.,* 1995), the major pathology of HD is a selective loss of GABAergic medium spiny projection neurons in the caudate and putamen (Vonsattel & DiFiglia, 1998). Mutant huntingtin, by virtue of its expanded polyglutamine tract, interacts with other proteins and perturbs many cellular functions (Harjes & Wanker, 2003; Li & Li, 2006).

Several mouse models have been established for investigating early pathological and molecular abnormalities in HD (Mangiarini *et al.,* 1996; Reddy *et al.,* 1998; Hodgson *et al.,* 1999; Schilling *et al.,* 1999; Shelbourne *et al.,* 1999; Wheeler *et al.,* 1999). The transgenic R6/1 and R6/2 mouse models were used in this study. Both of these transgenic lines express exon 1 of the human mutant *huntingtin* gene under the control of the human huntingtin promoter and two copies of the endogenous mouse *huntingtin* gene (Mangiarini *et al.,* 1996). These mice develop a progressive HD-like neurological phenotype in a CAG length-dependent fashion, whereby the R6/1 line containing ~115 CAG repeats within the transgene develops HD-like symptoms over a longer period of time than the R6/2 line that contains ~150 CAG repeats within the human huntingtin exon 1 transgene (Mangiarini *et al.,* 1996). We and others have found that the expression of several genes critical to striatal signaling are decreased in R6 and other transgenic HD mice prior to the onset of HD-like symptoms compared to the age-matched wild-type controls. These observations support the hypothesis that alterations in the steady-state levels of a specific subset of mRNAs are an early component of the pathological process

of HD (Cha, 2000; Denovan-Wright & Robertson, 2000; Luthi-Carter *et al.,* 2000; Menalled *et al.,* 2000; van Dellen *et al.,* 2000; Sipione *et al.,* 2002; Sugars & Rubinsztein, 2003).

Recently, we have shown that the steady-state levels of the PDE10A mRNA and protein decline during the course of disease progression in R6/1 and R6/2 transgenic HD mice and in HD human brains (Hebb *et al.,* 2004). The decrease in PDE10A mRNA is more rapid in R6/2 mice than in R6/1 mice, which parallels the rate of disease progression as measured by the development of neuronal intranuclear inclusions (NIIs), motor symptoms and weight loss (Mangiarini *et al.,* 1996). PDE10A is a signaling enzyme that hydrolyzes cAMP and cGMP in cells and belongs to a second messenger system, which has been shown to be affected in a pre-symptomatic age of R6/2 mice (Luthi-Carter *et al.,* 2000). It is highly expressed in the brain and the testis (Fujishige *et al.,* 1999a; Fujishige *et al.,* 1999b; Fujishige *et al.,* 2000), which would allow us to compare and contrast the effect of mutant huntingtin in different tissues. PDE10A belongs to a large PDE family that is regulated by alternative splicing and polyadenylation at the transcriptional level (Soderling *et al.,* 1999; Soderling & Beavo, 2000). This gives us a reference of basal regulation in order to understand how mutant huntingtin reduces transcription of this gene. Thus, given these reasons, we chose to study how the expression of the N-terminus of mutant huntingtin caused decreased transcription of the PDE10A gene in HD.

The goal of this chapter was to fully describe the temporal and spatial changes in the distribution of PDE10A mRNA, and to identify the promoters of the PDE10A gene utilized in the striatum and testis in R6 mice that express the N-terminus of mutant

huntingtin. Such information was required for the study of how mutant huntingtin was involved in reducing steady-state levels of mRNA in HD.

3.2 Results

Isolation of PDE10A splice variants from the mouse striatum and testis

Multiple PDE isoforms are expressed throughout the mammalian body either as products of different PDE gene family members or as products of the same gene through alternative splicing or transcription start site utilization (Conti & Jin, 2000). In humans, rats, and mice, PDE10A is highly expressed in the caudate and putamen (striatum) and testis (Fujishige *et al.,* 1999a; Fujishige *et al.,* 1999b; Loughney *et al.,* 1999; Soderling *et al.,* 1999; Hebb *et al.,* 2004). To study the regulation of PDE10A in HD, we first cloned the striatal-specific PDE10A cDNA. The full-length coding region of PDE10A from mouse striatal cDNA could not be amplified using a primer specific to the 5' end of the coding sequence of the mouse PDE10A cDNA (GenBank accession number AF110507) that was derived from RNA isolated from testis. Two EST clones derived from embryonic mouse brain (GenBank accession number AB041808 and AK014090) that had an unique sequence at their 5' ends compared to the testis PDE10A cDNA were identified in Genbank. Comparison of the cDNA and genomic DNA PDE10A sequences revealed that the sequence at the 5' ends of the brain ESTs corresponded to an exon 48 kb upstream of the exon annotated as exon 1 in the mouse PDE10A gene on chromosome 17. This exon, which corresponded to the 5' end of brain PDE10A cDNAs, was defined as exon 1a (Fig. 3-1A). RT-PCR was performed using 4

Figure 3-1. PDE10A mRNAs expressed in the striatum and the testis had different 5' exon sequences. A schematic representation of exon sequences included in PDE10A1 (A) and PDE10A2 (B) cDNAs are shown. Exons are depicted as open boxes and numbered according to the Sanger mouse genome database with the exception of exon 1a, which is located ~48 kb upstream of exon 1 in the mouse PDE10A genomic DNA sequence located on chromosome 17. The relative positions of translation start (M) and stop codons (TGA) are indicated by arrows. Asterisks indicate polyadenylation signal sites. The location of primers used in RT-PCR (P1-P4) (short black bars) and oligonucleotides used for *in situ* hybridization (HD40 and HD1) (hatch bars) are shown below the exon sequences. C. RT-PCR analysis of PDE10A variants in the mouse testis and striatum. Total RNA was prepared from wild-type mouse testis (lanes 1-4) and striatum (lanes 5-8). Primers used for PCR reaction are indicated below each lane. The relative mobility of molecular weight markers (1 kb Ladder, MBI Fermentas) are indicated on the left.

A

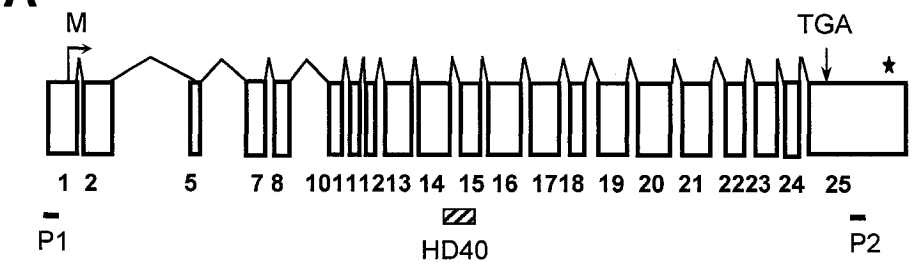

B

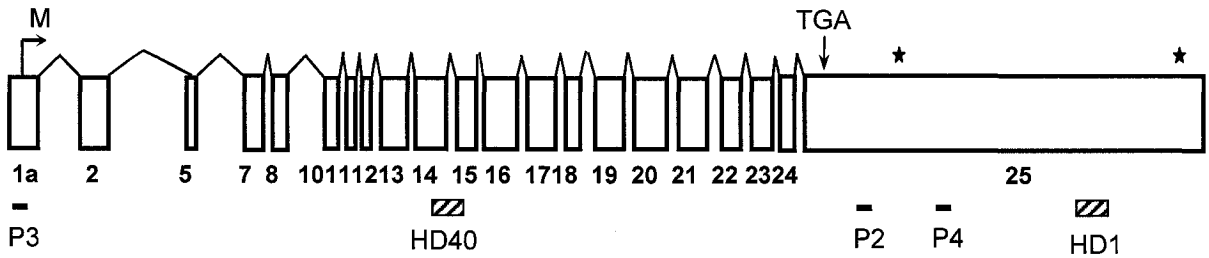

C

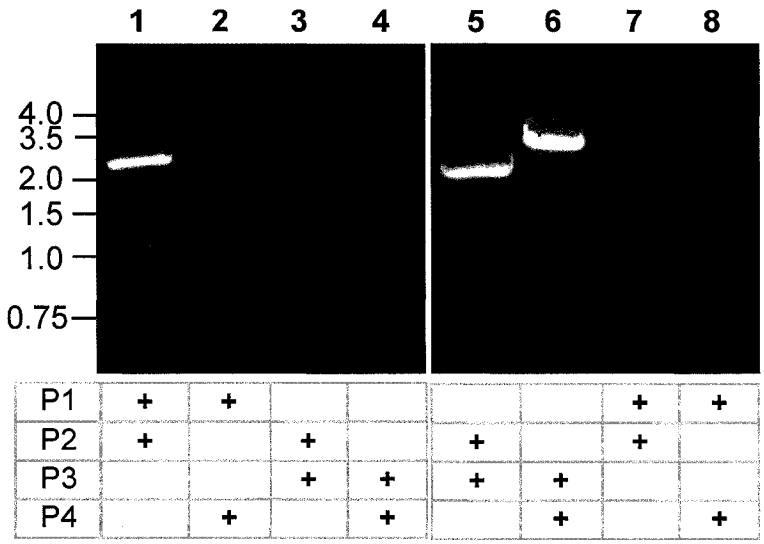

P1	+	+					+	+
P2	+		+		+		+	
P3			+	+	+	+		
P4		+		+		+		+

pairs of primers to determine which cDNAs were expressed in mouse striatum and testis (Fig. 3-1C). RT-PCR using primers P1/P2 and testis cDNA generated a single 2.5 kb product (Fig. 3-1C), however, no product was generated using P1/P2 and striatal cDNA. The primer pairs P3/P2 and P3/P4, however, amplified products of 2.5 kb and 3.5 kb, respectively, from striatal cDNA (Fig. 3-1C). Using testis cDNA as the template, a faint band of 2.5 kb was detected using P3/P2 but no PCR product was detected using primers P3/P4. Following cloning and sequencing of these PCR products, we determined that the striatal and testis PDE10A isoforms contained exon 1a or 1, respectively, and exons 2, 5, 7, 8 and 10-25. Therefore, although the PDE10A isoforms differed at their 5' ends, the cDNA sequence that encompassed the entire coding region of both isoforms was identical. We designated the isoform containing exon 1a PDE10A2 (GenBank accession number AY360383). In order to confirm the result from RT-PCR analysis, northern blotting was employed using a coding sequence probe common to both PDE10A1 and PDE10A2 cDNAs (Fig. 3-2). Northern blot analysis demonstrated that the most abundant PDE10A mRNA in the mouse striatum is PDE10A2, which contains the sequence of exon 1a and is ~ 9 kb in length. In the testis, the most abundant PDE10A mRNA is PDE10A1, which contains the sequence of exon 1 and is ~ 4 kb in length. The difference in length between PDE10A1 and PDE10A2 is due to the presence of a longer 3'UTR within exon 25 in PDE10A2 compared to PDE10A1 (Fig. 3-1A). A polyadenylation signal (AATAAA) is located 19 bp upstream of the 3' end of the PDE10A1 within exon 25, another polyadenylation signal (ATTAAAT) is located 27 bp upstream of the 3' end of the PDE10A2 within exon 25 (Fig. 3-1A). PDE10A2 encodes 797 amino acids with a predicted molecular mass of 90,443 Da. It consists of 22 amino

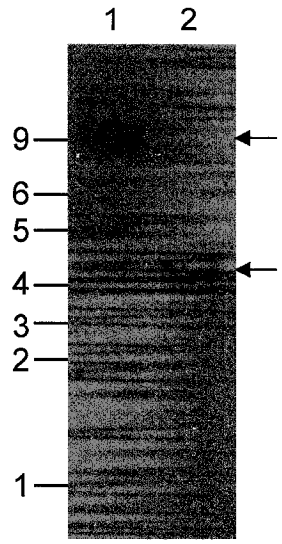

Figure 3-2. The most abundant PDE10A mRNAs in the mouse striatum and testis are 9 and 4 kb, respectively. Northern blot analysis was performed using total RNA isolated from the mouse striatum (lane 1) and the testis (lane 2). A 300 bp coding sequence of the PDE10A mRNA spanning exon 7-10 was radiolabelled with [α-^{32}P]dCTP and used as a probe for hybridization. The two sizes of transcripts detected are indicated by arrows on the right. The relative mobility of RNA molecular size markers (RNA millennium marker, Ambion) is shown on the left.

acids derived from exon 1a and amino acids 7-779 as reported for the PDE10A1 isoform. The 22 amino acids at the amino terminus are identical to the first 22 amino acids from the human PDE10A2 splice form (Soderling *et al.,* 1999). The proteins encoded by the mouse and human PDE10A2 genes are 95% identical at the amino acid level.

Transcription of PDE10A2 is decreased in HD mice

Previously, it has been shown that there is a decline in the steady-state levels of the coding region of PDE10A mRNA in the striatum of two strains of transgenic HD mice R6/1 and R6/2 (Hebb *et al.,* 2004). Since the steady-state abundance of mRNA is dependent on the net difference between the rate of synthesis and decay (Ross, 1995), the N-terminal mutant huntingtin-dependent decrease in PDE10A mRNA levels could be caused by a decreased rate of transcription of the PDE10A gene or decreased PDE10A mRNA stability. *In situ* hybridization analyses were performed using oligonucleotide probes complementary to the PDE10A2 3' UTR (HD1) and the coding region common to PDE10A1 and PDE10A2 (HD 40). There was no difference in PDE10A mRNA levels between the wild-type littermates of R6/1 or R6/2 mice using either probe (data not shown). Brain sections from wild-type and R6/1 transgenic HD mice between 3 and 29 weeks of age and R6/2 transgenic HD mice between 3 and 12 weeks of age were subjected to *in situ* hybridization analysis to determine the relative hybridization of the two probes. There was no statistically significant difference in the relative intensity of HD40-specific hybridization among different ages of wild-type mice. Levels of HD1-specific hybridization declined with increasing age in wild-type mice (Fig. 3-3A). The levels of HD1-specific hybridization were significantly different in 11 to 30 week-old

Figure 3-3. *In situ* hybridization analysis of PDE10A mRNA in R6/1 and R6/2 HD mouse striatum. Antisense probes HD40 and HD1 are complementary to sequences encoded by exon 14 and exon 25, which detected the coding sequence and the 3' UTR of the PDE10A2 transcript, respectively. Following *in situ* hybridization, optical density values were obtained by densitometric analyses from brain sections derived from four individual mice per age and genotype. The optical density values of the HD40- (open circles) and HD1-specific (closed circles) hybridization signal in the striatum are presented as mean ± standard error of the mean (SEM). SigmaPlot was used to fit curves that best describe the rate of decline (equation $Y = Y_0 + ae^{-b.X}$) in PDE10A mRNA levels in wild-type (A), R6/1 (B) and R6/2 (C) mice.

A

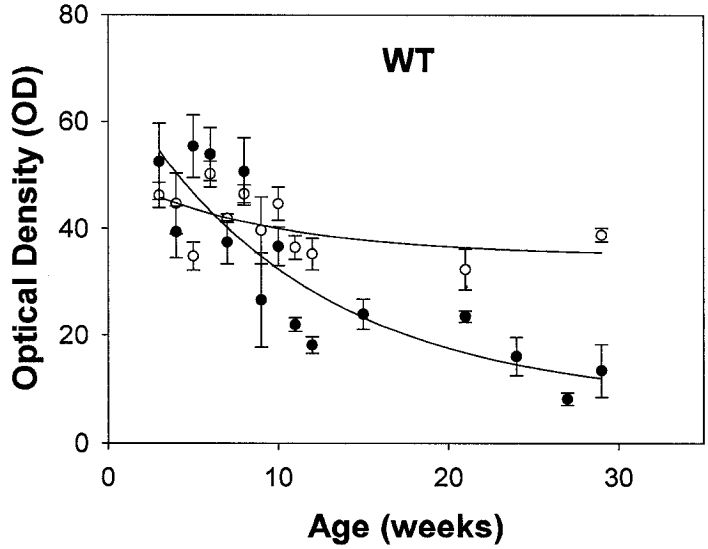
WT
Optical Density (OD)
Age (weeks)
0
20
40
60
80
0
10
20
30

B

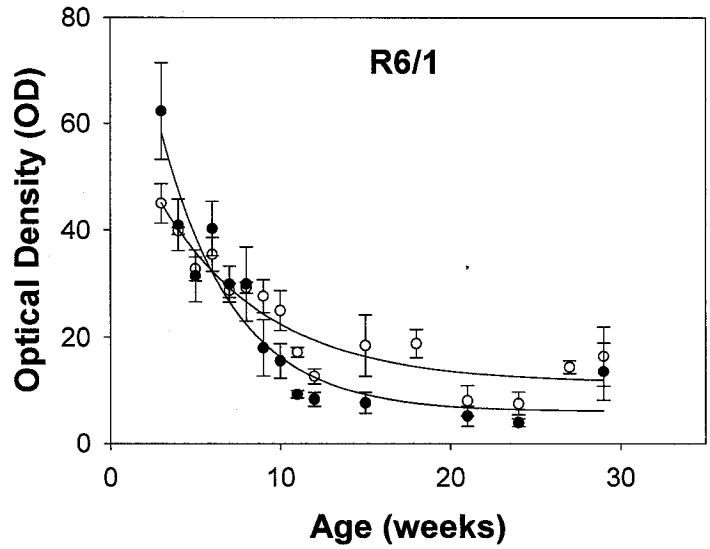
R6/1
Optical Density (OD)
Age (weeks)
0
20
40
60
80
0
10
20
30

C

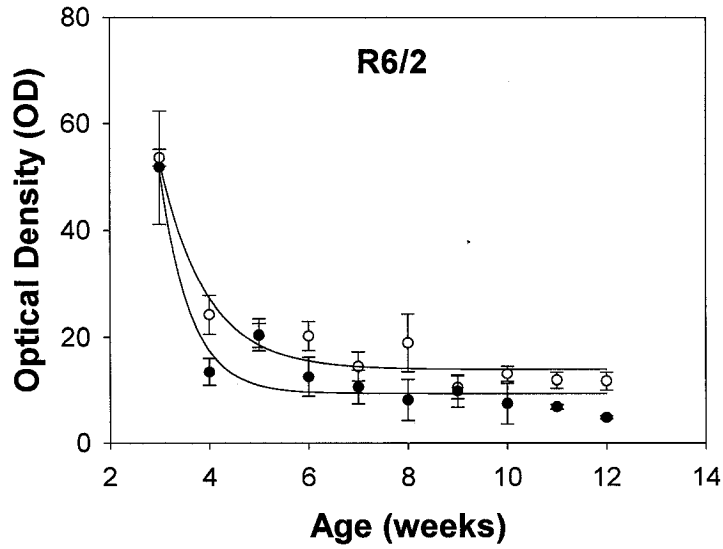
R6/2
Optical Density (OD)
Age (weeks)
0
20
40
60
80
2
4
6
8
10
12
14

compared to 3 week-old wild-type mice. In contrast, the decrease in the steady-state levels of the coding region and 3'UTR were described by a simple exponential decay curve in R6/1 and R6/2 mice (Fig. 3-3B and 3-3C). There was a significant difference in the levels of coding region- and 3' UTR-specific hybridization signal in all R6/2 mice older than 4 weeks of age compared to the levels in 3 week-old wild-type and R6/2 mice. Similarly, the levels of PDE10A mRNA that hybridized with the coding region- and 3' UTR-specific probes were significantly different from wild-type levels by 5 and 6 weeks of age in R6/1 mice. Comparison of the rate constant (b value) for each exponential decay curve revealed that the ratios of the rate constant for the decline in the coding region and 3'UTR were similar for both R6/1 (1.47) and R6/2 (1.54) mice demonstrating that the PDE10A mRNA coding sequence and the 3'UTR decline proportionally in both lines of R6 transgenic HD mice. The reduced steady-state level of PDE10A mRNA in the striatum of HD mice, therefore, did not appear to be associated with instability of PDE10A2 transcripts mediated by the striatum-specific extended 3'UTR.

In order to confirm that the decreased steady-state level of PDE10A mRNA in the striatum of HD mice was due to reduced transcription rather than post-transcriptional mRNA instability, we determined the copy number of PDE10A2 primary and mature transcripts in total RNA isolated from 3, 5, 6 and 12 week-old wild-type and R6/1 mouse striata using real-time quantitative RT-PCR (qRT-PCR) (Fig. 3-4). Since intron splicing of newly synthesized RNA occurs co-transcriptionally, quantitative measurement of the amount of primary transcripts at any given time indirectly reflects the rate of transcription (Elferink & Reiners, 1996). The gene-specific primer RT1 that is located at intron 1a and the gene-specific primer RT2 that is located at exon 5 were used in RT reactions,

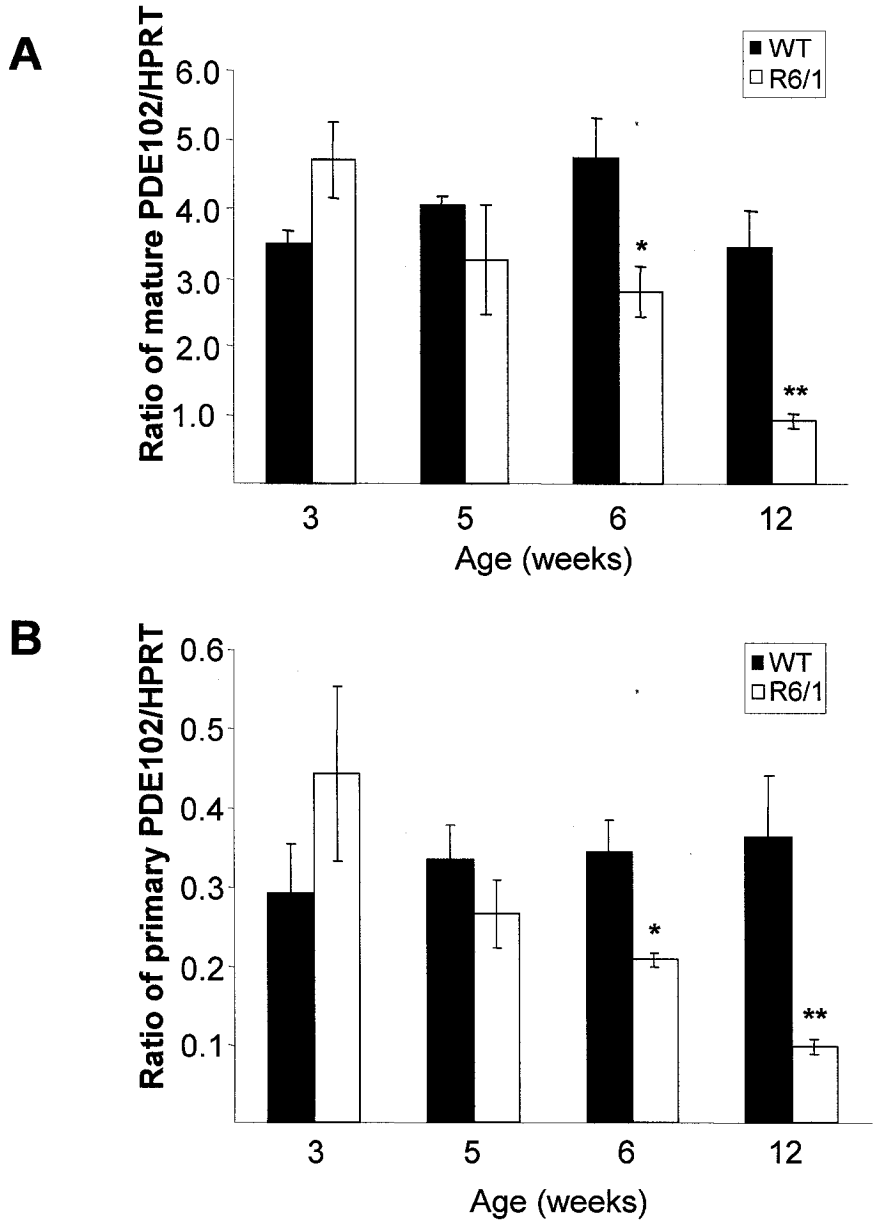

Figure 3-4. Levels of PDE10A2 mature and primary transcript decreased starting at 6 weeks of age in R6/1 mice. Copy number of mature and primary PDE10A2 transcript and HPRT cDNA were quantified by qRT-PCR. Total RNA was isolated from 3, 5, 6 and 12 week-old wild-type (WT, filled bars) and R6/1 (open bars) striatal tissues. cDNAs were obtained by reverse transcriptase reaction using gene-specific primers. The levels of mature and primary PDE10A2 transcripts were normalized to levels of HPRT. The ratio of mature (A) or primary (B) PDE10A2 cDNA to HPRT cDNA is presented as mean ± SEM (N = 5 for each age and genotype). *P<0.05, **P<0.001, significant difference between wild-type and R6/1. (Two-way ANOVA).

which allow us to specifically amplify primary transcripts and mature transcripts, respectively. The amounts of primary and mature PDE10A2 transcripts were normalized to the levels of hypoxanthine guanine phosphoribosyltransferase (HPRT) amplified from each cDNA sample. There was no difference in the levels of HPRT transcripts in striatal tissue isolated from 3 and 5 week-old wild-type or R6/1 mice (Luthi-Carter *et al.*, 2000). There was a significant decrease in the copy number of primary (Fig. 3-4B) and mature transcripts (Fig. 3-4A) in 6 ($P<0.05$) and 12 ($P<0.001$) week-old R6/1 mice striata compared to age-matched wild-type striata. The ratio of primary and mature PDE10A2 transcript (~1:10) remained constant in all samples tested demonstrating that the decline in PDE10A2 mature transcript was proportional to the decline in primary transcript levels. This observation, in conjunction with the previous regression analyses of PDE10A *in situ* hybridization signal density, was consistent with the hypothesis that the decreased steady-state levels of PDE10A2 mRNA in the striatum of transgenic HD mice was caused by altered transcription initiation rather than increased mRNA degradation.

In situ hybridization and quantitative RT-PCR both demonstrated that the earliest time point for the N-terminal exon 1-encoding mutant huntingtin to exert significant repression on transcription was at 6 weeks of age in R6/1 and 4 weeks of age in R6/2 mice. The *in situ* hybridization results also demonstrated that the rate of decline for the steady-state level of the PDE10A mRNA was faster in R6/2 than in R6/1 (Hebb *et al.*, 2004). These observations suggest that the difference in the rate of decline of the PDE10A mRNA between two transgenic HD mice strains could be due to the expression level of the N-terminal mutant huntingtin, the length of CAG repeats, or combination of both. A polyclonal antibody (Hum I) was raised against the human huntingtin-specific

peptide PQLPQPPPQAQPLLPQPQC located immediately downstream of the polyglutamine repeat within the protein sequence expressed by R6/1 and R6/2 mice (Rodriguez-Lebron *et al.*, 2005). Western blot analysis using the Hum I polyclonal antibody was used to determine the expression level of the mutant huntingtin transgene in forebrain lysate isolated from various ages of R6/1 and R6/2 mice. A 300 kDa Hum I-immunoreactive band was detected in brain extracts isolated from 3 week-old and 12 week-old R6/1 mice but not from wild-type mice of the same ages demonstrating the expression of the N-terminal mutant huntingtin protein in HD mice. The level of the N-terminal mutant huntingtin was higher in forebrain extracts from 12 weeks compared to 3 weeks suggesting that there was an age-dependent accumulation of mutant huntingtin transgene products in the forebrains of R6/1 mice (Fig. 3-5A). Subsequently, the levels of mutant huntingtin transgene products were examined in forebrain lysate of R6/1 and R6/2 mice at 3, 5, 9 and 12 weeks of age. The optical density of the detected N-terminal mutant huntingtin products in different ages was individually normalized to the optical density of an unchanged amido-black positive band (50 kDa) and the ratio was represented as relative optical density (Fig. 3-5B). The levels of the N-terminal mutant huntingtin were first detected in the forebrain of 3 week-old mice and increased significantly at 5 weeks of age and remained constant at the age of 9 and 12 weeks in R6/1 and R6/2. This suggests that the maximal level of expression was reached by 5 weeks of age in both R6/1 and R6/2 ($\ddagger P<0.01$, $\sim P<0.01$, N=3). Importantly, the expression level of the N-terminal mutant huntingtin in R6/2 mice was higher than that observed in R6/1 in all the ages examined (Fig. 3-5B. $*P<0.05$, N=3). The results indicated that the rate of decline for the steady-state levels of the PDE10A2 mRNA in the

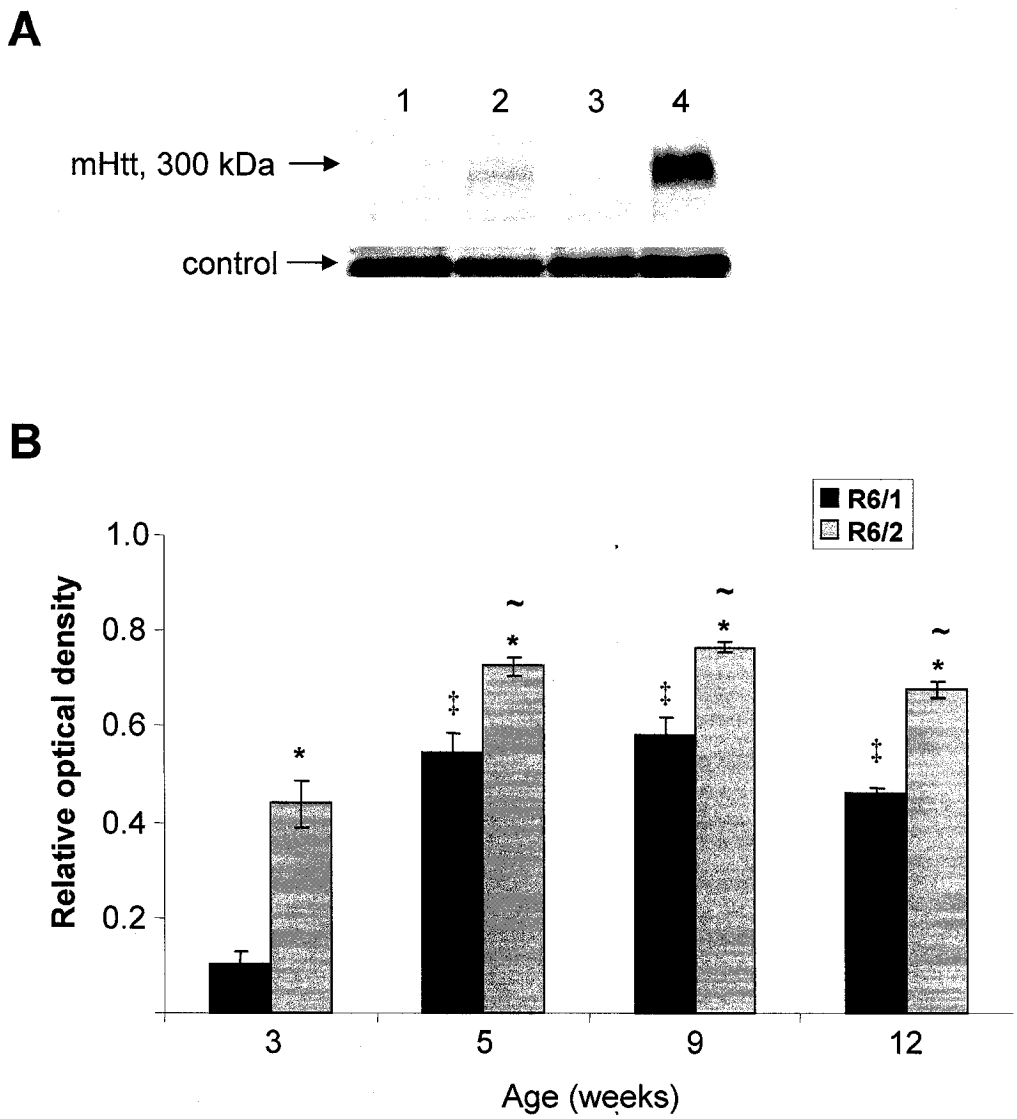

Figure 3-5. The levels of mutant huntingtin transgene product in the brains of R6/2 mice was significantly higher than in R6/1 mice at 3, 5, 9 and 12 weeks of age. Western blotting of mutant huntingtin protein was performed using protein extracts from the brains of 3 (lane 2) and 12 week-old R6/1 (lane 4) mice and their wild-type littermate controls (lane 1, 3) (A). Molecular weight of detected mutant huntingtin protein is indicated at the left of the panel A. A 50 kDa amido black-stained band served is used as a loading control. Densitometric analyses of the levels of detected mutant huntingtin protein in the brain extracts of 3, 5, 9 and 12 week-old R6/1 and R6/2 mice (B). The histogram shows the mean optical density (±SEM, N=3) of the levels of mutant huntingtin in R6/1 mice (black bars) and R6/2 mice (grey bars) normalized to the optical density of the 50 kDa control band. *P<0.05, significant difference between R6/1 and R6/2 at each age. ‡P<0.01, significant difference between 3 weeks and other weeks of R6/1 mice. ~P< 0.01, significant difference between 3 weeks and other weeks of R6/2 mice. (Two-way ANOVA).

striatum correlated with both the expression of the N-terminus of mutant huntingtin and the length of CAG repeat in R6 mice.

Identification of the transcription start sites

Based on the identification of two PDE10A isoforms with unique 5' ends, the promoters for PDE10A2 and PDE10A1 were likely located upstream of exon 1a and exon 1, respectively. To define transcription initiation sites, 5'RLM-RACE was carried out to determine the 5' end of full-length capped PDE10A mRNA present in striatal tissue isolated from wild-type mice. After nested PCR reactions using cDNA prepared from RNA adapter-ligated full-length mRNA, a mixture of PCR products of ~120-150 bp was observed that corresponded to the 5' ends of 7-methyl G capped PDE10A2 mRNAs (Fig. 3-6A). A PCR product of approximately 500 bp was detected that corresponded to the 5' ends of the PDE10A1 mRNAs (Fig. 3-6B). The 5'RLM-RACE products were cloned and several clones were sequenced. Two transcription start sites were identified at positions -337 and -307 relative to the position of the translation initiation codon (designated as +1) in exon 1a as illustrated as site A and B in Fig. 3-8A. One transcription start site was identified at -657 relative to the +1 site in exon 1 (Fig. 3-8B).

To determine whether the expression of the N-terminal mutant huntingtin in R6/1 mice differentially alters the relative amount of mRNA with 5' ends that corresponded to these transcription initiation sites, we used ribonuclease protection assays (RPA) to confirm the usage of start sites identified by 5'RLM-RACE and to determine the levels of transcripts derived from different start sites in both wild-type and R6/1 mice. Two clones that represent start sites corresponding to -337 (relative to +1 ATG start site) in exon 1a

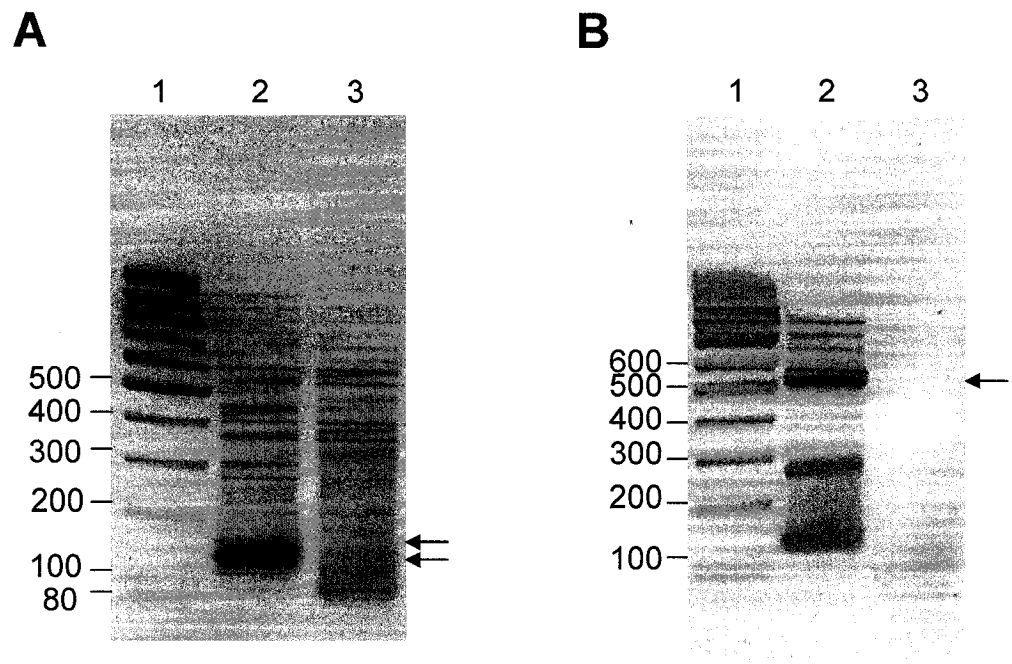

Figure 3-6. Determination of the 5' ends of PDE10A2 (A) and PDE10A1 (B) cDNA using 5' RNA-ligase mediated RACE. 5' RLM-RACE products were fractionated on 2% agarose gels. For A and B, lane 1 is 100 bp Ladder (MBI, Fermentas). Molecular weights are indicated to the left of each panel. Lane 2 is the experimental reaction that included tobacco acid pyrophosphotase treatment (+TAP). Lane 3 is the control reaction without TAP treatment. The PCR products from the +TAP reaction as indicated by arrows were cloned and sequenced.

(for PDE10A2) and -657 in exon 1 (for PDE10A1) were used to synthesize riboprobes RPA-P1 and RPA-P2, respectively. Three PDE10A2-specific transcripts were detected with a size of 112 nt, 82 nt and 71 nt, respectively, in 4 week-old wild-type and 9 week-old R6/1 striatal RNA (lane 7 and 8). The 112 nt and 82 nt protected RPA products corresponded to transcription initiation sites at positions -337 and -307, respectively, as identified by 5'RLM-RACE, which was designated as start site A (-337) and B (-307) in Fig. 3-8A. The size of the third protected band (71 nt) corresponded to position –296 that was depicted as start site C in Fig. 3-8A. The levels of 87 nt and 71 nt transcripts were both decreased in RNA isolated from the striatum of 9 week-old R6/1 mice compared to the levels detected in 4 week-old wild-type mice. The level of 112 nt transcript was relatively unchanged between RNAs from these two groups. A 245 nt protected transcript was detected using a full-length 304 nt β-actin probe in 4 week-old wild-type and 9 week-old R6/1 (Fig. 3-7, lanes 3 and 4) and the levels of protected β-actin transcript remained unchanged between these two groups. Two protected transcripts 460 nt and 322 nt were detected in both 4-week old wild-type and R6/1 mice using a 552 nt RPA-P2 riboprobe (Fig. 3-7B), which corresponded to start site 1 (-657) and 2 (-419) in the PDE10A1 cDNA shown in figure 3-8B. In contrast, the levels of the 460 nt and 322 nt transcripts did not change in the striatum of 4 week-old R6/1 mice compared to that in wild-type mice.

Regulation of the transcripts derived from start sites in HD mice striata

Since there were decreased levels of transcripts associated with specific start sites, we wanted to examine how the expression of the N-terminus of mutant huntingtin in R6/1

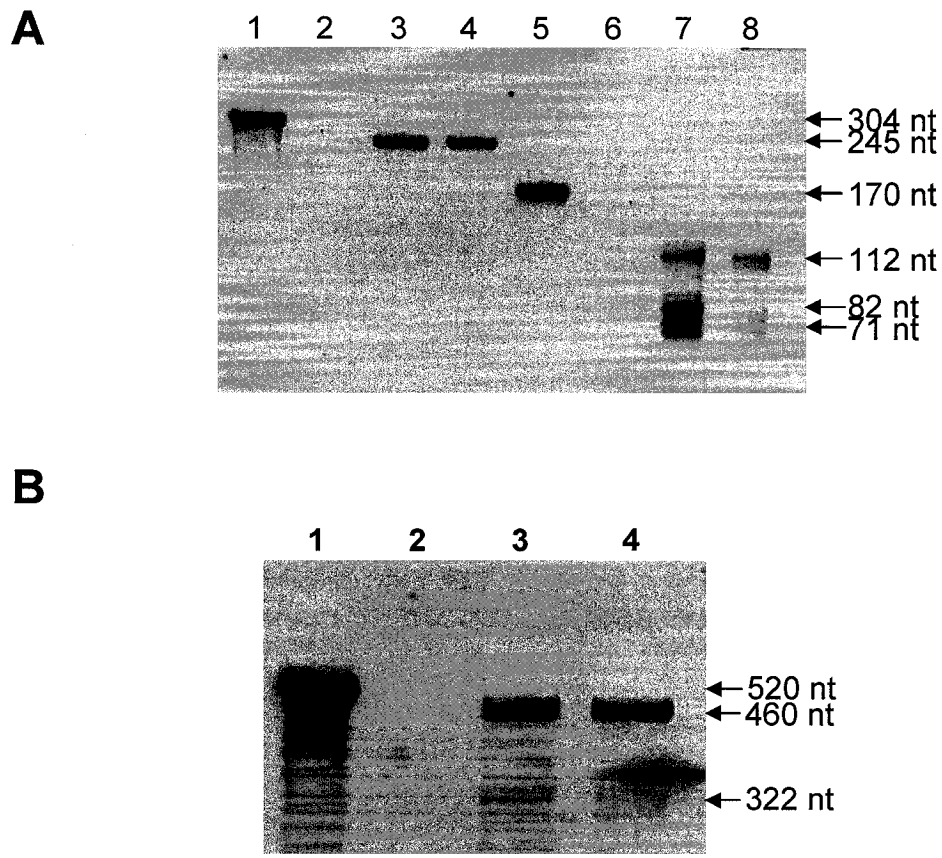

Figure 3-7. Determination of transcription start sites of the PDE10A2 mRNA (A) and the PDE10A1 mRNA (B) using RNase protection assays. RNase protection assays were performed with β-actin riboprobes (lane 1-4) and PDE10A2-specific full-length riboprobes (lane 5-8) using total RNA isolated from 4 week-old wild-type (lane 3, 7) and 9 week-old R6/1 mice striata (lane 4, 8) (A). The RPA products were fractionated on 12% denaturing polyacrylamide gels. Control reactions contained excess probe and yeast tRNA but no mouse RNA (lane 2, 6). RNase protection assays were performed with PDE10A1-specific riboprobes (lane 1-4) (B). Two protected bands were detected in RNA isolated from 4 week-old wild-type (lane 3) and R6/1 mice striata (lane 4). The protected products were fractionated on 5% denaturing polyacrylamide gels. No product was detected in the control reaction that contained excess probe and yeast tRNA but no mouse RNA (lane 2). The relative mobility and size of riboprobes and their protected products are indicated on the right of each panel.

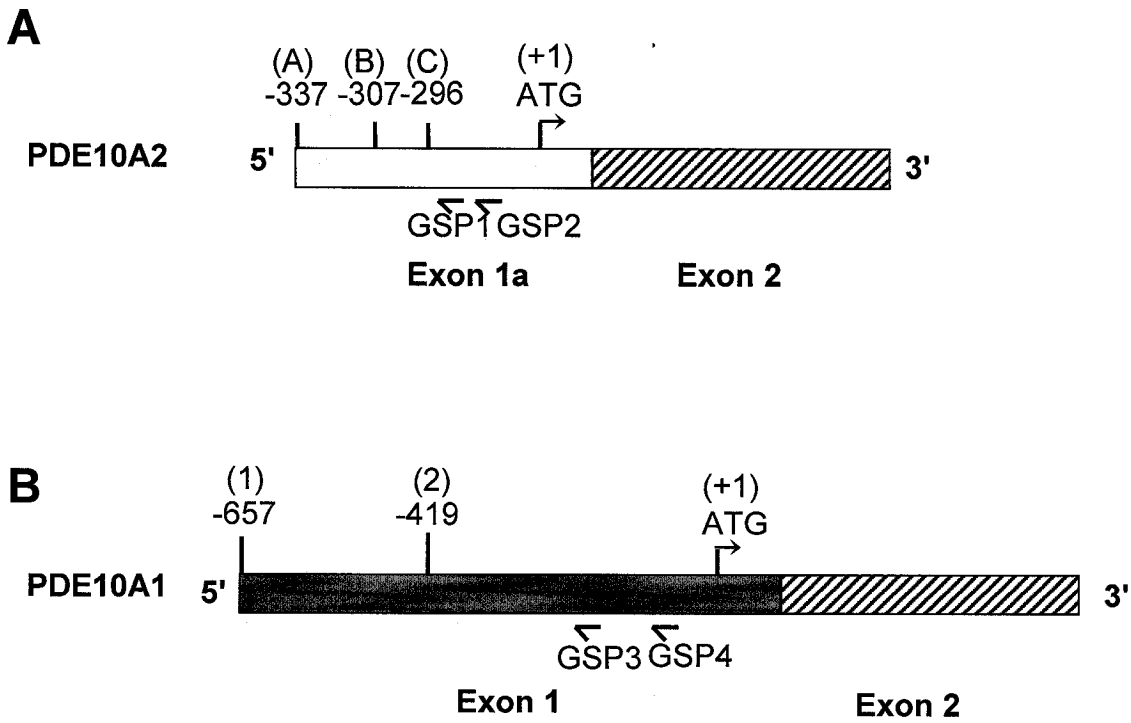

Figure 3-8. Schematic view of the 5' ends of PDE10A2 (A) and PDE10A1 (B) cDNAs. Exon 1a, exon 1 and exon 2 are illustrated as open, gray and hatched boxes, respectively. The positions of transcription start sites relative to the translation initiation codon (+1) of each cDNA were determined by comparing the sequences of the 5' ends of cloned 5' RLM-RACE clones with genomic DNA. Transcription start sites used for the PDE10A2 mRNA that were verified by RNase protection assays are indicated as A, B and C in A. Transcription start sites used in the PDE10A1 mRNA are numbered in B. The relative position of gene-specific primers used for 5' RLM-RACE are indicated by arrows.

mice exerts transcriptional repression from specific transcription start sites during the progression of HD. RPA was performed using the RPA-P1 and RPA-P2 riboprobes in RNAs isolated from 4, 9 and 22 week-old R6/1 HD mice and age-matched wild-type littermates. As shown in Fig. 3-9A, three protected bands were detected using the 170 nt RPA-P1. The size of these protected fragments corresponded to three transcription sites in exon 1a as A, B and C site, respectively (Fig. 3-8A). Transcripts derived from the three sites were equally abundant in 4 week-old wild-type and R6/1 HD mice suggesting that each transcription initiation site contributed equally to the population of PDE10A2 mRNAs in the mouse striatum (Fig. 3-9A). The mRNAs that initiated at position -307 (site A) and -296 (site B), which corresponded to the 82 and 71 nt protected bands in RPA, were decreased in 9 and 22 week-old R6/1 HD mice compared to wild-type mice. The steady-state level of PDE10A2 mRNA derived from transcription start sites B and C, therefore, were affected by the expression of the mutant huntingtin transgene in 9 and 22 week-old R6/1 mice. Densitometric analyses of the relative amount of each protected RNA band revealed that the levels of transcripts derived from sites B and C were decreased in R6/1 mice to ~50% of those observed in wild-type mice, while the level of the transcript derived from the site A in R6/1 mice was similar to that observed in wild-type mice (Fig. 3-9B). *In situ* hybridization using a probe complementary to the sequence between start site A and B (HD88) confirmed that there was no statistically significant difference in the levels of mRNA that initiated at site A between 16 week-old wild-type and R6/1 transgenic mice (data not shown). It was not possible to directly test whether the levels of transcripts that initiated at sites B and C decreased *in vivo*. The

Figure 3-9. PDE10A2 mRNAs that are derived from three transcription start sites differentially decreased in striatal tissue of R6/1 compared to wild-type mice. RNase protection assays of PDE10A2 mRNA were performed using 20 μg of total RNA isolated from 4 (lanes 1 and 2), 9 (lanes 3 and 4) and 22 (lanes 5 and 6) week-old wild-type (lanes 1, 3 and 5) and R6/1 (lanes 2, 4 and 6) mice striata (A). The RPA reaction products were fractionated on 12% denaturing polyacrylamide gels. The PDE10A2-specific full-length riboprobe was 170 nts in length (lane P). Three protected bands were detected. The relative mobility and size of these protected products are indicated. No product was observed in control reactions that contained excess probe and yeast tRNA but no mouse RNA (data not shown). Reactions using aliquots of the experimental RNAs (1 μg) and a β-actin-specific riboprobe were used to normalize the amount of input RNA for each sample (shown below panel A). The optical density of each protected PDE10A2-specific band normalized to the optical density of the β-actin protected band from each RNA sample is shown in the histogram in B and expressed as ratios of optical density for each band to those observed in 4 week-old wild-type mice. The identity of each band is indicated in the inserted legend.

A

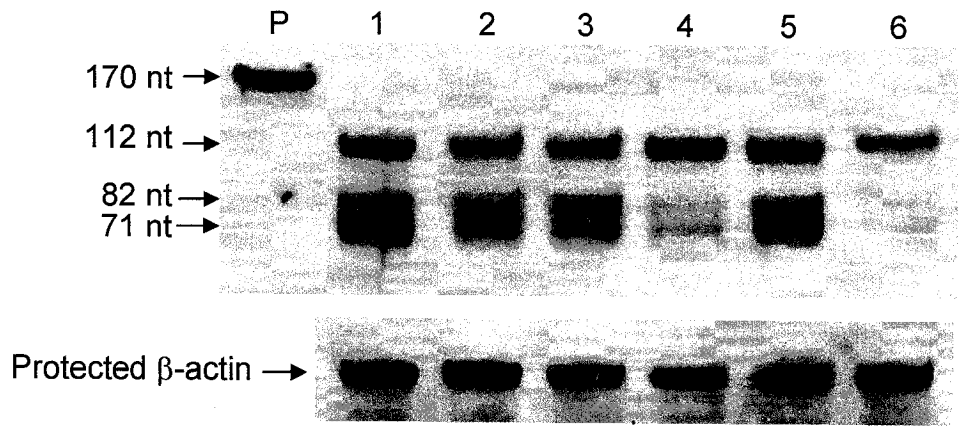
P
1
2
3
4
5
6
170 nt
112 nt
82 nt
71 nt
Protected β-actin

B

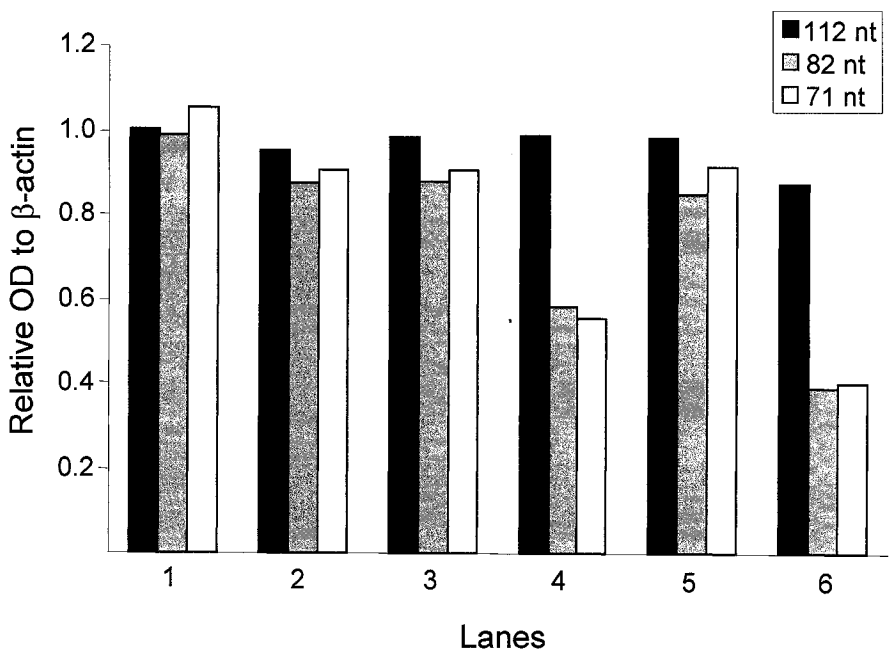
112 nt
82 nt
71 nt
Relative OD to β-actin
1.2
1.0
0.8
0.6
0.4
0.2
1
2
3
4
5
6
Lanes

levels of β-actin mRNA did not change over the time and were included in all assays as a control for the amount of input RNA (Fig. 3-9A).

In the striatum, PDE10A1 mRNA was not detected using standard RT-PCR conditions indicating that the levels of PDE10A1 were lower than the levels of PDE10A2 mRNA (Fig. 3-1C). However, a specific 498 bp product was amplified from the striatal RNA in 5'RLM-RACE reactions using exon1-specific primers. Similarly, two protected transcripts were detected using the RPA-P2 probe in RNA isolated from 4 week-old wild-type mice. Therefore, PDE10A1 was expressed in the striatum (Fig. 3-6B and 3-7B). We used RPA to determine whether the expression of PDE10A1 mRNA from different transcription start sites in the striatum was affected by the expression of the mutant huntingtin transgene. RPA was performed using striatal RNA from 4, 9 and 22 week-old R6/1 HD mice and age-matched wild-type mice. As shown in Fig. 3-10A, two major protected products of 460 and 322 nts were observed following RPA. Unlike the protected products corresponding to the 5' ends of PDE10A2 transcripts, the protected products of exon1-containing transcripts were only detected after an extended exposure of the RPA blot to the film demonstrating that PDE10A1-specific transcripts are relatively rare in the striatum. The 460 nts product corresponded to the expected size of PDE10A1 mRNA that was transcribed from the start site at – 657 bp (site 1) upstream of the ATG in exon 1. The 322 nts product corresponded to transcripts that initiated at position -419 (site 2) (Fig. 3-10A). The levels of protected products corresponding to PDE10A1 transcripts derived from site 1 in the promoter upstream of exon 1 in 9 and 22 week old R6/1 mice were ~60% of that observed in wild-type mice. The PDE10A1 mRNA derived from site 2, however, appeared to decrease with increasing age in wild-

Figure 3-10. PDE10A1 mRNAs that are derived from one transcription start site decreased in striatal tissue of R6/1 compared to wild-type mice. RNase protection assays of PDE10A1 mRNA were performed using 40 μg of total RNA isolated from 4 (lanes 1 and 2), 9 (lanes 3 and 4) and 22 (lanes 5 and 6) week-old wild-type (lanes 1, 3 and 5) and R6/1 (lanes 2, 4 and 6) mice striata (A). The protected products were fractionated on 5% denaturing polyacrylamide gels. The PDE10A1-specific full-length riboprobe was 520 nts (lane P). Two protected bands were detected. The relative mobility of these protected products and size are indicated. No product was observed in control reactions that contained excess probe and yeast tRNA but no mouse RNA (data not shown). Reactions using aliquots of the experimental RNAs (1 μg) and a β-actin-specific riboprobe were used to normalize the amount of input RNA for each sample. The optical density of each protected PDE10A1-specific band normalized to the optical density of the β-actin protected band from each RNA sample is shown in the histogram in B and expressed as ratios of optical density of each band to those observed in 4 week-old wild-type mice. The identity of each band is indicated in the inserted legend.

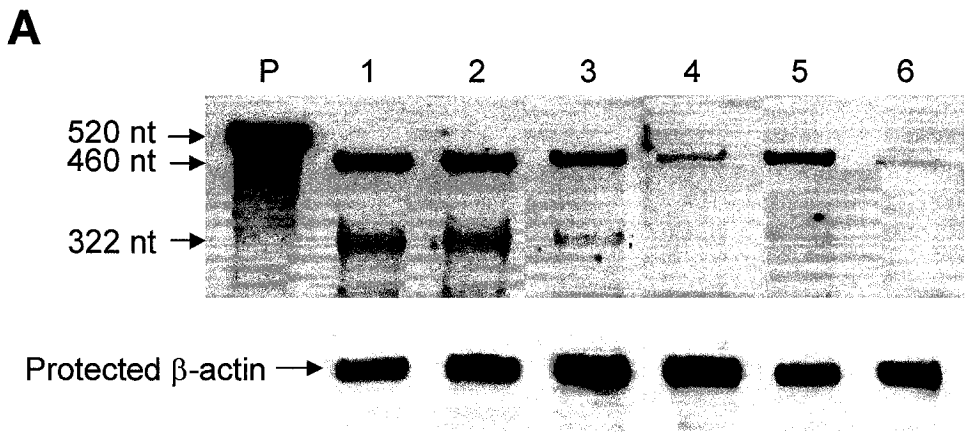
A
P
1
2
3
4
5
6
520 nt
460 nt
322 nt
Protected β-actin

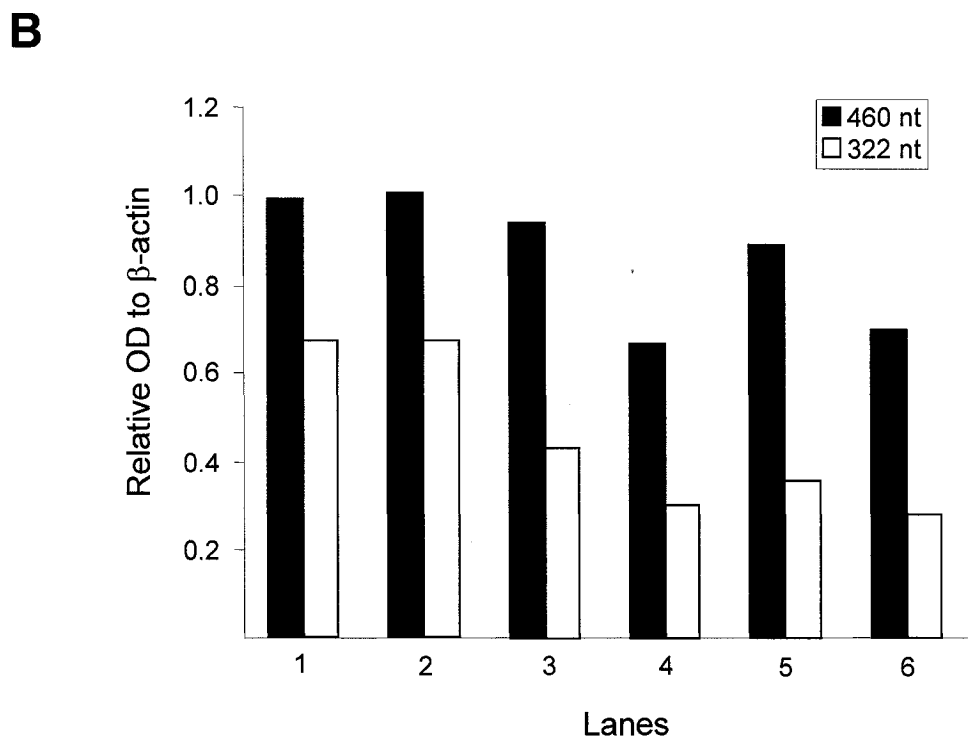
B
460 nt
322 nt
Relative OD to β-actin
1.2
1.0
0.8
0.6
0.4
0.2
1
2
3
4
5
6
Lanes

type and HD mice. Therefore, the steady-state levels of PDE10A1 mRNA that initiated from site 1 in the promoter upstream of exon 1 appeared to be affected by the N-terminus of mutant huntingtin while the levels of transcripts derived from site 2 were affected by age and not the genotype of the mice. Based on the relative abundance of PDE10A1 and PDE10A2 mRNA in the striatum and the observation that there is a significant loss of transcripts derived from sites B and C in the promoter upstream of exon 1a, it appears that the loss of PDE10A mRNA detected by *in situ* hybridization (Fig. 3-3) and northern blot analysis (Fig. 3-2) was due to loss of PDE10A2 mRNA that initiate at sites B and C in the exon 1a-specific promoter.

Next, we examined whether PDE10A mRNA levels in the testes were affected by the expression of the mutant huntingtin transgene in R6 mice. RNA was isolated from the testes of 4 and 9 week-old wild-type, R6/1and R6/2 mice and used as the substrate for RPA using probes specific to exon1a and exon 1. There were no protected bands in reactions containing testes RNA that were equivalent in size to the bands after RPA of striatal RNA using the 170 nt exon1a- or 520 nt exon1-specific probes (Fig. 3-11A) and 3.11B). Using the 520 nt exon1-specific probe, we did detect a faint 52 nt protected product in each sample of testes RNA following fractionation of the RPA products in 12% polyacrylamide gels (data not shown). We did not observe this 52 nt protected product when striatal RNA was included in the RPA reactions. This protected fragment corresponded to the 5' end of the testis-specific PDE10A1 cDNA described previously (Soderling *et al.*, 1999, GenBank Accession Number AF110507). The transcription of PDE10A1 and PDE10A2, therefore, initiate at different sites in the

Figure 3-11. PDE10A1 and PDE10A2 mRNAs initiated at different transcription start sites in the mouse testis and striatum. RNase protection assays with the PDE10A2-specific 170 nt riboprobe were performed using 20 μg of total testis RNA from 4 (2 and 3) and 9 (lanes 4, 5 and 6) week-old wild-type testis RNA (lanes 2 and 4), R6/1 testis RNA (lanes 3 and 5) and R6/2 testis RNA (A). The positive control reaction included striatal RNA isolated from the striatum of 4 week-old wild-type mice (lane 1). A β-actin-specific riboprobe was used to normalize input RNA in each sample. We did not observe any protected bands in testis RNA using the PDE10A2-specific riboprobe indicating that transcription of PDE10A2 mRNA initiates at different transcription start sites in the mouse testis compared to the striatum. RPAs with the PDE10A1-specific 520 nt riboprobe were performed using 20 μg of total testis RNA from 4 (2 and 3) and 9 (lanes 4, 5 and 6) week-old wild-type testis RNA (lanes 2 and 4), R6/1 testis RNA (lanes 3 and 5) and R6/2 testis RNA (B). The positive control reaction included striatal RNA isolated from the striatum of 4 week-old wild-type mice (lane 7). The relative mobility of the full-length probe is shown in lane P. Lane 1 contains excess riboprobe and yeast RNA but no mouse RNA. Input RNA was equivalent in each sample as shown by the β-actin riboprobe-protected bands shown below panels A and B.

A

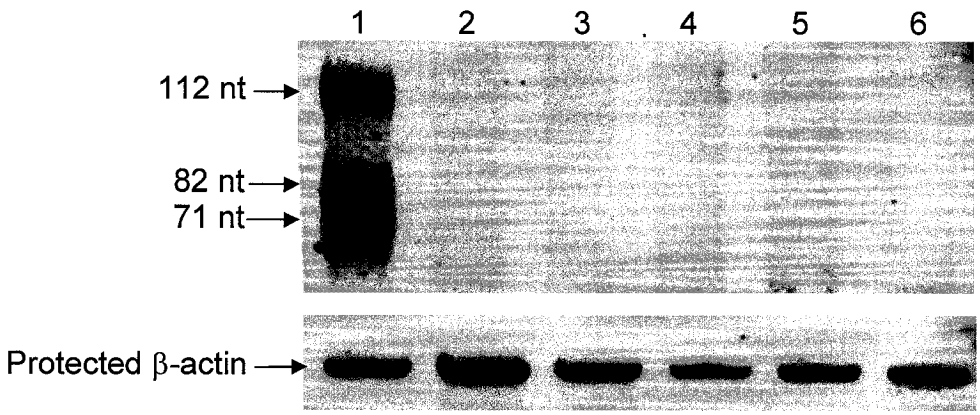
1
2
3
4
5
6
112 nt
82 nt
71 nt
Protected β-actin

B

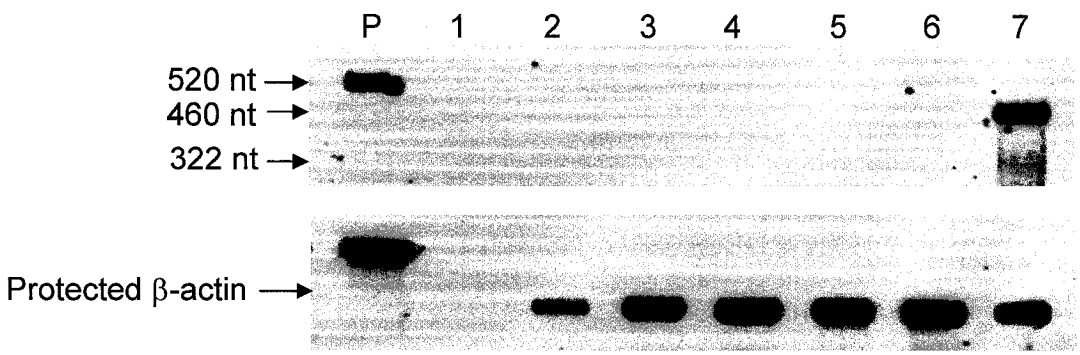
P
1
2
3
4
5
6
7
520 nt
460 nt
322 nt
Protected β-actin

striatum and testis and the levels of PDE10A1 and PDE10A2 transcripts were affected by the expression of the mutant huntingtin transgene in the striatum, but not in the testis.

Comparison of PDE10A2 promoter region between mouse and human

The genomic DNA sequence upstream of the identified transcription start sites in the mouse PDE10A2-specific exon 1a is highly GC-rich and does not contain typical TATA or CAAT boxes. Similarly, the human PDE10A2 and PDE5A promoters do not contain TATA or CAAT boxes (Fujishige *et al.,* 2000; Lin *et al.,* 2001). The mouse and human PDE10A2-specific promoters were aligned using CLUSTALW (Thompson *et al.,* 1994). The mouse PDE10A promoter was analysed for putative transcription factor regulatory elements using MatInspector 2.2 (Quandt *et al.,* 1995) and potential *cis*-acting regulatory elements that were conserved between the human and mouse PDE10A regulatory regions were identified (Fig. 3-12A and B). Numerous myeloid zinc finger 1 (MZF-1) and specificity protein (Sp1) binding elements were found distributed throughout the promoter region (Table 3-1). Several GC-rich transcription factor binding sites known to be involved in cell cycle regulation and differentiation such as early growth response protein 1 (NGFI-A and NGFI-C) and activator protein (AP) family proteins (AP4 and AP1) were also identified. One NF-kappaB and one AP4 *cis*-elements were identified between transcription start sites A and B, suggesting that NF-kappaB or AP4 may participate in the expression of PDE10A2 from transcription initiation sites B and C. We did not observe any cAMP response element (CRE) or nuclear receptor co-repressor (NCoR)-dependent recognition elements that were conserved in the PDE10A2-specific promoters.

Table 3-1. Conserved potential *cis* regulatory elements in the mouse and human PDE10A2 promoters.

Transcription factors[1]	Consensus Sequence	Number of sites	Position[2]
MZF-1	CCCC	11	-714, -539, -485, -480, -419, -329, -143, -134, -117, -93, +26
GC-1	GGAG	7	-659, -577, -522, -498, -394, -342, -11
Sp1	GGCG/GGAG	9	-970, -964, -933, -882, -736, -210, -60, -38, -23
AP4	CAGC	4	-894, -288, -63, +9
AP2	CCCA/CCCG	4	-708, -548, -327, -223
AHRARNT	CGTG/CACG	2	-813, -811
NF1	TGGC	2	-511, -357
NGFI-A	GCGGGGGCG	1	-587
NGFI-C	GCGG	1	-587
MyoD	CATC	1	-109
E47	GCAG	1	-103
NF-kappaB	TCCC	1	+16

[1]MZF-1, myeloid zinc finger 1; GC-1, GC-box elements; Sp1, specific protein 1, AP4/AP2, activation protein 4/2; NGFI-A, early growth response protein-1A; NGFI-C, early growth response protein-1C; AHRARNT, aryl hydrocarbon receptor /Ah receptor nuclear translocator heterodimers; NF-kappaB, nuclear factor kappaB; MyoD, myogenic regulatory factor D. NF1, nuclear factor –1.
[2]Number of 5'bp of recognition sequence relative to +1 of the mouse PDE10A promoter as shown in figure 3-8.

Figure 3-12. Comparison of mouse and human PDE10A2 promoter regions revealed that they are highly conserved. Schematic representation of the promoter region upstream of the PDE10A2-specific exon 1a showing the relative position of selected transcription factor recognition sites that are conserved in both the mouse and human PDE10A2-specific promoters is shown in A. The promoter region, 5' UTR and coding sequence are depicted as solid, hatched and gray bars, respectively. The position of conserved transcription factor binding sites relative to the 5' most transcription initiation site (site A, Fig. 3-7A) are indicated. CLUSTALW alignment of the mouse and human PDE10A2 promoter sequences is shown in B. The asterisks represent conserved nucleotides in the human PDE10A2-specific promoter compared to the mouse sequence. Dashes indicate insertion/deletions. The position indicated by +1 is the first of three major PDE10A2 transcription initiation sites in the mouse sequence and numbering on the left is relative to this +1 position. Arrows pointing to the right above the mouse PDE10A sequence represent transcription start sites identified in this study. The arrow pointing to the right below the human PDE10A sequence represents transcription start sites reported by Fujishige *et al.* (2000). The amino acid sequence of mouse and human PDE10A2 is shown above the aligned coding sequence.

A

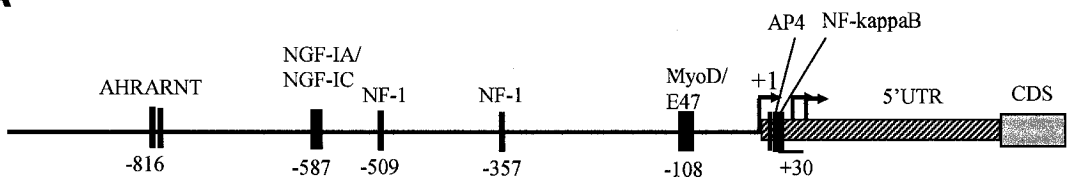

B

```
M AGCGGGCCAGGGGCACACACCACACGCAGAGTGCCAGGGTGCTGGGACCTGAGTTCCAGTGGACGCGCAACGTGGGCGCGGGCGGTGGCGGTTCGGGGAG -951
H ----ACT*G**T**GGGAG**TGG*****-*G***-*A**C*C*C*GGGC*C*C*A*-****G****G**G*C**-**GC*****C*****CGT******

M CGCCTGCTCCGCCAGTGGGCGTCTTCTGCCGCCGCCACCACCGCCGCCTCCACGGGCAGCAGCACTGCGGCGCTTTTCTCCGCTGCTCTGGAGCAGCCGC -851
H ************************************G*****A*****************G*************************T*C***A******

M CGCGGCTCAGGCGCCGGCCGGAGCTTGCACACACCACGCCACGCCCGCAGGCAGCGTCCCGGCAG--CCTCGCCA-GGCCGGGAAGGACGCGGATCGTGC -754
H **A*******C*****----****GC*****************T*****G**G***T*C**C*TC***A***CC****C**G*******C***T****

M GTACCAGCCCGCACCCCGGCGCAGCGATCGGGACTCGTCCCCCCGCCCGCGGTCCTATTGAATCCCAAAGGGAACACGATGTGAACCCCCGGGCCGGAGA -654
H *CG**T*AGG*T*G**A*****C*TCGC****G*CT*G*****A*G**CG******CCC*C*A*****GCC**G***A*******GA*TA*ACTG****G

M GGCACCCTAGACCCGAGAGGCGGACCGGACCAGAGCCTGGGCAGCGTCGCGGGGAGGGCCGCGTGCTGCGGGGGCGGAGCCCGCAGAGTCCGGGCC-GCCG -555
H *AAG**CG*****G******A*****A*G*AGCG*TTC****G**CGGCA****T****A***C*****************A*C***C**C****C****

M CGCCC-TCCCGCCTGC------CCCCCTTGCAAGCTGGGGAGGAGGGCCATGGCTAGCCCGGAGGAGCGGCTCGCTCCCCACCCCCAGGCCCCACTGCGG -462
H *****C*******C**GGCCTG****TCC**GGC*C********A--*******C****TC*******CT**T*******G********GT**C****CA

M GAGTCTGGGGACGAGCCCGGCCGTGTCC------AAGTCCCTCTGGAACCCCGGTGCGGCGCGGCCAGCGGGCGGAGTACAGTGGGCCTGAGCCTGGCCC -368
H *C*G*C**********G***T*C*G**CCGGCA**C***GC*C*********CT*A********G*****G****CG*G*C*****C*G***C*****

M GGGAGCTGCTTGGCTGCAGCCGGGAGGAGCTAGCGGCGCCCCCGCCCCTGTCCCGGTCCCTGTCTCCCGCAGGCCACGCCAGCCCCACTGGGGGCCCCAG -268
H CC***TG**C****C*TG******C*****GC**C*********G**C*C***------*C**CT*********G*C********G**********G*

M CGCCCTCTCCGCTCTCCGTGCCGGAGGCTGTGGTTGGGTGGCGGCCCGTGCTCCCTGGGCGCTTGCCTTCTCCTCCCCTGTCCCCTCCTCCTCCTTTTCA -168
H *********T**G*---*C*G***C*****C**C*****C********C*******T******C********G****GG***************--*-C**

M TCTTCCTGGTACTTCTGGCCGCCGCCCCCCCTCCCCCCTCCCCCTCTTGTCCCCTCCTCATCTGCCTTCCACCTCCCCGCGCGTCTCCCGAGAAGGGAGG -68
H ****T**TT**********************CG*********T**T**C*******************T**********T*********AG*********

                                                                    +1
M GCGCAGCGGCGGCTGGAGGAGGAGGAGGCGGCGGCGGCGATGCTGGCGGCCGCCGGCGGAGGAGGAGGACAAGAGGCAGCTCCCTTGAGCGTCCCCCCAGG +33
H *************-**C**C**C*---*A**A****************A**A---************************************A*CA*

M CAGTAGTCACCGCAGCAGCGGTGGCAGCAGCGGTGGCAGCGGCGGGCGGCGGCGGCTCTTCCTCTCGCCTGCGATTCAAGGCTTGCTGCTCCCTGCCCGC +133
H *************G**G**********G---------*************************************C*C**G***********T**A*****T

M GCCGGGCCCCGGCCATCTCCGCCGCCGCGGCTTCCCCTACACCCGGGTGCACGCCGCGCGGACTCCTCGGATTTTCCGGGCGCCGGCGGGGGCTGCCCTG +233
H *****T********GC*G********C*****C*****TGG**A**CC**C**********G****C*C*GC**C**C*********---------**A*

M GCCTCGGCCCCGGCTCTGCCGCCGGTGGCCGAACTCTTTGGCGGCCCCGAGGCGCCGCCTTCCCCCTTGCCACCGTTTGGCCGCTGCCCTTCGGCTCCGA +333
H **GG****------------------****A*****CGC****T****AG******AG****G****C***G***CGGCCG******T************

    M  E  D  G  P  S  N  N  A  S  C  F  R  R  L  T  E  C  F  L  S  P
M CATGGAAGATGGACCCTCTAACAATGCGAGTTGCTTCCGAAGGCTGACCGAGTGTTTCCTCAGCCCCA  +401
H ***************T*****T*********C**********************C*****G*******
```

3.3 Discussion

In this study, we demonstrated that PDE10A expression in the striatum and testis is regulated through differential promoter usage, alternative splicing and polyadenylation site selection giving rise to an abundant 9 kb mRNA that includes the sequence of exon 1a in the striatum and a 4 kb mRNA that includes the sequence of exon 1 in the testis. The use of different transcriptional units and exon splicing of a single PDE gene to regulate protein production in different tissues is common among different PDE genes in a variety of mammalian cells (Beavo, 1995; Conti & Jin, 2000; Soderling & Beavo, 2000). We also demonstrated that the expression of the N-terminus of mutant huntingtin in R6 HD transgenic mice decreased the rate of transcription from two of three transcription initiation sites on the promoter of the striatial-specific isoform, PDE10A2, and that the decreased transcription was associated with transcription start sites used in the striatum but not in the testis.

The levels of the N-terminus of mutant huntingtin in R6 mice determined the initial time and the rate of decline of the steady-state level of the PDE10A mRNA

The R6/1 and R6/2 transgenic HD mice both express exon 1 of the human *huntingtin* as a transgene under the control of the endogenous human huntingtin promoter. They differ in the length of CAG repeat (R6/1, [1]N89-115Q; R6/2, N89-150Q) and the site of transgene integration (Mangiarini *et al.*, 1996). Using a polyclonal antibody against an epitope downstream of the polyglutamine repeat region, we observed a higher level of expression of the N-terminus of mutant huntingtin protein in the brains of R6/2 compared

[1] The constructs used in this thesis are defined by the number of amino terminal amino acids of the human huntingtin sequence they express followed after the dash by the number of contiguous polyQ within the amino acid sequence.

to that in R6/1 mice. This is consistent with previous observations that the levels of transgene expression are about 31% and 75% of the endogenous huntingtin in R6/1 and R6/2, respectively (Mangiarini *et al.,* 1996). The size of the detected transgene product (~300 kDa) exceeded the predicted molecular weight for both the R6/2 and R6/1 transgene proteins, indicating that the Hum I antibody detected a form of the N-terminal mutant huntingtin that had formed a soluble protein aggregate, perhaps in association with other proteins, even though the samples were treated to dissociate protein complexes for gel electrophoresis. This observation agrees with previous findings that the N-terminal exon 1-encoding mutant huntingtin in R6 mice has a property of forming highly stable self-aggregates and aggregates with other proteins via the polyglutamine region (Davis *et al.,* 1997; Busch *et al.,* 2003).

The steady-state levels of the PDE10A (Hebb *et al.,* 2004), cannabinoid receptor 1 (CB1) (McCaw *et al.,* 2004), dopamine- and adenosine-regulated phosphoprotein (DARPP32) (Gomez *et al.,* 2006) and preproenkephalin mRNAs (Gomez and Denovan-Wright, unpublished result) start to decrease at 4~5 weeks of age in the striatum of R6/1 mice. The amount of detectable mutant huntingtin N89-115Q in R6/1 increased starting at ~ 4 weeks of age (Fig 3-5). It appeared that the amount of the N-terminal mutant huntingtin expressed correlated with when the mRNA levels started to be affected. It has been shown that the rate of decline for the steady-state levels of each transcript in the striatum of R6/2 mice is faster than in R6/1 mice (Hebb *et al.,* 2004; McCaw *et al.,* 2004; Gomez *et al.,* 2006). This could be attributed to the level of expression of transgene product, the length of CAG repeats within the transgene, the insertion site of the transgene, or a combination of all. The observation that R6/2 mice had a higher

expression and a faster rate of accumulation of the N-terminal mutant huntingtin compared to R6/1 mice provides evidence that the level of transgene expression may be one of the determining factors for the differential rate of decline of these transcripts in these two lines of HD transgenic mice.

In eukaryotes, the primary transcript is first synthesized during transcription followed by RNA processing that includes 5' end capping, co-transcriptional splicing of intron, and addition of a poly(A) tail, yielding a functional mRNA. However, the levels of mRNA measured at any one time reflect the balance between synthesis and mRNA turnover. Multiple copies of AU-rich response elements (AREs) are situated between the first and the second polyadenylation signal in exon 25 included in the extended 3' UTR in striatal PDE10A2. AREs influence mRNA stability and a subset of AREs enhance the rate of mRNA degradation by stimulating poly(A) shortening by 3' to 5' ribonucleases (Ross, 1995). We hypothesized that the decrease in the steady-state level of PDE10A2 mRNA in the striatum of HD mice (Hebb *et al.*, 2004) may have been caused by 3'UTR mRNA instability. In wild-type mice, the levels of PDE10A detected by a coding region-specific probe did not change with increasing age although the levels of mRNA containing the extended 3' UTR did decline suggesting that the 3' UTR may be less stable in older wild-type mice. In contrast, in R6 mice, the rate of decline in the PDE10A2 coding sequence was proportional to the rate of decline in the PDE10A2 3' UTR sequence. The decrease in both the coding and 3' UTR regions began at ~4 and 5-6 weeks of age in R6/2 and R6/1 mice, respectively. These observations suggest that the early decline of PDE10A mRNA in HD mice was not associated with the N-terminus of mutant huntingtin transgene-induced 3' UTR instability. Further, there was a significant

decline in the levels of primary and mature transcripts of PDE10A2 starting at 6 week-old R6/1 mice ($P<0.05$). The parallel decline of mature and primary transcripts of PDE10A indicated that the presence of the mutant huntingtin N89-115Q affected transcription initiation of PDE10A2 mRNA rather than post-transcriptional mRNA stability. Similarly, we have found that the rate of transcription of the CB1 (McCaw *et al.*, 2004) and DARPP-32 genes is reduced in 4 week-old R6/2 and 5-6 week-old R6/1 mice compared to wild-type mice (Gomez *et al.*, 2006). In each case, the initial time of decrease and rate of decrease was dependent on the length of polyglutamine repeats or the amount of mutant huntingtin transgene product expressed in the two R6 mouse strains or both.

The N-terminal mutant huntingtin selectively reduced transcription from specific transcription start sites on the PDE10A2 promoter

In the striatum, transcription initiates at three distinct sites in the PDE10A2-specific promoter. These sites, located within a 50 bp region, were identified by 5'RLM-RACE and RPA analysis. Similarly, cDNAs with 3 different 5' ends were identified for human PDE10A2 (Fujishige *et al.*, 2000). The relative position of the start sites in the mouse PDE10A2 gene did not correspond to any of the 5' ends identified in human PDE10A2 mRNAs. In contrast to the reported 5' cDNA ends of human PDE10A2, which are ~30 bp upstream from the ATG codon (Fujishige *et al.*, 2000), the farthest 5' transcription start site in exon 1a of the mouse PDE10A gene was 333 bp upstream of the ATG codon (Fig. 3-12).

Transcripts from transcription start site B and C were decreased while transcripts from site A were relatively unaffected by the expression of the N89-115Q in R6/1mice.

In contrast, the N89-115Q transgene product appears to ubiquitously exert repression on all transcription start sites used on the CB1 and DARPP32 genes (McCaw *et al.*, 2004; Gomez *et al.*, 2006). One likely scenario for specific transcriptional repression from start site B and C but not A is that transcription start sites B and C may be used in different populations of striatal neurons than start site A. These two populations of cells could have different concentrations of the N-terminal mutant huntingtin N89-115Q or other transcription factors that influence the activity of mutant huntingtin, thus leading to different levels of transcription from the PDE10A promoter. This scenario, therefore, would predict complete loss of transcripts from some cells but little change in mRNA levels in other cells. We have been unable to determine whether these mRNAs are produced by different subpopulations of neurons within the striatum. Emulsion autoradiography demonstrated that there was a uniform decrease in hybridization intensity of a PDE10A2-specific probe in R6/2 compared to wild-type mice (data not shown), suggesting that there are not distinct subpopulations of neurons that express PDE10A2 mRNA from specific start sites. However, this technique may lack precision for quantification of mRNA levels in neuronal subpopulations. A second scenario is that start sites A, B and C are used in the same cells and mutant huntingtin N89-115Q affects the activity of RNA pol II on site B and C extensively but less so on site A. This would predict even loss of transcripts throughout the striatal cells. Indeed, Hebb *et al.* (2004) observed that there is even distribution of the PDE10A mRNAs in the striatum, nucleus accumbens and olfactory tubercle of mice and rat and that there is even loss of transcripts in these brain regions in 10 week-old symptomatic R6/2 HD (N89-150Q) mice. This suggests that mutant huntingtin N89-115Q in R6/1 mice expressed within the same

striatal cells may have a different sensitivity on the transcription from site B and C than site A. Moreover, it has been shown that the preproenkephalin mRNA is preferentially lower in the spiny striatal neurons projecting to the lateral pallidum in early stages of HD, and the substance P mRNA in the medial pallidum is reduced only in later stages of HD (Richfield *et al.,* 1995). It remains to be determined whether transcripts from sites B and C are produced by neurons projecting to the lateral globus pallidum, which are affected early in HD and whether transcripts from site A are present in neurons projecting to the medial pallidum, which are affected late or whether all transcripts are produced by striatal neurons and differentially affected by the amino terminus of mutant huntingtin.

Mutant huntingtin may interact with specific transcription factors in the striatum to alter transcription initiation

Neuronal intranuclear inclusions (NIIs) are first observed in the brains of 8 week-old R6/1 mice and 4.5 week-old R6/2 mice and the proportion of striatal neurons containing NIIs increases to ~ 80% of the neuronal populations by about 15-16 weeks in R6/1 and 10 weeks in R6/2 mice. At the same time, the mean inclusion size also increases markedly (Davies *et al.,* 1997; Hansson *et al.,* 2001). The role of NIIs in the progression of HD is controversial, with evidence suggesting that they may have a deleterious or a neuroprotective function in the brain (Sisodia, 1998; Saudou *et al.,* 1998; Yu *et al.,* 2002; Bates, 2003; Shastry, 2003; Arrasate *et al.,* 2004). Since the first appearance of NIIs occur in the hippocampus and the cerebral cortex not the striatum (Davies *et al.,* 1997; DiFiglia *et al.,* 1997; Gutekunst *et al.,* 1999), it is unlikely that the neuronal inclusion is causative to the neurodegeneration that first appears in the striatum.

Saudou *et al.* (1998) have shown that the presence of neuronal inclusions in the nucleus does not correlate with huntingtin-induced cell death in cultured striatal neurons transfected with the N-terminal mutant huntingtin. Interaction of mutant huntingtin with the extended polyQ repeat of TATA box binding protein (TBP) can structurally destabilize the transcription factor, which is independent of the formation of insoluble aggregates (Schaffar *et al.*, 2004). PDE10A2 primary transcript levels were decreased in 6 week-old R6/1, which precedes the time that NIIs are detected in these mice. We have shown that the accumulation of the Hum I-immunoreactive mutant huntingtin N89-115Q in the increasing ages of R6/1 mice was directly correlated to the significant decrease in the steady-state level of PDE10A2 at 4-5 weeks of age in R6/1 mice. This indicates that this form of mutant huntingtin N89-115Q in R6/1 mice, not the visible nuclear inclusions which occur late, is likely the cause for the decreased mRNA in R6/1.

Mounting evidence has suggested that the soluble form of mutant huntingtin interacts with transcription factors to alter transcription of target genes (Saudou *et al.*, 1998; Dunah *et al.*, 2002; Li *et al.*, 2002; Yu *et al.*, 2002). Molecular modeling and X-ray diffraction have demonstrated that polyglutamine repeats in mutant huntingtin are capable of forming β-sheets with other polyglutamine-containing transcription factors via polar zippers *in vitro* (Perutz, 1995; Perez *et al.*, 1998). Yeast two-hybrid selection analyses have shown that mutant huntingtin can interact with NCoR to repress transcription from sequence-specific ligand-activated receptors such as the retinoid X-thyroid hormone receptor dimers and other nuclear receptors (Boutell *et al.*, 1999). Co-immunoprecipitation assays and cellular localization studies demonstrated that the polyglutamine region in mutant huntingtin can preferentially bind to TAFII130 and

suppress cAMP-responsive element binding protein (CREB)-dependent transcriptional activation (Shimohata *et al.*, 2000). Polyglutamine-containing transcription factor TATA-binding proteins (TBP)-positive structure has been also shown to co-localize with mutant huntingtin-labeled middle frontal gyrus in HD brains (van Roon-Mom *et al.*, 2002). Taken together, these studies suggest that the interaction of mutant huntingtin with factors that control transcription initiation may alter the steady-state levels of specific mRNAs. However, it remains to be determined how the interaction of mutant huntingtin with ubiquitous transcription factors and complexes would cause changes in the expression of a limited number of genes specifically in the striatum *in vivo*.

Comparison of promoter regions between the mouse and human PDE10A genes revealed several conserved transcription factor binding site sequences. The highly GC-rich PDE10A2 promoter region has nine Sp1 and eleven MZF-1 binding sites. The soluble form of mutant huntingtin can interact with Sp1, which is thought to cause decreased transcript levels of target genes such as the D2 receptor and nerve growth factor (NGF) in cultured HD cells and striatal tissues from HD patients (Dunah *et al.*, 2002; Li *et al.*, 2002). Although *in vitro* coimmunoprecipitation and binding assays demonstrated that Sp1 can interact with mutant huntingtin in a polyglutamine length-dependent fashion and that over expression of Sp1 reduced cell toxicity and other neuronal defects caused by intranuclear mutant huntingtin (Li *et al.*, 2002), it remains to be determined how only a specific subset of Sp1-regulated genes are affected by the expression of mutant huntingtin. For example, the promoter of the mouse β-actin gene contains several Sp1 binding sites, but transcript levels of β-actin do not change in HD mice (Luthi-Carter *et al.*, 2000). CREB-binding protein (CBP) and several transcription

factors having histone deacetylase activity can interact with the polyglutamine region in mutant huntingtin but it remains to be determined whether such interaction directly affects transcription (Shimohata *et al.,* 2000; Steffan *et al.,* 2000). Neuron restrictive silencing factor (NRSF), a *trans*-factor that has been shown to accumulate in the nucleus as result of the expression of mutant huntingtin, decreases the expression of brain-derived neurotrophic factor (BDNF) and other genes in the cortex (Zuccato *et al.,* 2003). We did not observe any CRE or neuron restrictive silencing element (NRSE) consensus sequence of the human and mouse PDE10A2 promoters from -900 to +50 region. Therefore, it is unlikely that CREB or NRSF are directly involved in the alterations of PDE10A2 transcription in R6 transgenic mice. Although mutant huntingtin has been shown to interact with NCoR and TBP (Boutell *et al.,* 1999; Kegel *et al.,* 2002; van Roon-Mom *et al.,* 2002), the lack of NCoR interacting- thyoid hormone receptor (THR)/retinoic acid receptor (RAR) response elements and TATA box in the PDE10A2 promoter suggest that NCoR and TBP may also not be directly responsible for decreased PDE10A2 transcription.

We have identified a striatal-specific PDE10A isoform, PDE10A2, and determined that in HD transgenic mice the expression of the N-terminal fragment of mutant huntingtin causes levels of PDE10A2 mRNA to decrease by altering transcription initiation early in HD progression from the PDE10A2 promoter. We have demonstrated that the amount and the rate of accumulation of mutant huntingtin transgene products in the brains of R6/1 and R6/2 mice correlated with the initial time and the rate of decline of the PDE10A2 mRNA in the striatum of these two HD mice. The N-terminal exon 1 encoding portion of mutant huntingtin N89-115Q appeared to exert transcriptional

repression in a promoter- and transcription start site-specific manner on the mouse PDE10A gene. It remains to be determined how the N-terminus of mutant huntingtin interferes with the interaction between *cis*- and *trans*- elements on the PDE10A2 promoter giving a specific reduction of the mRNA.

CHAPTER 4

Mutant Huntingtin Affected PDE10A2 Promoter Activity Prior to Altering DNA-Protein Interactions in Striatal Cells

4.1 Introduction

We determined that the N-terminus of mutant huntingtin in R6/1 mice decreased transcription initiation of several striatal-specific genes including PDE10A, CB1 and DARPP32 and that decreased transcription occurred early in a progressive series of changes that occur in multiple models of HD and in HD patients (Hebb *et al.*, 2004; McCaw *et al.*, 2004; Gomez *et al.*, 2006 and Chapter 3). Caspase-cleaved N-terminal fragments of mutant huntingtin accumulate in the nucleus and result in the formation of NIIs (Davies *et al.*, 1997; DiFiglia *et al.*, 1997; Lin *et al.*, 2001; Schilling *et al.*, 1999). It remains to be determined whether soluble or insoluble N-terminal mutant huntingtin directly altered transcription. We chose to study the regulation of the PDE10A2 promoter because the mutant huntingtin N89-115Q expressed in R6/1 mice exerted specific transcriptional repression on two of three transcription initiation sites (Chapter 3). It remains to be determined how N-terminal mutant huntingtin affected the interaction between *cis*- and *trans*- elements of the PDE10A2 promoter that give a transcriptional repression on specific start sites.

Many transcription factors have been shown to associate with mutant huntingtin *in vitro* and *ex vivo*. These factors include Sp1 (Dunah *et al.*, 2002; Li *et al.*, 2002), NcoR (Boutell *et al.*, 1999), CBP (McCampbell *et al.*, 2000; Nucifora *et al.*, 2001), TBP (van Roon-Mom *et al.*, 2002), p53 (Steffan *et al.*, 2000) and peroxisome proliferation activator receptor (PPAR) gamma-coactivator 1 alpha (PGC1-α) (Cui *et al.*, 2006). Hence, one of the theories for transcriptional dysregulation is that mutant huntingtin binds to and sequesters these factors into soluble or insoluble complexes thus compromising their normal function in transcription. We hypothesized that if sequestration of these factors by

mutant huntingtin occured in the brains of R6/1 mice, we would see reduced DNA binding activities of these, and perhaps other, factors on the PDE10A2 promoter.

In this study, we examined how the N-terminus of mutant huntingtin affected DNA binding activities of transcription factors using multiple techniques that measure protein-DNA interactions *in vitro* and determined where the N-terminus of mutant huntingtin exerted repression on the promoter of the PDE10A2 gene using several cell culture models of HD.

4.2 Results

Examination of protein-DNA interactions in vitro

To examine whether the human huntingtin transgene product (N89-115Q) in R6/1 mice altered the DNA binding activity of transcription factors *in vitro,* nuclear proteins containing soluble transcription factors were isolated from the forebrains of 5 week-old wild-type, 5 week-old R6/1, 16 week-old wild-type and 16 week-old R6/1 mice. Western analyses using an antibody raised against the human huntingtin-specific polyproline region immediately downstream of the polyQ repeat (Hum 1; Rodriguez-Lebron *et al.,* 2005) were performed to determine the distribution of the N89-115Q transgene product in the subcellular fractions isolated from the forebrains of wild-type and R6/1 HD mice. There was a ~300 kDa Hum 1-immunoreactive band present in protein fractions isolated from R6/1, but not wild-type mice. The relative mobility of this R6 mouse-specific immunoreactive band in western blots was observed in previous experiments (Rodriguez-Lebron *et al.,* 2005). In addition, this antibody cross-reacted with other cellular proteins that were equally abundant in wild-type and R6/1 mice. The level of mutant huntingtin

transgene product in total protein isolated from 16 week-old R6/1 mice was increased compared to the amount observed in total protein isolated from 5 week-old R6/1 mice (Fig. 4-1A). Low levels of mutant huntingtin transgene product were detected in the cytoplasmic fraction in both 5 week-old and 16 week-old R6/1 mice (Fig. 4-1A). There were similar levels of mutant huntingtin transgene product in the 300 mM NaCl-soluble nuclear fraction between 5 and 16 week-old R6/1 mice (Fig. 4-1B). The increased levels of mutant huntingtin transgene product in the 300 mM NaCl-insoluble protein fraction of 16 week-old R6/1 mice indicated that the increase in total mutant huntingtin transgene product in the forebrain of 16 week-old compared to 5 week-old R6/1 mice was mainly due to an increase in the amount of insoluble protein in the nuclear fraction.

Three hundred mM NaCl is known to extract many soluble transcription factors from nuclei (Sambrook *et al.*, 2001). Since the 300 mM NaCl soluble nuclear fraction contained the N-terminus of mutant huntingtin transgene product (Fig. 4-1) in both 5 week- and 16 week-old R6/1 mice, we decided to use this fraction to examine how the expression of N-terminus of exon 1-encoding mutant huntingtin (N89-115Q) altered the DNA binding activity of transcription factors in mice. We employed the Panomics TranSignal protein/DNA array technology to survey protein/DNA interactions. This technique is analogous to electromobility shift assay (EMSA) and allowed us to profile the DNA binding activities of 345 transcription factors simultaneously. A mixture of 345 unique biotin-labelled double-stranded oligonucleotides (TranSignal probe mix) was incubated with nuclear extract isolated from the forebrains of 5 week-old wild-type, 5 week-old R6/1 or 16 week-old R6/1 mice. At 5 weeks of age, transcription of the

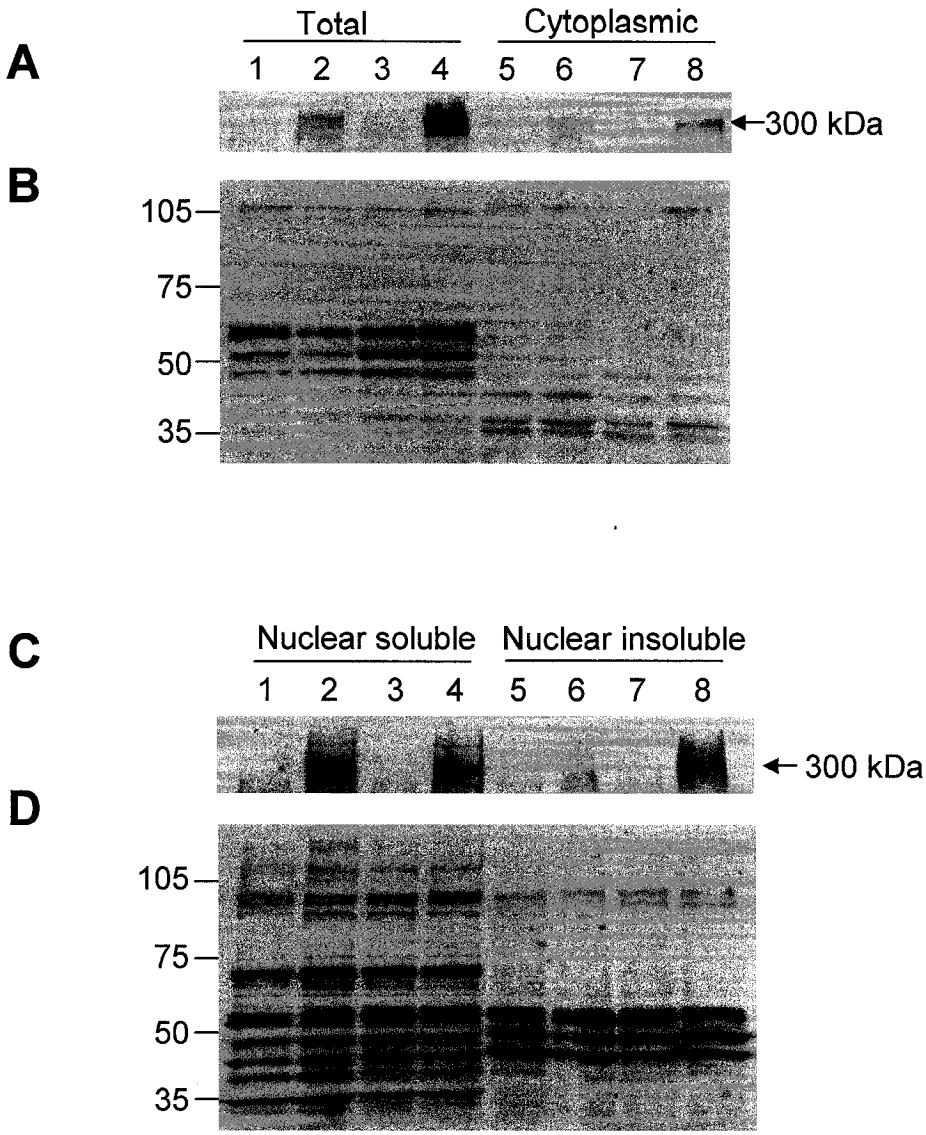

Figure 4-1. Mutant huntingtin was enriched in the 300 mM NaCl soluble nuclear fraction derived from the forebrain of 5 and 16 week-old R6/1 mice. SDS-PAGE was used to fractionate 40 μg of total protein (total), cytoplasmic protein (cytoplasmic), 300 mM NaCl soluble nuclear protein (nuclear soluble), and 300 mM NaCl insoluble nuclear protein (nuclear insoluble). Western blot analysis was performed using Hum I antibody. Proteins were isolated from 5 week-old wild-type (lanes 1 and 5), 5 week-old R6/1 (lanes 2 and 6), 16 week-old wild-type (lanes 3 and 7) and 16 week-old R6/1 (lanes 4 and 8) mice. Panels A and C show the high molecular weight mutant huntingtin protein detected with a 90 min exposure of the film. Panels B and D show lower molecular weight Hum 1-immunoreactive bands that were detected after a 10 min exposure of the film. The relative mobility of molecular weight markers (kDa) are indicated on the left. The Hum 1 immunoreactive band that is exclusively expressed in R6/1 transgenic mice is indicated by an arrow on the right side of each blot.

PDE10A2 gene and steady-state levels of the PDE10A2 mRNA started to decrease and the levels of the mutant huntingtin transgene product had reached detectable levels (Hebb *et al.*, 2004, Fig. 3-4; 3-5). By 16 weeks of age, the steady-state levels of PDE10A2 reached a new lower equilibrium level in the striatum of R6/1 mice and the mice have significant abnormalities in coordination and motor activity (Mangiarini *et al.*, 1996; Li *et al.*, 2005). Therefore, examination of DNA binding activities of nuclear extracts isolated from 5 and 16 week-old mice would elucidate changes that occur at the time when transcription was first affected in these mice and at a time after HD-like symptoms were evident in these mice following a period of expression of mutant huntingtin, respectively. Of 345 transcription factors on the array, 167 transcription factors were expressed in the striatum of 5 week-old wild-type (5 WT), 5 week-old R6/1 and 16 week-old R6/1 (16 R6/1) mice (Fig. 4-2, 4-4). There were 125 transcription factors/DNA interactions detected in both 5 week-old wild-type and R6/1 striatal nuclear extracts (Fig. 4-2). The mean optical density of the hybridization signal, minus local film background, for each spot in two different groups (5 WT versus 5 R6/1) were scatter-plotted (Fig. 4-2). We observed some variability in the intensity of hybridization signal related to the interaction between protein and biotin-labelled double-stranded probes between samples derived from 5 week-old R6/1 compared to 5 week-old wild-type mice. The ratio of the optical density of each spot detected in the blots prepared using 5 week-old R6/1 and 5 week-old wild-type 300 mM NaCl-soluble nuclear fractions indicated that the fold difference of 98% (120/125) of the detected transcription factors was within a two-fold difference and the remaining 5/125 interactions were very close to the two-fold difference

Figure 4-2. There was no difference in DNA binding activities of a large number of transcription factors present in 300 mM NaCl soluble nuclear extract derived from 5 week-old wild-type and R6/1 mice. TranSignal protein-DNA array analysis was performed using 5 μg of nuclear extract isolated from 5 week-old wild-type (A) and R6/1 (B) mice. The normalized optical density of each spot was plotted using SigmaPlot. The X axis represents the normalized optical density for each transcription factor using nuclear extract from 5 week-old wild-type mice. The Y axis represents the normalized optical density of the same transcription factor in the presence of nuclear extract from 5 week-old R6/1mice. Blue and red dash line indicates a 2-fold increase and 2-fold decrease in 5 week-old R6/1 mice compared to 5 week-old wild-type mice, respectively.

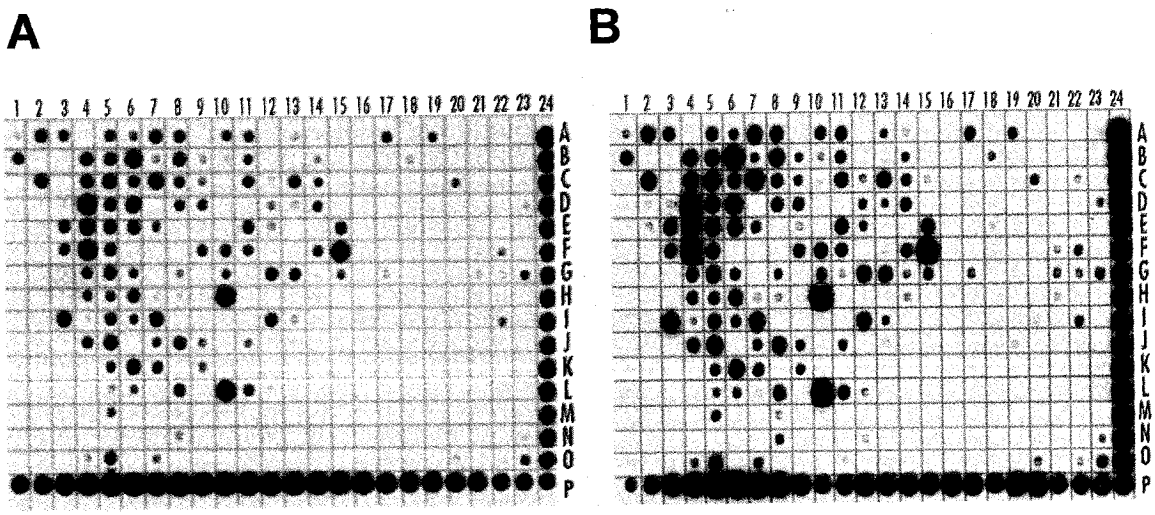
A
B
1 2 3 4 5 6 7 8 9 10 11 12 13 14 15 16 17 18 19 20 21 22 23 24
A B C D E F G H I J K L M N O P

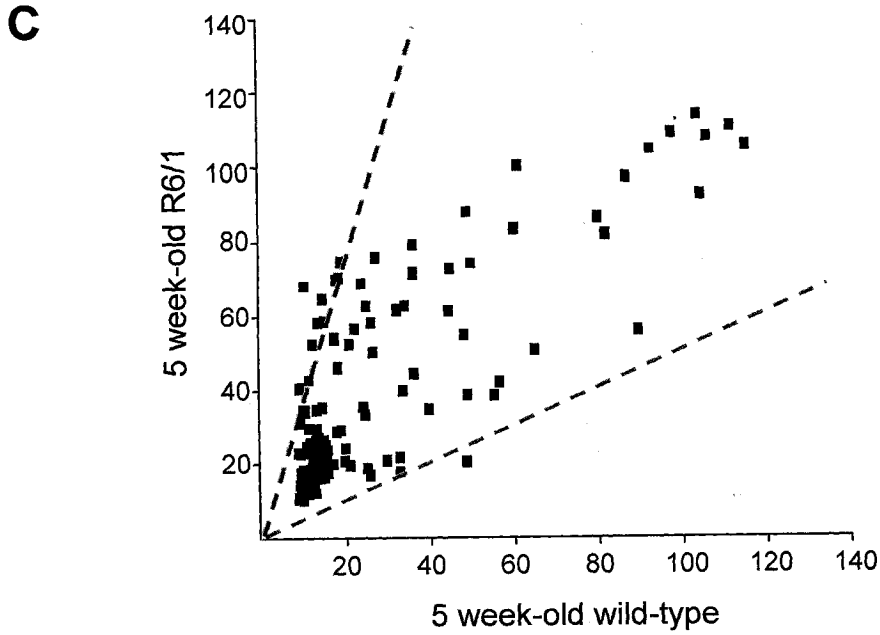
C
5 week-old R6/1
5 week-old wild-type
20
40
60
80
100
120
140

range; two-fold differences in relative hybridization are considered to be the inherent level of variability of these assays (Oweis *et al.*, 2006).

In order to verify the results from the TranSignal protein/DNA arrays, EMSAs were performed with selected consensus probes (Fig. 4-3). The consensus sequence for transcription factors thyroid hormone receptor (TR) (C4 in Fig. 4-2A,B), retinoid X receptor (RXR) (F3 in Fig. 4-2A,B) and vitamin D (1,25- dihydroxyvitamin D3) receptor (VDR) (F4, Fig. 4-2A,B) were chosen because the DNA binding activities detected using the TranSignal Array were very similar in 5 week-old R6/1 compared to wild-type mice (Fig. 4-2). In the TranSignal analysis, the DNA binding activity of AP1 showed the greatest increase in 5 week-old R6/1 compared to 5 week-old wild-type mice (slightly greater than two-fold). It has been shown that NFkappaB could interact with full-length mutant huntingtin *in vitro* using co-immunopreciptiation although it is unclear whether the change occurred early or late in disease progression (Takano *et al.*, 2002). The DNA binding activity of NFkappaB did not show any significant change between nuclear extracts isolated from 5 week-old wild-type and R6/1 mice in our assay. Sp1 and CREB were not detected in the TranSignal assay using the soluble nuclear proteins from 5 week-old wild-type and R6/1 mice but these factors have been shown to interact with mutant huntingtin *in vitro* using GST pull-down (Sp1, CREB) (Stefan *et al.*, 2000, 2001) and yeast two hybrid analyses (Sp1) (Dunah *et al.*, 2002; Li *et al.*, 2002). Individual EMSA analyses confirmed the TransSignal results that there was no significant difference in the DNA binding activities of TR, RXR, VDR, AP1, Sp1, CREB and NFkappaB between the nuclear extracts from the forebrains of 5 week-old wild-type and R6/1 mice (Fig. 4-3). We also tested several transcription factors with different relative signal abundance and

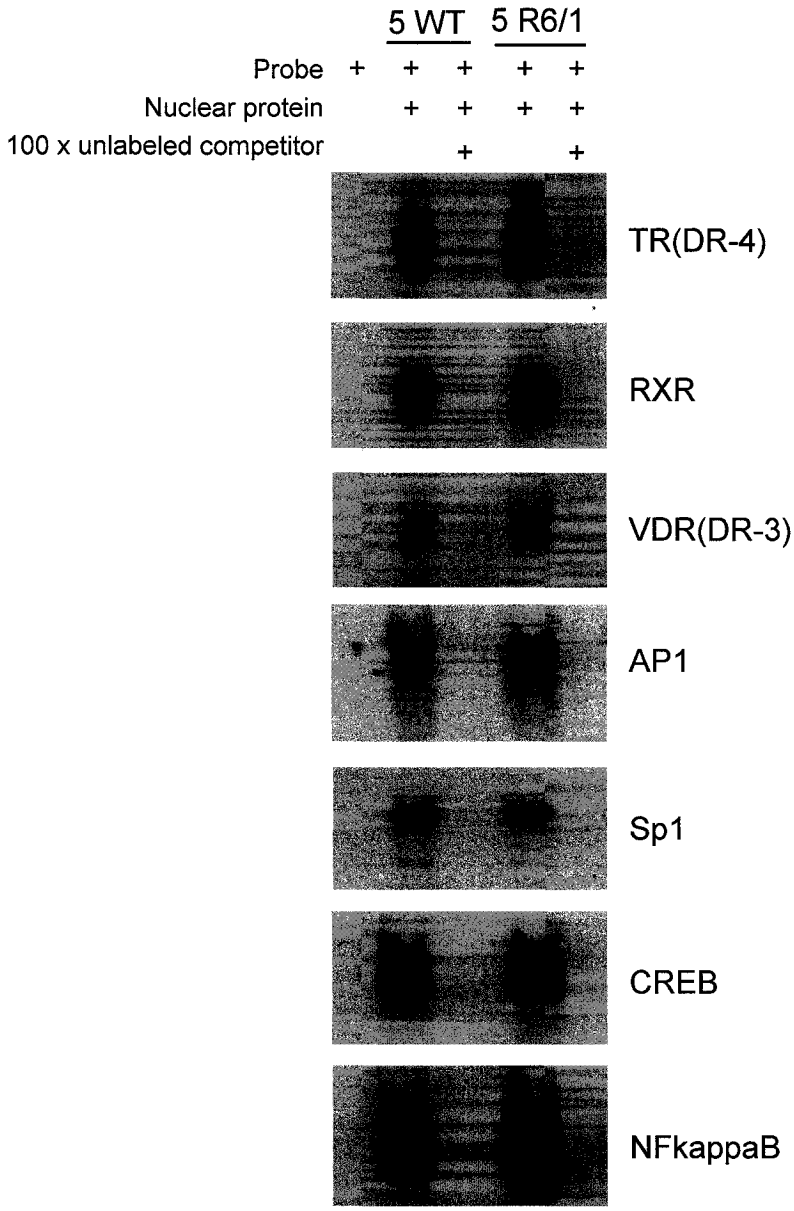

Figure 4-3. The DNA binding activities of the transcription factors TR, RXR, VDR, AP1, Sp1, CREB and NFkappaB were not affected in 5 week-old R6/1 mice. EMSAs were performed using radiolabelled double-stranded consensus sequences for TR, RXR, VDR, AP1, Sp1, CREB and NFkappaB and 5 μg of nuclear extracts derived from 5 week-old wild-type and R6/1 mice. Non-radiolabelled double-stranded consensus sequences (100X molar excess compared to radio-labelled probe) was used as a sequence-specific competitor. Each panel shows the protein-DNA complexes. The name of the factor that has been shown to bind to the double-stranded DNA consensus sequence used is indicated to the right.

found no difference in DNA binding activities between the two nuclear fractions (data not shown). Together, these analyses demonstrated that, in 5 week-old mice, the mutant huntingtin transgene product expressed in the forebrain of the R6/1 mice did not appear to alter the DNA binding activities of any of the set of transcription factors analyzed.

TranSignal protein/DNA array was also performed using 300 mM NaCl-soluble nuclear proteins isolated from the forebrain of 16 week-old R6/1 mice. The TranSignal results showed that the DNA binding activities of transcription factors were significantly different between nuclear extracts from 5 week-old wild-type and 16 week-old R6/1 mice (Fig. 4-4). DNA binding activity corresponding to a set of 73/167 transcription factors were approximately equal in both 5 WT and 16 R6/1 protein fractions. The DNA binding activity of 51/167 transcription factors were lower or undetected in the protein fractions isolated from 16 week-old R6/1 compared to wild-type mice. The DNA binding activity of 42/167 transcription factors were only detected or were higher in the nuclear fraction isolated from 16 week-old R6/1 compared to the nuclear fraction isolated from wild-type mice (Fig. 4-4). EMSA analyses were performed to confirm these findings. Using individual double-stranded probes, EMSA with 16 week-old wild-type and 16 week-old R6/1 soluble nuclear proteins revealed that there was an increase in the DNA binding activity of TR, RXR, Sp1, NFkappaB and CREB in 16 week-old R6/1 compared to wild-type mice. There was no difference in the DNA binding activity of VDR between nuclear extracts isolated from16 week-old wild-type and R6/1 mice. There was a significant decrease in the DNA binding activity of AP1 in 16 week-old R6/1 compared to 16 week-old wild-type mice (Fig. 4-5). The trend of alterations in DNA binding

Figure 4-4. The DNA binding activity of transcription factors were different between nuclear extract derived from 16 week-old R6/1 and wild-type mice. TranSignal protein-DNA array was performed using 5 μg of nuclear extract isolated from the forebrain of 5 week-old wild-type (A) and 16 week-old R6/1 mice (B). The OD value of each spot detected was plotted on the X axis (from blot A) and Y axis (from blot B). Solid circles represent the OD value of transcription factors that were highly enriched in 16 week-old R6/1 nuclear extract compared to 5 week-old wild-type nuclear extract. Open circle represent the OD value of transcription factors that were highly enriched in 5 week-old wild-type nuclear extract compared to 16 week-old R6/1 nuclear extract. Solid triangles represent OD for transcription factors that appeared equivalent in 5 week-old wild-type and 16 week-old R6/1 nuclear extracts. The dash line indicates the predicted correlation between X and Y if there is no difference in binding activity between two groups.

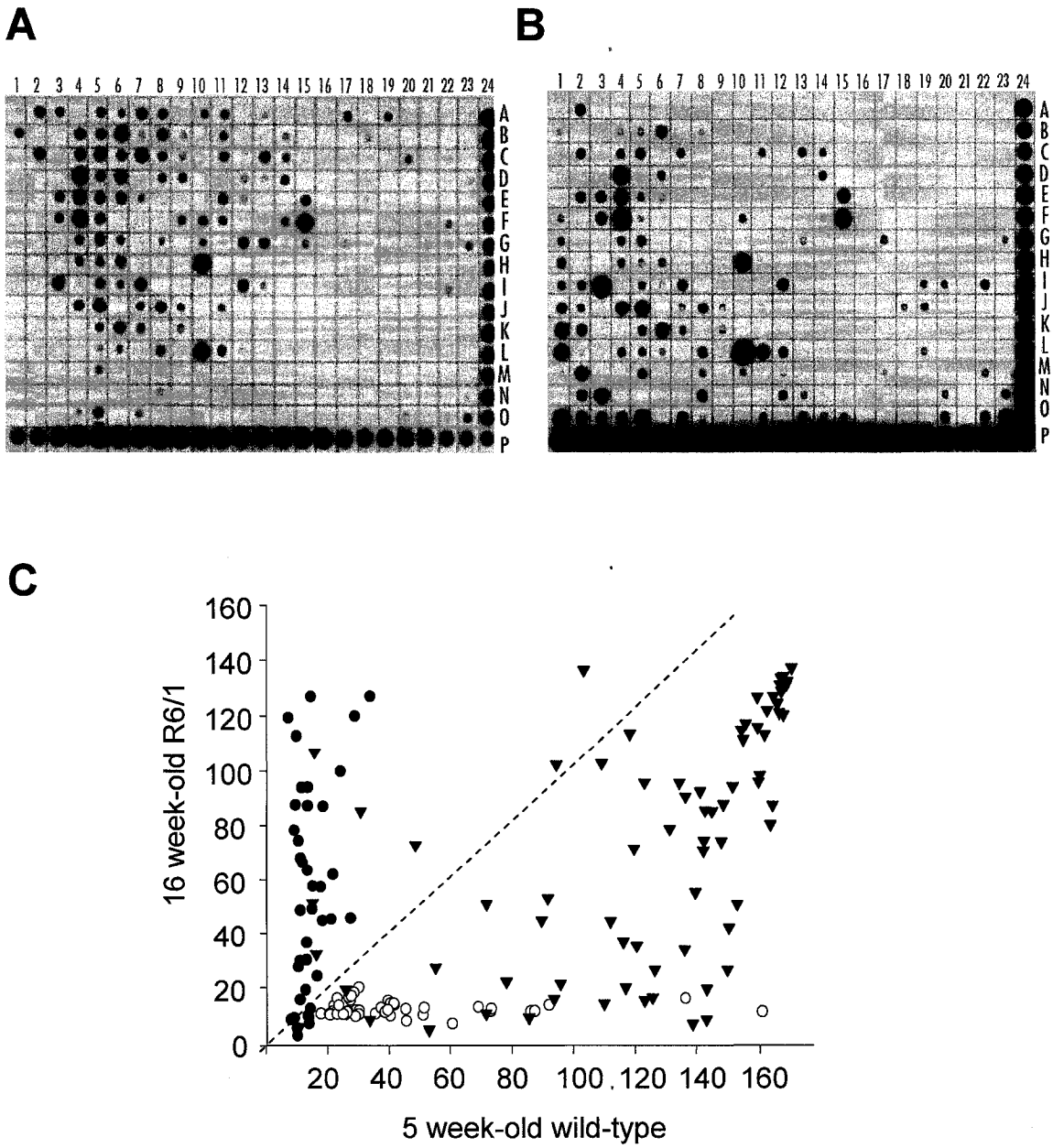
A
B
C
1 2 3 4 5 6 7 8 9 10 11 12 13 14 15 16 17 18 19 20 21 22 23 24
A B C D E F G H I J K L M N O P
160
140
120
100
80
60
40
20
0
16 week-old R6/1
20 40 60 80 100 120 140 160
5 week-old wild-type

Figure 4-5. The DNA binding activity of transcription factors TR, RXR, VDR, AP1, Sp1, CREB and NFkappaB were affected in 16 week-old wild-type mice. EMSAs were performed using radiolabelled double-stranded consensus sequences for TR, RXR, VDR, AP1, Sp1, CREB and NFkappaB and 5 μg of nuclear extracts derived from 16 week-old wild-type and R6/1 mice. Non-radiolabelled double-stranded consensus sequences (100X molar excess compared to radiolabelled probe) was used as a sequence-specific competitor. Each panel shows the protein-DNA complexes. The name of the corresponding consensus sequence used is indicated on the right.

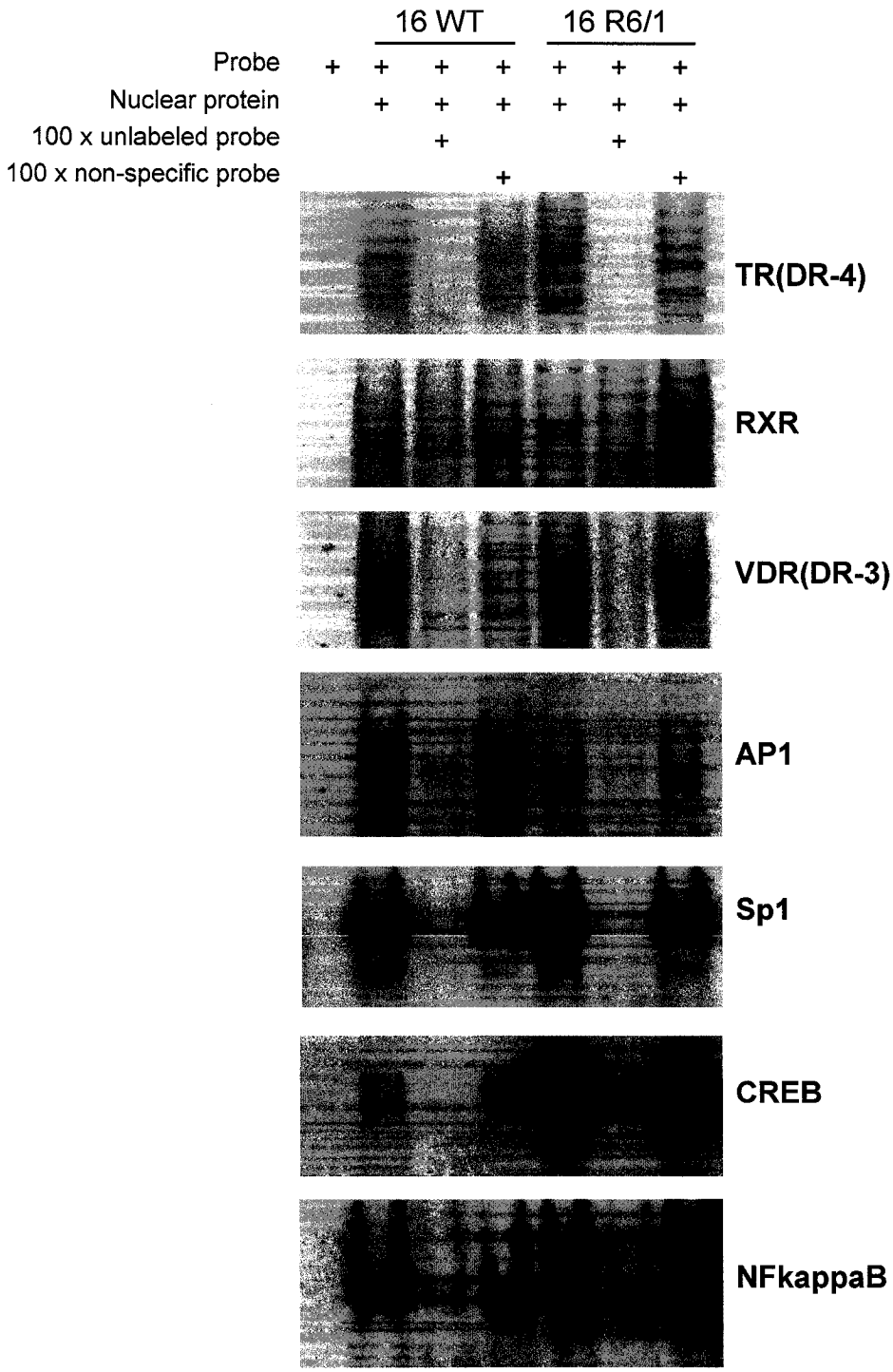
16 WT
16 R6/1
Probe
Nuclear protein
100 x unlabeled probe
100 x non-specific probe
TR(DR-4)
RXR
VDR(DR-3)
AP1
Sp1
CREB
NFkappaB

activity of transcription factors in 16 week-old R6/1 mice compared to wild-type mice in EMSA analyses was consistent with the TranSignal array analysis (Fig. 4-4).

The transcription factors detected in TranSignal array are listed and grouped by functional families, including cell growth, differentiation and proliferation, basal transcription machinery and chromatin modification, cytokine-related signal transduction, brain function and development, lipid and insulin metabolism, cardiac functions as well as those involved in conditional stresses (Table 4-1).

Next, we selectively examined the protein levels of several transcription factors that were tested in EMSA to determine whether changes in DNA binding activities in 16 week-old R6/1 mice relative to younger R6/1 mice and wild-type mice was related to relative protein level within 300 mM NaCl soluble nuclear fractions. Western analyses using antibodies for nerve growth factor-induced clone A (NGF-IA), VDR, CREB, and NFkappaB indicated that the expression levels of these factors did not change in the soluble nuclear fraction isolated from the forebrains of 5 week-old and 16 week-old R6/1 mice compared to 5 week-old wild-type mice (Fig. 4-6). The unchanged expression of VDR was consistent with the unchanged DNA binding activity of VDR in both 5 and 16 week-old R6/1 mice. For NGF-IA, CREB and NFkappaB, it appeared that at 5 weeks of age, the N-terminus of mutant huntingtin in these mice (N89-115Q) did not alter either the DNA binding activity or the levels of expression of these factors. However, long-term expression of the N-terminus of mutant huntingtin altered the DNA binding activity, but not the protein level, of CREB and NFkappaB. We also measured the protein levels of Sp1 and found that Sp1 protein levels increased in total proteins of 15 week-old R6/1 mice but that there was no difference in Sp1 levels among 6- and 9-week-old wild-type

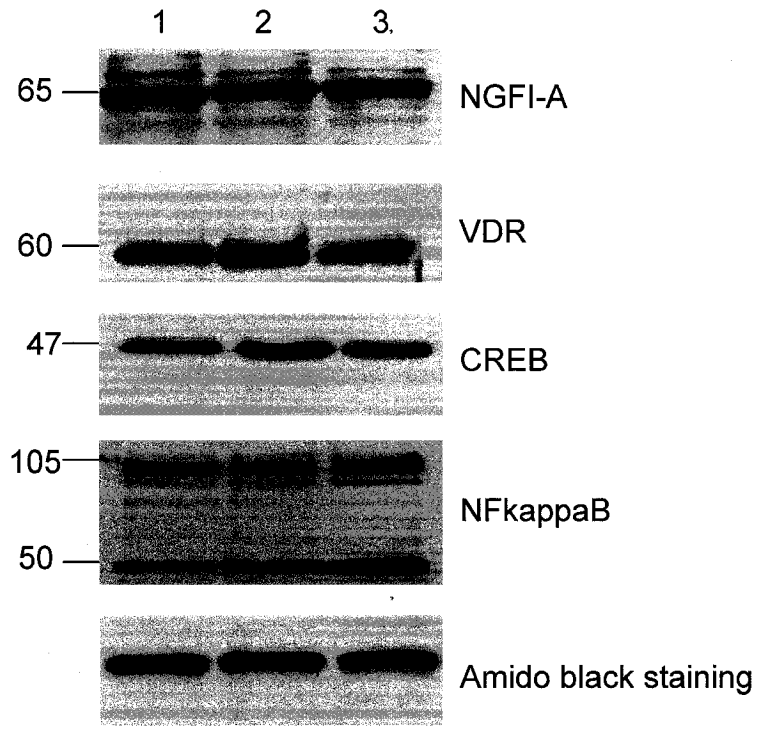

Figure 4-6. There was no difference in the protein levels of the transcription factors NGFI-A, VDR, CREB, and NFkappaB amongst 5 week-old wild-type, 5 week-old R6/1 and 16 week-old R6/1 mice. Western blot analysis was performed on 20 μg of 300 mM nuclear soluble proteins isolated from 5 week-old wild-type (lane 1), 5 week-old R6/1 (lane 2), 16 week-old R6/1 (lane 3) forebrain. The size (kDa) and identity of each transcription factor tested are shown on the left and right side of each panel, respectively. An example of amino black staining of one of western blots is shown.

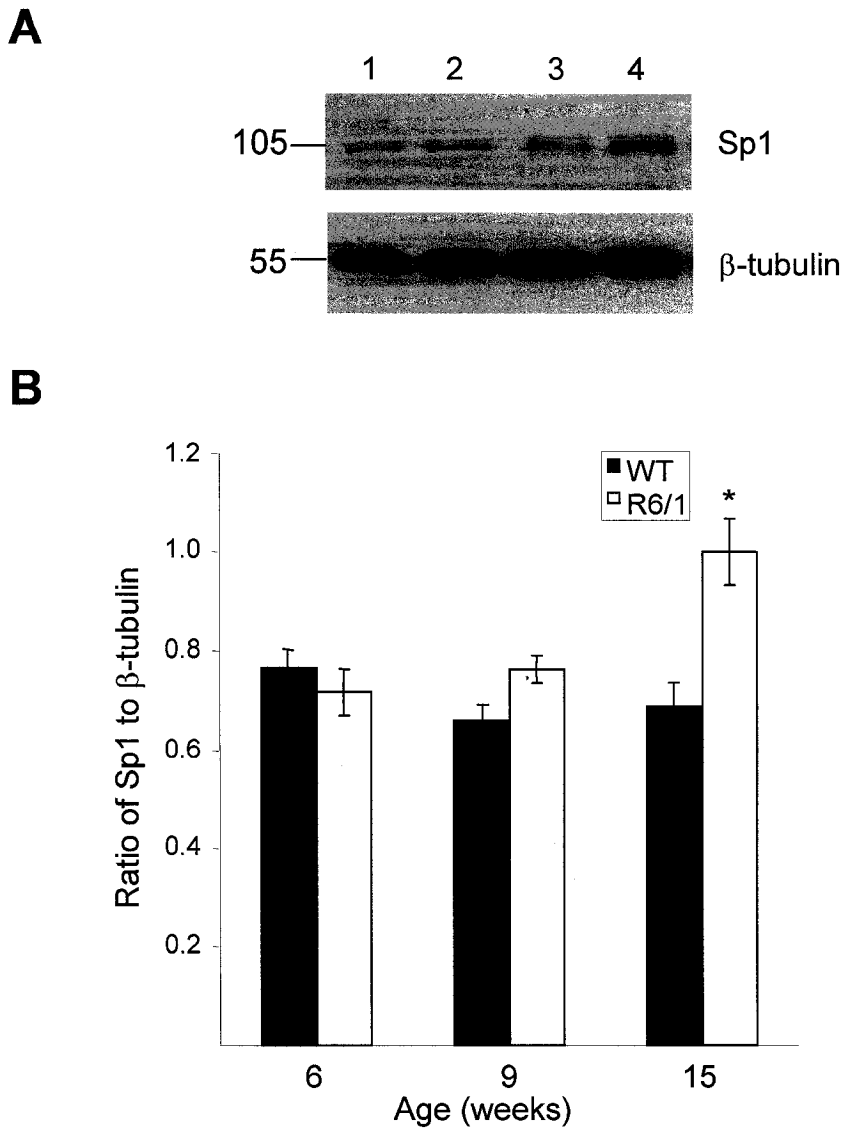

Figure 4-7. The level of Sp1 was higher in nuclear forebrain extract of 16 week-old R6/1 compared to 5 week-old wild-type and R6/1 mice. Western blotting analysis of Sp1 was performed with 20 μg of total proteins from the total protein lysate isolated from the striatum of 6 (lanes 1, 2) and 15 (lanes 3, 4) week-old wild-type (lanes 1, 3) and R6/1 (lanes 2, 4 mice) mice (A). The size (kDa) of Sp1 and β-tubulin are shown on the left. The optical density of Sp1 immunoreactivity was normalized to the optical density of β-tubulin immunoreactivity. A histogram of the ratio of the average optical density of the signal for Sp1 and β-tubulin was shown in B. The ratio was determined for four animals per age and genotype (N=4, mean ± SEM). *P<0.05, significant difference between wild-type and R6/1. (One-way ANOVA).

Table 4-1. List of transcription factors detected in TranSignal protein/DNA arrays.

Abbrev[1]	Name of transcription factors	5 WT[2]	5 R6/1	16 R6/1
Cell growth, differentiation and proliferation				
AP-2	activating enhancer binding protein 2	X[3]	X	X
COUP-TF	nuclear receptor subfamily 2	X	X	X
CREB-BP1	cAMP response element binding protein	X	X	X
c-Rel	NFkappaB p75kDa protein	X	X	X
PPAR	peroxisome proliferative activated receptor	X	X	
PRE	progesterone receptor	X	X	
TR	thyroid hormone receptor	X	X	X
MRE	metal response factor	X	X	X
Ikaros	Ikaros protein (zinc-finger protein)	X	X	
PARP	poly(ADP-ribose) synthetase/polymerase	X	X	X
PPARγ	peroxisome proliferator activated receptor-gamma	X	X	
RREB (1)	ras-responsive transcription element	X	X	
RSRFC4	ras-responsive transcription element	X	X	
Skn	octamer-binding site in epidermis (POU domain factor)	X	X	X
XBP-1	x-box binding protein 1	X	X	X
AML1	acute myeloid leukemia 1; aml1 oncogene	X	X	X
AREB6	Atp1a1 regulatory element binding protein 6	X	X	
CACC	CACC binding protein	X	X	X
CCAAT	CCAAT binding protein	X	X	
CSBP	conserved sequence-binding protein 1	X	X	
CTCF	CCCTC binding factor	X	X	
E12	E2A immunoglobulin enhancer binding factors	X	X	X
EKLF(1)	erythroid kruppel-like factor gene	X	X	X
EKLF(2)	erythroid kruppel-like factor gene	X	X	
Elf-1	E74-like factor 1,a novel Ets family member	X	X	
HOXD9,10	HOXD9,10	X	X	
KTP1	keratinocyte transcriptional protein-1	X	X	X

Abbrev[1]	Name of transcription factors	5 WT[2]	5 R6/1	16 R6/1
MTF	MRE-binding transcription factor-1	X	X	
MyoG	myogenic factor G	X	X	X
PPUR(1)	purine-rich sequences binding sequence	X	X	
PPUR(2)	purine-rich sequences binding sequence	X	X	
Pur-1	purine-binding transcription factor	X	X	X
PYR	pyrimidine-rich domain binding factor	X	X	X
RFX1,2,3,	regulatory factor x	X	X	X
SIF1	sucrase-isomaltase factor 1	X	X	
TREF1, 2	transferrin receptor binding protein	X	X	
c-myb binding protein	c-myb binding protein	X	X	
CYP1A1	cytochrome P450-c	X	X	X
PAX1	Pax-1DNA-binding transcription factor	X	X	
pax2	Pax-2DNA-binding transcription factor	X	X	
Pax5(2)	Pax5 DNA-binding transcription factor	X	X	
NF-A3	nuclear factor A3			X
NFκB(2)	Nuclear factor kappa	X	X	X
RFX1/2/3	a transactivator of hepatitis B virus enhancer	X	X	
RORE	RAR-related orphan receptor	X	X	
Snail	zinc-finger transcription factor Snail	X	X	X
Surf-2(2)	Surfeit locus protein 2	X	X	X
Thy-1binding protein	Thy binding protein	X	X	X
XBP1(2)	X-box binding protein 1	X	X	X
RAR (DR-5)	RAR: retinoic acid receptor	X	X	X
RXR (DR-1)	RXR: retinoid X receptor	X	X	X
Smad 3/4	MADH3/4: MAD, mothers against decapentaplegic homolog3/4	X	X	X
Stat4	signal transducer and activator of transcription 4			X
Stat5	signal transducer and activator of transcription 5			X

Abbrev[1]	Name of transcription factors	5 WT[2]	5 R6/1	16 R6/1
TR(DR-4)	thyroid hormone receptor	X	X	X
USF-1	upstream transcription factor	X	X	X
VDR(DR-3)	vitamin D (1,25- dihydroxyvitamin D3) receptor	X	X	X
AP-1	Fos, FosB, Fra1, Fra2, Jun, JunB	X	X	
CREB	CREB1: cAMP responsive element binding protein 1			X
Ets	v-ets erythroblastosis virus E26 oncogene homolog (avian)			X
GRE	GR:glucocorticord receptor	X	X	X
NF-E1 (YY1)	YY1 transcription factor			X
NF-E2	nuclear factor (erythroid-derived 2), 45kDa			X
Stat3	signal transducer and activator of transcription 3			X
E47	E2A immunoglobulin enhancer bind factors E12/E47			X
EVI-1	ecotropic viral integration site 1(zinc finger oncogene)	X	X	X
FKHR	forkhead box O1A human	X	X	X
MSP1	the sequences are the same as SAA except SP1 binding site is removed	X	X	X
hTERT-MT-Box	tentative new binding domain	X	X	
MUSF1	the sequences are the same as SAA except USF binding site is removed	X	X	X
MZF1	myeloid-specific retinoic acid-responsive zinc finger factor 1	X	X	
NF-Y	nuclear Y box factor	X	X	X
PARP	poly(ADP-ribose) synthetase/polymerase	X	X	X
Pax3	paired box gene 3	X	X	X
Pax4	paired box gene 4	X	X	X
Pax6	paired box gene 6	X	X	X
Pax8	paired box gene 8			X
LyF-1	transcriptional factor in lymphoid cell lines	X	X	X
RIPE3a1	rat insulin promoter element 3	X	X	
TGF	Transforming Growth Factor			X
TREF1, 2	transferrin receptor (TR) binding protein	X	X	X
ACF	albumin CCAAT-binding factor			X
EGR1	Early growth factor1			X

Abbrev[1]	Name of transcription factors	5 WT[2]	5 R6/1	16 R6/1
LXRE1	nuclear receptor subfamily 1, group H, member 2			X
Myb(2)	myeloblastosis viral oncogene homolog	X	X	X
PBGD binding protein	porphobilinogen deaminase			X
Stat1/Stat3	signal transducer and activator of transcription 1/3			X
YB1	Y-box binding protein 1	X	X	X
Basal transcription machinery and chromatin modification				
TFIID	TBP: TATA box binding protein	X	X	X
HiNF	histone gene transcription factors	X	X	X
TEF1(2)	TFIID activator		X	X
E4F, ATF	E4F transcription factor 1	X	X	X
CBF	CAAT box binding factor			X
CDP	CCAAT displacement protein			X
E2F-1	E2F transcription factor 1	X	X	X
Elk1	member of ETS oncogene family	X	X	X
GATA-1	GATA binding protein 1, globin transcription factor 1	X	X	
GATA-1/2	GATA binding protein 1/2, globin transcription factor	X	X	X
GATA-2	GATA binding protein 2, globin transcription factor 2	X	X	X
GATA-4	GATA binding protein 4, globin transcription factor 4	X	X	X
GATA-6	GATA binding protein 6, globin transcription factor 6	X	X	X
CACC	CACC binding protein	X	X	X
CCAAT	CCAAT binding protein	X	X	
CCAC	CCAC binding protein	X	X	X
CSBP	conserved sequence-binding protein 1	X	X	
CTCF	CCCTC binding factor	X	X	
E12	E2A immunoglobulin enhancer binding factors E12	X	X	X
HMG	high mobility group proteins	X	X	X
PEBP	polyoma enhancer binding protein			X
PEBP2	polyoma enhancer binding protein			X
CP1, CTF, CBTF	CCAAT-box-binding transcription factor			X

Abbrev[1]	Name of transcription factors	5 WT[2]	5 R6/1	16 R6/1
HiNF-B/H1TF1	Human H1 Histone Gene Promoter CCAAT Box Binding Protein			X
MDBP(1)	methylated DNA-binding protein			X
TFE3	Transcription factor E3			X
Tf-LF	Transcription elongation factor			X
Cytokine-related signalling transduction				
GAS/ISRE	interferon activated factors	X	X	X
Pbx1	pre-B-cell leukemia transcription factor 1	X	X	
IRF-1, IRF-2	interferon regulatory factor 1/2 binding element	X	X	X
ISRE (1)	interferon-a stimulated response element	X	X	X
ICSBP	interferon consensus sequence binding protein	X	X	
NFIL-2	5' upstream activating sequences (UAS) of the human IL-2 gene	X	X	
Fra-1/JUN	Fos-related antigen	X	X	
NFATc	nuclear factor of activated T-cells, cytoplasmic,			X
HSE	heat shock transcription factor	X	X	X
Pax-5	paired box gene 5, B-cell lineage specific activator protein			X
Beta-response element	Beta-response element	X	X	X
EVI-1	ecotropic viral integration site 1, zinc finger oncogene	X	X	X
FKHR	forkhead box O1A (rhabdomyosarcoma) human	X	X	X
Afxh (Foxo4)	myeloid/lymphoid or mixed-lineage leukemia	X	X	X
ISRE	Interferon-a stimulated response element	X	X	X
MBP-1(1)	HIV-EP1; MHC-binding protein 1; PRDII-BF1			X
Brain function and development				
GRE	GR:glucocorticord receptor response element	X	X	X
OCT-1	POU domain, class 2, transcription factor 1			X
WT1 (1)	Wilms tumor 1	X	X	X

Abbrev[1]	Name of transcription factors	5 WT[2]	5 R6/1	16 R6/1
GAG	amyloid precursor protin (APP) regulatory element	X	X	X
NZF-3	neural zinc finger factor 3	X	X	
MyTI	myelin transcription factor I	X	X	
HFH-2	forkhead box D3	X	X	X
HFH-3	forkhead box I1	X	X	
HFH-8	forkhead box F1a (HNF-3/Fkh Homolog-8)	X	X	
Skn	octamer-binding site in epidermis (POU domain factor)	X	X	X
Lipid and insulin metabolism				
ADR1	alcohol dehydrogenase regulatory gene1binding element	X	X	
Freac-4	forkhead box D1	X	X	
Freac-7	forkhead box L1	X	X	X
Freac-2 (1)	forkhead box F2 (mouse)	X	X	
ORE	osmotic response element	X	X	
XRE	xenobiotic response element	X	X	X
Isl-1	Islet-1	X	X	
LF-A1	liver-specific TF	X	X	X
RIPE3a1	rat insulin promoter element 3(RIPE3)can confer either positive regulation in insulin-producing cells	X	X	
ISGF	Interferon-Stimulated Response factor	X	X	
PTF1	pancreas specific transcription factor	X	X	
FAST-1	FOXH1: forkhead box H1			X
AhR/Arnt	aryl hydrocarbon receptor/aryl hydrocarbon receptor nuclear translocator		X	X
HNF-3 b	hepatocyte nuclear factor 3 beta	X	X	
ARP	apolipoprotein AI regulatory protein	X	X	
SIF1	Sucrase-isomaltase factor 1	X	X	
HFH-11B/11a	Hepatocyte Nuclear Factor 3/ fork head homolog 11			X
Cardiac functions				
CdxA/NKX2	Caudal-type homeodomain protein/ cardiac-specific homo box	X	X	
CEF1	cTnC (Slow/Cardiac Troponin C)	X	X	X

Abbrev[1]	Name of transcription factors	5 WT[2]	5 R6/1	16 R6/1
CEF2	cTnC (Slow/Cardiac Troponin C)	X	X	X
CETP-CRE	CETP (Cholesteryl ester transfer protein)	X	X	X
E4BP4	nuclear factor, interleukin 3 regulated	X	X	X
HNF-3 b	hepatocyte nuclear factor 3 beta	X	X	
MEF-1	MEF-1Myocyte enhancing factor1	X	X	X
CEA	carcinoembryonic antigen gene	X	X	X
Conditional stresses				
HSE	heat shock transcription factor	X	X	X
MRE	Metal response factor	X	X	X
Anti-oxidant RE	Anti-oxidant responsive element			X
HIF-1	hypoxia-inducible factor 1	X	X	X

[1]Abbreviation.
[2]Nuclear extracts used in this analysis were isolated from the forebrains of 5 week-old wild-type (5 WT), 5 week-old R6/1 (5 R6/1) and 16 week-old R6/1 (16 R6/1) mice.
[3]X, protein interaction with the transcription factor recognition sequence was detected in TranSignal protein/DNA arrays

and R6/1 mice compared to wild-type counterparts (Fig. 4-7). There was a relative increase in Sp1-specific DNA binding in 16 week-old R6/1 compared to wild-type mice (Fig. 4-5). Increased Sp1 DNA-binding activity, therefore, correlated with increased Sp1 protein levels in older R6/1 mice.

Mutant huntingtin decreased the activity of the PDE10A promoter construct in *ex vivo*

The N-terminal portion of mutant huntingtin in R6/1 mice (N89-115Q) did not alter the DNA binding activity of transcription factors at the time that the rate of transcription of several striatal genes started to decrease. We hypothesized that the N-terminus of mutant huntingtin may have interfered with the transactivation of transcription factors of affected promoters to decrease transcription. We chose to use a cell culture model of HD to examine whether intracellular N-terminus mutant huntingtin repressed transcription of the PDE10A2 promoter, whether this effect would be observed in the absence of native chromatin structure on the promoter and how the N-terminal fragment of mutant huntingtin exerted transcriptional repression in a gene-specific manner.

ST14A cells that were originally derived from primary cells isolated from the embryonic day 14 rat striatum (Cattaneo & Conti, 1998) were employed as a cell culture model of HD to study the regulation of the PDE10A2 promoter. It is known that PDE10A mRNA and protein are highly expressed in the rat striatum (Fujishige *et al.*, 1999). ST14A derivative cell lines N548wt-15Q and N548hd-128Q stably express equivalent amounts of the N-terminal 548 amino acids of the human huntingtin protein with 15 and

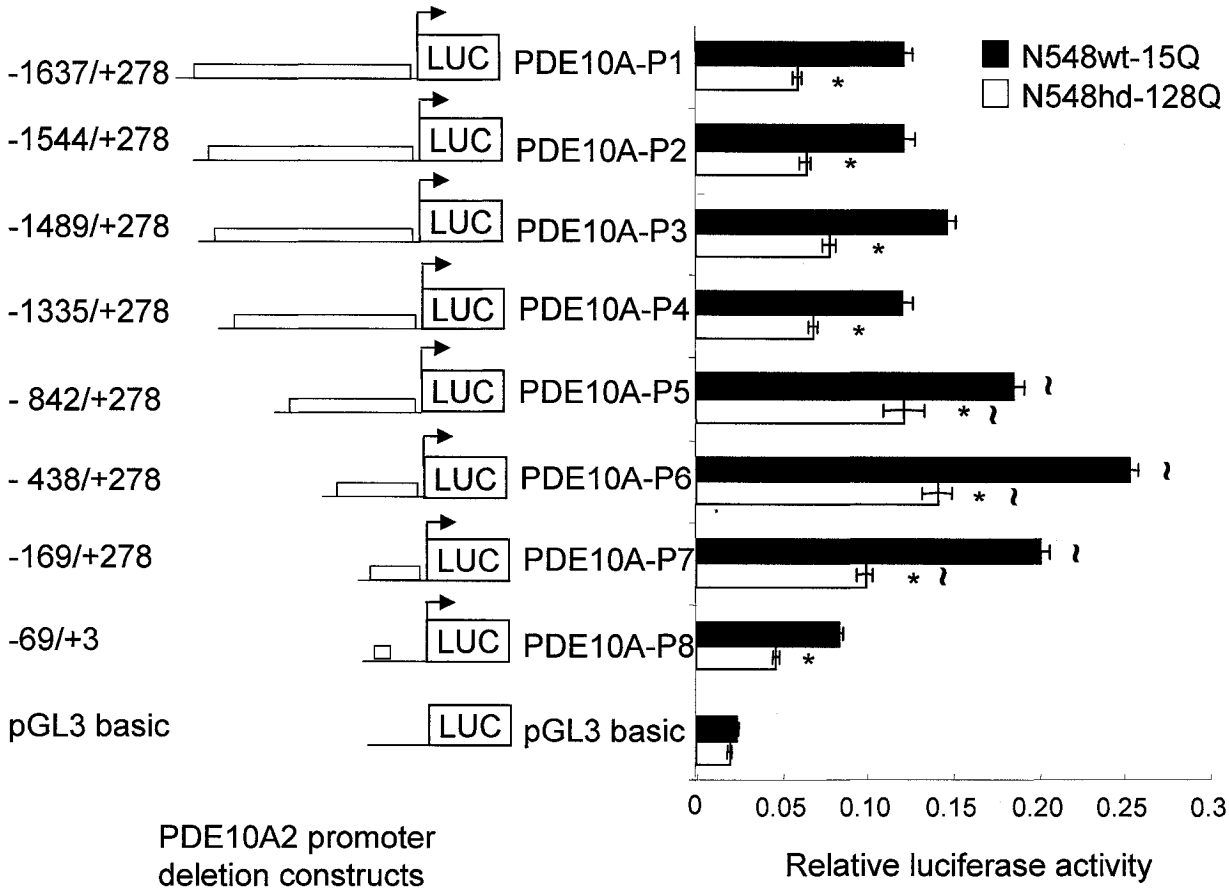

Figure 4-8. The -169/+3 region of the PDE10A2 promoter conferred sensitivity to mutant huntingtin expressed in N548hd-128Q cells. Schematic representations of deletion constructs of the PDE10A2 promoter are shown on the left. Numbers indicates the region of the PDE10A2 promoter relative to the transcription start site +1 contained in each construct (-1637+278). Deletion constructs for the PDE10A-pGL3 constructs and the promoter-less pGL3 vector were co-transfected with phRL-TK into N548wt-15Q (solid bars) and the N548hd-128Q cells (open bars). Firefly luciferase activity of each construct was normalized to *Renilla* luciferase activity of the co-transfected control phRL-TK. The relative luciferase activity was expressed as a mean (±SEM, N=12 for each construct per cell line). *P<0.05, significant difference between deletion constructs expressed in N548hd-128Q compared to N548wt-15Q cells ; ~P<0.05, significant difference between deletion constructs and the PDE10A-P1 (-1637/+278) construct in each cell line (Two-way ANOVA).

128 polyglutamines, respectively (Rigamonti *et al.*, 2000). The proteins expressed include sequence encoded by exons 1 and 2 of the human *HD* gene. The 548 amino acids portion of human huntingtin can be detected as 72 kDa and 115 kDa proteins, using the MAB2166 antibody (data not shown).

To determine which part of the PDE10A2 promoter conferred mutant huntingtin-mediated transcriptional repression, a series of promoter deletion constructs were created that spanned the -1637 to +278 region of the PDE10A2 promoter (Fig. 4-8). Each of the constructs was co-transfected with a thymidine kinase promoter-driven construct (phRL-TK) that expresses *Renilla* luciferase into N548wt-15Q and N548hd-128Q cells. phRL-TK construct served as a control plasmid for normalizing variability among transfections and variability of expression due to differences between N548wt-15Q and N548hd-128Q cell lines. The ratio of PDE10A2 promoter-dependent firefly luciferase relative to control TK promoter-dependent *Renilla* luciferase activity (N=12) for each promoter deletion construct was determined 48 hrs after transfection. Each promoter deletion construct had a lower activity in N548hd-128Q cells compared to N548wt-15Q cells. The ratio of the activity for each construct in N548hd-128Q was ~0.5-0.6 of that observed in N548wt-15Q cells suggesting that all constructs were equally affected by the expression of the N-terminus of mutant huntingtin. The activity of all promoter deletion constructs was higher than the basal activity from the promoter-less vector pGL3. There was a significant increase in PDE10A2 promoter activity when the region spanning -1335 to -438 was removed from the promoter construct. There was a significant decrease in promoter activity when the region from -438 to -169 was deleted. This suggests that there were repressor elements present between -1335 and -438 and activator elements

present between -438 and -169 bp of the PDE10A2 promoter but that this promoter was regulated in the same way in N548wt-15Q and N548hd-128Q cells. If specific *cis*-elements conferred sensitivity to mutant huntingtin, they would have to reside within the -169 to +3 region of the PDE10A2 promoter.

Expression of the stably transfected N548hd-128Q construct lowered the activity of all deletion constructs of the PDE10A2 promoter. We hypothesized that the decreased promoter activity in N548hd-128Q cells may have been due to a decrease in the interaction between the promoter DNA and transcription factors. We examined the protein-DNA interactions with the -169/+3 region of the PDE10A2 promoter, which was the smallest promoter that had mutant huntingtin-sensitive promoter activity. *In vitro* DNase I footprinting was employed to determine if there was a difference in the distribution of proteins on the -170/+209 region of the PDE10A2 promoter using nuclear extracts isolated from 5 week-old wild-type and R6/1 mice or nuclear extracts isolated from N548wt-15Q and N548hd-128Q cells (Fig. 4-9). The results showed that a number of DNase I hypersensitive sites and several regions protected from DNase I digestion were observed within the -170 to +70 region of the PDE10A2 promoter. However, there was no difference in the footprinting patterns using nuclear extracts isolated from the forebrains of 5 week-old wild-type and R6/1 mice or between nuclear extracts isolated from N548wt-15Q and N548hd-128Q cells. Moreover, a similar DNase I footprint was observed using nuclear extracts isolated from mice and N548 cells. The N-terminal fragment of mutant huntingtin expressed in R6/1 mice at 5 weeks of age or the N-terminal fragment of mutant huntingtin protein expressed in immortalized striatal cells

Figure 4-9. *In vitro* DNase I footprinting revealed that there was no difference in the distribution of proteins on the -169/+3 PDE10A2 promoter region using nuclear extracts derived from wild-type and R6/1 mice or between nuclear extracts isolated from N548wt-15Q and N548hd-128Q cells. Schematic representation of the PDE10A2 promoter region is shown as a black line (A). The transcription start site +1 is indicated with an arrow. The probe used in *in vitro* DNase I footprinting spanned the -170/+209 of the promoter region (hatched bar). The 5' end-labelled probe was incubated either with 10 μg of bovine serum albumin (P), or with soluble nuclear proteins isolated from 5 week-old wild-type mice (lane 1), 5 week-old R6/1 mice (lane 2), N548wt-15Q cells (lane 3), or N548hd-128Q cells (lane 4). The relative positions of a radiolabelled PhiX174 DNA/*Hinf*I markers (Fermentas) are indicated on the left. The position of DNase I hypersensitive sites (arrows) and the relative positions of the sequence of transcription factor binding sites implicated by DNase I footprinting are indicated on the right. Myeloid zinc finger protein (MZF) is predicted to bind to -135/-130, -90/-85 and +25/+30; Myeloid-associated zinc finger protein (MAZ), -140/-135, -85/-80; Specific protein 1 (Sp1), -140/-130; Zinc finger transcription factor binding protein (ZBP89), -140/-130; Nerve growth factor-induced protein factor C (NGF-IC), - 39/-30; Early response gene-1 (Egr-1/NGFIA), -30/-25 and +20/+25. Nuclear factor kappa B (NFkappaB), olfactory neuron-specific factor 1 (OLF1) and B-cell specific activating protein (PAX5), winged helix protein (WHN), -9/+20. Neuron restrictive silencing factor (NRSF), +58/+70.

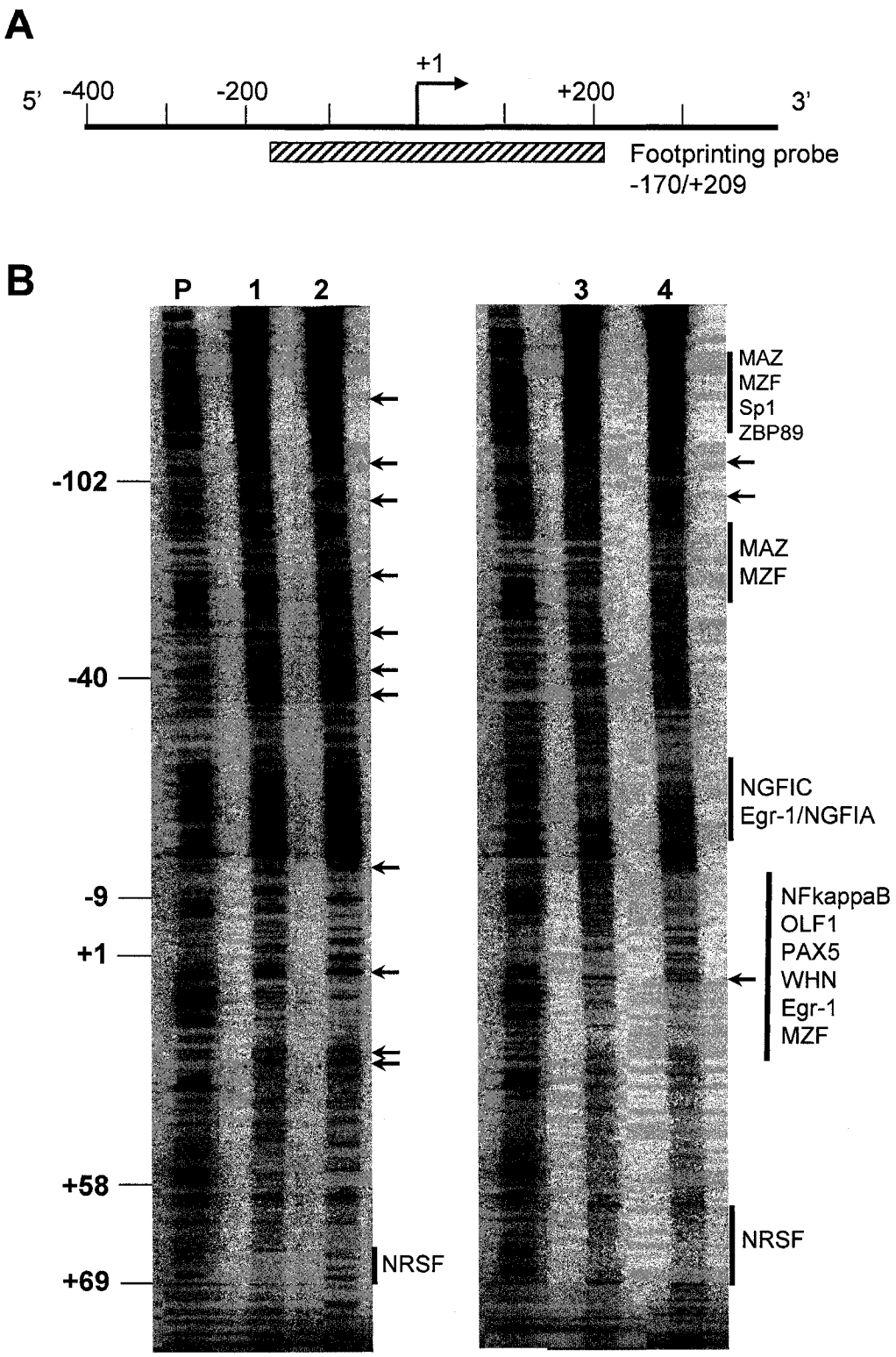
A
5'
-400
-200
+1
+200
3'
Footprinting probe
-170/+209
B
P
1
2
3
4
-102
-40
-9
+1
+58
+69
NRSF
MAZ
MZF
Sp1
ZBP89
MAZ
MZF
NGFIC
Egr-1/NGFIA
NFkappaB
OLF1
PAX5
WHN
Egr-1
MZF
NRSF

(N548hd-128Q) did not alter the relative amount or ability of transcription factors to bind to the PDE10A2 core promoter region. Sequence analysis of this region and comparison of the sequence and footprinting pattern allowed us to identify the recognition elements of transcription factors that may contribute to PDE10A2 expression (Fig. 4-9).

Although the *in vitro* DNase I footprinting provided us with information regarding where and what transcription factors could potentially bind to the PDE10A2 core promoter region, this technique uses excess nuclear protein in relation to the amount of DNA in each reaction. *In vitro* DNase I footprinting, therefore, cannot indicate the affinity of different transcription factors for the DNA. Gel-shift assays were performed to examine protein-DNA interactions on the minimal PDE10A2 promoter that had reduced activity in the presence of the N-terminus of mutant huntingtin using excess radiolabelled DNA in comparison to protein. There were five protein-DNA complexes formed between nuclear proteins isolated from N548wt-15Q and N548hd-128Q cells and a radiolabelled EMSA probe spanning the -170 to +20 region of the PDE10A2 promoter (Fig. 4-10). There were 3 major protein-DNA complexes formed between nuclear proteins isolated from 5 week-old wild-type and R6/1 mice and the same EMSA probe. However, no alteration in the amounts of protein-DNA complexes was observed in nuclear proteins from 5 week-old R6/1 mice or from N548hd-128Q cells compared to wild-type nuclear extracts. The N-terminal portion of mutant huntingtin in the nucleus of 5 week-old R6/1 mice or in the N548hd-128Q cells did not alter the protein-DNA interactions on the core PDE10A2 promoter although this region conferred sensitivity to mutant huntingtin-mediated transcriptional repression *in vivo* and *ex vivo*.

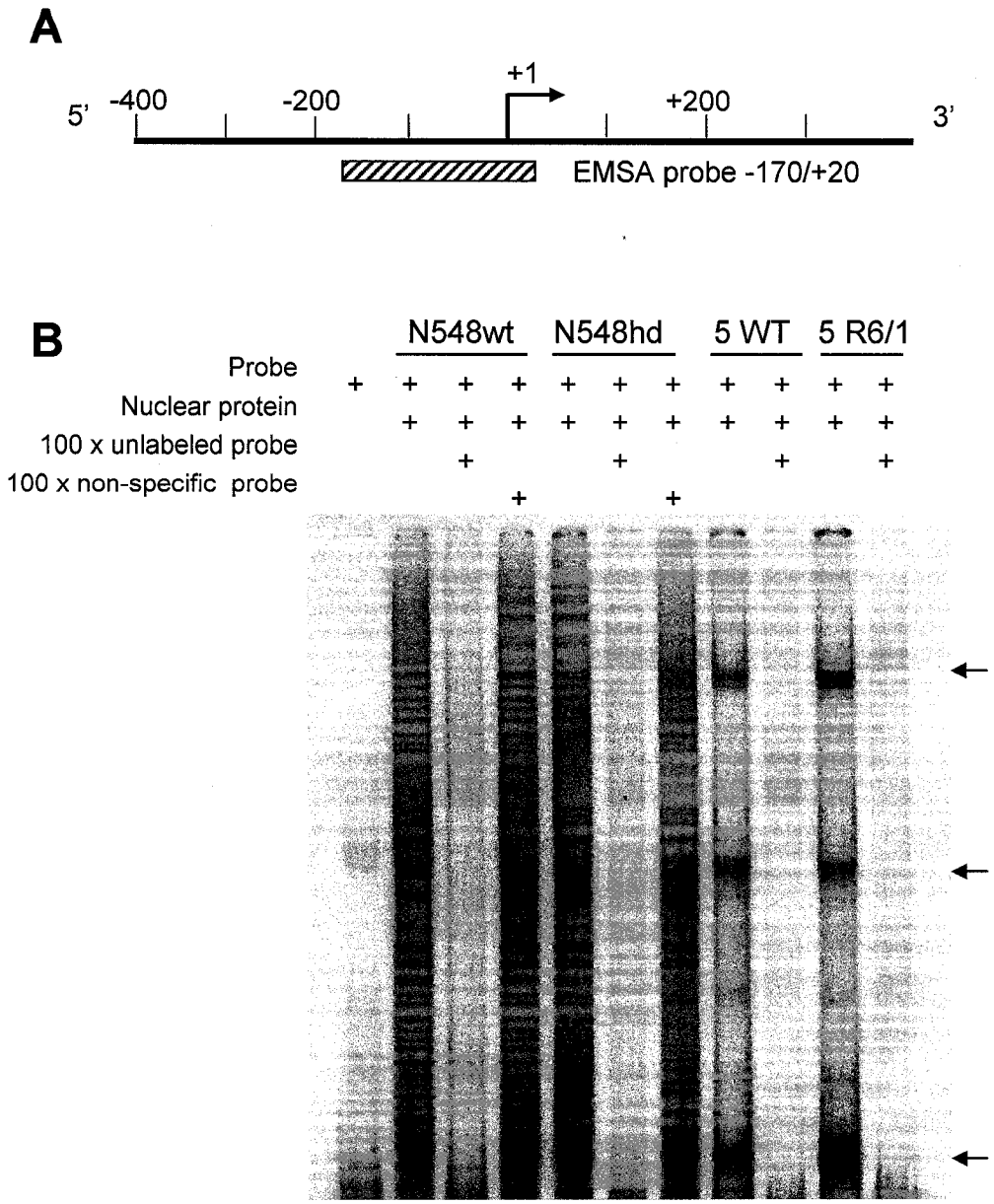

Figure 4-10. EMSA analysis of the -170/+20 region of the PDE10A2 promoter did not reveal differences in the binding of protein complexes to DNA between extracts isolated from N548wt-15Q and N548hd-128Q cells or between extracts isolated from 5 week-old wild-type and R6/1 mice. A schematic view of the PDE10A2 promoter region (black line) and the EMSA probe spanning the -170/+20 region of the promoter (hatched bar) is shown in A. The nuclear extract, probe and competitor components for each reaction are indicated above the autoradiogram in B. Competitors were unlabelled EMSA probes (100 X molar excess compared to radiolabelled probe), non-specific probes were unlabelled double-stranded DNA containing a CREB consensus sequence(100X molar excess compared to radiolabelled probe). The arrows indicate the three abundant protein/DNA complexes.

Although the N-terminus of mutant huntingtin expressed in N548wt-128Q cells decreased the activity of all PDE10A2 promoter constructs, it was possible that the difference in PDE10A2 promoter activity was due to differences between the two cell lines that had been induced by the long-term expression of the N-terminal portion of the mutant huntingtin protein. Therefore, we examined the activity of the PDE10A2 promoter in the presence of transiently expressed N-terminus of mutant huntingtin in ST14A parental cells. Plasmids that expressed exon 1 of the human huntingtin gene with either 22Q (N89-22Q) or 115Q (N89-115Q) were co-transfected with different promoter PDE10A-pGL3 constructs (Fig. 4-11A) or with GAD65-pGL3 (Fig. 4-11B). Acute expression of N89-115Q decreased the activity of the full-length PDE10A2 promoter construct (P1, -1637/+278) and the most active PDE10A2 promoter construct (P6, -428/+278) (Fig. 4-11A), whereas it did not decrease the activity of the GAD65 promoter construct (-509/+552) relative to the activity observed in the presence of N89-22Q (Fig. 4-11B). Relative to control vector, acutely expressed N89-22Q and N89-115Q decreased the activity of the PDE10A2 (P6, P1) promoter by 40% and the GAD promoter construct by 20%, which demonstrated that the N-terminus of human huntingtin, regardless of polyQ length, had a repressive effect on transcription and that N89-115Q had an additional repressive effect on the PDE10A2 but not the GAD65 promoter.

In contrast to the results observed in ST14A cells, the acute expression of N89-115Q in human embryonic kidney cell line (HEK293) did not decrease the activity of the PDE10A2 promoter construct (P6, -428/+278) compared to the activity of the promoter observed in these cells in the presence of N89-22Q (Fig. 4-11C). Moreover, N89-115Q and N89-22Q did not decrease the activity of the PDE10A2 (P6) compared to the control

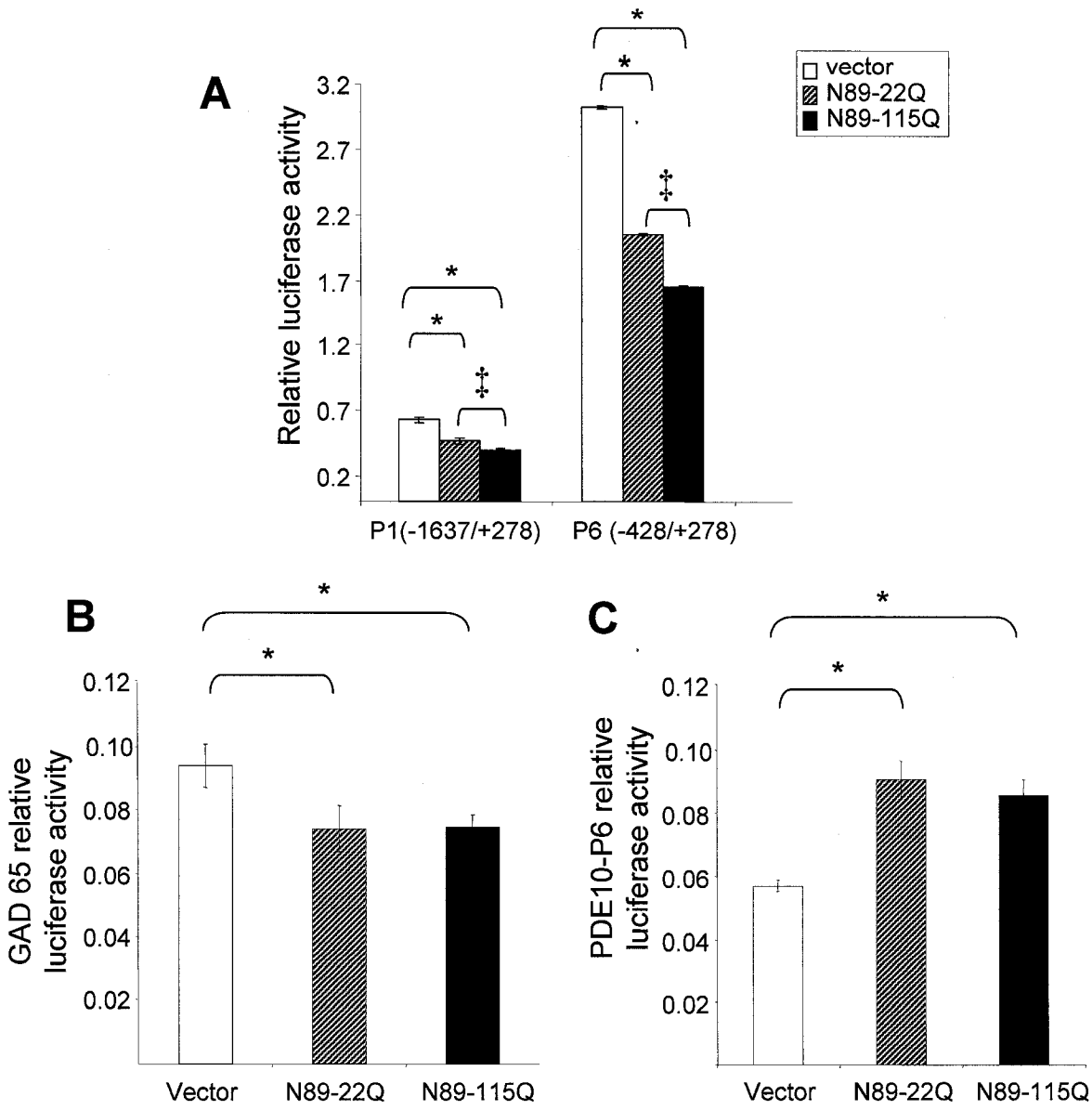

Figure 4-11. Transiently expressed N89-115Q decreased the activity of the -438/+278 region of the PDE10A2 promoter in a cell- and promoter- specific manner. PDE10A deletion constructs PDE10A-P1 (-1637/+278) (P1) and PDE10A-P6 (-438/+278) (P6) were co-transfected with phRL-TK, pCMV vector (vector), or with plasmid expressing exon 1 of human huntingtin with 22 CAG repeats (N89-23Q) or 115 CAG repeats (N89-115Q) into ST14A cells (A) and HEK293 cells (C). A GAD65 promoter construct was co-transfected with phRL-TK and pCMV vector, or N89-23Q or N89-115Q in ST14A cells. The ratio of the firefly/*Renilla* luciferase activity was expressed as mean (±SEM, N=12). **P*<0.05, significant difference in promoter activity between vector and N89-22Q or N89-115Q. ‡*P*<0.05, significant difference in promoter activity between N89-22Q and N89-115Q. (One-way ANOVA).

vector, suggesting that both repression of transcription via the N-terminus of huntingtin and the additive polyQ-specific repression were mediated by cell-specific factors.

Examination of ex vivo protein-DNA interactions

We decided to examine how the transient expression of the N-terminus of mutant huntingtin altered the protein-DNA interaction in cultured cells. TransReporter Protein/DNA arrays (Panomics) were employed to simultaneously determine the activity of 24 transcription factors in response to transient expression of the N-terminus of mutant huntingtin. The TransReporter Plasmid mix was co-transfected with a control vector or with the comparable plasmid expressing exon 1 of human huntingtin with 22 CAG repeats (N89-22Q) or 115 CAG repeats (N89-115Q) into ST14A cells for 48 hrs. RNA was then isolated and reverse transcribed to synthesize biotinylated cDNA probes. The biotinylated cDNA probes were allowed to hybridize with the TransReporter blot. Since the plasmid mix contained 24 different reporter vectors, each of which contained several copies of a specific *cis*-acting element, a promoter and a unique tag sequence, the amount of cDNA probes that can hybridize to the membrane reflected the efficiency of transcription, which was dependent on the interaction between *cis*-elements and endogenous transcription factors in ST14A cells. A list of transcription factors surveyed using the TransReporter array membrane is shown in Table 4-2. Transcription factors detected on the membrane are shown in Fig. 4-12. Out of 24 transcription factors on the membrane, only nine factors were active in ST14A cells.

The optical density for each detected transcription factor was normalized by subtracting the optical density of the background for each array. The relative

Table 4-2. Transcription factors in TranReporter protein/DNA arrays and in TranSignal protein/DNA arrays.

Abbrev[1]	Name of transcription factors[2]	22Q	115Q	5 WT[3]	5 R6/1	16 R6/1
MR	MRE-binding transcription factor-1			X[4]	X	X
Myc	c-Myc oncogenic transcription factor					
MZF1	zinc finger protein 42 (myeloid-specific retinoic acid- responsive)			X	X	
NF-1	Nuclear factor 1					
NFAT	nuclear factor of activated T-cells					X
NF-E2	nuclear factor (erythroid-derived 2), 45kDa					X
NFκB	nuclear factor of kappa light polypeptide gene enhancer in B-cells					X
NRF-1	nuclear respiratory factor 1					
NRF-2	nuclear respiratory factor 2					
OCT-1	POU domain, class 2, transcription factor 1					X
p53	TP53: tumor protein p53					X
PAX5	paired box gene 5					X
Pax8	paired box gene 8					
PBX1	pre-B-cell leukemia transcription factor 1			X	X	
PIT1	growth hormone factor 1					
PPARa	peroxisome proliferator activated receptor alpha					
PPARg	peroxisome proliferator activated receptor gamma	X	X			
PR	pathogenesis-related response elements				X	
RARE	retinoic acid receptor elements	X	X	X	X	X
RB	retinoblastoma tumor suppressor protein					
RXRE	retinoid X receptor elements	X	X	X	X	X
Smad 3/4	signaling mothers against decapentaplegic homolog 3 / 4			X	X	X

Abbrev[1]	Name of transcription factors[2]	22Q	115Q	5 WT[3]	5 R6/1	16 R6/1
Sp1	specific protein 1					
SRE	sterol regulatory element binding transcription factor					
SRF	serum response factor					
SRY	testis determining factor binding domain					
STAT1 p84/p91	signal transducer and activator of transcription 1 (84 kDa/94 kDa dimmer)					
STAT1(GAS)	signal transducer and activator of transcription 1 (interferon activated factors)					
STAT3	signal transducer and activator of transcription 3	X	X			X
STAT4	signal transducer and activator of transcription 4	X	X			X
STAT5	signal transducer and activator of transcription 5					X
STAT5/6	signal transducer and activator of transcription 5/6					
TA-luc	TATA box binding element	X	X			
Tax/CREB	TAX &CREB complex-responsive element	X	X			
TCF/LEF	T cell factor/lymphocyte enhancer binding factor					
TFE3	transcription factor E3					
TR(DR-4)	thyroid hormone receptor			X	X	X
USF1	USF: upstream transcription factor			X	X	X
VDR(DR-3)	vitamin D (1,25- dihydroxyvitamin D3) receptor	X	X	X	X	X
v-MAF	v-maf musculoaponeurotic fibrosarcoma oncogene homolog (avian)	X	X			
Xbp-1	X-box-binding protein 1					

Abbrev[1]	Name of transcription factors[2]	22Q	115Q	5 WT[3]	5 R6/1	16 R6/1
YY1	Ying-Yang transcription factor 1					X

[1]Abbreviation.

[2] Specific transcription factor sequence tags detected by RNA derived from ST14A cells that had been co-transfected with the TransReporter protein/DNA plasmid mix and pCMV-Exon 1-22Q (22Q) or pCMV-Exon 1-115Q (115Q).

[3]Factors detected in TranSignal protein/DNA arrays using nuclear extracts isolated from the forebrains of 5 week-old wild-type (5 WT), 5 week-old R6/1 (5 R6/1) and 16 week-old R6/1 (16 R6/1) mice.

[4]X, factors detected in TransReporter and TranSignal protein/DNA arrays.

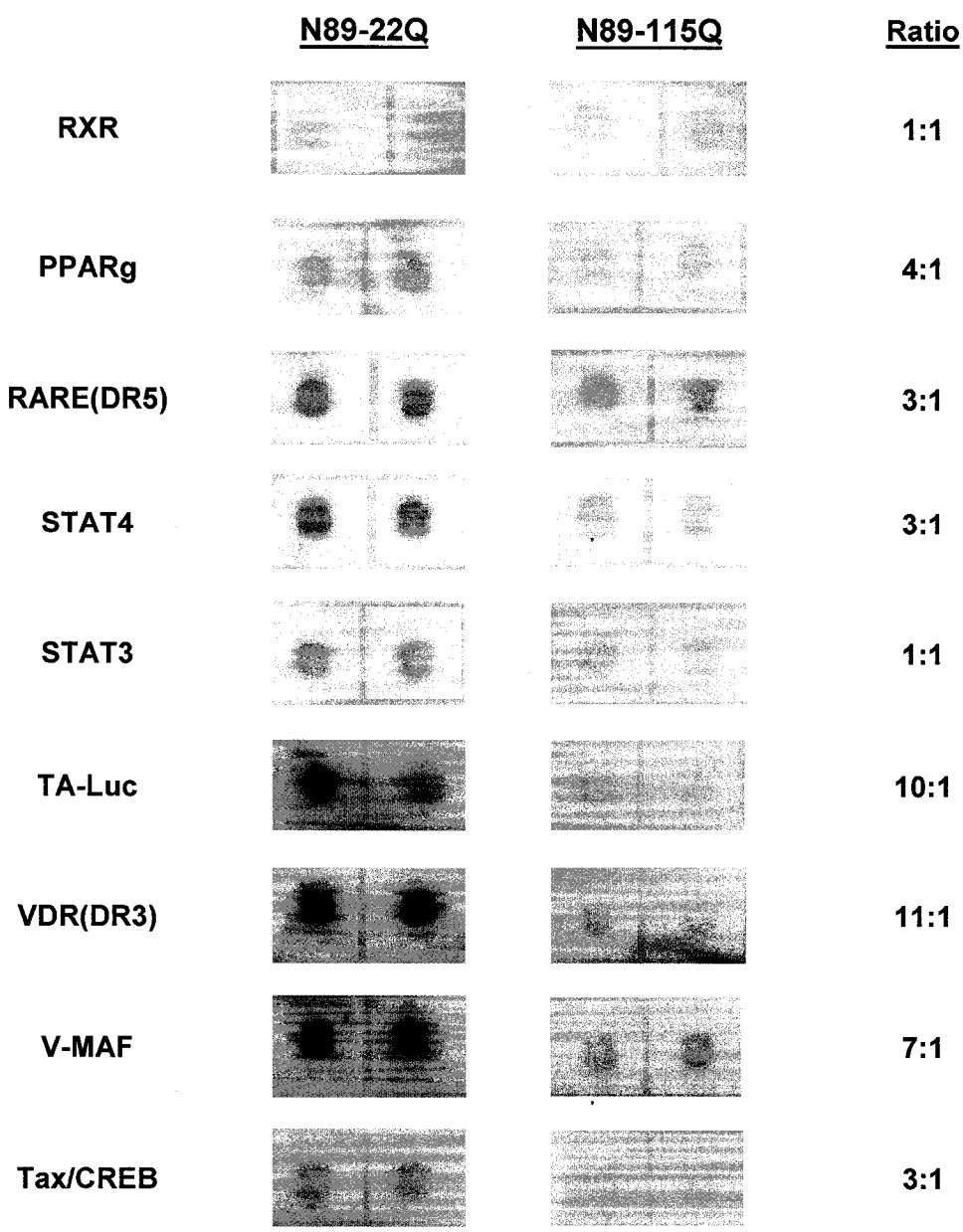

Figure 4-12. TransReporter protein/DNA array showed that transiently expressed mutant huntingtin N89-115Q decreased the activity of transcription factors PPARg, RAR, STAT4, TA-luc, VDR (DR-3), V-MAF, Tax/CREB in ST14A cells.
TransReporter protein/DNA array was performed by co-transfecting the TransReporter plasmid mix and plasmid expressing N89-22Q or N89-115Q into ST14A cells. The level of signal reflects the relative amount of RNA synthesized from constructs that contain the consensus DNA binding sites for the transcription factors indicated. The optical density of detected spots was normalized to the optical density of background and the ratio of normalized values of 22Q to 115Q is listed on the right of each panel.

hybridization of RXR and STAT3 tags did not appear to differ between the two conditions. The ratio of the relative activity of each promoter under the regulation of different *cis*-elements in the presence of N89-22Q and N115Q was obtained by dividing the normalized optical density to the normalized optical density for RXR. Seven specific tag sequences had lower levels of hybridization signal in the presence of N89-115Q (Fig. 4-12). Decreased hybridization of these tag sequences on the array indicated decreased transcriptions from the promoters that have specific *cis*-elements for corresponding transcription factors in ST14A cells. It appeared that reduced levels of detected sequence tags in the presence of N89-115Q in ST14A cells were not equally proportional, indicating that the expression of N89-115Q differentially affected the amount of mRNA derived from different transcription binding to their *cis*-elements in ST14A cells. Different levels of tag sequences for different ranscription factors binding to their *cis*-elements were detected, which showed high (VDR), medium (STAT4) and low (Tax/CREB). However, they all appeared to be lower in the presence of N89-115Q suggesting a universal repression. Based on previous evidence that the N89-115Q form of mutant huntingtin in the forebrain nuclear extract in R6/1 mice did not alter the DNA binding or the expression levels of these factors, it is likely that the transiently expressed N89-115Q affected functional interaction between specific transcription factors and the RNA pol II enzyme without altering DNA binding.

We performed EMSA analysis to examine the protein-DNA interaction of the transcription factors that were altered by the N-terminus of mutant huntingtin N89-115Q in TransReporter assays. The DNA-binding activities of transcription factors RAR, RXR, STAT4 and VDR were determined using nuclear extracts isolated from ST14A cell

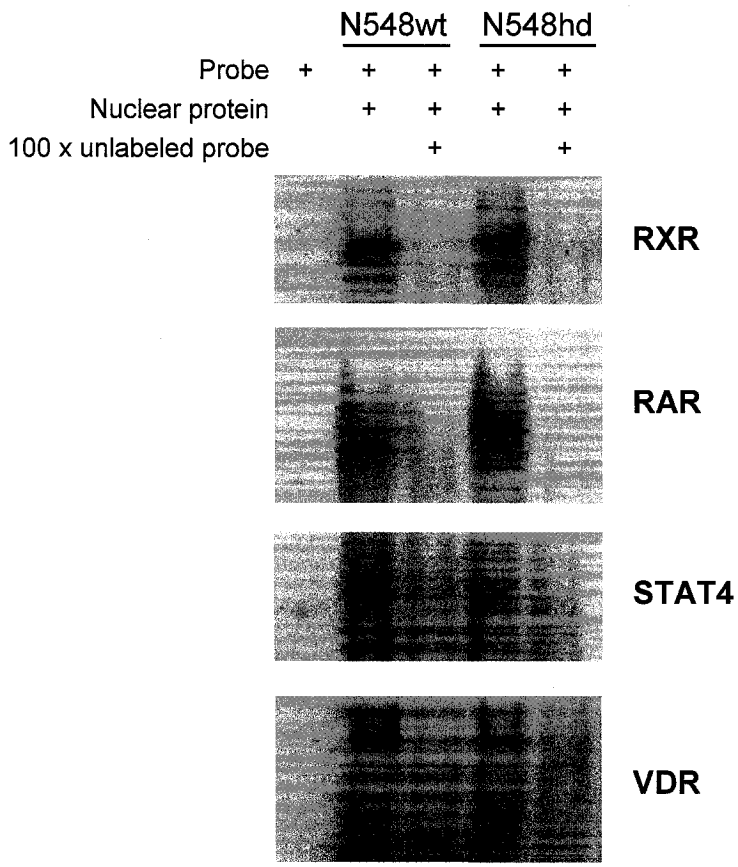

Figure 4-13. EMSA analyses demonstrated that there was no difference in DNA binding activity of transcription factors RAR, RXR, STAT4 and VDR in the nucleus of N548wt-22Q and N548hd-128Q cells. EMSA analyses were performed with a radiollabeled consensus probe and 5 μg of cell nuclear extracts. Protein-DNA complexes were separated from free probes on a 4% native polyacrylamide gel. Competitor DNAs were non-radiolabelled double-stranded consensus sequences (100X molar excess compared to radiolabelled probe). The name of detected protein-DNA complexes is indicated on the right.

derivatives, N548wt-15Q and N548hd-115Q (Fig. 4-13). Indeed, the levels of protein-DNA complexes were similar between nuclear extracts from N548wt-15Q and N548hd-128Q cells. This suggests that the stably expressed N-terminus of mutant huntingtin did not alter the DNA binding activity of these transcription factors although their transcriptional activities were decreased by the transiently expressed mutant huntingtin N89-115Q.

4.3 Discussion

Mutant huntingtin protein has been shown to interact with several ubiquitous polyglutamine-containing transcription factors, such as CBP, Sp1, TBP, TAFII130, p53 and N-CoR via insoluble or soluble complexes in the nucleus, which has been assumed to compromise their normal function (Boutell *et al.,* 1999; McCampbell *et al.,* 2000; Shimohata *et al.,* 2000; Steffan *et al.,* 2000; Nucifora *et al.,* 2001; Dunah *et al.,* 2002; Li *et al.,* 2002; van Roon-Mom *et al.,* 2002). Using similar methods, it has also been demonstrated that mutant huntingtin is capable of interacting with other proteins that are not transcription factors (Harjes & Wanker, 2003). The effect of mutant huntingtin on DNA binding activities of transcription factors and whether such alteration can ultimately affect transcription remain largely unknown. We did not detect any difference in the DNA binding of a screen of 345 transcription factors using nuclear extracts isolated from forebrains of 5 week-old wild-type and R6/1 mice. The N-terminal product of human huntingtin with an expanded polyglutamine repeat (N89-115Q) started to decrease the steady-state levels of the PDE10A2 mRNA in 5 week-old R6/1 mice (Fig. 3-5). At 16 weeks of age, when PDE10A2 transcripts reached a new lower equilibrium level in the

striatum of R6/1 mice (Fig. 3-3), there were significant alterations in the DNA binding activities of some transcription factors detected in TranSignal. In parallel to TranSignal, we did not detect any change in the amount of transcription factors following expression of N89-115Q in 5 week-old R6/1 mice but there were some changes in 16 week-old R6/1 mice. Using a functional reporter system, we found that the transiently expressed N89-115Q decreased the transactivation, but not the DNA binding activities, of several transcription factors. Moreover, the transiently expressed N89-115Q decreased the activity of the core PDE10A2 promoter region (-170/+70) but did not affect the distribution or the DNA binding of transcription factors on this region.

The N-terminus of mutant huntingtin likely exerts a direct effect on transcription at 5 weeks not 16 weeks in R6/1 mice.

Microarray studies have documented many changes in gene expression in different models and some changes are observed in all models. It is not known which changes in gene expression are a direct effect of the presence of mutant huntingtin, compensatory effects to mutant huntingtin-induced changes, or which changes that reflect the processes of cell dysfunction (Luthi-Carter *et al.,* 2000; 2002a, 2002b; Chan *et al.,* 2002; Desplats *et al.,* 2006; Hodges *et al.,* 2006). Common findings of these microarray data on different animal models of HD and among HD patients are decreased expression of neuropeptides such as enkephalin and proteins involved in signal transduction such as G-protein coupled receptors (CB1), phosphoproteins (DARPP-32) and phosphodiesterases (PDE10A). Decreased steady-state levels of the striatal-specific mRNAs such as PDE10A2 (this study), CB1 (McCaw *et al.,* 2004), DARPP32 (Gomez *et*

al., 2006), and enkephalin (Gomez and Denovan-Wright, unpublished data) at 5-6 weeks of age in the striatum of R6/1 mice indicates that these changes are likely to be one of the earliest steps for mutant huntingtin-mediated neuronal dysfunction. Our data suggest that the direct effect of the N-terminal fragment of mutant huntingtin on the transcription of these genes in 5 week-old R6/1 mice does not include the modulation of the DNA binding activity of transcription factors that could potentially bind to the promoters of these HD-affected genes. Although changes in the DNA binding activity of transcription factors occurred in the forebrain of 16 week-old R6/1 mice, these changes are likely to be an indirect effect that results from early or protracted expression of mutant huntingtin transgene product. The altered striatal mRNAs found in brain samples from human subjects with HD corroborate the array findings from HD mouse models, further supporting the notion that altered gene expression specifically in the caudate putamen/striatum is essential to the pathologic deficits and neurodegeneration processes in HD (Desplats *et al.,* 2006). This study also concluded that genes that are highly expressed in the striatum are preferentially affected by mutant huntingtin. In fact, of the 54 genes surveyed, over half occurred in fully symptomatic 6 month-old R6/1 mice and only 16 of 54 were decreased in 10 week-old R6/1 mice. Of the 16 changes many were transcription factors. The authors argued that these transcription factors may be causal to HD. However, their own analysis showed that the regulation of these factors was altered by mutant huntingtin showing that the changes in these transcription factors are a consequence of altered transcription and not the primary cause of altered transcription.

We observed that there was an increased level of mutant huntingtin transgene product in the insoluble nuclear fraction in 16 week-old R6/1 compared to 5 week-old

R6/1 whereas there were similar levels of mutant huntingtin N89-115Q in the soluble nuclear fractions in both 5 and 16 week-old R6/1 mice (Fig. 4-1C). This suggests that the soluble N-terminus mutant huntingtin reached a maximal level of expression at 5 weeks of age and remains constant from 5 to 16 weeks. We determined that there was a exponential decay of the levels of the PDE10A mRNA in increasing ages of R6/1 mice (Fig 3-3) and that levels of transcripts did not reduce to zero but reached a new lower equilibrium level starting at 8-10 weeks until 30 weeks in the striatum of R6/1 mice. This implies that the constant level of soluble N-terminus mutant huntingtin from 5 to 16 weeks leads to a sustained but lower level of transcription of those genes.

The observations that a similar level of the DNA binding activities of transcription factors detected in nuclear extract from 5 week-old wild-type and R6/1 mice indicates that these factors are important in regulating cell growth, differentiation and proliferation. Factors that play a role in cytokine-related signaling transduction, brain development and lipid and insulin metabolism are also listed (Table 4-1). However, it is important to know that factors listed in one functional category may not be exclusive to other functions because they may simultaneously regulate transcription of genes involved in multiple cellular pathways. The DNA binding activity of the nuclear hormone receptor family was all detected in 5 week-old wild-type, 5 week-old R6/1 and 16 week-old R6/1, including peroxisome proliferators activated receptor (PPAR), thyroid hormone receptors (TR), vitamin D receptors (VDR), retinoid acid receptors (RAR) and retinoid X receptors (RXR). In addition, the transactivation activity of VDR, RAR and RXR was also detected in ST14A cells expressing the same transgene product N89-22Q or N89-115Q in TransReporter assays (Fig. 4-10 and Table 4-2). These observations suggest that the

nuclear hormone receptor family is expressed at a significant level in the forebrains of 5 week-old mice and in the ST14A cells that can be detected in TranSignal and TransReporter assays, respectively. It appeared that their transactivation, but not the DNA binding activity, are directly associated with the N-terminus mutant huntingtin-mediated transcriptional repression.

Functionally, retinoid signaling initiated RAR/RXR and PPAR/RAR dimer formation has been implicated as a necessary step for expressing genes for the development of the nervous system in the embryonic or early postnatal brains as well as in the adult brains (Lane & Bailey, 2005). Retinoid acid is synthesized in mesostriatal and mesolimic dopaminergic neurons and can regulate the expression of dopamine D2 receptors, one of striatal genes that are affected in HD (Samad *et al.*, 1997; Thomas, 2006), thus retinoid related transcriptional regulation is likely to be affected by mutant huntingtin. Retinoid signaling pathways have also been implicated in the pathophysiology of Alzheimer's disease (Goodman & Pardee, 2003) and schizophrenia (Goodman, 1998). Nuclear co-repressor (N-CoR) is part of a complex that represses transcription in combination with the thyroid hormone receptor, RAR and other orphan nuclear receptors. The yeast two-hybrid system has identified the protein-protein interaction between mutant huntingtin and N-CoR (Boutell *et al.*, 1999) and expression of mutant 103Q protein in PC12 cells appears to enhance the ability of N-CoR to repress transcription (Yohrling *et al.*, 2003). Therefore, the expression of N-terminus mutant huntingtin protein N89-115Q may perturb the function or the homeostasis of nuclear hormone receptor-mediated transcription in the HD brains.

The protein-DNA interactions in vitro does not support the previously proposed sequestration model

The DNA binding activities of 42 transcription factors were detected in 16 week-old R6/1, but not 5 week-old R6/1 or wild-type mice (Fig. 4-4). This group of factors showed increased DNA binding activities in 16 week-old R6/1 compared to wild-type mice in individual EMSA analyses (Fig. 4-5). Increased Sp1 DNA binding activity and levels of protein expression have been demonstrated in nuclear proteins isolated from 12 week-old R6/2 mice compared to wild-type mice (Chen-Plotkin *et al.*, 2006). In combination with our data, the increased DNA binding activity of Sp1 at late stage of HD is likely a compensatory effect but not a direct effect as a result of long-term expression of the N-terminus of mutant huntingtin N89-115Q in R6/1 mice. Similarly, Obrietan and Hoyt (2004) found that there is an increased phosphorylation of CREB at Ser-133, which leads to the increased CREB DNA binding activity when they cross-bred a HD transgenic mouse model (R6/2) with a transgenic mouse that expresses a CRE-regulated gene. This study supports our data that there was a robust increase in the DNA binding activity of transcription factor CREB at 16 week but not 5 week-old R6/1 mice in the TranSignal and EMSA analyses. Increased DNA binding for CREB was only seen in late stage of HD, and increased binding is likely a long-term effect not an immediate effect of mutant huntingtin.

There have been other studies reporting that mutant huntingtin is capable of interacting with Sp1 and sequestering it away from the promoter thus compromising transcription (Dunah *et al.*, 2002; Li *et al.*, 2002; Yu *et al.*, 2002). Nucifora *et al.* (2000) reported that sequestration of CBP into NIIs by mutant huntingtin interrupts CREB-

mediated transcription. Mutant huntingtin is able to interact with CBP *in vitro* using GST pull-down and in cell culture (Stephan *et al.*, 2000). These studies imply that mutant huntingtin is likely to decrease the DNA binding activity of CREB as a result of mutant huntingtin sequestering CREB-binding protein, CBP. Takano *et al.* (2000) demonstrated that huntingtin protein in *Drosophila* interacts with NFkappaB in HeLa cell nuclear extract using co-immunoprecipitation assays. If mutant huntingtin sequestered Sp1, CREB and NFkappB *in vivo* as implied in these studies and if it was true *in vivo* at time when transcription was perturbed, we would have seen a reduced DNA binding activity of Sp1, CREB and NFkappaB in nuclear extract isolated from 5 week-old R6/1 mice compared to wild-type mice. However, we did not see any reduction in the levels of the protein-DNA complexes in nuclear extract containing the N-terminus of mutant huntingtin in mice nor did we see a reduced migration of the protein-DNA complexes in EMSA. In addition, in Western blot analysis, we did not see any alteration of the levels of these transcription factors in nuclear extract that contained physiologically relevant amounts of mutant huntingtin. Since these studies used *in vitro* binding techniques GST pull-down to examine the interaction between overexpressed factors and employed an overexpression system, where there may be sufficient protein interactions between otherwise weakly associating factors *in vivo,* therefore such a highly artificial system may not recapitulate the *in vivo* situation. Combining the EMSA and Western blot analysis, the N-terminus of mutant huntingtin at the physiological concentration did not appear to sequester transcription factors away from the promoter nor to alter the levels of transcription factors at the time when transcription was reduced. We conclude that the affected transcription by mutant huntingtin in 5 weeek-old R6/1 mice is unlikely due to

mutant huntingtin-mediated sequestration of transcription factors from the affected promoter in these mice.

Many genes contain Sp1 consensus sites on their promoters, including those that are not affected by mutant huntingtin, such as β-actin (Gustafson & Kedes, 1989). Therefore, Sp1 alone can not explain the specific transcriptional dysregulation exerted by mutant huntingtin. Dunah *et al.* (2002) determined that introduction of Sp1 alone into cells expressing the N-terminus of mutant huntingtin can not rescue the decreased D2 promoter activity and that only Sp1 in combination with TAFII130, one of the components in the basal transcription machinery, can reverse the repression. This suggests that mutant huntingtin is likely to affect the activity of both TAFII130 and Sp1 and cause transcriptional repression. Recently, Cornett *et al.* (2006) determined that different sizes of N-terminal fragments of mutant huntingtin adopt different misfolded structures in the nucleus leading to different affinities for Sp1 and that inhibition of Sp1 activity is mutant huntingtin-context dependent. This study suggests a possibility that different sizes of mutant huntingtin binding to Sp1 with different affinities allows mutant huntingtin specifically and selectively to decrease transcription from different promoters. Therefore, these studies all suggest that Sp1 alone can not explain how mutant huntingtin gives a specific transcriptional repression on certain genes not others.

The N-terminus of mutant huntingtin affects the transactivation not the DNA binding of transcription factors in *ex vivo.*

Transiently expressed mutant huntingtin N89-115Q decreased the activity of the full-length (P1) and the strongest (P6) PDE10A2 promoter construct in ST14A cells but

not in HEK293 cells. This observation suggests that the transiently expressed mutant huntingtin N89-115Q was able to exert transcriptional repression in a system that is free of interneuronal signaling and chromatin structure but that cell specific factors contribute to control of expression of mutant huntingtin-affected genes. It is possible that N89-115Q in combination with striatal- or brain-specific factor exerts transcriptional repression on the PDE10A promoter, or factors in HEK293 cells protect the transcriptional machinery from N89-115Q-mediated repression. Thus, the N-terminal exon 1-encoding part of mutant huntingtin has a cellular context-dependent effect. The transiently expressed N89-115Q altered the activity of the PDE10A2 promoter but not the GAD65 promoter, suggesting that both PDE10A2 and GAD65 promoter constructs are active in ST14A cells and that this immortalized striatal cell line contains the necessary transcription factors to drive the expression of each construct. GAD65, the enzyme for synthesizing GABA in the CNS, has been shown to co-localize with enkephalin in medium spiny projection neurons in the striatum of mice brains (Menalled *et al.*, 2000). The GAD65 mRNA is not altered in the striatum of two mouse models of HD, transgenic animals expressing exon 1 of the human huntingtin gene with 144Q and knock-in mice containing a chimeric mouse/human exon 1 with 71Q or 94Q (Menalled *et al.*, 2000). It appears that mutant huntingtin N89-115Q exerts a gene-specific transcriptional repression as observed in animal models of HD. It is hypothesized that unaffected genes may adopt a condensed chromatin structure thus preventing the accessibility of mutant huntingtin to affect the transcription (Emerson, 2002; Sadri-Vakili & Cha, 2006). Since the transiently expressed N89-115Q did not decrease the promoter activity even on a naked plasmid DNA that is free of chromatin structure, which recapitulates the *in vivo*

situation, it is unlikely that a condense chromatin structure of the GAD65 gene prevents the accessibility of mutant huntingtin *in vivo*. It is possible that factors in striatal cells directly block the mutant huntingtin effect on the GAD65 promoter.

The levels of the tag sequences produced from reporter constructs following the binding of active RAR and VDR to their *cis*-elements were lower but not absent in cells expressing N89-22Q compared to cells expressing N89-115Q. This observation suggests that the transiently expressed mutant huntingtin N89-115Q likely modulates the transactivation of these factors without totally blocking their communications with RNA pol II holoenzyme, causing a reduced but not silenced transcription. Consistently, the reduced steady-state levels of the PDE10A2, CB1, DARPP32 and preproenkephalin mRNAs do not continue to decline and finally reach a level of mRNA that is undetectable, but maintain at a new lower equilibrium level after 8-9 weeks in R6/1 mice (this study, McCaw *et al.*, 2004; Gomez *et al.*, 2006; Gomez and Denovan-Wright, unpublished data). This suggests that the maximal effect of the N-terminus mutant huntingtin is reached by 8 weeks in R6/1 and the transcription is not blocked but suppressed. The N-terminus of mutant huntingtin N89-115Q did not appear to alter DNA binding activities of transcription factors at the time when transcription was first perturbed in R6/1 mice. Transactivation of some, but not all transcription factors, was affected in ST14A cells expressing N89-115Q. It remains to be determined how mutant huntingtin affects the transactivation of transcription factors to decrease transcription initiation and what transcriptional complexes that mutant huntingtin is likely to associate with to exert repression.

CHAPTER 5

The N-Terminus of Mutant Huntingtin Affected Transcription *in Vitro*

5.1 Introduction

Based on the work presented in chapters 3 and 4, we hypothesized that soluble N-terminus mutant huntingtin exerts transcriptional repression on the PDE10A2 promoter by interacting with specific factors in the basal transcription machinery or by interfering with communication between activators and the core transcription complexes. To test these hypotheses, we employed an *in vitro* transcription system and purified, soluble N-terminus huntingtin protein with different polyQ length. The *in vitro* transcription system utilized HeLa nuclear extracts, which contain a variety of transcription activators, DNA binding proteins and other enzymatic machinery for accurate transcription initiation by RNA polymerase II. Transcription using this system exhibits basal and regulated RNA polymerase-mediated transcription *in vitro* (Dignam *et al.,* 1983; Sawadogo & Roeder, 1985). For our purposes, this simple system has several advantages over cell culture or *in vivo* systems. We can examine protein-protein interactions on the functional promoter, easily manipulate the defined system by adding components and we can specifically study transcription initiation events. Our goal was to determine whether the N-terminus of mutant huntingtin affected transcription factor binding and/or the assembly of the transcription pre-initiation complexes on the PDE10A2 and GAD65 promoters.

Information obtained from this functional *in vitro* system will allow us to formulate testable hypotheses, which then can be tested both *ex vivo* and *in vitro*. For example, Zhai *et al.* (2005) showed that the N-terminal 540 amino acids of mutant huntingtin disrupts the formation of functional TFIIF complexes by interacting with one of the TFIIF subunits RAP30 and that transcription of the dopamine D2 receptor gene was decreased when mutant huntingtin was present. It appeared that the fragment

containing 40-60 amino acids of RAP30 subunit interacted with mutant huntingtin. We wanted to test if the 40-60 aa of RAP30 could function as a dominant-negative molecule in a cell culture model of HD to block mutant huntingtin-mediated decrease in promoter activity. Slepko *et al.* (2006) demonstrated that non-pathological length polyQ enhances the aggregation of a pathologic length polyQ47 peptide *in vitro* in a concentration and polyQ length-dependent manner. We hypothesized that if a normal length polyQ peptide enhanced aggregation of pathologic length polyQ *in vitro*, we would see an alleviation of the repressive effect of soluble recombinant N171-87Q protein on *in vitro* transcription of the PDE10A2 promoter. These two proof-of-principle experiments would provide us approaches to test the functions of potential mutant huntingtin binding partners in a functional system.

5.2 Results

Soluble N171-87Q reduced transcription of the PDE10A2 and GAD65 genes in vitro.

We produced and purified histidine-tagged recombinant protein composed of the N-terminal 171 amino acids of human huntingtin with either 23 polyglutamines (N171-23Q) or 87 polyglutamines (N171-87Q) (Li *et al.*, 2002). *In vitro* transcription reactions were performed using a PCR fragment spanning -392/+278 region of the PDE10A2 promoter as the template and increasing amounts of recombinant N171-23Q or N171-87Q protein. Transcripts corresponding to five transcription start sites were detected in each reaction demonstrating that this template was transcriptionally active *in vitro* (Fig. 5-1). The positions of these start sites were -272 (1), -74 (2), -55 (3), +46 (4) and +60 (5) relative to the most 5' transcription start site (+1, site A) identified in the striatum of

wild-type mice (Chapter 3, Fig. 3-8). The location of the transcription start sites used *in vitro* did not match exactly with the three major start sites (+1, +30, +40) identified *in vivo*. The start site at +46 (4) was in close proximity to start site C (+40) used in striatal cells. It appeared that the levels of the 352 and 333 nt transcripts were lower than the levels of the 550, 232 and 218 nt transcripts. The start sites that produced 550, 232 and 218 nt transcripts were used more frequently to initiate transcription within the -392/+278 region of the PDE10A2 promoter *in vitro*. Increasing concentrations of recombinant mutant huntingtin protein N171-87Q proportionately decreased the levels of transcripts derived from each start site and it appeared that the levels of each of the different sizes of transcript were equally affected by the presence of N171-87Q. The amount of 550 nt transcript was significantly decreased in the presence of 1.5 pmol of N171-87Q to ~ 20% of levels observed in the presence of N171-23Q huntingtin and in the absence of recombinant protein (Fig. 5-1C). The presence of the extended polyglutamine tract within N171-87Q protein, therefore, directly reduced transcription *in vitro*.

In vitro transcription was also performed using a PCR fragment spanning the -508/+600 region of the GAD65 promoter and increasing amounts of recombinant N171-23Q or N171-87Q protein. Six different sizes of transcripts were detected that corresponded to six transcription start sites. These start sites were located at -202 (1), +98 (2), +164 (3), +204 (4), +232 (5), +273 (6) relative to the most 5' transcription start site (+1) identified by Makinae *et al.* (2000) in the mouse GAD65 gene (Fig. 5-2). Seven start sites were identified *in vivo* (Makinae *et al.*, 2000) and four of these corresponded to sites (3, 4, 5 and 6) used *in vitro*. Levels of the 802, 436 and 327 nt transcripts were

Figure 5-1. The N-terminus of mutant huntingtin (N171-87Q) decreased transcription of the PDE10A2 -392/+278 promoter region *in vitro*. Schematic representation of the PDE10A2 promoter is shown as a black line (A). The transcription start site (+1) (site A) identified in wild-type mice is indicated with an rightward-pointing arrow. The DNA template used in *in vitro* transcription spanned -392/+278 of the PDE10A2 gene (hatched bar). *In vitro* transcription reactions were performed with the DNA template in the presence of HeLa nuclear extract and increasing amounts of recombinant N171-23Q and N171-87Q proteins (pmol). The RNA products were fractioned on denaturing 4% PAGE gels. A representative experiment is shown in B. The relative positions of radiolabelled and denatured PhiX174 DNA/*Hinf*I markers (Fermentas) are indicated on the left. The sizes of synthesized transcripts are indicated on the right (nt). The numbers in the brackets correspond to transcription start sites indicated as downward-pointing arrows in A. A histogram of normalized OD values for the 550 nt transcript is shown in C (N=3, $\pm$SEM). *P<0.05, significant difference between the levels of transcripts detected in the presence of recombinant proteins and the level of transcript detected in the presence of HeLa alone. (Two-way ANOVA).

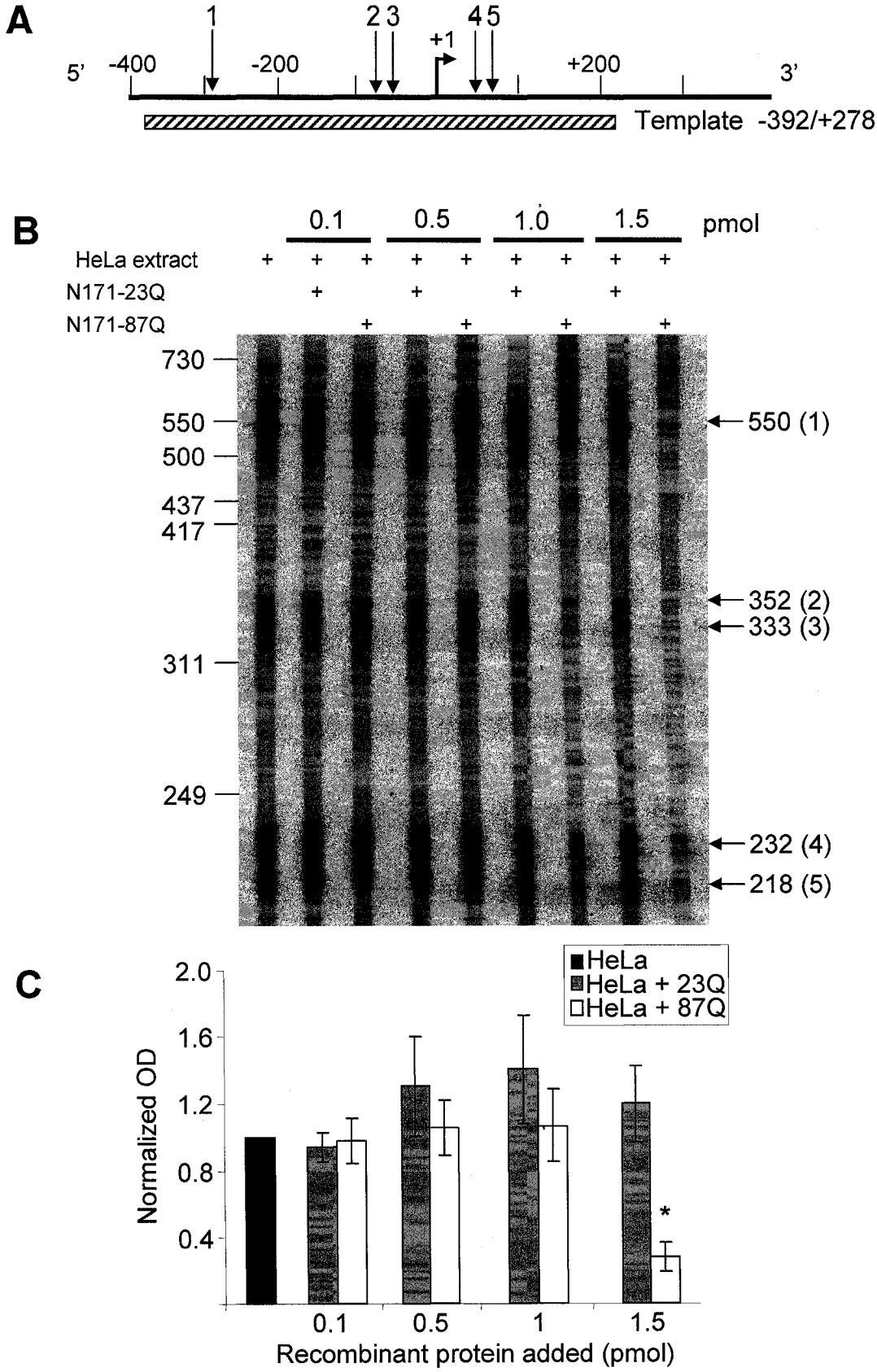
A
1
2 3
4 5
+1
5'
-400
-200
+200
3'
Template -392/+278
B
0.1
0.5
1.0
1.5
pmol
HeLa extract
N171-23Q
N171-87Q
730
550
500
437
417
311
249
550 (1)
352 (2)
333 (3)
232 (4)
218 (5)
C
HeLa
HeLa + 23Q
HeLa + 87Q
Normalized OD
2.0
1.6
1.2
0.8
0.4
*
0.1
0.5
1
1.5
Recombinant protein added (pmol)

Figure 5-2. N171-87Q decreased transcription of the GAD65 -508/+600 promoter *in vitro*. Schematic representation of the GAD65 promoter is shown as a black line (A). The most 5' transcription start site (+1) identified by Makinae *et al.* (2000) is indicated with a rightward-pointing arrow. The DNA template used in *in vitro* transcription reactons spanned -508/+600 of the mouse GAD65 gene (hatched bar). In vitro transcription reactions were performed with the DNA template in the presence of HeLa nuclear extract and increasing amounts of recombinant N171-23Q and N171-87Q proteins (pmol). The RNA products were fractioned on a denaturing 4% PAGE gel shown in B. The relative positions of a radiolabelled and denatured PhiX174 DNA/*Hinf*I markers (Fermentas) are indicated on the left. The sizes of synthesized transcripts are indicated on the right (nt). The numbers in the brackets correspond to transcription start sites indicated as downward-pointing arrows in A. A histogram of normalized optical density values for the 436 nt transcript is shown in C (N=3, $\pm$SEM). *P<0.05, significant difference between the levels of transcripts detected in the presence of recombinant proteins and the level of transcript detected in the presence of HeLa alone. (Two-way ANOVA).

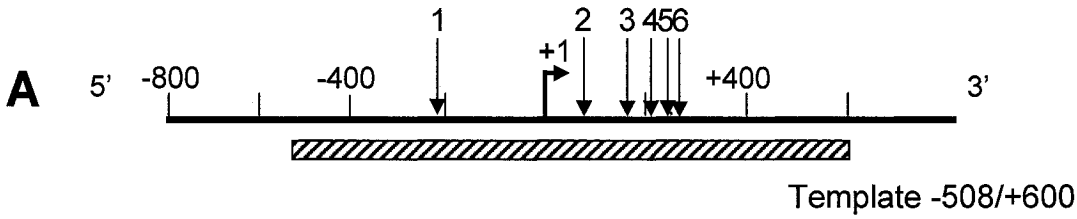
A
5'
-800
-400
+1
+400
3'
1
2
3
4
5
6
Template -508/+600

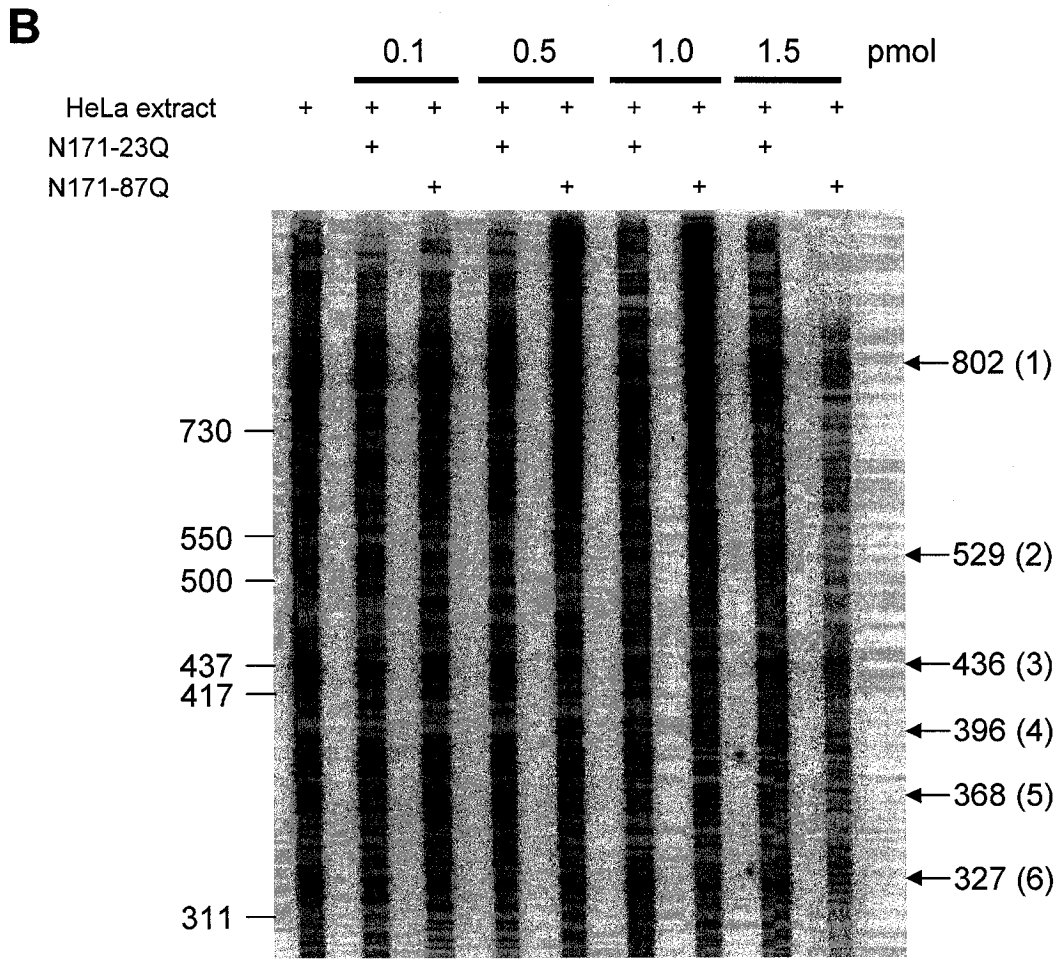
B
0.1
0.5
1.0
1.5
pmol
HeLa extract
N171-23Q
N171-87Q
730
550
500
437
417
311
802 (1)
529 (2)
436 (3)
396 (4)
368 (5)
327 (6)

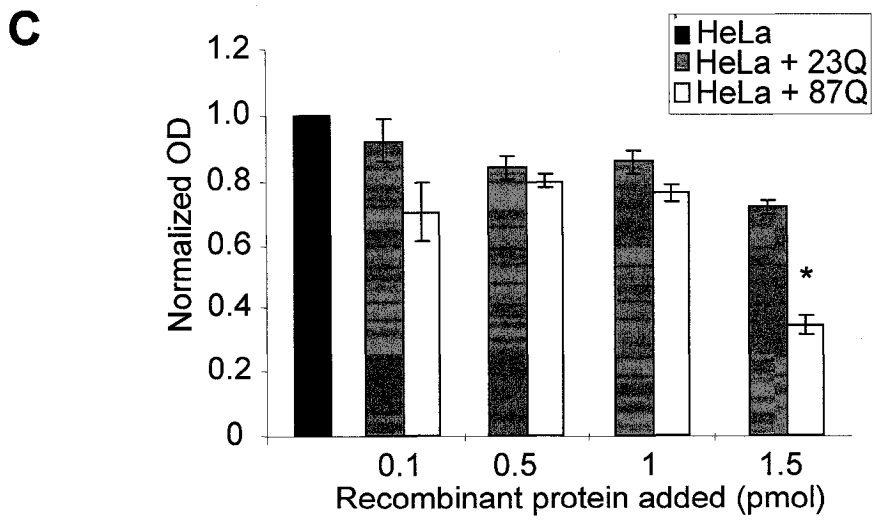
C
HeLa
HeLa + 23Q
HeLa + 87Q
Normalized OD
1.2
1.0
0.8
0.6
0.4
0.2
0
*
0.1
0.5
1
1.5
Recombinant protein added (pmol)

sites 1, 3, and 6 of the mouse GAD65 promoter were utilized more frequently than start sites 2, 4, and 5 *in vitro* (Fig. 5-2). Levels of each transcript remained constant in the presence of 0.1, 0.5 and 1.0 pmol of either N171-23Q or N171-87Q compared to the levels of transcripts detected in HeLa nuclear extract alone. However, in the presence of 1.5 pmol of N171-87Q, levels of transcripts decreased to ~40% of the levels detected in reactions containing HeLa alone or HeLa and 0.1, 0.5 or 1.0 pmol of N-terminal human huntingtin (Fig. 5-2C). It appeared that the presence of 1.5 pmol of N171-87Q affected the activity of both the PDE10A2 and GAD65 promoters and that the PDE10A2 promoter may have been more sensitive than the GAD65 promoter to the amount of recombinant N171-87Q present in the reactions.

In vivo, levels of GAD65 mRNA are not altered in the striatum of a HD transgenic model expressing exon 1 of the human *huntingtin* gene with 144Q and a knock-in HD model containing a chimeric mouse/human exon 1 with 71Q or 94Q (Menalled *et al.,* 2000). Transient expression of N89-115Q in ST14A cells did not affect GAD65 promoter activity (Chapter 4, Fig. 4-11). We hypothesized that brain-specific factors in ST14A cells and in the mouse striatum may provide a protective effect on the GAD65 promoter *in vivo* and *ex vivo*. *In vitro* transcription was performed in the presence of 1.5 pmol of N171-87Q supplemented with 15 μg of nuclear factors isolated from the forebrains of 5 week-old wild-type mice. It appeared that levels of 232 nt and 218 nt transcripts from the PDE10A2 promoter were reduced in the presence of forebrain nuclear extract compared to the levels observed in reactions containing HeLa extract or HeLa extract and 1.5 pmol of N171-23Q (Fig. 5-3A). Forebrain nuclear extract, however, did not further reduce levels of each transcript in reactions containing HeLa

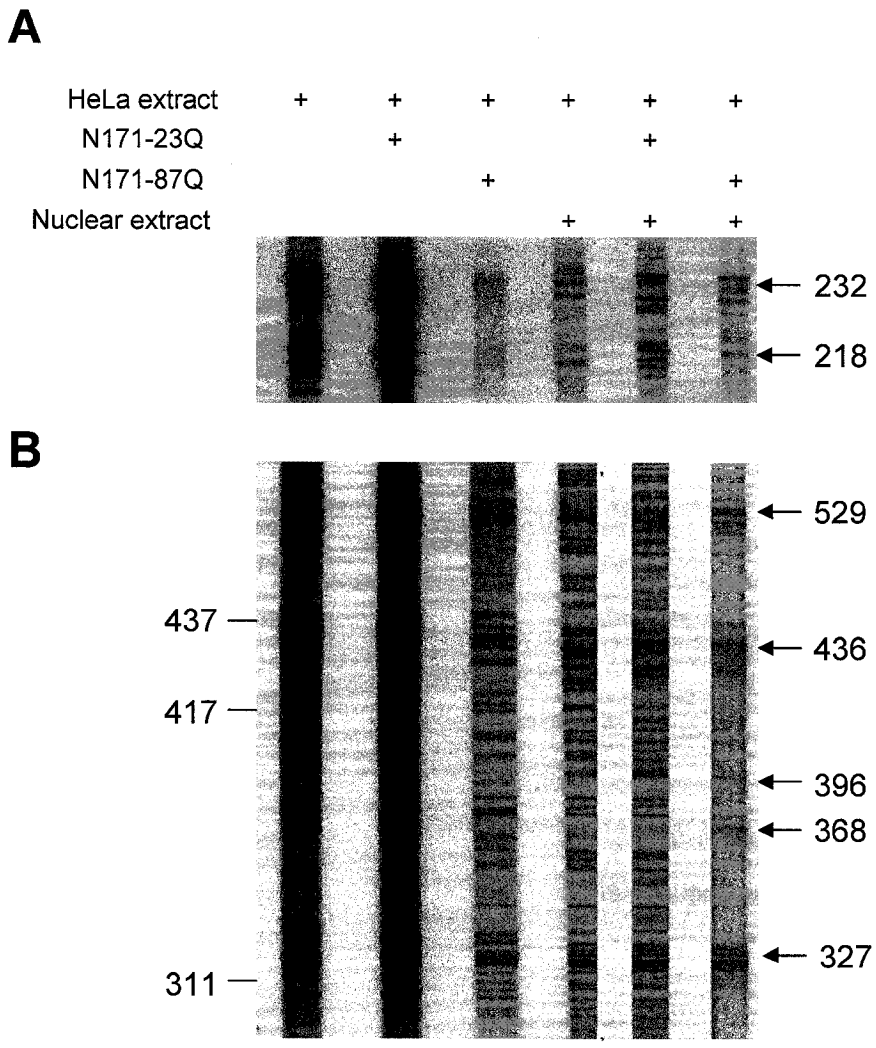

Figure 5-3. Addition of forebrain nuclear extract decreased transcription from the PDE10A2 and GAD65 promoters *in vitro*. *In vitro* transcription of the PDE10A2 (A) and the GAD65 (B) promoters in the presence or absence of 15 μg of forebrain nuclear extract isolated from 5 week-old wild-type mice and 1.5 pmol of N171-23Q or N171-87Q as indicated. The RNA products were fractioned on denaturing 4% PAGE gels. The relative positions of a radiolabelled and denatured PhiX174 DNA/*Hinf*I markers (Fermentas) are indicated on the left. The sizes of synthesized transcripts are indicated on the right (nt).

extract and 1.5 pmol of N171-87Q. Forebrain nuclear extract decreased the basal transcription supported by HeLa nuclear extract but did not alter the N171-87Q-mediated repressive effect on the PDE10A2 promoter (-392/+278). Similarly, forebrain nuclear extract decreased the basal transcription of the GAD65 promoter (-508/+600) supported by HeLa alone as well as transcription supported by HeLa extract in the presence of 1.5 pmol of N171-23Q. Thus, forebrain nuclear extract did not increase transcription or prevent N171-87Q-induced repression of the PDE10A2 and GAD65 promoters (Fig. 5-3B).

We wanted to determine whether the presence of N171-87Q altered the abundance of specific proteins that bound to the PDE10A2 and GAD65 promoters in this active transcription system. A flow scheme of the steps used to isolate proteins that interacted with the Dynabead-coupled PDE10A2 or GAD65 promoters is illustrated in figure 5-5. Biotinylated PDE10A2 and GAD65 promoter fragments attached to streptavidin-coated magnetic Dynabeads were used as templates for transcription. Four different sizes of transcripts were produced from the Dynabead-coupled PDE10A2 promoter, and 3 of these 4 sites corresponded closely to the four transcription start sites observed using non-Dynabead-coupled PDE10A2 template (Fig. 5-4A). The 352 nt transcript derived from start site 2 that was located at position -74 relative to the most 5' transcription start site identified *in vivo* (+1) was not detected suggesting that the Dynabead-labelling of the PDE10A2 promoter rendered this site inactive. Four different sizes of transcripts were synthesized from the Dynabead-coupled GAD65 promoter (Fig. 5-4B), three of which corresponded to transcription start site 1, 3, and 5 identified using the non-Dynabead-coupled GAD65 promoter as shown in figure 5-2. The 477 nt

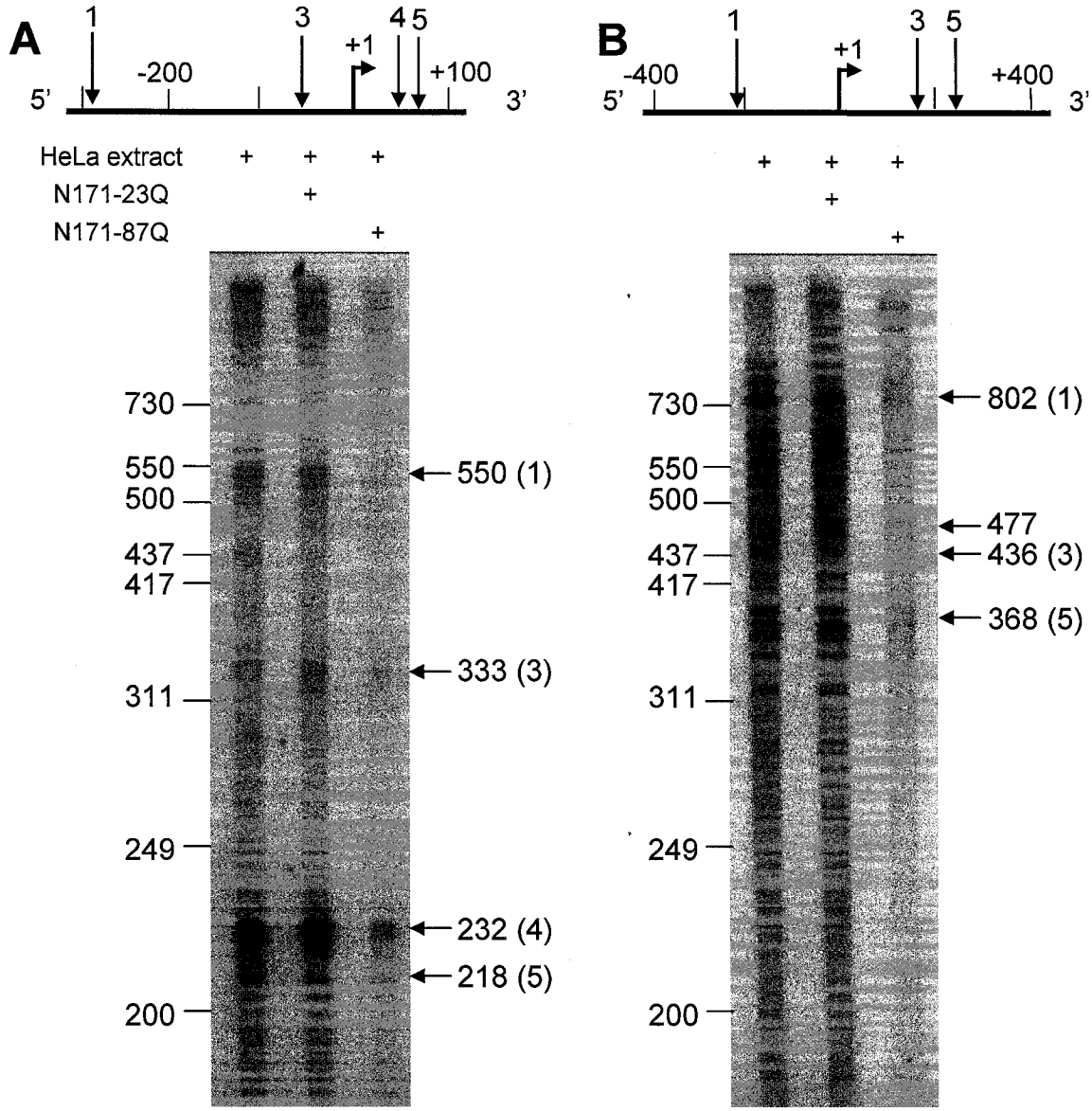

Figure 5-4. N171-87Q decreased transcription of the Dynabead-coupled PDE10A (-392/+278) and GAD65 promoter (-508/+600) *in vitro*. *In vitro* transcription was performed with Dynabead-coupled PDE10A2 and Dynabead-coupled GAD65 promoter fragments in the presence of HeLa nuclear extract and 1.5 pmol of N171-23Q or N171-87Q as indicated. The RNA products were fractioned on a denaturing 4% PAGE gel. The relative positions of a radiolabelled and denatured PhiX174 DNA/*Hinf*I markers (Fermentas) are indicated on the left. Schematic representations of the PDE10A and the GAD65 promoter are shown above each graph as a black line in A and B, respectively. The sizes of detected transcripts are indicated on the right (nt). The numbers in the bracket correspond to transcription start site indicated as downward-pointing arrows in A.

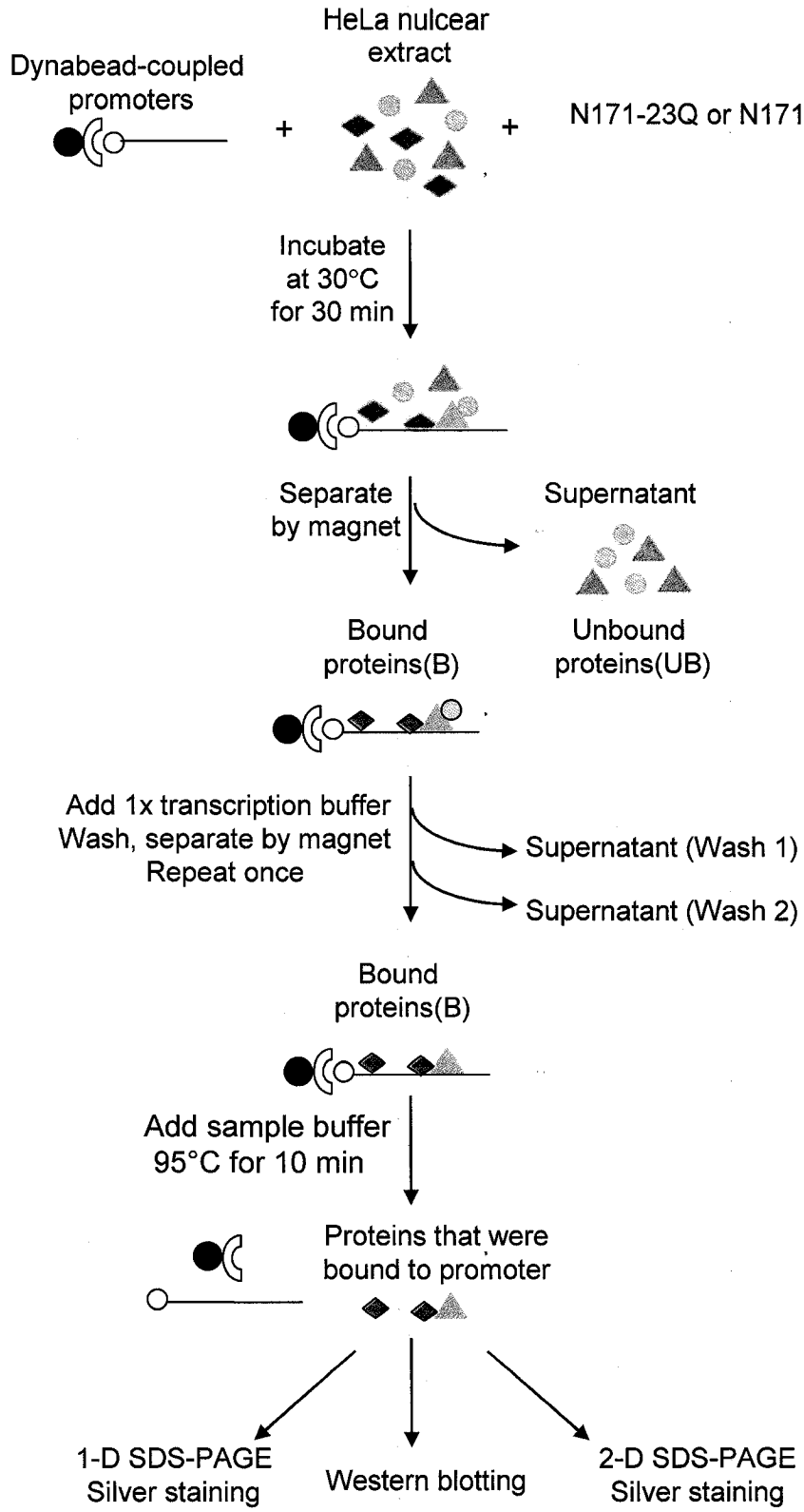

Figure 5-5. A flow scheme of isolating proteins that bound to the Dynabead-coupled PDE10A2 and GAD65 promoters.

transcript corresponded to a new site +123 relative to +1 site identified *in vivo* (Menalled *et al.*, 2000). Although Dynabead labeling of the PDE10A2 and GAD65 promoters slightly altered transcription start sites usage *in vitro*, the presence of Dynabead at the end of these DNA templates did not alter N171-87Q-induced transcriptional repression (Fig. 5-4).

As 1.5 pmol of N171-87Q was able to reduce transcription from the Dynabead-coupled PDE10A2, we wanted to determine whether N171-87Q was among proteins that bound to the promoter or among proteins that did not bind to the promoter. Western blot analysis was performed using an anti-histidine antibody which recognizes the histidine-tag at the N-terminus of recombinant N171-23Q (~28 kDa) and N171-87Q (~35 kDa)(Fig. 5-6). Both N171-23Q and N171-87Q were present in proteins that bound to the Dynabead-coupled PDE10A2 promoter. N171-23Q or -87Q was not detected in washes 1 or 2, (Fig. 5-6A). Comparing the levels of detected fusion proteins, we observed that N171-23Q was present at equal amount in proteins that bound to the promoter (Bound, B) and proteins that did not bind (Unbound, UB) and that N171-87Q appeared to be more abundant in the unbound fraction than the bound fraction (arrows). This antibody also detected two other proteins present in HeLa nuclear extract in reactions that contain HeLa, HeLa plus N171-23Q, and HeLa plus N171-87Q. The two proteins present in HeLa nuclear extract that cross reacted with the anti-histidine antibody were approximately 38 and 40 kDa. There was an another anti-histidine immunoreactive band migrating at ~70 kDa in the lanes containing unbound protein of the reaction containing HeLa extract and N171-87Q and in the control lane that contained N171-87Q alone (far left), indicating that the 70 kDa band may be an aggregation of N171-87Q

Figure 5-6. N171-23Q and N171-87Q were both present in the protein population that bound to the Dynabead-coupled PDE10A2 promoter. HeLa nuclear proteins were allowed to bind to the Dynabead-coupled PDE10A2 promoter in the presence of 1.5 pmol of N171-23Q or N171-87Q. Bound proteins (B), unbound proteins (UB), proteins that were present in the first wash of the Dynabead-coupled DNA (wash 1, W1) and proteins that were present in the second wash(wash 2, W2) were isolated as illustrated in figure 5-5. Western blot analysis of these proteins using an anti-histidine antibody is shown in A. 1.5 pmol of N171-23Q and N171-87Q were used as positive controls for the immunolabelling and their mobility is shown on the right. Silver stained SDS-PAGE analysis is shown in B. The total proteins in the reaction before magnet separation are indicated under the heading total. The relative mobility of molecular weight markers (kDa) are indicated on the left.

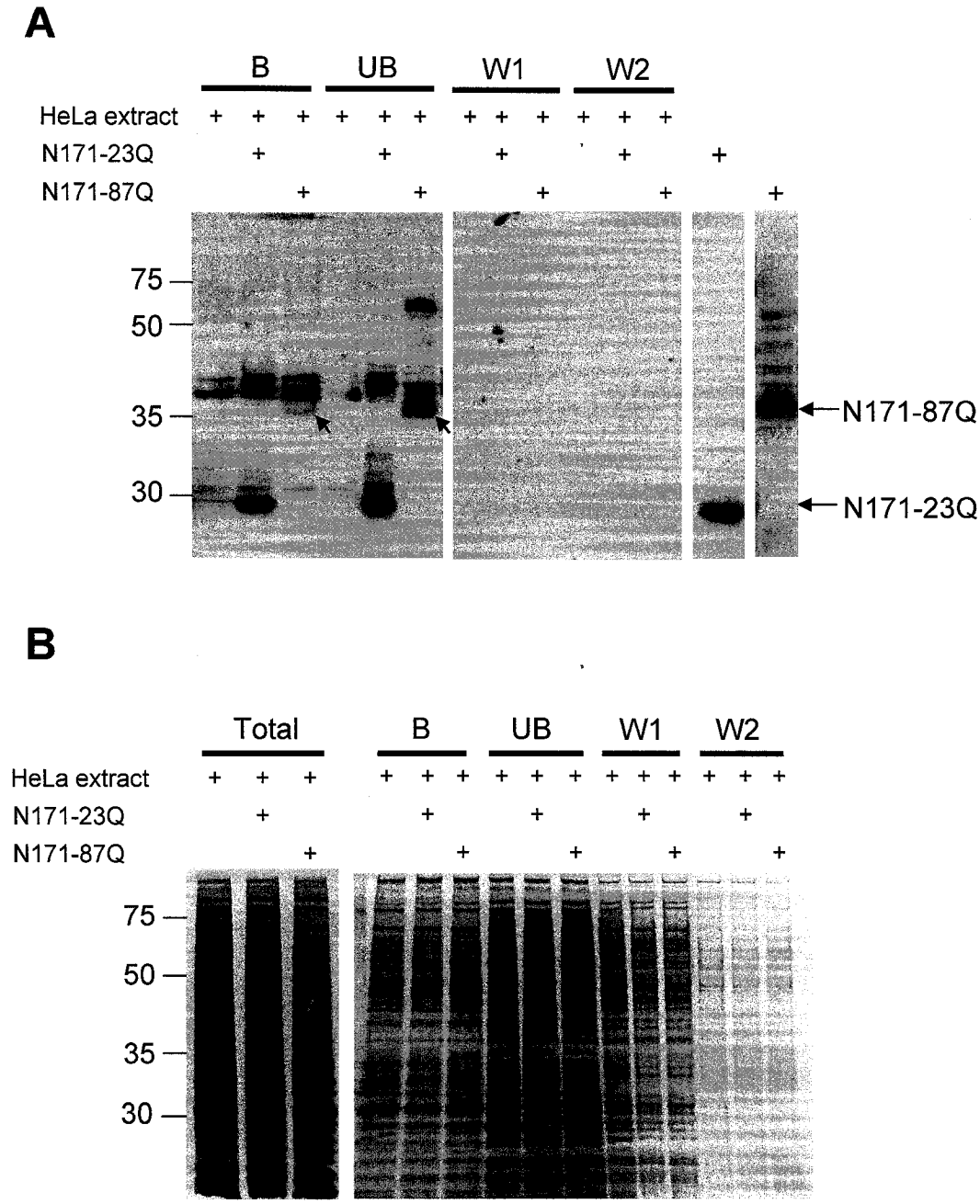
A
B
UB
W1
W2
HeLa extract
N171-23Q
N171-87Q
75
50
35
30
N171-87Q
N171-23Q
B
Total
B
UB
W1
W2
HeLa extract
N171-23Q
N171-87Q
75
50
35
30

monomers that form dimers with the concentrations used that are resistant to SDS and heat dissociation (Fig. 5-6A). Silver staining of these fractionated protein fractions indicated that the bound proteins and the unbound proteins each had a different banding pattern suggesting they each contained a unique protein population. A comparable analysis was also performed on proteins that bound to the Dynabead-coupled GAD65 promoter and there appeared that certain proteins were enriched in the bound fraction compared to the unbound fraction. Similarly, we found that N171-87Q was also present in both the bound and the unbound fractions for the GAD65 promoter (data not shown).

We compared the proteins that directly interacted with the PDE10A2 and GAD65 promoters on silver-stained one-dimensional (1-D) SDS-PAGE gels and determined that there were some common and some unique proteins bound to each promoter as indicated by arrows in figure 5-7, demonstrating that the subsets of proteins present in the HeLa nuclear extract provided promoter-specific proteins to preinitiation complexes in addition to common proteins that interacted with both promoters. Whether the reproducible, but subtle differences, in the abundance of proteins that bound to the Dynabead-coupled PDE10A2 and GAD65 promoters in the presence of N171-87Q affects transcription remains to be determined. Two-dimensional SDS-PAGE analysis was performed on proteins that bound to the Dynabead-coupled PDE10A2 promoter. Many of the proteins that bound these promoters had the same isoelectric points (PI), molecular weight (MW) and apparent abundance in complexes whether N171-23Q or N171-87Q was present. However, the presence of N171-23Q or N171-87Q altered the relative abundance of several proteins (Fig. 5-7B).

Figure 5-7. One-dimensional and two-dimensional SDS-PAGE analyses of proteins that bound to the Dynabead-coupled promoters in the presence of N171-23Q and N171-87Q. HeLa nuclear proteins were allowed to bind to Dynabead-coupled PDE10A2 and GAD65 promoters in the presence of 1.5 pmol of N171-23Q or N171-87Q. Proteins that were bound to the Dynabead-coupled PDE10A2 promoter (-428/+278) (lanes 1 and 2) and proteins that bound to the Dynabead-coupled GAD65 promoter (-508/+600) (lanes 3 and 4) were isolated as shown in figure 5-6A, and then fractioned on 7.5% SDS-PAGE gels followed by silver staining (A). 1.5 pmol of N171-23Q (lane 1 and 3) or 1.5 pmol of N171-87Q (lane 2 and 4) was included in the reactions. The relative mobilities of molecular weight markers (kDa) are indicated on the left. Bound proteins that are enriched on each promoter are indicated by arrows on the right. Proteins that were bound to the Dynabead-coupled PDE10A2 promoter (-428/+278) in the presence of N171-23Q or N171-87Q were fractioned by two-dimensional SDS-PAGE. A portion of 2-D SDS-PAGE analysis of bound proteins is shown in B. The relative mobility of molecular weight markers (kDa) in the second dimension are indicated on the left.

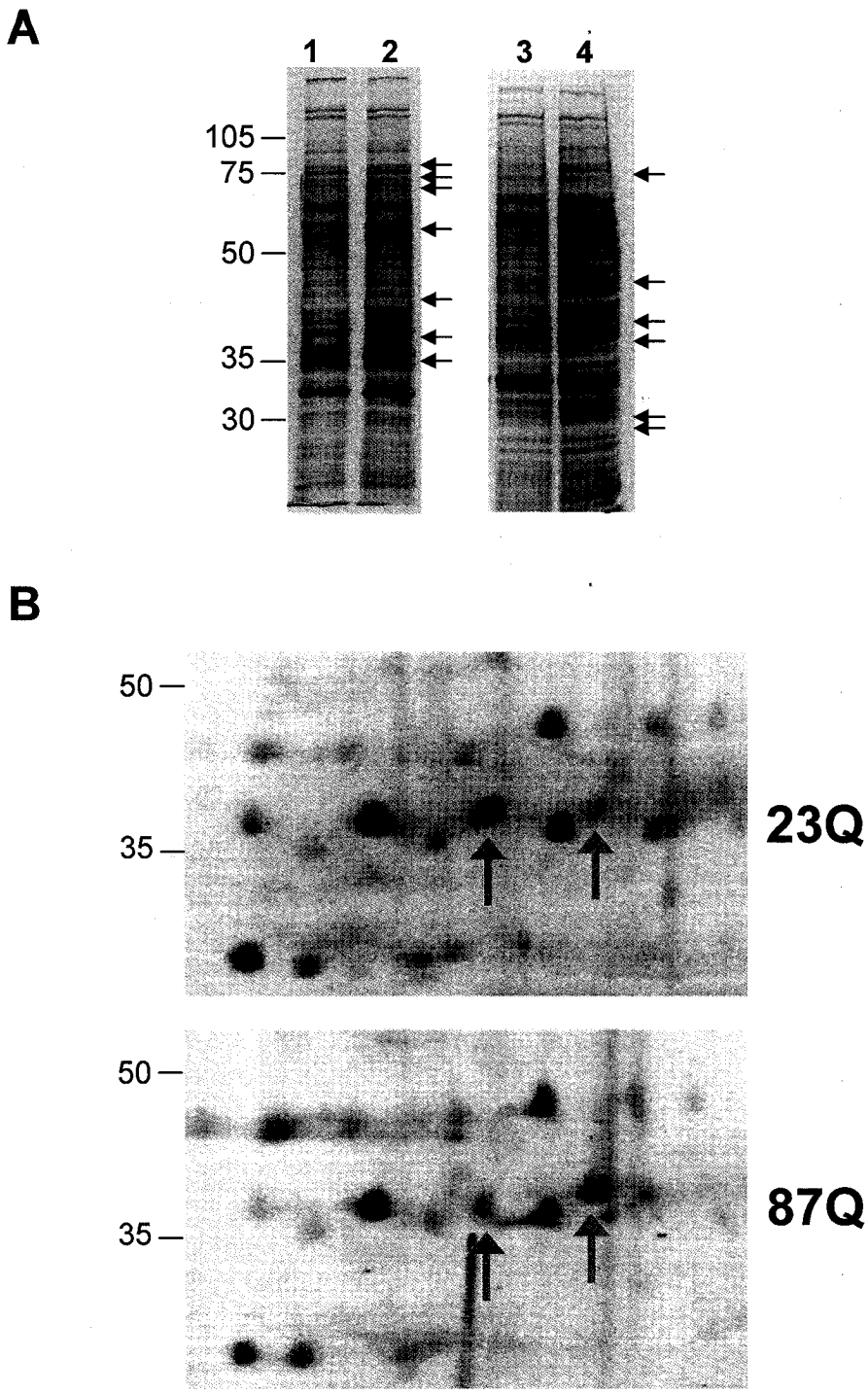
A
1
2
3
4
105
75
50
35
30
B
50
35
23Q
50
35
87Q

Reducing the levels of huntingtin increased transcription of the PDE10A2 promoter in ex vivo.

Transient expression of N89-22Q in ST14A cells decreased the activities of PDE10A2 and GAD65 promoters. We hypothesized that the N-terminus of huntingtin protein probably decreased transcription in striatal cells. A RNA interference (RNAi) approach was used to reduce the expression of the N-terminus of huntingtin in N548wt-15Q and N548hd-128Q cell lines and to see how reducing levels of huntingtin affects transcription. A small hairpin RNA construct (shRNA.htt) that expresses a 21 nt antisense RNA complementary to the 413-436 nt of the human huntingtin mRNA (GenBank assession number, NM002111) (Harper *et al.*, 2005) or a control vector that did not express any short hairpin RNA (shRNA) were co-transfected with the PDE10A2-pGL3 (-438/+278, P6) and transfection efficiency control construct phRL-TK into N548wt-15Q and N548hd-128Q cells. The activity of PDE10A2-pGL3 (-438/+278) in the presence of shRNA.htt increased in N548wt-15Q and N548-128Q cells compared to the promoter activity in the presence of shRNA vector (Fig. 5-8). The relative activity of PDE10A2-pGL3 (-438/+278) was increased by 1.3 and 2.0 fold in N548wt-15Q and N548hd-128Q cells, respectively, compared to the promoter activity in the absence of anti-N-terminal huntingtin shRNA.htt in each cell line. Despite differences in the fold increase compared to cells that did not express the shRNA, the promoter activity reached the same level in two cell lines in the presence of shRNA.htt. Western blot using MAB2166 antibody and densitometric analysis of the immunoreactive bands demonstrated that the expression of the shRNA.htt reduced the protein levels of the 75 kDa N-terminus of huntingtin expressed in N548wt-15Q cells by ~50% (Fig. 5-8B, 5-

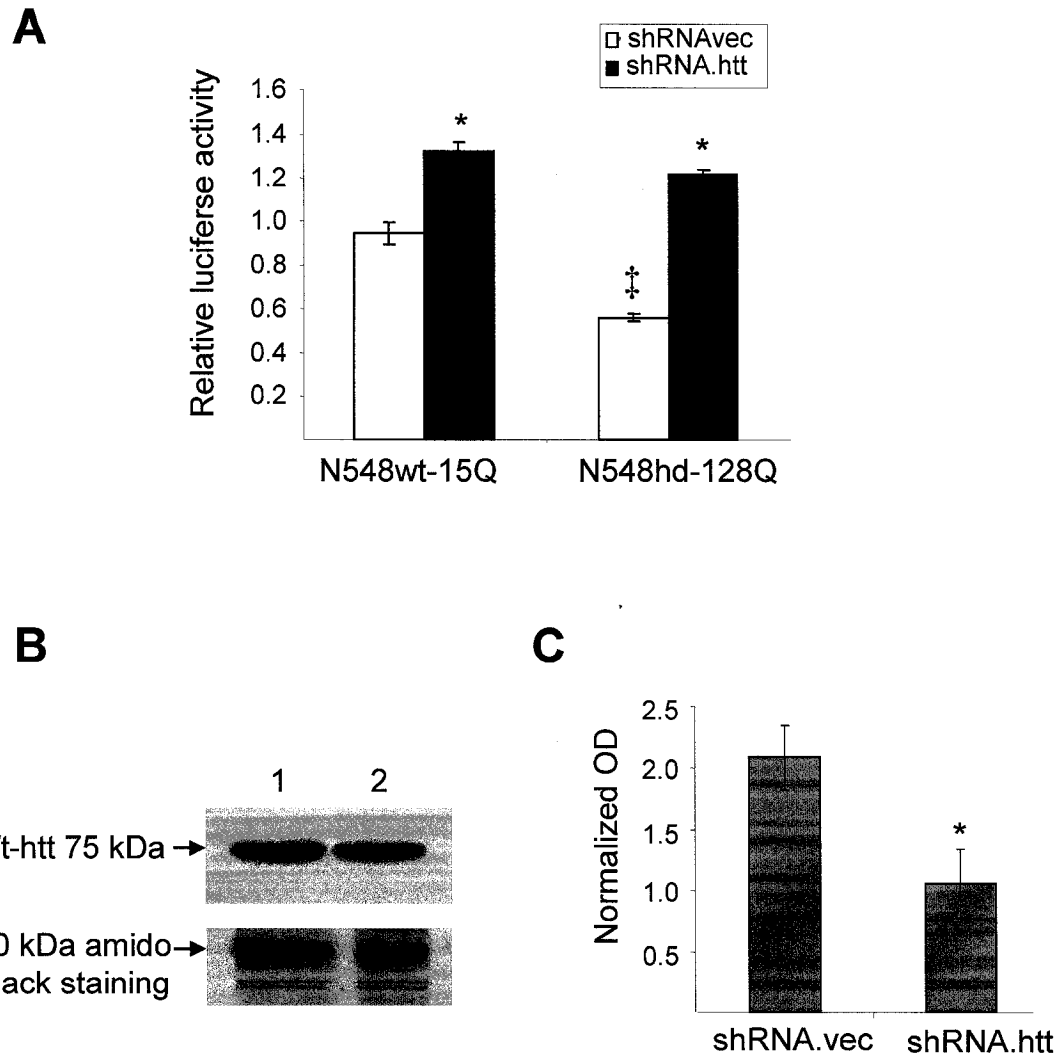

Figure 5-8. Expression of shRNA.htt reduced levels of human huntingtin in N548wt-15Q and N548hd-128Q cells and alleviated the N-terminus of mutant huntingtin-induced repression of PDE10A2 promoter activity. PDE10A2-pGL3 (P6, -428/+278) plasmid DNA was co-transfected with shRNA.htt or shRNA.vec into N548wt-15Q and N548hd-128Q cells. Firefly luciferase activity was normalized to *Renilla* luciferase activity and results were expressed as relative luciferase activity shown in A. Western blotting analysis using MAB2166 antibody is shown in B. The size of detected wild-type huntingtin protein from N548wt-15Q cells transfected with either shRNA vector (lane 1) or shRNA.htt (lane 2) is indicated on the left. A 50 kDa amido black-stained band was used as a loading control. Optical denstiy of the wild-type huntingtin protein were normalized to a 50 kDa amido black-stained protein and results were expressed as normalized OD (±SEM, N=3). *P<0.05, significant difference between shRNA.vec and shRNA.htt. ‡P<0.05, significant difference between N548wt-15Q cells and N548hd-128Q. (Two-away ANOVA).

8C), which is similar to the efficacy of knockdown reported in a previous study (Harper *et al.*, 2005). A low level of mutant huntingtin N548hd-128Q was detected in N548hd-128Q cells, suggesting that the extended polyQ tract in N548 reduced MAB2166-immunoreactivity due to an altered conformation of N548 containing 128Q (Davies *et al.*, 1997). Therefore, it was not possible to measure whether shRNA.htt reduced the levels of mutant huntingtin in N548hd-128Q cells. There was an increase in promoter activity when N-terminal huntingtin levels were decreased in N548wt-15Q cells, suggesting that the N-terminal huntingtin protein repressed transcription in these cells and that the presence of an extended polyglutamine tract within the N-terminus had an additive repressive effect on transcription.

Previously, Zhai *et al.* (2006) demonstrated that mutant huntingtin protein interacts with amino acids 40 to 60 of the RAP30 subunit of TFIIF, a key component in the core transcription machinery, thus interfering with the formation of the RAP30-RAP74 native complex and they hypothesized that this interaction was the cause of mutant huntingtin-induced transcriptional regulation. Human TFIIF consists of two subunits, RAP30 and RAP74 that, as a complex, directly bind to RNA pol II and function to recruit PolII to TFIID/TFIIB complex. TFIIF is a required component for transcription of all genes (Robert *et al.*, 1998). We hypothesized that a peptide composed of amino acids 40 to 60 of RAP30 would act as a dominant negative molecule interacting with and blocking the effects of mutant huntingtin, thus allowing the endogenous RAP30 and RAP74 to associate and fulfill their normal function in transcription as TFIIF. Co-transfection of a construct that expressed amino acids 40-60 of RAP30 [pCDNA4-RAP30 (40-60)] and PDE10A2-pGL3 (-438/+278) into N548wt-15Q and N548hd-128Q cells did

not alter the ratio of PDE10A2-dependent firefly to *Renilla* luciferase activity (Fig. 5-9A) even though pCDNA4-RAP30 (40-60) affected transcription. There was a 1.4 fold increase of firefly luciferase activity driven by the PDE10A2 promoter in the presence of pCDNA4-RAP30(40-60) and a 1.6 fold increase of the *Renilla* luciferase activity driven by the thymidine kinase promoter in the presence of pCDNA4-RAP30(40-60) in both cell lines (Fig. 5-9B, C). Increased firefly and *Renilla* promoter activities in both N548wt-15Q and N548hd-128Q cells in the presence of RAP30 (40-60 aa) indicated that this peptide was affecting promoter activity within these cells and increased general transcription independent of the length of the polyQ within the amino terminus of mutant huntingtin.

Recently, Slepko *et al.* (2006) demonstrated that synthesized polyQ peptides, which are lengths corresponding to non-pathological polyQ repeats, enhance the aggregation of a pathologic length polyQ47 peptide *in vitro* in a concentration and polyQ length-dependent manner. Co-expression of a wild-type huntingtin contruct (Exon 1-20Q) in a fruitfly model of HD (Exon 1-93Q) accelerates aggregate formation and neurodegeneration. Although this study showed that aggregate formation causes neurodegeneration of photoreceptor neurons in *Drosophila*, a large amount of evidence indicates the aggregation process is independent of neurodegeneration but associated with neuronal dysfunction (Saudou *et al.*, 1998; Arrasate *et al.*, 2004; Schaffar *et al.*, 2004; Slow *et al.*, 2005). We hypothesized that if a normal length polyQ peptide enhanced aggregation of a pathologic length polyQ *in vitro* regardless of whether or not such aggregates affect cell survival *ex vivo*, we would see an alleviation of the repressive

Figure 5-9. Expression of a portion of the RAP30 protein increased the firefly luciferase activity driven by the PDE10A2 promoter and the *Renilla* luciferase activity driven by the TK promoter in N548wt-15Q and N548hd-128Q cells. PDE10A2-pGL3 (P6, -428/+278) was co-transfected with phRL-TK, pcDNA4 vector or pCDNA4-RAP30 (amino acids 40-60 into N548wt-15Q and N548hd-128Q cells. Firefly luciferase activity was normalized to *Renilla* luciferase activity and results were expressed as relative luciferase activity in A. Average firefly luciferase activity is shown in B. Average *Renilla* luciferase activity is shown in C (±SEM, N=12). **P*<0.05, significant difference between pcDNA4 vector or pCDNA4-RAP30 (40-60 aa), ‡*P*<0.05, significant difference between N548wt-15Q cells and N548hd-128Q (Two-away ANOVA).

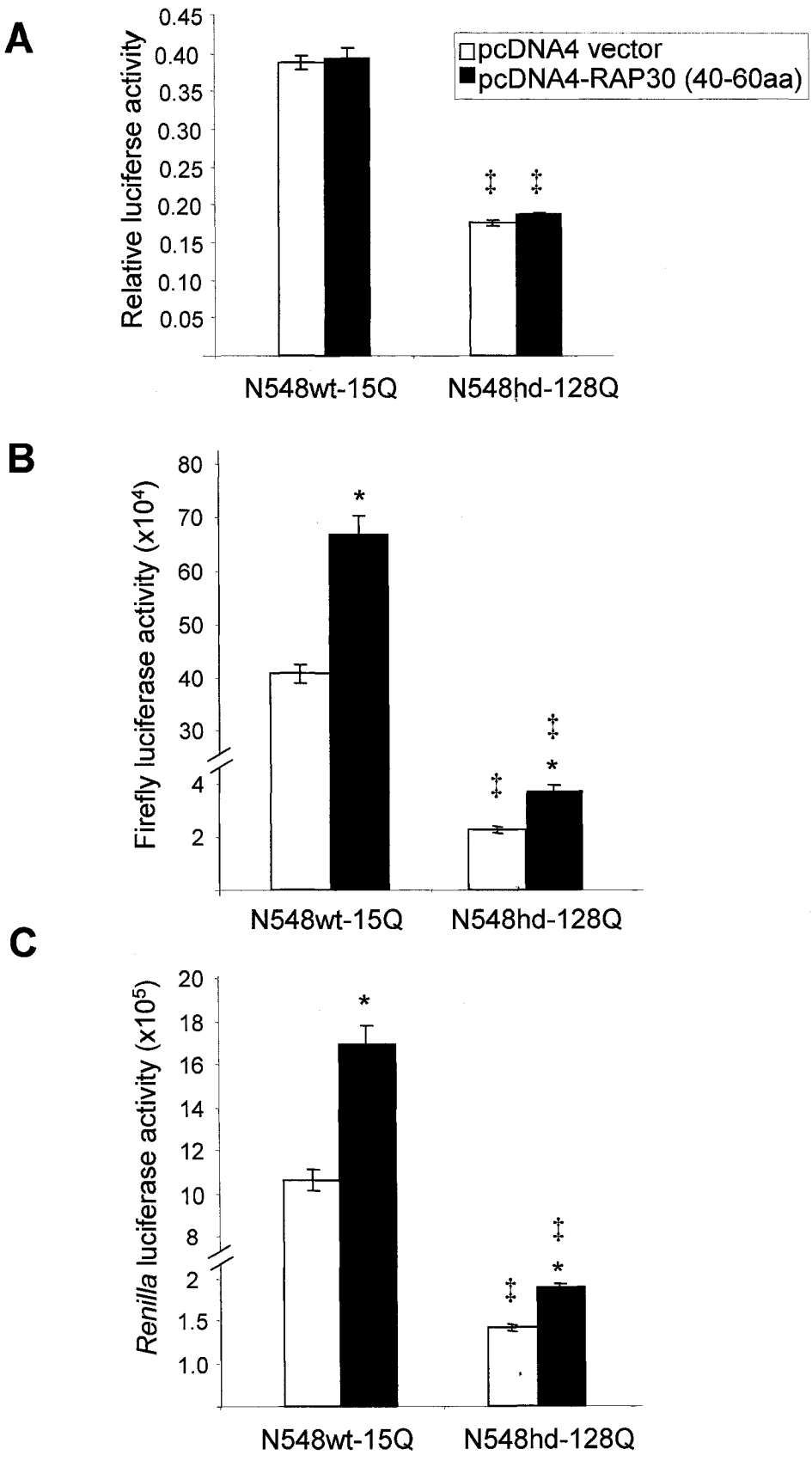
A
Relative luciferse activity
0.45
0.40
0.35
0.30
0.25
0.20
0.15
0.10
0.05
□pcDNA4 vector
■pcDNA4-RAP30 (40-60aa)
‡ ‡
N548wt-15Q
N548hd-128Q
B
Firefly luciferase activity (x10⁴)
80
70
60
50
40
30
4
2
*
‡
‡ *
N548wt-15Q
N548hd-128Q
C
Renilla luciferase activity (x10⁵)
20
18
16
14
12
10
8
2
1.5
1.0
*
‡
‡ *
N548wt-15Q
N548hd-128Q

effect of soluble recombinant N171-87Q protein in *in vitro* transcription reactions of the PDE10A2 promoter. To test this possibility, we obtained a synthetic peptide that contained 20 contiguous glutamines and two lysine residues on each side (polyQ) and a control peptide containing the polyproline-rich sequence found downstream of the polyQ repeat in human huntingtin (amino acids 51 to 70; 19) (polyP) to determine whether preincubation of polyQ peptide and N171-87Q would affect transcription of the PDE10A2 promoter *in vitro.* Levels of the 232 nt and 218 nt transcripts did not change in reactions containing 1.5 pmol of N171-23Q or N171-87Q that had been preincubated with 1.5 or 15 pmol of polyQ or polyP compared to the level of these transcripts in reactions without polyQ or polyP peptides. A ten min preincubation with either a 10:1 or 1:1 ratio of polyQ or polyP peptide to N171-23Q or N171-87Q did not affect transcription from the PDE10A2 promoter *in vitro.* It is possible that either the concentrations of peptides used were not high enough to initiate the aggregation process or there was not enough time for aggregation to occur. Before we used a high dose of polyQ and polyP to test whether they blocked the repressive effect of N171-87Q, we tested whether a high dose of peptides would affect transcription in the absence of N171-87Q. In fact, increasing amounts of polyP (2 pmol, 20 pmol, 200 pmol, 0.5 nmol, 1 nmol, 5 nmol) did not alter the amount of product transcribed from the PDE10A2 promoter (data not shown). The same amounts of polyQ peptide did not alter transcription with the exception of the highest dose (5 nmol). In the presence of 5 nmol polyQ, transcript levels were reduced suggesting that this dose of polyQ could decrease transcription directly (data not shown). When we preincubated 2 pmol and 20 pmol of polyP and polyQ peptide with 2 pmol of N171-87Q that corresponded to 1:1 and 10:1

Figure 5-10. Preincubation of N171-87Q and a peptide with 20 polyglutamines [polyQ(20)] alleviated the N171 mediated transcriptional repression in a dose-dependent manner on the PDE10A2 promoter. N171-23Q and N171-87Q were pre-incubated with a peptide composed of 20 glutamines (polyQ) or a 19 amino acid polyproline-rich peptide (polyP) for10 min (A) or for 2.5 hrs (B) before *in vitro* transcription reactions. The relative amount of polyQ or polyP and N171-87Q contained in each *in vitro* transcription reaction are indicated. The equivalent amounts of polyP used in each reaction were aligned below. The 232 and 218 nt transcripts from the PDE10A2 promoter are shown.

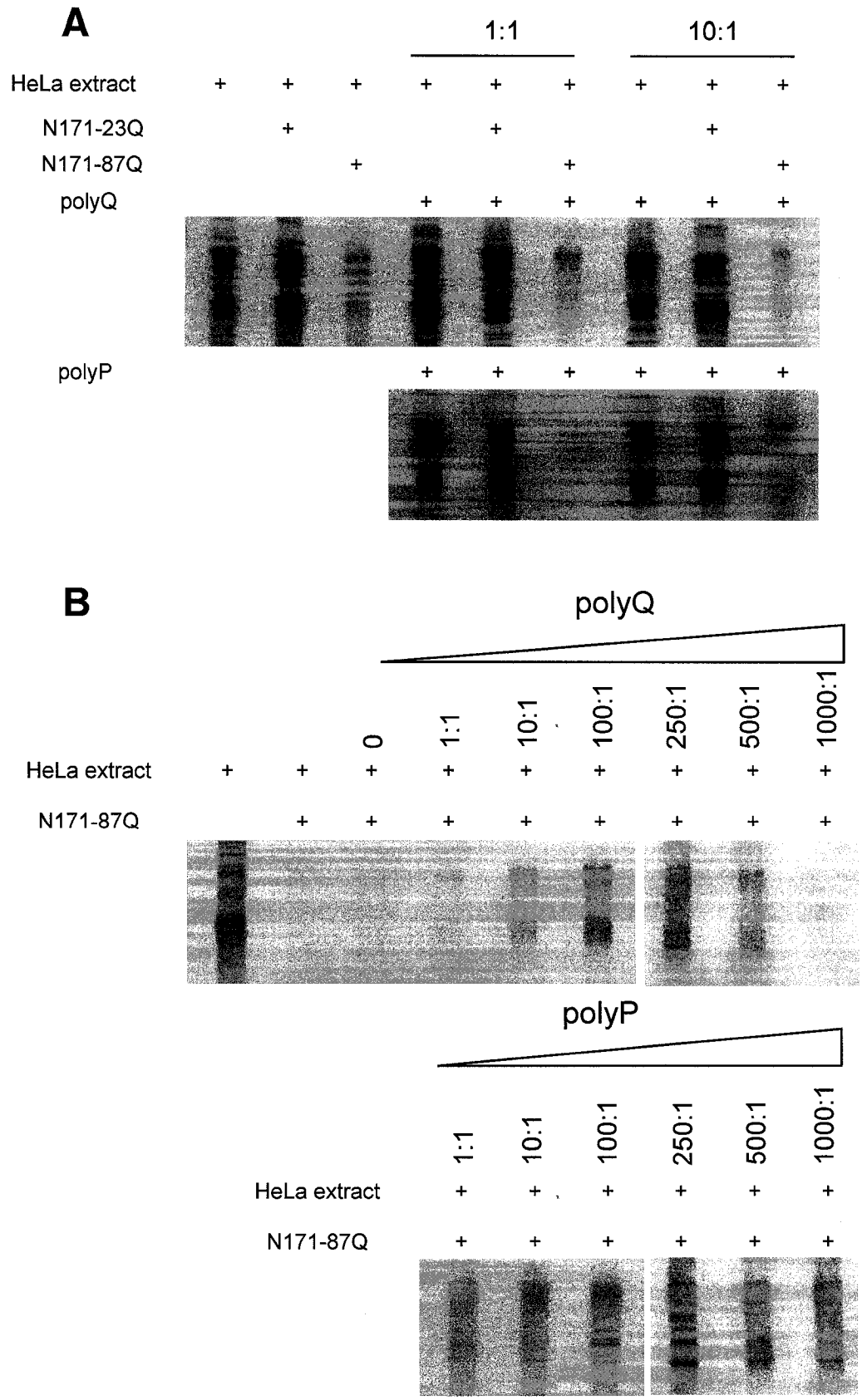
A
1:1
10:1
HeLa extract
N171-23Q
N171-87Q
polyQ
polyP
B
polyQ
0
1:1
10:1
100:1
250:1
500:1
1000:1
HeLa extract
N171-87Q
polyP
1:1
10:1
100:1
250:1
500:1
1000:1
HeLa extract
N171-87Q

ratio of peptides to N171-87Q for 2.5 hrs before *in vitro* transcription, we did not see any changes in the levels of transcripts, suggesting that extended preincubation of these peptides with N171-87Q did not reverse N171-87Q-mediated repression (Fig. 5-10B). However, when the ratios of both peptides to N171-87Q were increased to 100:1, 250:1 and 500:1 (200 pmol, 0.5 nmol, 1 nmol of peptides to 2 pmol of N171-87Q), there was a dose-dependent increase of the levels of PDE10A2 transcripts compared to the levels of transcripts from HeLa and N171-87Q (Fig. 5-10B). A 1000:1 ratio (5 nmol) of polyQ to N171-87Q reduced transcript levels. This suggests that 1000:1 ratio had combinatory effects, one was from the amount of peptide that blocked the N171-87Q-mediated repression and another was from the repressive effect of the polyQ peptide itself when it reached more than 1 nmol. Thus, it appears that at a ratio of 100:1, 250:1 and 500:1 between polyQ or polyP peptides and N171-89Q, there was a dose-dependent de-repression of N171-89Q-involved transcription from the PDE10A2 promoter. This data suggests that decreasing the soluble level of N171-87Q by promoting it to form aggregates alleviates its repressive effect on transcription in a dose-dependent manner.

5.3 Discussion

Transcription initiation is a highly orchestrated process that requires the assembly of promoter-specific DNA binding proteins and the core RNA pol II transcription machinery for the formation of a preinitiation complex at the transcription initiation site (Hampsey, 1998; Lemon & Tjian, 2000; Asturias, 2004). In this study, we wanted to study how polyQ in the context of the N-terminus of mutant huntingtin caused gene-specific transcriptional repression in a cell-free, functional transcription system and how

the presence of mutant huntingtin altered protein assembly for transcription initiation on the core promoter of the PDE10A2 gene.

Soluble mutant huntingtin directly affected transcription independent of chromatin structure.

One of the fundamental mechanisms controlling the selectivity of gene expression is through limiting the ability of transcription factors to access promoter sequences by packaging genes into chromatin (Emerson, 2002). During RNA pol II-mediated transcription, accessibility of transcription factors to DNA and recruitment of RNA pol II basal transcription complexes to promoters is regulated by modulation of nucleosomal structure through ATP-dependent remodeling and histone modification. The amino-terminus of huntingtin protein interacts with proteins CBP and p300/CAF that have histone acetyltransferase activity and such interaction leads to recruitment of these factors into aggregates compromising their ability in histone acetylation (Nucifora *et al.,* 2001; Steffan *et al.,* 2000). It is proposed that decreased histone acetylation induced by mutant huntingtin results in decreased transcription seen in many genes in HD and that histone modification might be an underlying mechanism of transcriptional dysregulation in HD (Sadri-Vakili & Cha, 2006). This concept has been supported by beneficial effects of histone deacetylase (HDAC) inhibitors in animal models of HD, which, in theory, augment histone acetylation and compensate for decreased transcription (Steffan *et al.,* 2000; Bates, 2001; Nucifora *et al.,* 2001; Ferrante *et al.,* 2003; Hockly *et al.,* 2003). We found that soluble mutant huntingtin N171-87Q directly caused decreased transcription of DNA fragments of the PDE10A and GAD65 promoters that were free of chromatin

structure (Widlak *et al.,* 1997). This effect was polyQ length-dependent, which recapitulates the effects observed *in vivo,* and confirms that mutant huntingtin protein exerts a toxic "gain-of-function" (Chapter 3, Fig.3-3 and Hebb *et al.,* 2004). The observed repression *in vitro* is unlikely due to soluble mutant huntingtin interfering with chromatin modifying activities such as histone acetylation or deacetylation, because the DNA templates that are free of proteins were added to the system. Our findings are consistent with a previous study showing that soluble mutant huntingtin is able to decrease transcription on a chromatin structure-free, dopamine D2 receptor promoter fragment using *in vitro* reconstituted basal transcription factors and RNA pol II (Zhai *et al.,* 2005). The authors also found that the addition of HDAC inhibitors in the *in vitro* system has no effect on mutant huntingtin-mediated transcription, emphasizing that chromatin modification is not a required regulatory event for mutant huntingtin to exert transcriptional repression. Therefore, histone modifications on chromatin structure of genes is unlikely the only theme in transcriptional dysregulation in HD.

Forebrain nuclear proteins decreased transcription in vitro.

The activity of the GAD65 promoter was not affected by the N-terminus of mutant huntingtin *in vivo* and *ex vivo* (Chapter 4, Fig. 4-11, Menalled *et al.,* 2000). However, soluble N171-87Q decreased transcription from the GAD65 promoter *in vitro* suggesting that HeLa nuclear extract may not contain brain-specific factors that protect the GAD65 promoter from the activity of mutant huntingtin or this system does not faithfully recapitulate all aspects for accurate neuronal transcription. The addition of forebrain nuclear extract decreased transcription from the PDE10A2 promoter to a level

that there was no further measurable repressive effect from N171-87Q. These results differ with the result on the cytomegalovirus (CMV) promoter where the addition of wild-type forebrain nuclear extract increased expression of the CMV promoter *in vitro* (Hogel, Gomez and Denovan-Wright, unpublished data) and accentuated the repression caused by N171-87Q. These data suggest that the N-terminal mutant huntingtin act synergistically with forebrain nuclear proteins to reduce transcription on the CMV promoter. It is possible that forebrain nuclear extract interacting with N171-87Q alters transcription of promoters with lower activity than CMV, such as PDE10A2, but we were unable to detect such effects using this *in vitro* system.

Mutant huntingtin was associated with the transcription preinitiation complexes

Transcription initiation starts with the assembly of the preinitiation complex on the promoter (Conaway & Conaway, 1993). The proteins from HeLa nuclear proteins in the presence of recombinant N171-23 or -87Q that bind to the promoter before the addition of dNTP can be isolated by magnet separation of Dynabead-coupled promoter. Both soluble N171-23Q and N171-87Q were localized to protein fractions that bound to the PDE10A2 and GAD65 promoters, suggesting that both proteins were likely present in the complexes ready for transcription initiation. It is unlikely that these proteins act as DNA binding proteins to directly bind to DNA, since we did not see any difference in protein binding pattern on the PDE10A2 promoter fragment in *in vitro* DNase I footprinting between reactions containing HeLa nuclear extract alone or HeLa extract in the presence of N171-23Q or N171-87Q (data not shown). It is possible that both N171-23Q and N171-87Q act as bridging molecules by associating with DNA binding proteins

that physically bind to the promoter. This suggests that sequences in N171 can interact with basal factors and that 87Q within N171 mediates transcriptional repression. It is important to note that, while N171-23Q is an experimental control *in vitro*, the comparable part of the normal huntingtin protein does not accumulate in the nucleus *in vivo*. Future experiments to identify proteins that affect promoter activity will compare protein populations isolated from transcription reactions without N-terminal mutant huntingtin, and reactions containing N171-23Q and N171-87Q. Ideally, we would want to examine how the pathological length polyQ alone alters transcription initiation *in vitro*. However, pathological length polyQ is not soluble.

Many mutant huntingtin-binding partners have been identified through *in vitro* binding assays and several of them are basal transcription components such as TAFII130 or TAF4 , TFIIF (Dunah *et al.,* 2002; Zhai *et al.,* 2005). TFIIF is composed of two subunits, RAP30 and RAP74, and the association of these two subunits is critical for the production of a functional TFIIF in the core transcription machinery. It has been shown that RAP30 interacts with the N-terminus of mutant huntingtin. This interaction disrupts the formation of a functional TFIIF complex and causes abnormal transcription of the dopamine D2 receptor promoter (Zhai *et al.,* 2006). These authors hypothesized that dysfunctional TFIIF is the cause for transcriptional dysregulation in HD. However, over-expression of amino acids 40 to 60 of RAP30 increased both firefly activity derived from PDE10A2 promoter and *Renilla* luciferase activity from the TK promoter but did not alter the ratio between the two in cells expressing either wild-type (N548wt-15Q) and mutant huntingtin (N548hd-128Q). This suggests that RAP30 does not appear to be the target inhibited by mutant huntingtin to give a specific transcriptional repression on the

PDE10A2 promoter. Over-expression of full-length RAP30 in primary striatal cells expressing the N-terminus of mutant huntingtin alleviates transcriptional repression on the D2 promoter and cell toxicity induced by mutant huntingtin (Zhai *et al.*, 2005). However, the promoter activity in their study was measured by normalizing luciferase activity derived from the D2 promoter to the amount of protein present in each lysate. This normalization is questionable since the transfection efficiency is not properly controlled by normalizing the luciferase activity to total protein lysate. In contrast, the PDE10A2 promoter activity was obtained by normalizing the activity of firefly to *Renilla* activity within the same cells. This internal normalization accurately reflected the mutant huntingtin effect. Our result indicates that expressing RAP30 (40-60 aa) can increase the absolute promoter activity, but not the ratio of firefly to *Renilla* luciferase activity in cells expressing N548hd-128Q. It is unlikely that RAP30 blocks mutant huntingtin effects specifically on the PDE10A2 promoter in N548hd-128Q cells.

polyQ and polyP peptides alleviated transcriptional repression by N171-87Q

The formation of NIIs is a process that is independent from mutant huntingtin-induced dysregulation of transcription, cell death and the development of HD symptoms in animal models of HD (Saudou *et al.*, 1998; Yu *et al.*, 2002; Schaffar *et al.*, 2004). We showed that preincubation of N171-87Q with polyQ and polyP peptides blocked the repressive effect of N171-87Q. It appeared that normal length polyQ peptide can only initiate the aggregation with N171-87Q at certain concentrations, which gave a concentration dependent de-repression of transcription *in vitro*. This finding agrees with previous observations that aggregate formation is a nucleation-dependent polymerization

process (Slepko *et al.*, 2006). In this process, mutant huntingtin may exist as disordered monomers and it starts to form fibrils via spontaneous aggregation (Slepko *et al.*, 2006). Thus, proteins containing sterically accessible polyQ segments can serve to elongate or enhance the growth of polyQ-based aggregates (Huang *et al.*, 1998; Perez *et al.*, 1998). Slepko *et al.* (2006) also showed that co-expression of exon 1 of wild-type huntingtin with 20Q together with exon 1 of mutant huntingtin with 94Q in *Drosophila* accelerates the aggregation process leading to a faster neurodegeneration seen in photoreceptor neurons in *Drosophila*. Similarly, an earlier study showed that exon 1-containing mutant huntingtin promotes the aggregation of wild-type huntingtin *in vitro*, causing the formation of SDS-resistant co-aggregates with a fibrillar morphology. However, this N-terminus mutant huntingtin did not promote the aggregation of the polyQ-containing transcription factors neuronal OCT3 and PQBP-1 (Busch *et al.*, 2003). These observations suggest that mutant huntingtin is able to form aggregates with wild-type huntingtin which appears to be a highly selective process that not only depends on polyQ tract length but also on the surrounding amino acid sequence. The data suggest that co-aggregation of wild-type huntingtin and mutant huntingtin may limit the concentration of soluble mutant huntingtin *in vivo*.

The observations that both polyQ and polyP peptides alleviated the repression of transcription suggests that soluble N171-87Q likely interferes with transcription through interacting with polyQ and polyP region of transcription factors in the preinitiation complexes. The short peptides at a high concentration efficiently block such interactions. It is known that transactivation domains of most of transcription factors contain a polyglutamine and a polyproline rich region (Gerber *et al.*, 1994). Thus, soluble N171-

87Q is likely to affect transcription by interacting with transactivation domains of transcription factors. This complements the observations in Chapter 4 where the N-terminus of mutant huntingtin did not appear to affect DNA binding of transcription factors but likely affected transactivation domain of factors.

Western analysis of a 1-D gel of proteins that bound to the PDE10A2 and GAD65 promoters indicated association of N171-23Q or N171-87Q with these proteins. Several attempts to detect N171-23Q or N171-87Q on 2-D gels were not successful (data not shown). Nevertheless, the silver staining of bound proteins on 2-D gels suggested that N171-87Q altered the intensity of individual proteins but not did not appear to cause small changes in isoelectric point or molecular weight indicating that N171-87Q is unlikely to post-translationally modify transcription factors that form preinitiation complexes on this promoter. Determining the identity of these factors and how these factors are functionally involved in mutant huntingtin-mediated transcriptional repression are ongoing studies in the laboratory.

CHAPTER 6

Conclusions

6.1 Summary

Although it is known that inheritance of one copy of the *HD* gene with an extended CAG repeat causes HD and that the huntingtin protein is expressed throughout the brain and body, the exact mechanism(s) whereby this genetic mutation causes all of the changes that progressively alter brain function remains poorly defined. Unlike most other neurodegenerative disorders, HD patients can be unambiguously identified decades before the appearance of disease symptoms or measurable changes in brain structure or function. For this reason, a clear understanding of how mutant huntingtin directly initiates the cascade of events that make up the natural course of HD may lead to novel targets to intervene or prevent the development of HD. HD is currently without effective management strategies.

The goal of this study was to contribute to our understanding of the mechanism whereby mutant huntingtin directly affects gene expression, which occurs early in disease progression and initiates a cascade of events that lead to changes in neuronal function. We studied the spatial and temporal regulation of PDE10A in the brains of transgenic models of HD (R6/1 and R6/2). Different mechanisms of transcriptional dysregulation were tested in cell culture models of HD and an *in vitro* transcription system using soluble, purified recombinant huntingtin proteins. We determined that the N-terminus of mutant huntingtin reduced the steady-state level of PDE10A2 mRNA by affecting the rate of transcription initiation from two of three transcription start sites *in vivo* in the striatum of R6/1 mice. Previous studies that demonstrated interactions between mutant huntingtin and transcription factors (Huang *et al.*, 1998; Boutell *et al.*, 1999; Kazantseve *et al.*, 1999; Nucifora *et al.*, 2000; Steffan *et al.*, 2000; Dunah *et al.*, 2002; McCampbell

et al., 2000) were based on the unproven assumption that mutant huntingtin affected transcription initiation. Mutant huntingtin did not alter the DNA binding activity of transcription factors *in vitro* or alter protein-PDE10A2 promoter interactions *in vitro* or *ex vivo*. The soluble, and not the aggregated form, of mutant huntingtin reduced transcription. Mutant huntingtin repressed, but did not completely block, transcription. We developed a system to 1) identify proteins that interact with mutant huntingtin and affect transcription and 2) to test the effect of such interactions *in vitro*. We also demonstrated that N-terminus mutant huntingtin-dependent transcriptional repression could be alleviated by pre-incubating purified, soluble N-terminus mutant huntingtin N171-87Q with non-pathological length polyQ and polyP peptides.

6.2 Mutant Huntingtin Is Incorporated Into the Transcriptionally-Active Complexes

Previously, three models of the mechanism of transcriptional dysregulation in HD were proposed (Sugars & Rubinsztein, 2003; Thomas, 2006; Fig. 6-1). First, polyQ in the context of the N-terminus of mutant huntingtin may allow this part of mutant huntingtin to directly function as a transcription factor. In this model, N-terminus mutant huntingtin would be a DNA binding protein that displaces other polyQ-containing transcription activators or recruits co-repressors (Fig. 6-1A, 1). Second, N-terminus mutant huntingtin may interact with or sequester transcription factors and prevent these factors from forming functional complexes on promoters (Fig. 6-1A, 2). Third, mutant huntingtin may directly alter transcription by interacting with specific components in the core transcription machinery including TAFII130 (Dunah *et al.*, 2002) and TFIIF (Zhai *et*

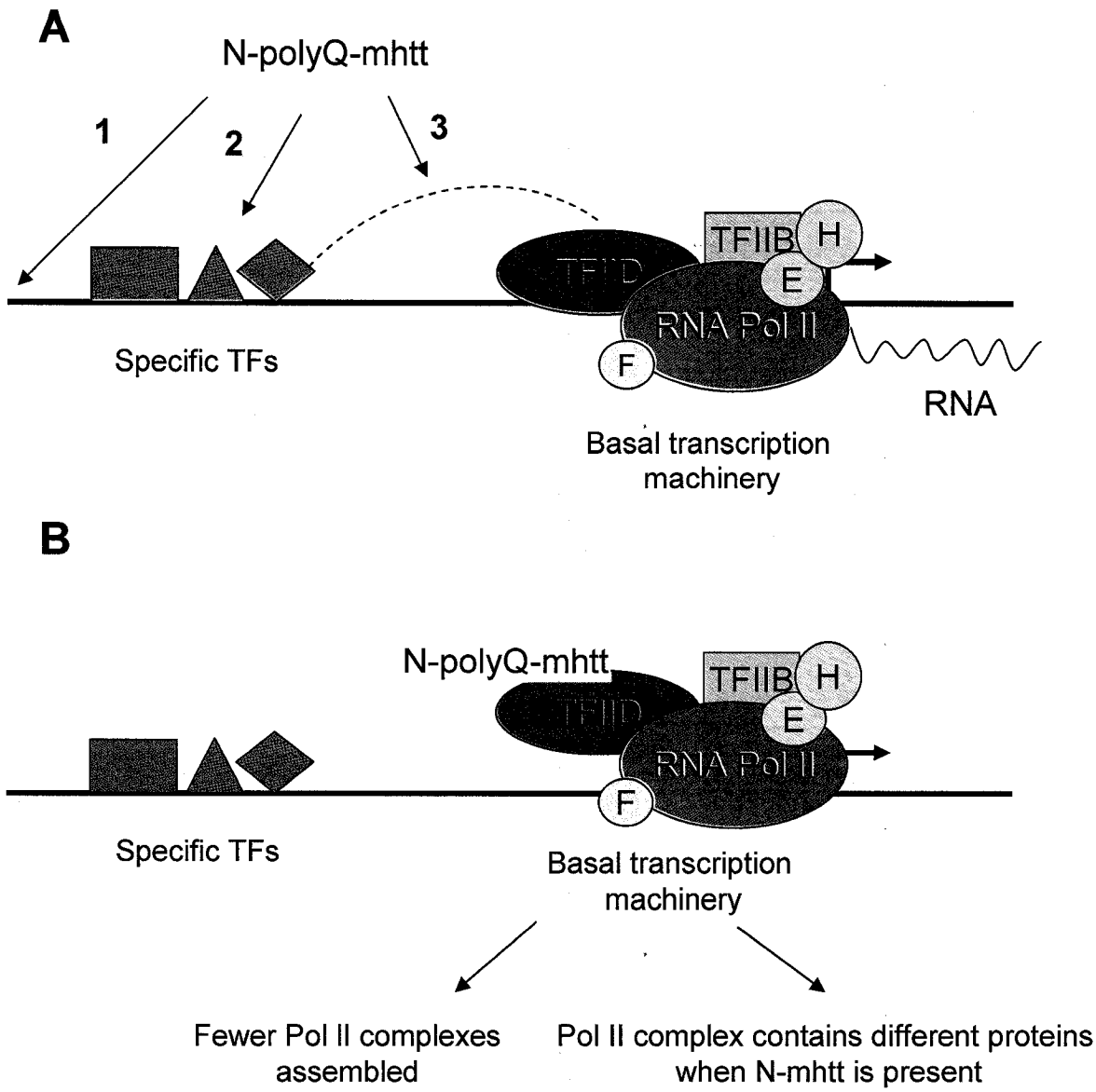

Figure 6-1. Models of N-terminus mutant huntingtin-mediated transcriptional dysregulation. As shown in part A, N-terminus mutant huntingtin (N-mhtt) could act as a DNA binding protein on affected promoters (1), sequester transcription factors away from the promoter (2) or block the communication between promoter-specific factors and the core pol II transcription machinery (3). Our data supports the hypothesis that mutant huntingtin is associated with components of the active transcription machinery. As shown in B, N-terminus mutant huntingtin could cause fewer complexes to be assembled or alter the composition of complexes that do assemble. The change in complex may lead to reduced transcription.

al., 2005) (Fig. 6-1A, 3) and block communication between sequence specific factors and the core pol II complex (Fig. 6-1A, 3).

In this study, we determined that the N-terminus of mutant huntingtin affected transcription initiation at a specific promoter of the PDE10A2 gene *in vivo*, *ex vivo* and *in vitro.* Mutant huntingtin did not affect the ability of transcription factors to bind to DNA nor did it act as a DNA binding protein itself on the PDE10A2 promoter region we examined. Thus, our data do not support model 1 or 2 (Fig. 6-1A). Our data demonstrate that the N-terminus of mutant huntingtin associates with proteins that assemble at the minimal promoter and affects transcription initiation. This observation is consistent with numerous other studies that have shown interactions between the proteins that together make up a functional pol II complex with co-activators (Shimohata *et al.,* 2000; Dunah *et al.,* 2002; Zhai *et al.,* 2005). There are two theories that could explain why such association would cause reduced transcription. First, mutant huntingtin could block interactions between interacting proteins and cause less frequent productive assembly of transcription factors at the transcription start site, which would result in less mRNA synthesis (Fig. 6-1B). Second, the N-terminus of mutant huntingtin could alter the composition of transcriptionally-active complexes at the transcription start sites leading to the assembly of pol II complexes that have reduced rates of transcription (Fig. 6-1B). Because the presence of N171-87Q did not appear to alter the amount of protein that associated with the promoter but did affect the relative abundance of specific promoter-bound proteins on the PDE10A2 promoter, our data supported the second theory whereby the composition of functional pol II complexes was altered by N-terminus mutant huntingtin.

6.3 Composition of the Basal Transcription Machinery and Cell- And Promoter-Specificity In the Presence of Mutant Huntingtin

A key unresolved issue in HD research is the definition of the basis for mutant huntingtin-dependent cell-, gene- and promoter-specific transcriptional repression. It is generally thought that Pol II transcription complex is largely invariable and that the temporal and spatial regulation of gene expression in multicellular organisms is controlled by tissue-specific transcription factors that act upstream of the core promoter to recruit the Pol II complex. Increasing evidence, however, has demonstrated that TFIID , within the Pol II complex, is composed of various TBP and TBP-associating factors (TAFs). Such variability in TFIID has emerged as one of critical components that leads to a highly versatile, cell-type specific and promoter-specific transcription apparatus (Hochheimer & Tjian, 2003). For example, TBP-related factor 2 (TRF2) in mice and humans is highly expressed in testis compared to other tissues and is important for gene expression during spermatogenesis based on evidence obtained from TRF2 knockout mice (Rabenstein *et al.*, 1999). Cell type-specific expression of TAF4 has also been demonstrated (Freiman *et al.*, 2001). TAF4 is highly expressed in B cells and interacts with B cell-specific regulators including NFkappaB/Rel family transcription factors to regulate gene expression in B cells (Ainbinder *et al.*, 2002). Differential association of TRF2 with TFIIA or TFIIB gives promoter-selective gene expression in *Drosophila* (Goodrich & Tjian, 1994). Our preliminary analysis of PDE10A2 promoter-bound proteins by 2D-PAGE suggests that the presence of soluble mutant huntingtin alters the composition of transcription initiation complexes. Thus, it seems likely that the extended polyQ at the N-terminus of mutant huntingtin results in differential association of

different components of the general transcription machinery, which ultimately causes the cell type- and gene-specific transcriptional repression by mutant huntingtin.

6.4 Future Work

Our data support the theory that mutant huntingtin alters the composition of pol II complexes that are bound to the PDE10A2 promoter. It did not appear that N-terminus mutant huntingtin affected the overall ability to assemble or stabilities of protein complexes at the PDE10A2 promoter. The first step in our future work will be to identify proteins that are more or less abundant within PDE10A2 promoter-bound pol II complexes in the presence of N171-87Q. Preliminary 2D comparative analysis presented here (Fig. 5-7) will be replicated and include comparisons between reactions containing HeLa extract, HeLa extract and N171-22Q and HeLa extract and N171-87Q. Proteins which are present in complexes that have lower activity in the presence of N-terminus mutant huntingtin will be subjected to Tandem Mass Spectrometry for identification. We will then determine whether such interactions are mediated through the polyQ region or the polyQ region in the context of the N-terminus of mutant huntingtin and determine whether over-expression or depletion of specific proteins affect mutant huntingtin-induced transcriptional repression *in vitro*, in cell culture models, and animal models of HD. We will perform parallel studies using several mutant huntingtin-sensitive and –resistant promoters. This systematic approach will give us confidence that the interaction between mutant huntingtin and any specific protein has a functional consequence on transcription and pinpoint the fundamental mechanism that causes early pathogenesis of

HD. Using the information obtained, we may ultimately be able to formulate strategies to rescue mutant huntingtin-altered transcription.

REFERENCES

Agrawal, N., Pallos, J., Slepko, N., Apostol, B.L., Bodai, L., Chang, L.W., Chiang, A.S., Thompson, L.M. & Marsh, J.L. (2005) Identification of combinatorial drug regimens for treatment of Huntington's disease using Drosophila. *Proceedings of the National Academy of Sciences of the United States of America*, **102**, 3777-3781.

Ainbinder, E., Revach, M., Wolstein, O., Moshonov, S., Diamant, N. & Dikstein, R. (2002) Mechanism of rapid transcriptional induction of tumor necrosis factor alpha-responsive genes by NF-kappaB. *Mol Cell Biol*, **22**, 6354-6362.

Albright, S.R. & Tjian, R. (2000) TAFs revisited: more data reveal new twists and confirm old ideas. *Gene*, **242**, 1-13.

Ambrose, C.M., Duyao, M.P., Barnes, G., Bates, G.P., Lin, C.S., Srinidhi, J., Baxendale, S., Hummerich, H., Lehrach, H., Altherr, M. & et al. (1994) Structure and expression of the Huntington's disease gene: evidence against simple inactivation due to an expanded CAG repeat. *Somatic cell and molecular genetics*, **20**, 27-38.

Arrasate, M., Mitra, S., Schweitzer, E.S., Segal, M.R. & Finkbeiner, S. (2004) Inclusion body formation reduces levels of mutant huntingtin and the risk of neuronal death. *Nature*, **431**, 805-810.

Asturias, F.J. (2004) Another piece in the transcription initiation puzzle. *Nature structural & molecular biology*, **11**, 1031-1033.

Augood, S.J., Faull, R.L., Love, D.R. & Emson, P.C. (1996) Reduction in enkephalin and substance P messenger RNA in the striatum of early grade Huntington's disease: a detailed cellular in situ hybridization study. *Neuroscience*, **72**, 1023-1036.

Bae, B.I., Xu, H., Igarashi, S., Fujimuro, M., Agrawal, N., Taya, Y., Hayward, S.D., Moran, T.H., Montell, C., Ross, C.A., Snyder, S.H. & Sawa, A. (2005) p53 mediates cellular dysfunction and behavioral abnormalities in Huntington's disease. *Neuron*, **47**, 29-41.

Bates, E.A., Victor, M., Jones, A.K., Shi, Y. & Hart, A.C. (2006) Differential contributions of Caenorhabditis elegans histone deacetylases to huntingtin polyglutamine toxicity. *J Neurosci*, **26**, 2830-2838.

Bates, G. (2003) Huntingtin aggregation and toxicity in Huntington's disease. *Lancet*, **361**, 1642-1644.

Bates, G., Harper, P.S. & Jones, L. (2002) *Huntington's disease*. Oxford University Press, Oxford ; New York.

Beal, M.F., Brouillet, E., Jenkins, B.G., Ferrante, R.J., Kowall, N.W., Miller, J.M., Storey, E., Srivastava, R., Rosen, B.R. & Hyman, B.T. (1993) Neurochemical and histologic characterization of striatal excitotoxic lesions produced by the mitochondrial toxin 3-nitropropionic acid. *J Neurosci*, **13**, 4181-4192.

Beal, M.F., Kowall, N.W., Ellison, D.W., Mazurek, M.F., Swartz, K.J. & Martin, J.B. (1986) Replication of the neurochemical characteristics of Huntington's disease by quinolinic acid. *Nature*, **321**, 168-171.

Beavo, J.A. (1995) Cyclic-Nucleotide Phosphodiesterases - Functional Implications Of Multiple Isoforms. *Physiological Reviews*, **75**, 725-748.

Bhide, P.G., Day, M., Sapp, E., Schwarz, C., Sheth, A., Kim, J., Young, A.B., Penney, J., Golden, J., Aronin, N. & DiFiglia, M. (1996) Expression of normal and mutant huntingtin in the developing brain. *J Neurosci*, **16**, 5523-5535.

Bibb, J.A., Yan, Z., Svenningsson, P., Snyder, G.L., Pieribone, V.A., Horiuchi, A., Nairn, A.C., Messer, A. & Greengard, P. (2000) Severe deficiencies in dopamine signaling in presymptomatic Huntington's disease mice. *Proceedings of the National Academy of Sciences of the United States of America*, **97**, 6809-6814.

Bjorkqvist, M., Fex, M., Renstrom, E., Wierup, N., Petersen, A., Gil, J., Bacos, K., Popovic, N., Li, J.Y., Sundler, F., Brundin, P. & Mulder, H. (2005) The R6/2 transgenic mouse model of Huntington's disease develops diabetes due to deficient beta-cell mass and exocytosis. *Human molecular genetics*, **14**, 565-574.

Bodner, R.A., Outeiro, T.F., Altmann, S., Maxwell, M.M., Cho, S.H., Hyman, B.T., McLean, P.J., Young, A.B., Housman, D.E. & Kazantsev, A.G. (2006) Pharmacological promotion of inclusion formation: a therapeutic approach for Huntington's and Parkinson's diseases. *Proceedings of the National Academy of Sciences of the United States of America*, **103**, 4246-4251.

Bonelli, R.M. & Hofmann, P. (2004) A review of the treatment options for Huntington's disease. *Expert Opin Pharmacother*, **5**, 767-776.

Borlongan, C.V., Koutouzis, T.K. & Sanberg, P.R. (1997) 3-Nitropropionic acid animal model and Huntington's disease. *Neurosci Biobehav Rev*, **21**, 289-293.

Borrell-Pages, M., Zala, D., Humbert, S. & Saudou, F. (2006) Huntington's disease: from huntingtin function and dysfunction to therapeutic strategies. *Cell Mol Life Sci*, **63**, 2642-2660.

Boutell, J.M., Thomas, P., Neal, J.W., Weston, V.J., Duce, J., Harper, P.S. & Jones, A.L. (1999) Aberrant interactions of transcriptional repressor proteins with the Huntington's disease gene product, huntingtin. *Human molecular genetics*, **8**, 1647-1655.

Brandt, J., Strauss, M.E., Larus, J., Jensen, B., Folstein, S.E. & Folstein, M.F. (1984) Clinical correlates of dementia and disability in Huntington's disease. *J Clin Neuropsychol*, **6**, 401-412.

Brinkman, R.R., Mezei, M.M., Theilmann, J., Almqvist, E. & Hayden, M.R. (1997) The likelihood of being affected with Huntington disease by a particular age, for a specific CAG size. *American journal of human genetics*, **60**, 1202-1210.

Brouillet, E., Conde, F., Beal, M.F. & Hantraye, P. (1999) Replicating Huntington's disease phenotype in experimental animals. *Prog Neurobiol*, **59**, 427-468.

Busch, A., Engemann, S., Lurz, R., Okazawa, H., Lehrach, H. & Wanker, E.E. (2003) Mutant huntingtin promotes the fibrillogenesis of wild-type huntingtin: a potential mechanism for loss of huntingtin function in Huntington's disease. *J Biol Chem*, **278**, 41452-41461.

Caramins, M., Halliday, G., McCusker, E. & Trent, R.J. (2003) Genetically confirmed clinical Huntington's disease with no observable cell loss. *Journal of neurology, neurosurgery, and psychiatry*, **74**, 968-970.

Cattaneo, E. & Conti, L. (1998) Generation and characterization of embryonic striatal conditionally immortalized ST14A cells. *Journal of neuroscience research*, **53**, 223-234.

Cha, J.H., Frey, A.S., Alsdorf, S.A., Kerner, J.A., Kosinski, C.M., Mangiarini, L., Penney, J.B., Jr., Davies, S.W., Bates, G.P. & Young, A.B. (1999) Altered neurotransmitter receptor expression in transgenic mouse models of Huntington's disease. *Philosophical transactions of the Royal Society of London*, **354**, 981-989.

Cha, J.H., Kosinski, C.M., Kerner, J.A., Alsdorf, S.A., Mangiarini, L., Davies, S.W., Penney, J.B., Bates, G.P. & Young, A.B. (1998) Altered brain neurotransmitter receptors in transgenic mice expressing a portion of an abnormal human huntington disease gene. *Proceedings of the National Academy of Sciences of the United States of America*, **95**, 6480-6485.

Cha, J.H.J. (2000) Transcriptional dysregulation in Huntington's disease. *Trends In Neurosciences*, **23**, 387-392.

Chai, Y., Koppenhafer, S.L., Shoesmith, S.J., Perez, M.K. & Paulson, H.L. (1999) Evidence for proteasome involvement in polyglutamine disease: localization to nuclear inclusions in SCA3/MJD and suppression of polyglutamine aggregation in vitro. *Hum Mol Genet*, **8**, 673-682.

Chai, Y., Wu, L., Griffin, J.D. & Paulson, H.L. (2001) The role of protein composition in specifying nuclear inclusion formation in polyglutamine disease. *J Biol Chem*, **276**, 44889-44897.

Chan, E.Y., Luthi-Carter, R., Strand, A., Solano, S.M., Hanson, S.A., DeJohn, M.M., Kooperberg, C., Chase, K.O., DiFiglia, M., Young, A.B., Leavitt, B.R., Cha, J.H., Aronin, N., Hayden, M.R. & Olson, J.M. (2002) Increased huntingtin protein length reduces the number of polyglutamine-induced gene expression changes in mouse models of Huntington's disease. *Human molecular genetics*, **11**, 1939-1951.

Chen-Plotkin, A.S., Sadri-Vakili, G., Yohrling, G.J., Braveman, M.W., Benn, C.L., Glajch, K.E., DiRocco, D.P., Farrell, L.A., Krainc, D., Gines, S., MacDonald, M.E. & Cha, J.H. (2006) Decreased association of the transcription factor Sp1 with genes downregulated in Huntington's disease. *Neurobiol Dis*, **22**, 233-241.

Conaway, R.C. & Conaway, J.W. (1993) General initiation factors for RNA polymerase II. *Annual review of biochemistry*, **62**, 161-190.

Conti, M. & Jin, S.L.C. (2000) The molecular biology of cyclic nucleotide phosphodiesterases *Progress In Nucleic Acid Research And Molecular Biology, Vol 63*, pp. 1-38.

Cornett, J., Smith, L., Friedman, M., Shin, J.Y., Li, X.J. & Li, S.H. (2006) Context-dependent dysregulation of transcription by mutant huntingtin. *J Biol Chem*, **281**, 36198-36204.

Courey, A.J. & Tjian, R. (1988) Analysis of Sp1 *in vivo* reveals multiple transcriptional domains, including a novel glutamine-rich activation motif. *Cell*, **55**, 887-898.

Cui, L., Jeong, H., Borovecki, F., Parkhurst, C.N., Tanese, N. & Krainc, D. (2006) Transcriptional repression of PGC-1alpha by mutant huntingtin leads to mitochondrial dysfunction and neurodegeneration. *Cell*, **127**, 59-69.

Davies, S.W., Turmaine, M., Cozens, B.A., DiFiglia, M., Sharp, A.H., Ross, C.A., Scherzinger, E., Wanker, E.E., Mangiarini, L. & Bates, G.P. (1997) Formation of neuronal intranuclear inclusions underlies the neurological dysfunction in mice transgenic for the HD mutation. *Cell*, **90**, 537-548.

Denovan-Wright, E.M., Newton, R.A., Armstrong, J.N., Babity, J.M. & Robertson, H.A. (1998) Acute administration of cocaine, but not amphetamine, increases the level of synaptotagmin IV mRNA in the dorsal striatum of rat. *Brain Res Mol Brain Res*, **55**, 350-354.

Denovan-Wright, E.M. & Robertson, H.A. (2000) Cannabinoid receptor messenger RNA levels decrease in a subset of neurons of the lateral striatum, cortex and hippocampus of transgenic Huntington's disease mice. *Neuroscience*, **98**, 705-713.

Desplats, P.A., Kass, K.E., Gilmartin, T., Stanwood, G.D., Woodward, E.L., Head, S.R., Sutcliffe, J.G. & Thomas, E.A. (2006) Selective deficits in the expression of striatal-enriched mRNAs in Huntington's disease. *J Neurochem*, **96**, 743-757.

DiFiglia, M., Sapp, E., Chase, K.O., Davies, S.W., Bates, G.P., Vonsattel, J.P. & Aronin, N. (1997) Aggregation of huntingtin in neuronal intranuclear inclusions and dystrophic neurites in brain. *Science*, **277**, 1990-1993.

Dignam, J.D., Lebovitz, R.M. & Roeder, R.G. (1983) Accurate transcription initiation by RNA polymerase II in a soluble extract from isolated mammalian nuclei. *Nucleic Acids Res*, **11**, 1475-1489.

Dragatsis, I., Levine, M.S. & Zeitlin, S. (2000) Inactivation of Hdh in the brain and testis results in progressive neurodegeneration and sterility in mice. *Nature genetics*, **26**, 300-306.

Dunah, A.W., Jeong, H., Griffin, A., Kim, Y.M., Standaert, D.G., Hersch, S.M., Mouradian, M.M., Young, A.B., Tanese, N. & Krainc, D. (2002) Sp1 and TAFII130 transcriptional activity disrupted in early Huntington's disease. *Science*, **296**, 2238-2243.

Durr, A., Hahn-Barma, V., Brice, A., Pecheux, C., Dode, C. & Feingold, J. (1999) Homozygosity in Huntington's disease. *Journal of medical genetics*, **36**, 172-173.

Duyao, M., Ambrose, C., Myers, R., Novelletto, A., Persichetti, F., Frontali, M., Folstein, S., Ross, C., Franz, M., Abbott, M. & et al. (1993) Trinucleotide repeat length instability and age of onset in Huntington's disease. *Nature genetics*, **4**, 387-392.

Elferink, C.J. & Reiners, J.J. (1996) Quantitative RT-PCR on CYP1A1 heterogeneous nuclear RNA: A surrogate for the *in vitro* transcription run-on assay. *Biotechniques*, **20**, 470-477.

Emerson, B.M. (2002) Specificity of gene regulation. *Cell*, **109**, 267-270.

Ferrante, R.J., Kowall, N.W., Beal, M.F., Richardson, E.P., Jr., Bird, E.D. & Martin, J.B. (1985) Selective sparing of a class of striatal neurons in Huntington's disease. *Science*, **230**, 561-563.

Ferrante, R.J., Kubilus, J.K., Lee, J., Ryu, H., Beesen, A., Zucker, B., Smith, K., Kowall, N.W., Ratan, R.R., Luthi-Carter, R. & Hersch, S.M. (2003) Histone deacetylase inhibition by sodium butyrate chemotherapy ameliorates the neurodegenerative phenotype in Huntington's disease mice. *J Neurosci*, **23**, 9418-9427.

Freiman, R.N., Albright, S.R., Zheng, S., Sha, W.C., Hammer, R.E. & Tjian, R. (2001) Requirement of tissue-selective TBP-associated factor TAFII105 in ovarian development. *Science*, **293**, 2084-2087.

Fujishige, K., Kotera, J. & Omori, K. (1999a) Striatum- and testis-specific phosphodiesterase PDE10A - Isolation and characterization of a rat PDE10A. *European Journal Of Biochemistry*, **266**, 1118-1127.

Fujishige, K., Kotera, J., Michibata, H., Yuasa, K., Takebayashi, S., Okumura, K. & Omori, K. (1999b) Cloning and characterization of a novel human phosphodiesterase that hydrolyzes both cAMP and cGMP (PDE10A). *Journal Of Biological Chemistry*, **274**, 18438-18445.

Fujishige, K., Kotera, J., Yuasa, K. & Omori, K. (2000) The human phosphodiesterase PDE10A gene - Genomic organization and evolutionary relatedness with other PDEs containing GAF domains. *European Journal Of Biochemistry*, **267**, 5943-5951.

Fusco, F.R., Chen, Q., Lamoreaux, W.J., Figueredo-Cardenas, G., Jiao, Y., Coffman, J.A., Surmeier, D.J., Honig, M.G., Carlock, L.R. & Reiner, A. (1999) Cellular localization of huntingtin in striatal and cortical neurons in rats: lack of correlation with neuronal vulnerability in Huntington's disease. *J Neurosci*, **19**, 1189-1202.

Geevasinga, N., Richards, F.H., Jones, K.J. & Ryan, M.M. (2006) Juvenile Huntington disease. *Journal of paediatrics and child health*, **42**, 552-554.

Gomez, G.T., Hu, H., McCaw, E.A. & Denovan-Wright, E.M. (2006) Brain-specific factors in combination with mutant huntingtin induce gene-specific transcriptional dysregulation. *Molecular and cellular neurosciences*, **31**, 661-675.

Goodman, A.B. & Pardee, A.B. (2003) Evidence for defective retinoid transport and function in late onset Alzheimer's disease. *Proceedings of the National Academy of Sciences of the United States of America*, **100**, 2901-2905.

Goodman, A.B. (1998) Three independent lines of evidence suggest retinoids as causal to schizophrenia. *Proceedings of the National Academy of Sciences of the United States of America*, **95**, 7240-7244.

Goodrich, J.A. & Tjian, R. (1994) TBP-TAF complexes: selectivity factors for eukaryotic transcription. *Curr Opin Cell Biol*, **6**, 403-409.

Graham, R.K., Deng, Y., Slow, E.J., Haigh, B., Bissada, N., Lu, G., Pearson, J., Shehadeh, J., Bertram, L., Murphy, Z., Warby, S.C., Doty, C.N., Roy, S., Wellington, C.L., Leavitt, B.R., Raymond, L.A., Nicholson, D.W. & Hayden, M.R. (2006) Cleavage at the caspase-6 site is required for neuronal dysfunction and degeneration due to mutant huntingtin. *Cell*, **125**, 1179-1191.

Greene, J.G., Porter, R.H., Eller, R.V. & Greenamyre, J.T. (1993) Inhibition of succinate dehydrogenase by malonic acid produces an "excitotoxic" lesion in rat striatum. *J Neurochem*, **61**, 1151-1154.

Gusella, J.F., MacDonald, M.E., Ambrose, C.M. & Duyao, M.P. (1993) Molecular genetics of Huntington's disease. *Archives of neurology*, **50**, 1157-1163.

Gustafson, T.A. & Kedes, L. (1989) Identification of multiple proteins that interact with functional regions of the human cardiac alpha-actin promoter. *Mol Cell Biol*, **9**, 3269-3283.

Gutekunst, C.A., Li, S.H., Yi, H., Mulroy, J.S., Kuemmerle, S., Jones, R., Rye, D., Ferrante, R.J., Hersch, S.M. & Li, X.J. (1999) Nuclear and neuropil aggregates in Huntington's disease: relationship to neuropathology. *J Neurosci*, **19**, 2522-2534.

Hackam, A.S., Singaraja, R., Wellington, C.L., Metzler, M., McCutcheon, K., Zhang, T., Kalchman, M. & Hayden, M.R. (1998) The influence of huntingtin protein size on nuclear localization and cellular toxicity. *J Cell Biol*, **141**, 1097-1105.

Hampsey, M. (1998) Molecular genetics of the RNA polymerase II general transcriptional machinery. *Microbiol Mol Biol Rev*, **62**, 465-503.

Handley, O.J., Naji, J.J., Dunnett, S.B. & Rosser, A.E. (2006) Pharmaceutical, cellular and genetic therapies for Huntington's disease. *Clin Sci (Lond)*, **110**, 73-88.

Hantraye, P., Riche, D., Maziere, M. & Isacson, O. (1990) A primate model of Huntington's disease: behavioral and anatomical studies of unilateral excitotoxic lesions of the caudate-putamen in the baboon. *Exp Neurol*, **108**, 91-104.

Harjes, P. & Wanker, E.E. (2003) The hunt for huntingtin function: interaction partners tell many different stories. *Trends Biochem Sci*, **28**, 425-433.

Harper, J.D. & Lansbury, P.T., Jr. (1997) Models of amyloid seeding in Alzheimer's disease and scrapie: mechanistic truths and physiological consequences of the time-dependent solubility of amyloid proteins. *Annual review of biochemistry*, **66**, 385-407.

Harper, P.S. (1992) The epidemiology of Huntington's disease. *Hum Genet*, **89**, 365-376.

Harper, S.Q., Staber, P.D., He, X., Eliason, S.L., Martins, I.H., Mao, Q., Yang, L., Kotin, R.M., Paulson, H.L. & Davidson, B.L. (2005) RNA interference improves motor and neuropathological abnormalities in a Huntington's disease mouse model. *Proceedings of the National Academy of Sciences of the United States of America*, **102**, 5820-5825.

Hebb, A.L. & Robertson, H.A. (2007) Role of phosphodiesterases in neurological and psychiatric disease. *Current opinion in pharmacology*, **7**, 86-92.

Hebb, A.L., Robertson, H.A. & Denovan-Wright, E.M. (2004) Striatal phosphodiesterase mRNA and protein levels are reduced in Huntington's disease transgenic mice prior to the onset of motor symptoms. *Neuroscience*, **123**, 967-981.

Heiser, V., Scherzinger, E., Boeddrich, A., Nordhoff, E., Lurz, R., Schugardt, N., Lehrach, H. & Wanker, E.E. (2000) Inhibition of huntingtin fibrillogenesis by specific antibodies and small molecules: implications for Huntington's disease therapy. *Proceedings of the National Academy of Sciences of the United States of America*, **97**, 6739-6744.

Helmlinger, D., Tora, L. & Devys, D. (2006) Transcriptional alterations and chromatin remodeling in polyglutamine diseases. *Trends Genet*, **22**, 562-570.

Hermel, E., Gafni, J., Propp, S.S., Leavitt, B.R., Wellington, C.L., Young, J.E., Hackam, A.S., Logvinova, A.V., Peel, A.L., Chen, S.F., Hook, V., Singaraja, R., Krajewski, S., Goldsmith, P.C., Ellerby, H.M., Hayden, M.R., Bredesen, D.E. & Ellerby, L.M. (2004) Specific caspase interactions and amplification are involved in selective neuronal vulnerability in Huntington's disease. *Cell Death Differ*, **11**, 424-438.

Hilditch-Maguire, P., Trettel, F., Passani, L.A., Auerbach, A., Persichetti, F. & MacDonald, M.E. (2000) Huntingtin: an iron-regulated protein essential for normal nuclear and perinuclear organelles. *Human molecular genetics*, **9**, 2789-2797.

Hochheimer, A. & Tjian, R. (2003) Diversified transcription initiation complexes expand promoter selectivity and tissue-specific gene expression. *Genes Dev*, **17**, 1309-1320.

Hockly, E., Richon, V.M., Woodman, B., Smith, D.L., Zhou, X., Rosa, E., Sathasivam, K., Ghazi-Noori, S., Mahal, A., Lowden, P.A., Steffan, J.S., Marsh, J.L., Thompson, L.M., Lewis, C.M., Marks, P.A. & Bates, G.P. (2003) Suberoylanilide hydroxamic acid, a histone deacetylase inhibitor, ameliorates motor deficits in a mouse model of Huntington's disease. *Proceedings of the National Academy of Sciences of the United States of America*, **100**, 2041-2046.

Hodges, A., Strand, A.D., Aragaki, A.K., Kuhn, A., Sengstag, T., Hughes, G., Elliston, L.A., Hartog, C., Goldstein, D.R., Thu, D., Hollingsworth, Z.R., Collin, F., Synek, B., Holmans, P.A., Young, A.B., Wexler, N.S., Delorenzi, M., Kooperberg, C., Augood, S.J., Faull, R.L., Olson, J.M., Jones, L. & Luthi-Carter, R. (2006) Regional and cellular gene expression changes in human Huntington's disease brain. *Human molecular genetics*, **15**, 965-977.

Hodgson, J.G., Agopyan, N., Gutekunst, C.A., Leavitt, B.R., LePiane, F., Singaraja, R., Smith, D.J., Bissada, N., McCutcheon, K., Nasir, J., Jamot, L., Li, X.J., Stevens, M.E., Rosemond, E., Roder, J.C., Phillips, A.G., Rubin, E.M., Hersch, S.M. & Hayden, M.R. (1999) A YAC mouse model for Huntington's disease with full-length mutant huntingtin, cytoplasmic toxicity, and selective striatal neurodegeneration. *Neuron*, **23**, 181-192.

Hollenbach, B., Scherzinger, E., Schweiger, K., Lurz, R., Lehrach, H. & Wanker, E.E. (1999) Aggregation of truncated GST-HD exon 1 fusion proteins containing normal range and expanded glutamine repeats. *Philosophical transactions of the Royal Society of London*, **354**, 991-994.

Hoogeveen, A.T., Willemsen, R., Meyer, N., de Rooij, K.E., Roos, R.A., van Ommen, G.J. & Galjaard, H. (1993) Characterization and localization of the Huntington disease gene product. *Human molecular genetics*, **2**, 2069-2073.

Hu, H., McCaw, E.A., Hebb, A.L., Gomez, G.T. & Denovan-Wright, E.M. (2004) Mutant huntingtin affects the rate of transcription of striatum-specific isoforms of phosphodiesterase 10A. *The European journal of neuroscience*, **20**, 3351-3363.

Igarashi, S., Morita, H., Bennett, K.M., Tanaka, Y., Engelender, S., Peters, M.F., Cooper, J.K., Wood, J.D., Sawa, A. & Ross, C.A. (2003) Inducible PC12 cell model of Huntington's disease shows toxicity and decreased histone acetylation. *Neuroreport*, **14**, 565-568.

Jana, N.R., Tanaka, M., Wang, G. & Nukina, N. (2000) Polyglutamine length-dependent interaction of Hsp40 and Hsp70 family chaperones with truncated N-terminal huntingtin: their role in suppression of aggregation and cellular toxicity. *Human molecular genetics*, **9**, 2009-2018.

Jensen, P., Sorensen, S.A., Fenger, K. & Bolwig, T.G. (1993) A study of psychiatric morbidity in patients with Huntington's disease, their relatives, and controls. Admissions to psychiatric hospitals in Denmark from 1969 to 1991. *Br J Psychiatry*, **163**, 790-797.

Kahlem, P., Green, H. & Djian, P. (1998) Transglutaminase action imitates Huntington's disease: selective polymerization of Huntingtin containing expanded polyglutamine. *Mol Cell*, **1**, 595-601.

Kazantsev, A.G. & Hersch, S.M. (2007) Drug targeting of dysregulated transcription in Huntington's disease. *Prog Neurobiol.*

Kegel, K.B., Meloni, A.R., Yi, Y., Kim, Y.J., Doyle, E., Cuiffo, B.G., Sapp, E., Wang, Y.M., Qin, Z.H., Chen, J.D., Nevins, J.R., Aronin, N. & DiFiglia, M. (2002) Huntingtin is present in the nucleus, interacts with the transcriptional corepressor C-terminal binding protein, and represses transcription. *Journal Of Biological Chemistry*, **277**, 7466-7476.

Lafosse, J.M., Corboy, J.R., Leehey, M.A., Seeberger, L.C. & Filley, C.M. (2007) MS vs. HD: can white matter and subcortical gray matter pathology be distinguished neuropsychologically? *J Clin Exp Neuropsychol*, **29**, 142-154.

Lane, M.A. & Bailey, S.J. (2005) Role of retinoid signalling in the adult brain. *Prog Neurobiol*, **75**, 275-293.

Lemon, B. & Tjian, R. (2000) Orchestrated response: a symphony of transcription factors for gene control. *Genes Dev*, **14**, 2551-2569.

Levine, M.S., Klapstein, G.J., Koppel, A., Gruen, E., Cepeda, C., Vargas, M.E., Jokel, E.S., Carpenter, E.M., Zanjani, H., Hurst, R.S., Efstratiadis, A., Zeitlin, S. & Chesselet, M.F. (1999) Enhanced sensitivity to N-methyl-D-aspartate receptor activation in transgenic and knockin mouse models of Huntington's disease. *Journal of neuroscience research*, **58**, 515-532.

Li, J.Y., Popovic, N. & Brundin, P. (2005) The use of the R6 transgenic mouse models of Huntington's disease in attempts to develop novel therapeutic strategies. *NeuroRx*, **2**, 447-464.

Li, S. & Li, X.J. (2006) Multiple pathways contribute to the pathogenesis of Huntington disease. *Molecular neurodegeneration*, **1**, 19.

Li, S.H., Cheng, A.L., Zhou, H., Lam, S., Rao, M., Li, H. & Li, X.J. (2002) Interaction of Huntington disease protein with transcriptional activator Sp1. *Mol Cell Biol*, **22**, 1277-1287.

Li, X.J., Li, S.H., Sharp, A.H., Nucifora, F.C., Jr., Schilling, G., Lanahan, A., Worley, P., Snyder, S.H. & Ross, C.A. (1995) A huntingtin-associated protein enriched in brain with implications for pathology. *Nature*, **378**, 398-402.

Lin, C.H., Tallaksen-Greene, S., Chien, W.M., Cearley, J.A., Jackson, W.S., Crouse, A.B., Ren, S., Li, X.J., Albin, R.L. & Detloff, P.J. (2001) Neurological abnormalities in a knock-in mouse model of Huntington's disease. *Human molecular genetics*, **10**, 137-144.

Loughney, K., Snyder, P.B., Uher, L., Rosman, G.J., Ferguson, K. & Florio, V.A. (1999) Isolation and characterization of PDE10A, a novel human 3 ', 5 '-cyclic nucleotide phosphodiesterase. *Gene*, **234**, 109-117.

Lovestone, S., Hodgson, S., Sham, P., Differ, A.M. & Levy, R. (1996) Familial psychiatric presentation of Huntington's disease. *Journal of medical genetics*, **33**, 128-131.

Luesse, H.G., Schiefer, J., Spruenken, A., Puls, C., Block, F. & Kosinski, C.M. (2001) Evaluation of R6/2 HD transgenic mice for therapeutic studies in Huntington's disease: behavioral testing and impact of diabetes mellitus. *Behavioural brain research*, **126**, 185-195.

Luthi-Carter, R., Apostol, B.L., Dunah, A.W., DeJohn, M.M., Farrell, L.A., Bates, G.P., Young, A.B., Standaert, D.G., Thompson, L.M. & Cha, J.H. (2003) Complex alteration of NMDA receptors in transgenic Huntington's disease mouse brain: analysis of mRNA and protein expression, plasma membrane association, interacting proteins, and phosphorylation. *Neurobiol Dis*, **14**, 624-636.

Luthi-Carter, R., Hanson, S.A., Strand, A.D., Bergstrom, D.A., Chun, W., Peters, N.L., Woods, A.M., Chan, E.Y., Kooperberg, C., Krainc, D., Young, A.B., Tapscott, S.J. & Olson, J.M. (2002a) Dysregulation of gene expression in the R6/2 model of polyglutamine disease: parallel changes in muscle and brain. *Human molecular genetics*, **11**, 1911-1926.

Luthi-Carter, R., Strand, A., Peters, N.L., Solano, S.M., Hollingsworth, Z.R., Menon, A.S., Frey, A.S., Spektor, B.S., Penney, E.B., Schilling, G., Ross, C.A., Borchelt, D.R., Tapscott, S.J., Young, A.B., Cha, J.H.J. & Olson, J.M. (2000) Decreased expression of striatal signaling genes in a mouse model of Huntington's disease. *Human molecular genetics*, **9**, 1259-1271.

Luthi-Carter, R., Strand, A.D., Hanson, S.A., Kooperberg, C., Schilling, G., La Spada, A.R., Merry, D.E., Young, A.B., Ross, C.A., Borchelt, D.R. & Olson, J.M. (2002b) Polyglutamine and transcription: gene expression changes shared by DRPLA and Huntington's disease mouse models reveal context-independent effects. *Human molecular genetics*, **11**, 1927-1937.

Mangiarini, L., Sathasivam, K., Seller, M., Cozens, B., Harper, A., Hetherington, C., Lawton, M., Trottier, Y., Lehrach, H., Davies, S.W. & Bates, G.P. (1996) Exon 1 of the HD gene with an expanded CAG repeat is sufficient to cause a progressive neurological phenotype in transgenic mice. *Cell*, **87**, 493-506.

Marsh, J.L. & Thompson, L.M. (2006) Drosophila in the study of neurodegenerative disease. *Neuron*, **52**, 169-178.

Martindale, D., Hackam, A., Wieczorek, A., Ellerby, L., Wellington, C., McCutcheon, K., Singaraja, R., Kazemi-Esfarjani, P., Devon, R., Kim, S.U., Bredesen, D.E., Tufaro, F. & Hayden, M.R. (1998) Length of huntingtin and its polyglutamine tract influences localization and frequency of intracellular aggregates. *Nature genetics*, **18**, 150-154.

McCampbell, A., Taylor, J.P., Taye, A.A., Robitschek, J., Li, M., Walcott, J., Merry, D., Chai, Y., Paulson, H., Sobue, G. & Fischbeck, K.H. (2000) CREB-binding protein sequestration by expanded polyglutamine. *Human molecular genetics*, **9**, 2197-2202.

McCaw, E.A., Hu, H., Gomez, G.T., Hebb, A.L., Kelly, M.E. & Denovan-Wright, E.M. (2004) Structure, expression and regulation of the cannabinoid receptor gene (CB1) in Huntington's disease transgenic mice. *European journal of biochemistry / FEBS*, **271**, 4909-4920.

Meade, C.A., Deng, Y.P., Fusco, F.R., Del Mar, N., Hersch, S., Goldowitz, D. & Reiner, A. (2002) Cellular localization and development of neuronal intranuclear inclusions in striatal and cortical neurons in R6/2 transgenic mice. *J Comp Neurol*, **449**, 241-269.

Menalled, L., Zanjani, H., MacKenzie, L., Koppel, A., Carpenter, E., Zeitlin, S. & Chesselet, M.F. (2000) Decrease in striatal enkephalin mRNA in mouse models of Huntington's disease. *Experimental Neurology*, **162**, 328-342.

Mende-Mueller, L.M., Toneff, T., Hwang, S.R., Chesselet, M.F. & Hook, V.Y. (2001) Tissue-specific proteolysis of Huntingtin (htt) in human brain: evidence of enhanced levels of N- and C-terminal htt fragments in Huntington's disease striatum. *J Neurosci*, **21**, 1830-1837.

Metzler, M., Gan, L., Wong, T.P., Liu, L., Helm, J., Liu, L., Georgiou, J., Wang, Y., Bissada, N., Cheng, K., Roder, J.C., Wang, Y.T. & Hayden, M.R. (2007) NMDA receptor function and NMDA receptor-dependent phosphorylation of huntingtin is altered by the endocytic protein HIP1. *J Neurosci*, **27**, 2298-2308.

Miller, T.W., Zhou, C., Gines, S., MacDonald, M.E., Mazarakis, N.D., Bates, G.P., Huston, J.S. & Messer, A. (2005) A human single-chain Fv intrabody preferentially targets amino-terminal Huntingtin's fragments in striatal models of Huntington's disease. *Neurobiol Dis*, **19**, 47-56.

Nance, M.A. (1998) Huntington disease: clinical, genetic, and social aspects. *Journal of geriatric psychiatry and neurology*, **11**, 61-70.

Nance, M.A., Mathias-Hagen, V., Breningstall, G., Wick, M.J. & McGlennen, R.C. (1999) Analysis of a very large trinucleotide repeat in a patient with juvenile Huntington's disease. *Neurology*, **52**, 392-394.

Nasir, J., Floresco, S.B., O'Kusky, J.R., Diewert, V.M., Richman, J.M., Zeisler, J., Borowski, A., Marth, J.D., Phillips, A.G. & Hayden, M.R. (1995) Targeted disruption of the Huntington's disease gene results in embryonic lethality and behavioral and morphological changes in heterozygotes. *Cell*, **81**, 811-823.

Nguyen, H.P., Kobbe, P., Rahne, H., Worpel, T., Jager, B., Stephan, M., Pabst, R., Holzmann, C., Riess, O., Korr, H., Kantor, O., Petrasch-Parwez, E., Wetzel, R., Osmand, A. & von Horsten, S. (2006) Behavioral abnormalities precede neuropathological markers in rats transgenic for Huntington's disease. *Human molecular genetics*, **15**, 3177-3194.

Nucifora, F.C., Jr., Sasaki, M., Peters, M.F., Huang, H., Cooper, J.K., Yamada, M., Takahashi, H., Tsuji, S., Troncoso, J., Dawson, V.L., Dawson, T.M. & Ross, C.A. (2001) Interference by huntingtin and atrophin-1 with cbp-mediated transcription leading to cellular toxicity. *Science*, **291**, 2423-2428.

Obrietan, K. & Hoyt, K.R. (2004) CRE-mediated transcription is increased in Huntington's disease transgenic mice. *J Neurosci*, **24**, 791-796.

Oweis, S., Wu, L., Kiela, P.R., Zhao, H., Malhotra, D., Ghishan, F.K., Xie, Z., Shapiro, J.I. & Liu, J. (2006) Cardiac glycoside downregulates NHE3 activity and expression in LLC-PK1 cells. *Am J Physiol Renal Physiol*, **290**, F997-1008.

Perez, M.K., Paulson, H.L., Pendse, S.J., Saionz, S.J., Bonini, N.M. & Pittman, R.N. (1998) Recruitment and the role of nuclear localization in polyglutamine-mediated aggregation. *Journal Of Cell Biology*, **143**, 1457-1470.

Perutz, M.F. (1995) Glutamine repeats as polar zippers: their role in inherited neurodegenerative disease. *Mol Med*, **1**, 718-721.

Poirier, M.A., Li, H., Macosko, J., Cai, S., Amzel, M. & Ross, C.A. (2002) Huntingtin spheroids and protofibrils as precursors in polyglutamine fibrilization. *J Biol Chem*, **277**, 41032-41037.

Polli, J.W. & Kincaid, R.L. (1992) Molecular cloning of DNA encoding a calmodulin-dependent phosphodiesterase enriched in striatum. *Proceedings of the National Academy of Sciences of the United States of America*, **89**, 11079-11083.

Qiu, Z., Norflus, F., Singh, B., Swindell, M.K., Buzescu, R., Bejarano, M., Chopra, R., Zucker, B., Benn, C.L., DiRocco, D.P., Cha, J.H., Ferrante, R.J. & Hersch, S.M. (2006) Sp1 is up-regulated in cellular and transgenic models of Huntington disease, and its reduction is neuroprotective. *J Biol Chem*, **281**, 16672-16680.

Quandt, K., Frech, K., Karas, H., Wingender, E. & Werner, T. (1995) MatInd and MatInspector: New fast and versatile tools for detection of consensus matches in nucleotide sequence data. *Nucleic Acids Research*, **23**, 4878-4884.

Rabenstein, M.D., Zhou, S., Lis, J.T. & Tjian, R. (1999) TATA box-binding protein (TBP)-related factor 2 (TRF2), a third member of the TBP family. *Proceedings of the National Academy of Sciences of the United States of America*, **96**, 4791-4796.

Reddy, P.H., Williams, M., Charles, V., Garrett, L., Pike-Buchanan, L., Whetsell, W.O., Jr., Miller, G. & Tagle, D.A. (1998) Behavioural abnormalities and selective neuronal loss in HD transgenic mice expressing mutated full-length HD cDNA. *Nature genetics*, **20**, 198-202.

Rego, A.C. & de Almeida, L.P. (2005) Molecular targets and therapeutic strategies in Huntington's disease. *Curr Drug Targets CNS Neurol Disord*, **4**, 361-381.

Reyes-Irisarri, E., Perez-Torres, S. & Mengod, G. (2005) Neuronal expression of cAMP-specific phosphodiesterase 7B mRNA in the rat brain. *Neuroscience*, **132**, 1173-1185.

Richfield, E.K., Maguire-Zeiss, K.A., Cox, C., Gilmore, J. & Voorn, P. (1995) Reduced expression of preproenkephalin in striatal neurons from Huntington's disease patients. *Ann Neurol*, **37**, 335-343.

Rigamonti, D., Bauer, J.H., De-Fraja, C., Conti, L., Sipione, S., Sciorati, C., Clementi, E., Hackam, A., Hayden, M.R., Li, Y., Cooper, J.K., Ross, C.A., Govoni, S., Vincenz, C. & Cattaneo, E. (2000) Wild-type huntingtin protects from apoptosis upstream of caspase-3. *J Neurosci*, **20**, 3705-3713.

Riley, B.E. & Orr, H.T. (2006) Polyglutamine neurodegenerative diseases and regulation of transcription: assembling the puzzle. *Genes Dev*, **20**, 2183-2192.

Robert, F., Douziech, M., Forget, D., Egly, J.M., Greenblatt, J., Burton, Z.F. & Coulombe, B. (1998) Wrapping of promoter DNA around the RNA polymerase II initiation complex induced by TFIIF. *Mol Cell*, **2**, 341-351.

Rodriguez-Lebron, E., Denovan-Wright, E.M., Nash, K., Lewin, A.S. & Mandel, R.J. (2005) Intrastriatal rAAV-mediated delivery of anti-huntingtin shRNAs induces partial reversal of disease progression in R6/1 Huntington's disease transgenic mice. *Mol Ther*, **12**, 618-633.

Rosas, H.D., Koroshetz, W.J., Chen, Y.I., Skeuse, C., Vangel, M., Cudkowicz, M.E., Caplan, K., Marek, K., Seidman, L.J., Makris, N., Jenkins, B.G. & Goldstein, J.M. (2003) Evidence for more widespread cerebral pathology in early HD: an MRI-based morphometric analysis. *Neurology*, **60**, 1615-1620.

Rosenblatt, A., Brinkman, R.R., Liang, K.Y., Almqvist, E.W., Margolis, R.L., Huang, C.Y., Sherr, M., Franz, M.L., Abbott, M.H., Hayden, M.R. & Ross, C.A. (2001) Familial influence on age of onset among siblings with Huntington disease. *American journal of medical genetics*, **105**, 399-403.

Ross, C.A., Margolis, R.L., Rosenblatt, A., Ranen, N.G., Becher, M.W. & Aylward, E. (1997) Huntington disease and the related disorder, dentatorubral-pallidoluysian atrophy (DRPLA). *Medicine (Baltimore)*, **76**, 305-338.

Ross, J. (1995) mRNA stability in mammalian cells. *Microbiol Rev*, **59**, 423-450.

Rubinsztein, D.C. (2002) Lessons from animal models of Huntington's disease. *Trends Genet*, **18**, 202-209.

Rubinsztein, D.C., Leggo, J., Coles, R., Almqvist, E., Biancalana, V., Cassiman, J.J., Chotai, K., Connarty, M., Crauford, D., Curtis, A., Curtis, D., Davidson, M.J., Differ, A.M., Dode, C., Dodge, A., Frontali, M., Ranen, N.G., Stine, O.C., Sherr, M., Abbott, M.H., Franz, M.L., Graham, C.A., Harper, P.S., Hedreen, J.C., Hayden, M.R. & et al. (1996) Phenotypic characterization of individuals with 30-40 CAG repeats in the Huntington disease (HD) gene reveals HD cases with 36 repeats and apparently normal elderly individuals with 36-39 repeats. *American journal of human genetics*, **59**, 16-22.

Sadri-Vakili, G. & Cha, J.H. (2006) Mechanisms of disease: Histone modifications in Huntington's disease. *Nat Clin Pract Neurol*, **2**, 330-338.

Sambrook, J., MacCallum, P. & Russel, D. (2001) Molecular Cloning: A Laboratory Manual. Cold Spring Harbor Laboratory Press; New York.

Samad, T.A., Krezel, W., Chambon, P. & Borrelli, E. (1997) Regulation of dopaminergic pathways by retinoids: activation of the D2 receptor promoter by members of the retinoic acid receptor-retinoid X receptor family. *Proceedings of the National Academy of Sciences of the United States of America*, **94**, 14349-14354.

Sanchez, I., Mahlke, C. & Yuan, J. (2003) Pivotal role of oligomerization in expanded polyglutamine neurodegenerative disorders. *Nature*, **421**, 373-379.

Saudou, F., Finkbeiner, S., Devys, D. & Greenberg, M.E. (1998) Huntingtin acts in the nucleus to induce apoptosis but death does not correlate with the formation of intranuclear inclusions. *Cell*, **95**, 55-66.

Sawadogo, M. & Roeder, R.G. (1985) Factors involved in specific transcription by human RNA polymerase II: analysis by a rapid and quantitative *in vitro* assay. *Proceedings of the National Academy of Sciences of the United States of America*, **82**, 4394-4398.

Schaffar, G., Breuer, P., Boteva, R., Behrends, C., Tzvetkov, N., Strippel, N., Sakahira, H., Siegers, K., Hayer-Hartl, M. & Hartl, F.U. (2004) Cellular toxicity of polyglutamine expansion proteins: mechanism of transcription factor deactivation. *Mol Cell*, **15**, 95-105.

Scherzinger, E., Sittler, A., Schweiger, K., Heiser, V., Lurz, R., Hasenbank, R., Bates, G.P., Lehrach, H. & Wanker, E.E. (1999) Self-assembly of polyglutamine-containing huntingtin fragments into amyloid-like fibrils: implications for Huntington's disease pathology. *Proceedings of the National Academy of Sciences of the United States of America*, **96**, 4604-4609.

Schilling, G., Becher, M.W., Sharp, A.H., Jinnah, H.A., Duan, K., Kotzuk, J.A., Slunt, H.H., Ratovitski, T., Cooper, J.K., Jenkins, N.A., Copeland, N.G., Price, D.L., Ross, C.A. & Borchelt, D.R. (1999) Intranuclear inclusions and neuritic aggregates in transgenic mice expressing a mutant N-terminal fragment of huntingtin. *Human molecular genetics*, **8**, 397-407.

Sharp, A.H., Loev, S.J., Schilling, G., Li, S.H., Li, X.J., Bao, J., Wagster, M.V., Kotzuk, J.A., Steiner, J.P., Lo, A., Hedreen, J., Sisodia, S., Snyder, S.H., Dawson, T.M., Ryugo, D.K. & Ross, C.A. (1995) Widespread Expression Of Huntingtons-Disease Gene (It15) Protein Product. *Neuron*, **14**, 1065-1074.

Shastry, B.S. (2003) Neurodegenerative disorders of protein aggregation. *Neurochemistry international*, **43**, 1-7.

Shehadeh, J., Fernandes, H.B., Zeron Mullins, M.M., Graham, R.K., Leavitt, B.R., Hayden, M.R. & Raymond, L.A. (2006) Striatal neuronal apoptosis is preferentially enhanced by NMDA receptor activation in YAC transgenic mouse model of Huntington disease. *Neurobiol Dis*, **21**, 392-403.

Shelbourne, P.F., Killeen, N., Hevner, R.F., Johnston, H.M., Tecott, L., Lewandoski, M., Ennis, M., Ramirez, L., Li, Z., Iannicola, C., Littman, D.R. & Myers, R.M. (1999) A Huntington's disease CAG expansion at the murine Hdh locus is unstable and associated with behavioural abnormalities in mice. *Human molecular genetics*, **8**, 763-774.

Shimohata, T., Nakajima, T., Yamada, M., Uchida, C., Onodera, O., Naruse, S., Kimura, T., Koide, R., Nozaki, K., Sano, Y., Ishiguro, H., Sakoe, K., Ooshima, T., Sato, A., Ikeuchi, T., Oyake, M., Sato, T., Aoyagi, Y., Hozumi, I., Nagatsu, T., Takiyama, Y., Nishizawa, M., Goto, J., Kanazawa, I., Davidson, I., Tanese, N., Takahashi, H. & Tsuji, S. (2000) Expanded polyglutamine stretches interact with TAF(II)130, interfering with CREB-dependent transcription. *Nature genetics*, **26**, 29-36.

Sipione, S., Rigamonti, D., Valenza, M., Zuccato, C., Conti, L., Pritchard, J., Kooperberg, C., Olson, J.M. & Cattaneo, E. (2002) Early transcriptional profiles in huntingtin-inducible striatal cells by microarray analyses. *Human molecular genetics*, **11**, 1953-1965.

Sisodia, S.S. (1998) Nuclear inclusions in glutamine repeat disorders: are they pernicious, coincidental, or beneficial? *Cell*, **95**, 1-4.

Sittler, A., Walter, S., Wedemeyer, N., Hasenbank, R., Scherzinger, E., Eickhoff, H., Bates, G.P., Lehrach, H. & Wanker, E.E. (1998) SH3GL3 associates with the Huntingtin exon 1 protein and promotes the formation of polygln-containing protein aggregates. *Mol Cell*, **2**, 427-436.

Slepko, N., Bhattacharyya, A.M., Jackson, G.R., Steffan, J.S., Marsh, J.L., Thompson, L.M. & Wetzel, R. (2006) Normal-repeat-length polyglutamine peptides accelerate aggregation nucleation and cytotoxicity of expanded polyglutamine proteins. *Proceedings of the National Academy of Sciences of the United States of America*, **103**, 14367-14372.

Slow, E.J., Graham, R.K., Osmand, A.P., Devon, R.S., Lu, G., Deng, Y., Pearson, J., Vaid, K., Bissada, N., Wetzel, R., Leavitt, B.R. & Hayden, M.R. (2005) Absence of behavioral abnormalities and neurodegeneration *in vivo* despite widespread neuronal huntingtin inclusions. *Proceedings of the National Academy of Sciences of the United States of America*, **102**, 11402-11407.

Smith, D.L., Portier, R., Woodman, B., Hockly, E., Mahal, A., Klunk, W.E., Li, X.J., Wanker, E., Murray, K.D. & Bates, G.P. (2001) Inhibition of polyglutamine aggregation in R6/2 HD brain slices-complex dose-response profiles. *Neurobiol Dis*, **8**, 1017-1026.

Smith, R., Chung, H., Rundquist, S., Maat-Schieman, M.L., Colgan, L., Englund, E., Liu, Y.J., Roos, R.A., Faull, R.L., Brundin, P. & Li, J.Y. (2006) Cholinergic neuronal defect without cell loss in Huntington's disease. *Human molecular genetics*, **15**, 3119-3131.

Soderling, S.H. & Beavo, J.A. (2000) Regulation of cAMP and cGMP signaling: new phosphodiesterases and new functions. *Curr Opin Cell Biol*, **12**, 174-179.

Soderling, S.H., Bayuga, S.J. & Beavo, J.A. (1999) Isolation and characterization of a dual-substrate phosphodiesterase gene family: PDE10A. *Proceedings of the National Academy of Sciences of the United States of America*, **96**, 7071-7076.

Steffan, J.S., Bodai, L., Pallos, J., Poelman, M., McCampbell, A., Apostol, B.L., Kazantsev, A., Schmidt, E., Zhu, Y.Z., Greenwald, M., Kurokawa, R., Housman, D.E., Jackson, G.R., Marsh, J.L. & Thompson, L.M. (2001) Histone deacetylase inhibitors arrest polyglutamine-dependent neurodegeneration in Drosophila. *Nature*, **413**, 739-743.

Steffan, J.S., Kazantsev, A., Spasic-Boskovic, O., Greenwald, M., Zhu, Y.Z., Gohler, H., Wanker, E.E., Bates, G.P., Housman, D.E. & Thompson, L.M. (2000) The Huntington's disease protein interacts with p53 and CREB-binding protein and represses transcription. *Proceedings of the National Academy of Sciences of the United States of America*, **97**, 6763-6768.

Stevens, C.D., Altshuler, L.L., Bogerts, B. & Falkai, P. (1988) Quantitative study of gliosis in schizophrenia and Huntington's chorea. *Biological psychiatry*, **24**, 697-700.

Sugars, K.L. & Rubinsztein, D.C. (2003) Transcriptional abnormalities in Huntington disease. *Trends In Genetics*, **19**, 233-238.

Tagawa, K., Marubuchi, S., Qi, M.L., Enokido, Y., Tamura, T., Inagaki, R., Murata, M., Kanazawa, I., Wanker, E.E. & Okazawa, H. (2007) The induction levels of heat shock protein 70 differentiate the vulnerabilities to mutant huntingtin among neuronal subtypes. *J Neurosci*, **27**, 868-880.

Takano, H. & Gusella, J.F. (2002) The predominantly HEAT-like motif structure of huntingtin and its association and coincident nuclear entry with dorsal, an NF-kB/Rel/dorsal family transcription factor. *BMC neuroscience*, **3**, 15.

Tao, T. & Tartakoff, A.M. (2001) Nuclear relocation of normal huntingtin. *Traffic (Copenhagen, Denmark)*, **2**, 385-394.

The Huntington's Disease Collaborative Research Group. (1993) A novel gene containing a trinucleotide repeat that is expanded and unstable on Huntington's disease chromosomes. *Cell*, **72**, 971-983.

Thomas, E.A. (2006) Striatal specificity of gene expression dysregulation in Huntington's disease. *Journal of neuroscience research*, **84**, 1151-1164.

Thompson, J.D., Higgins, D.G. & Gibson, T.J. (1994) Clustal-W - Improving The Sensitivity Of Progressive Multiple Sequence Alignment Through Sequence Weighting, Position-Specific Gap Penalties And Weight Matrix Choice. *Nucleic Acids Research*, **22**, 4673-4680.

Trettel, F., Rigamonti, D., Hilditch-Maguire, P., Wheeler, V.C., Sharp, A.H., Persichetti, F., Cattaneo, E. & MacDonald, M.E. (2000) Dominant phenotypes produced by the HD mutation in STHdh(Q111) striatal cells. *Human molecular genetics*, **9**, 2799-2809.

Trottier, Y., Biancalana, V. & Mandel, J.L. (1994) Instability of CAG repeats in Huntington's disease: relation to parental transmission and age of onset. *Journal of medical genetics*, **31**, 377-382.

Trottier, Y., Devys, D., Imbert, G., Saudou, F., An, I., Lutz, Y., Weber, C., Agid, Y., Hirsch, E.C. & Mandel, J.L. (1995) Cellular localization of the Huntington's disease protein and discrimination of the normal and mutated form. *Nature genetics*, **10**, 104-110.

Trushina, E., Singh, R.D., Dyer, R.B., Cao, S., Shah, V.H., Parton, R.G., Pagano, R.E. & McMurray, C.T. (2006) Mutant huntingtin inhibits clathrin-independent endocytosis and causes accumulation of cholesterol *in vitro* and *in vivo*. *Human molecular genetics*, **15**, 3578-3591.

van Dellen, A., Welch, J., Dixon, R.M., Cordery, P., York, D., Styles, P., Blakemore, C. & Hannan, A.J. (2000) N-acetylaspartate and DARPP-32 levels decrease in the corpus striatum of Huntington's disease mice. *Neuroreport*, **11**, 3751-3757.

van Roon-Mom, W.M.C., Reid, S.J., Jones, A.L., MacDonald, M.E., Faull, R.L.M. & Snell, R.G. (2002) Insoluble TATA-binding protein accumulation in Huntington's disease cortex. *Molecular Brain Research*, **109**, 1-10.

Vonsattel, J.P., Myers, R.H., Stevens, T.J., Ferrante, R.J., Bird, E.D. & Richardson, E.P., Jr. (1985) Neuropathological classification of Huntington's disease. *J Neuropathol Exp Neurol*, **44**, 559-577.

Vonsattel, J.P.G. & DiFiglia, M. (1998) Huntington disease. *Journal Of Neuropathology And Experimental Neurology*, **57**, 369-384.

Wang, G.H., Mitsui, K., Kotliarova, S., Yamashita, A., Nagao, Y., Tokuhiro, S., Iwatsubo, T., Kanazawa, I. & Nukina, N. (1999) Caspase activation during apoptotic cell death induced by expanded polyglutamine in N2a cells. *Neuroreport*, **10**, 2435-2438.

Wanker, E.E., Rovira, C., Scherzinger, E., Hasenbank, R., Walter, S., Tait, D., Colicelli, J. & Lehrach, H. (1997) HIP-I: a huntingtin interacting protein isolated by the yeast two-hybrid system. *Human molecular genetics*, **6**, 487-495.

Wellington, C.L., Ellerby, L.M., Hackam, A.S., Margolis, R.L., Trifiro, M.A., Singaraja, R., McCutcheon, K., Salvesen, G.S., Propp, S.S., Bromm, M., Rowland, K.J., Zhang, T., Rasper, D., Roy, S., Thornberry, N., Pinsky, L., Kakizuka, A., Ross, C.A., Nicholson, D.W., Bredesen, D.E. & Hayden, M.R. (1998) Caspase cleavage of gene products associated with triplet expansion disorders generates truncated fragments containing the polyglutamine tract. *J Biol Chem*, **273**, 9158-9167.

Wexler, N.S., Lorimer, J., Porter, J., Gomez, F., Moskowitz, C., Shackell, E., Marder, K., Penchaszadeh, G., Roberts, S.A., Gayan, J., Brocklebank, D., Cherny, S.S., Cardon, L.R., Gray, J., Dlouhy, S.R., Wiktorski, S., Hodes, M.E., Conneally, P.M., Penney, J.B., Gusella, J., Cha, J.H., Irizarry, M., Rosas, D., Hersch, S., Hollingsworth, Z., MacDonald, M., Young, A.B., Andresen, J.M., Housman, D.E., De Young, M.M., Bonilla, E., Stillings, T., Negrette, A., Snodgrass, S.R., Martinez-Jaurrieta, M.D., Ramos-Arroyo, M.A., Bickham, J., Ramos, J.S., Marshall, F., Shoulson, I., Rey, G.J., Feigin, A., Arnheim, N., Acevedo-Cruz, A., Acosta, L., Alvir, J., Fischbeck, K., Thompson, L.M., Young, A., Dure, L., O'Brien, C.J., Paulsen, J., Brickman, A., Krch, D., Peery, S., Hogarth, P., Higgins, D.S., Jr. & Landwehrmeyer, B. (2004) Venezuelan kindreds reveal that genetic and environmental factors modulate Huntington's disease age of onset. *Proceedings of the National Academy of Sciences of the United States of America*, **101**, 3498-3503.

Wexler, N.S., Young, A.B., Tanzi, R.E., Travers, H., Starosta-Rubinstein, S., Penney, J.B., Snodgrass, S.R., Shoulson, I., Gomez, F., Ramos Arroyo, M.A. & et al. (1987) Homozygotes for Huntington's disease. *Nature*, **326**, 194-197.

Weydt, P., Pineda, V.V., Torrence, A.E., Libby, R.T., Satterfield, T.F., Lazarowski, E.R., Gilbert, M.L., Morton, G.J., Bammler, T.K., Strand, A.D., Cui, L., Beyer, R.P., Easley, C.N., Smith, A.C., Krainc, D., Luquet, S., Sweet, I.R., Schwartz, M.W. & La Spada, A.R. (2006) Thermoregulatory and metabolic defects in Huntington's disease transgenic mice implicate PGC-1alpha in Huntington's disease neurodegeneration. *Cell metabolism*, **4**, 349-362.

Wheeler, V.C., Auerbach, W., White, J.K., Srinidhi, J., Auerbach, A., Ryan, A., Duyao, M.P., Vrbanac, V., Weaver, M., Gusella, J.F., Joyner, A.L. & MacDonald, M.E. (1999) Length-dependent gametic CAG repeat instability in the Huntington's disease knock-in mouse. *Human molecular genetics*, **8**, 115-122.

Wheeler, V.C., White, J.K., Gutekunst, C.A., Vrbanac, V., Weaver, M., Li, X.J., Li, S.H., Yi, H., Vonsattel, J.P., Gusella, J.F., Hersch, S., Auerbach, W., Joyner, A.L. & MacDonald, M.E. (2000) Long glutamine tracts cause nuclear localization of a novel form of huntingtin in medium spiny striatal neurons in HdhQ92 and HdhQ111 knock-in mice. *Human molecular genetics*, **9**, 503-513.

Widlak, P., Gaynor, R.B. & Garrard, W.T. (1997) *In vitro* chromatin assembly of the HIV-1 promoter. ATP-dependent polar repositioning of nucleosomes by Sp1 and NFkappaB. *J Biol Chem*, **272**, 17654-17661.

Wolfgang, W.J., Miller, T.W., Webster, J.M., Huston, J.S., Thompson, L.M., Marsh, J.L. & Messer, A. (2005) Suppression of Huntington's disease pathology in Drosophila by human single-chain Fv antibodies. *Proceedings of the National Academy of Sciences of the United States of America*, **102**, 11563-11568.

Wood, N.I., Pallier, P.N., Wanderer, J. & Morton, A.J. (2007) Systemic administration of Congo red does not improve motor or cognitive function in R6/2 mice. *Neurobiol Dis*, **25**, 342-353.

Wood, S.J., Wypych, J., Steavenson, S., Louis, J.C., Citron, M. & Biere, A.L. (1999) alpha-synuclein fibrillogenesis is nucleation-dependent. Implications for the pathogenesis of Parkinson's disease. *J Biol Chem*, **274**, 19509-19512.

Xie, Z., Adamowicz, W.O., Eldred, W.D., Jakowski, A.B., Kleiman, R.J., Morton, D.G., Stephenson, D.T., Strick, C.A., Williams, R.D. & Menniti, F.S. (2006) Cellular and subcellular localization of PDE10A, a striatum-enriched phosphodiesterase. *Neuroscience*, **139**, 597-607.

Yamamoto, A., Lucas, J.J. & Hen, R. (2000) Reversal of neuropathology and motor dysfunction in a conditional model of Huntington's disease. *Cell*, **101**, 57-66.

Yohrling, G.J., Farrell, L.A., Hollenberg, A.N. & Cha, J.H. (2003) Mutant huntingtin increases nuclear corepressor function and enhances ligand-dependent nuclear hormone receptor activation. *Molecular and cellular neurosciences*, **23**, 28-38.

Yu, Z.X., Li, S.H., Nguyen, H.P. & Li, X.J. (2002) Huntingtin inclusions do not deplete polyglutamine-containing transcription factors in HD mice. *Human molecular genetics*, **11**, 905-914.

Zeitlin, S., Liu, J.P., Chapman, D.L., Papaioannou, V.E. & Efstratiadis, A. (1995) Increased apoptosis and early embryonic lethality in mice nullizygous for the Huntington's disease gene homologue. *Nature genetics*, **11**, 155-163.

Zemskov, E.A. & Nukina, N. (2003) Impaired degradation of PKCalpha by proteasome in a cellular model of Huntington's disease. *Neuroreport*, **14**, 1435-1438.

Zeron, M.M., Fernandes, H.B., Krebs, C., Shehadeh, J., Wellington, C.L., Leavitt, B.R., Baimbridge, K.G., Hayden, M.R. & Raymond, L.A. (2004) Potentiation of NMDA receptor-mediated excitotoxicity linked with intrinsic apoptotic pathway in YAC transgenic mouse model of Huntington's disease. *Molecular and cellular neurosciences*, **25**, 469-479.

Zeron, M.M., Hansson, O., Chen, N., Wellington, C.L., Leavitt, B.R., Brundin, P., Hayden, M.R. & Raymond, L.A. (2002) Increased sensitivity to N-methyl-D-aspartate receptor-mediated excitotoxicity in a mouse model of Huntington's disease. *Neuron*, **33**, 849-860.

Zhai, W., Jeong, H., Cui, L., Krainc, D. & Tjian, R. (2005) *In vitro* analysis of huntingtin-mediated transcriptional repression reveals multiple transcription factor targets. *Cell*, **123**, 1241-1253.

Zuccato, C., Tartari, M., Crotti, A., Goffredo, D., Valenza, M., Conti, L., Cataudella, T., Leavitt, B.R., Hayden, M.R., Timmusk, T., Rigamonti, D. & Cattaneo, E. (2003) Huntingtin interacts with REST/NRSF to modulate the transcription of NRSE-controlled neuronal genes. *Nature genetics*, **35**, 76-83.